Mediators of intercellular communication in immune responses

van Asten, S.D.

Publication date
2022
Document Version
Final published version

Citation for published version (APA):
van Asten, S. D. (2022). *Mediators of intercellular communication in immune responses.*

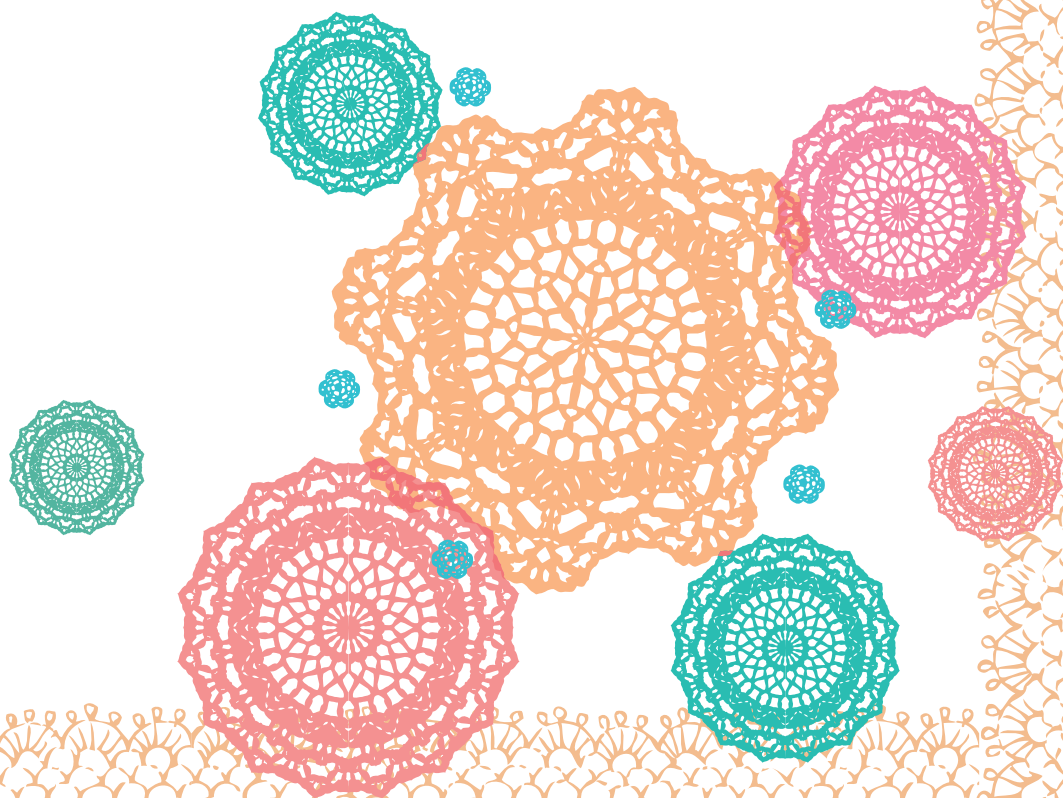# MEDIATORS OF INTERCELLULAR COMMUNICATION IN IMMUNE RESPONSES

SASKIA DÉSIRÉE VAN ASTEN

Mediators of Intercellular Communication in Immune Responses

Saskia Désirée van Asten

Mediators of Intercellular Communication in Immune Responses

ACADEMISCH PROEFSCHRIFT

ter verkrijging van de graad van doctor

aan de Universiteit van Amsterdam

op gezag van de Rector Magnificus

prof. dr. ir. K.I.J. Maex

ten overstaan van een door het College voor Promoties ingestelde commissie,

in het openbaar te verdedigen in de Agnietenkapel

op maandag 20 juni 2022, te 14:00 uur

door Saskia Désirée van Asten

geboren te Lelystad

Promotiecommissie

Promotor: prof. dr. S.M. van Ham   Universiteit van Amsterdam

Co-promotor: dr. R.M. Spaapen   Sanquin Research

Overige leden: prof. dr. J.G. Borst   Universiteit Leiden
                   prof. dr. ing. A.H.C. van Kampen   Universiteit van Amsterdam
                   prof. dr. T.B.H. Geijtenbeek   Universiteit van Amsterdam
                   prof. dr. E.C. de Jong   Universiteit van Amsterdam
                   prof. dr. L. Meyaard   Universiteit Utrecht
                   dr. J.J. García-Vallejo   Vrije Universiteit Amsterdam
                   prof. dr. C. Jalink   Universiteit van Amsterdam

Faculteit der Natuurwetenschappen, Wiskunde en Informatica

Table of contents

CHAPTER 1

General introduction and scope of this thesis

A functional immune system requires good communication

The human immune system protects against a wide variety of pathogens as well as cancer. It must therefore be sensitive to many different cues. It has a multitude of tricks up its sleeve, including protein complexes that can flag and even lyse bacteria and immune cells that can identify and kill dysfunctional cells. Different groups of pathogens require different strategies, as for example extracellular helminths have to be handled differently than viruses which reside intracellularly (1, 2). Yet threats do not come solely from the outside: genetic mutations may cause the body's own cells to transform and develop into cancer. Finding and clearing transformed cells is part of the immune system's capabilities (3).

To fight the different infections and cancer development, the immune system employs multiple specialized cell types, including cells that can generate and remember a pathogen-specific response. Communication is of vital importance for a functional immune system. Both immune and non-immune cells must be made aware of an infection to create a response that makes the environment inhospitable to pathogens or transformed cells. In addition, the correct specialized immune cells must be instructed to execute a suitable immune response while preventing activation of unsuitable immune cells and thereby risking tissue damage (4). Once the threat is over the effector functions of the immune system must be counteracted and returned to immune homeostasis to prevent (further) damage to the site of inflammation (5).

The messages leading to immune responses and the subsequent return to homeostasis are both predominantly communicated through extracellular receptors expressed by cells, which trigger or inhibit intracellular signaling pathways leading to modified gene expression or other cellular processes such as polarization or inside-out signaling (6–9). The repertoire of expressed receptors will determine which ligands a cell can recognize, and consequently which messages can be received. The ligands that bind these receptors may be soluble, expressed on the surface of host cells or expressed on the surface of pathogens (6–9). Soluble signaling molecules include small molecules, peptides, and secreted proteins. While direct cell-cell contact occurs only locally, soluble signaling molecules can influence nearby cells expressing the corresponding receptors (paracrine), including the secretory cell itself (autocrine), as well as cells located in other organs after transportation through the bloodstream (endocrine) (10). Immune cells can migrate through the body and thereby physically contact distant cells (11, 12). Migration allows immune cells to come in direct contact with other immune cells in lymphoid organs to convey an alarm signal, or with infected or dysfunctional cells to kill them. Cells receive a multitude of stimulating and inhibitory signals which combined determine their response. The potential responses include activation, proliferation, migration, maturation, differentiation, inactivation, and apoptosis. All of these responses occur at one or more stages during an immune response.

1

The innate immune system is the first responder

The general first-response strategies are collectively called the innate immune system since they use rather unspecific immune mechanisms that are imprinted in the human genome. Pathogens that circumvent the anatomical barriers and thereby invade the human body must be discovered as soon as possible to prevent pathogen replication and further spreading of the pathogen. Similarly, when the body's own cells become transformed they must be removed to prevent oncogenesis. The immune system is constantly vigilant for foreign material and transformed cells using different strategies.

Pathogens can be recognized by pattern recognition receptors (PRRs) expressed on the cell-surface of innate immune cells and intracellularly in most cells including non-immune cells (6). PRRs identify molecules that are expressed by pathogens but not by healthy human cells, such as bacterial lipopolysaccharides and viral double-stranded DNA (collectively called pathogen associated molecular patterns; PAMPs). In addition, they recognize damage-associated molecular patterns which are host-derived molecules that should not be present extracellularly under healthy conditions (13).

Non-immune cells may recognize when they have been infected by a virus through expression of PRRs that sense intracellular viral RNA or DNA. Ligation of PRRs induces secretion of type I interferons (IFNs) in these non-immune cells (Fig. 1A) (14). Neighboring cells that express the IFN receptor (IFNAR) are now warned of an infection, yet there is a striking difference in response between non-immune and immune cells. In non-immune cells, IFNAR activation results in inhibition of transcription, translation, and proliferation (15). As viruses make use of the molecular machinery of their host cell, inhibiting these processes inhibits viral replication. In multiple immune cell types IFNs act as a pro-inflammatory signal to stimulate their effector functions, although more signals are required for full activation (16–18).

Ligation of PRRs activates innate immune cells and induces secretion of multiple cytokines and chemokines to promote an immune response (6). These soluble proteins make blood vessels leaky, allowing other soluble proteins to enter the site of inflammation. An example is mannose-binding lectin (MBL) that circulates in blood and can bind to sugar moieties found on the surface of pathogens (19). Binding of MBL to pathogens initiates a protein activation cascade of the complement system resulting in the direct killing of bacteria by creating holes in the bacterial cell wall, the recruitment of other immune cells and phagocytosis of these bacteria by these immune cells (19). MBL is only one of several soluble proteins that opsonize pathogens for clearance by the immune system.

Activated innate immune cells also secrete chemokines to attract more immune cells and initiate effector mechanisms dependent on the type of danger sensed. Neutrophils and macrophages can engulf pathogens and kill them once taken up; a process called phagocytosis (20, 21). Natural killer (NK) cells assess the balanced expression of a set of receptors on human cells to determine whether it should kill the cell as aberrant expression may be caused by viral infection or be a characteristic of a tumor cell (22). Thus, the innate
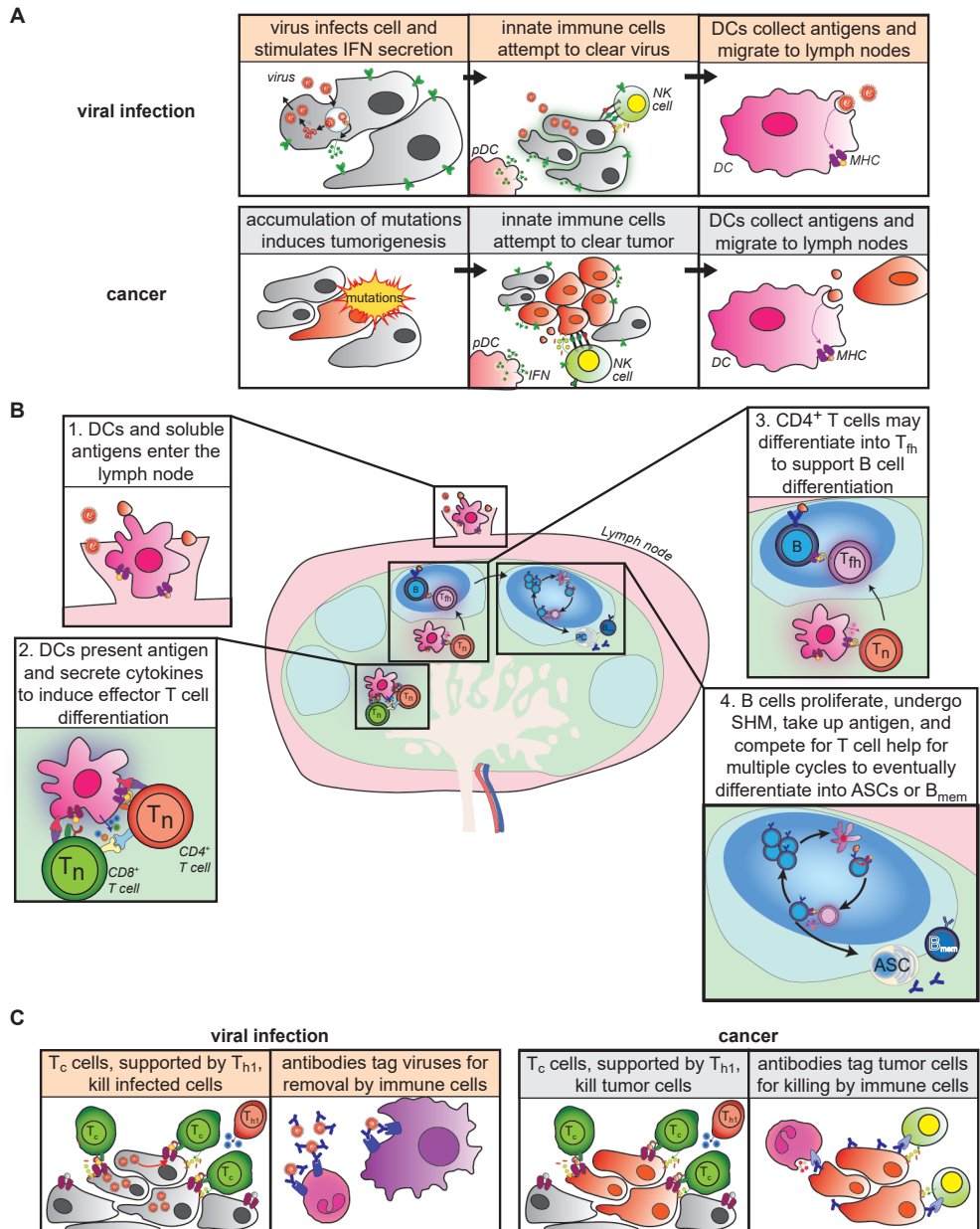
Figure 1. The immune response in viral infection and cancer. (A) Innate immune cells attempt to clear a viral infection (upper panels) or tumor cells (lower panels), while dendritic cells (DCs) collect antigen to bring to cells of the adaptive immune system in the lymph nodes. (B) In the lymph node, recognition of their cognate antigen combined with co-stimulation leads to the activation of T and B cells. Depending on the received signals, T cells may become effector cytotoxic T cells or any of the helper subsets. Proliferating B cells may form a germinal center reaction, during which they undergo somatic hyper mutation (SHM) which may improve their B cell receptor. Successful B cells receive T cell help and differentiate either into memory B cells or antibody secreting cells (ASCs) (C) Cytotoxic T cells (T_c) kill infected- or tumor cells, supported by T helper 1 cells (T_{h1}). Antibodies produced by ASCs opsonize viral particles or tumor cells for clearance by other cells of the immune system.

immune system can find and remove extra- and intracellular pathogens as well as tumor cells by sensing their presence using a diverse set of relatively unspecific receptors and soluble proteins and can alert other immune cells through secreted proteins and direct cell-cell contact (Fig. 1A). Yet, often pathogens cannot be removed solely by the innate immune system or only after prolonged inflammatory processes and tissue damage.

The adaptive immune system mounts a tailored response

The B and T lymphocytes of the adaptive immune system are able to create a highly tailored response towards pathogens and tumor cells. B and T lymphocytes develop unique receptors during their development, called B cell receptor (BCR) and T cell receptor (TCR) respectively, through random gene rearrangement. It is estimated that the pool of T cells within an individual harbors at least 10^5 different TCRs, with some estimations surpassing 10^8 unique TCRs (23, 24). Molecules recognized by BCRs and TCRs during an immune response are called antigens. Pathogens or tumor cells express many different antigens.

During the initial innate immune response, dendritic cells take up antigens, are activated through PRRs, mature and then migrate from the site of inflammation to the lymph nodes to activate the T lymphocytes that recognize the specific antigen (Fig. 1B) (11, 25). Concurrently antigens enter the lymph nodes by passive transport in the lymph which may be recognized by B cells through their BCR (25). Out of the vast number of unique BCRs and TCRs only a few will recognize the antigens at hand. The B and T cells expressing these antigen receptors must come in contact with their cognate antigen. Upon first encounter with a unique pathogen or tumor these will be naive lymphocytes that have not yet come into contact with their cognate antigen before. Naive lymphocytes require multiple signals next to antigen receptor engagement to become fully activated including membrane-bound ligands and soluble cytokines and chemokines. The different signals required for full activation are further discussed below. Upon successful activation, naive lymphocytes proliferate to greatly increase their number and differentiate into specialized effector cells that aid in the removal of the pathogen or transformed cells (Fig. 1C). This proliferation and differentiation may take days up to a few weeks to complete. After resolving the infection a few lymphocytes will remain as memory cells. Memory cells circulate the body, stay at the first site of infection as tissue resident cells, and live in specialized niches ready to be reactivated when necessary. Upon a secondary encounter with a pathogen, memory cells can respond much faster as the antigen receptor activation threshold is lowered and are therefore more time effective in resolving infections than naive lymphocytes.

T cell activation and differentiation requires multiple interactions

Because of their pro-inflammatory and cytolytic capacity, effector T cells can cause

tissue damage, thus unnecessary priming must be avoided. Four different communication signals are therefore required to fully activate naive T cells and to instruct them of their objective.

To ensure only the T cells recognizing the threat are activated, the first essential signal is activation of the TCR. TCRs can bind to their cognate antigen presented by major histocompatibility complexes (MHC) on the surface of any nucleated cell (26). MHC class I (MHCI) and class II (MHCII) molecules continuously present peptides derived from intracellular and extracellularly derived proteins. CD8$^+$ T cells recognize peptides presented by MHCI while CD4$^+$ T cells are restricted to MHCII (26). Under healthy conditions the peptides presented by the MHC molecules will be derived from the body's own wild type proteins. These peptides should not activate any T cell as T cells expressing a TCR recognizing the body's own wild type peptides are negatively selected during development (27). During infections, the presented peptide repertoire may include bacteria- or virus-derived proteins. In addition, transformed cells may present peptides derived from mutated genes (28). Thus, using antigen presentation, cells can communicate to T cells that they have been infected or contain mutated genes, while professional antigen presenting cells (APCs) such as DCs can inform T cells on the presence of pathogens and tumor cells both intra- and extracellularly. TCR stimulation alone is not sufficient for full naive T cell activation as TCR stimulation alone does not stimulate T cell proliferation or differentiation, but instead causes a T cell to undergo apoptosis or become anergic (29).

As a second signal T cells require activation of other cell surface receptors. The interaction of CD28 molecules expressed on the surface of the T cells with CD80 and CD86 expressed by activated APCs provides strong costimulation, which combined with TCR activation may be sufficient for full activation (30–32). APCs can further promote T cell activation through interactions between surface proteins. For example, interaction of CD137L on the APC with CD137 on T cells induces cytolytic activity, and the interaction of CD70 on the APC with CD27 on the T cell promotes proliferation (33–35).

In addition to direct cell-cell contact, T cell differentiation is supported by secreted proteins called cytokines. Cytokines may be secreted by other immune cells, including innate immune cells, to communicate what type of effector T cells are required. For example, IL-12 secreted by DCs stimulates CD4$^+$ T cells to become IFN-γ secreting helper cells (Th$_1$) that support cytotoxic T cells (36, 37). Effector T cells encompass cytotoxic T cells, which can kill infected cells as well as tumor cells, and several types of specialized T helper cells which promote a specific immune response through cytokine secretion. T helper functions include supporting B cell differentiation and promoting cytotoxicity of other immune cells. The variety of effector T cell types is described in more detail in chapter 4. Most CD8$^+$ T cells differentiate into cytotoxic T cells, while most CD4$^+$ T cells become helper cells. Cytotoxic T cell is therefore often used synonymously for CD8$^+$ T cells, however, CD4$^+$ T cells can also be cytotoxic cells and CD8$^+$ T cells also secrete cytokines.

The fourth signal consists of molecules that enable T cell migration towards tissues where they should exert their effector functions. By expressing a certain chemokine receptor, immune cells can enter and migrate within tissues where the corresponding ligand(s) are expressed. Target tissues include inflamed tissue where they must clear infections, as well as specific areas of the lymph node where immune cells requiring T cell help are located. For example, naive T cells and certain memory T cells express the chemokine receptor CCR7, thus they can enter lymph nodes which express CCL21 to determine whether their cognate antigen is being presented there (38–40). Th$_1$ and cytotoxic T cells express CXCR3 which enables migration into inflamed tissues that secrete CXCL9 and CXCL10 (41).

In addition to the pro-inflammatory signals described above, anti-inflammatory interactions exist to ensure that the T cell response lasts only as long as required and cannot go out of control. Shortly after initial activation, CD28 must compete with CTLA-4, likewise expressed by the T cell, for engagement with CD80/CD86 expressed by the APC (42). Consequently, the APC must have received ample pro-inflammatory signals to ensure sufficient expression of CD80/CD86, which will happen during prolonged inflammation. After activation T cells are further regulated to minimize collateral tissue damage and to stop their pro-inflammatory effector functions once the threat is over. After activation T cells express additional molecules, such as PD-1, that inhibit T cell effector functions when bound to their ligand (43–45). Other cells, including non-immune cells, can inhibit PD-1 expressing cells through interaction with its ligand PD-L1 (44, 46). In addition, a subset of CD4+ T cells called T regulatory cells is specialized in the suppression of an immune response through expression of inhibitory molecules and cytokines (47). The strength and duration of a T cell response depends on the balance of pro-inflammatory signals and anti-inflammatory signals.

B cell differentiation is a multistep process supported by other immune cells

B cells take up soluble antigen or phagocytose small pathogens and particles using the BCR, which are processed intracellularly to generate peptides which can be presented by MHC II (48). B cells require help from CD4+ T cells in secondary lymphoid organs to become long-lived antibody secreting cells or memory cells (49). Once a B cell finds DC-activated CD4+ T cells that are specific for the B cell's presented pathogen peptides, these cells will co-stimulate each other to induce the others' differentiation into the relevant effector cells. The CD4+ T cell becomes a helper cell specialized in stimulating B cells called a follicular T helper cell (T$_{fh}$, Fig. 1B) (49). The B cells will proliferate and undergo somatic hypermutation (SHM), by which point-mutations are introduced in the antigen-binding loops of BCR which might generate a BCR that binds the pathogen more effectively (50). In first instance, these random mutations may be beneficial, neutral, or detrimental for pathogen recognition. A BCR with higher binding affinity for the antigen allows B cells to more efficiently take up pathogen (particles) and present their peptides on MHCII, while detrimental mutations cause the opposite effect (51). Efficient B cells will be able

to receive T cell help because they present more of the pathogen's peptides on MHCII, while B cells lacking T cell help will go into apoptosis, a process termed affinity maturation. The T_{fh} cell derived activation and pro-survival signals B cells compete for include the interaction of CD40 on B cells with CD40L on T cells, ICOSL with ICOS, and the secreted cytokines IL-4 and IL-21 (49, 51). B cells will undergo multiple rounds of proliferation and somatic hypermutation followed by selection in so called germinal center reactions (52). Successful B cells will differentiate into memory B cells or into antibody secreting cells (plasmablasts and plasma cells). Plasma cells are long-lived cells that migrate to the bone marrow where they may secrete antibodies for years. Antibodies are soluble versions of the BCR. They may reach the site of inflammation through the blood and can reach the site of infection when blood vessels have become leaky through the action of other immune cells. They thwart pathogens by neutralizing extracellular toxins, flagging pathogens for phagocytosis by other immune cells, or by initiating the classical route of the complement system which also leads to their degradation (53). In conclusion, through the secretion of antibodies, B cells differentiated into plasmablasts and plasma cells cooperate with other elements of the immune system to remove extracellular particles and pathogens.

Pathogens and transformed cells foil immunological communication

The immune system uses its extensive and highly specialized communication system to coordinate immune responses. Unfortunately, both pathogens and transformed cells may prevent detection and clearance by inhibiting or even abusing any point of immunological communication described above. Viruses and tumor cells use similar strategies to avoid detection and suppress an immune response. A few examples are described in the next paragraph.

In addition to promoting an anti-viral immune response as explained above, IFNs can suppress tumor progression and promote an anti-tumor response (54–57). Yet viruses and tumor cells can be less sensitive to IFNs by inhibiting IFN production or downstream IFNAR signaling (58, 59). Both transformed cells and viruses may downregulate MHCI to avoid detection by CD8^{+} T cells, while employing other mechanisms to prevent detection by NK cells (60–62). In addition, they may stimulate expression of immune suppressing signals such as PD-L1 in neighboring cells or express this inhibitory molecule themselves (44, 63, 64). Tumors may also create an immune-suppressive microenvironment by attracting and maintaining suppressive immune cells such as myeloid-derived suppressor cells and T_{reg} cells (65).

When a tumor or pathogen efficiently prevents or inhibits an immune response, they can continue to thrive and further damage tissue locally or even systemically. When the communication systems of the immune system fail, therapeutic intervention is essential to support the failing parts of the immune system. Immunotherapy is an umbrella term for multiple strategies that aim to either educate the immune system of the threat, to provide functional immune proteins or cells, or to reduce suppressive signaling (66). For

example, vaccines can show the immune system characteristics of a pathogen or tumor cell so that immune cells may respond faster to emerging threats (67–70). Therapeutic antibodies can be administered to support an immune system that is unable or inefficient in producing them (71). Autologous T cells may be reactivated *ex vivo* and returned to a patient (72). To develop successful immunotherapy, it is important to understand which mechanisms pathogens and tumors use to avoid immune clearance and to find additional methods of boosting an immune response.

High-throughput screening to better understand communication in immunology

Further research is required to enhance our understanding of immunological communication to support therapy development. The most common screening methods applied these days are transcriptome analyses by RNAseq or genome-wide knockout screens by CRISPR/Cas9 (73, 74). These represent screening methods of two fundamentally different categories, since the first searches for new correlations (comparative screening) and the second for causal relationships (forward screening).

In more detail, in comparative screens each sample is assigned to one of two groups (healthy subjects vs a patient group, stratified patient groups, treated vs non-treated cells *in vitro*, etc.), a large set of data is gathered per sample (e.g. genome wide gene expression), and then the results are compared between the two groups to identify key differences that may or may not be causally related (74). Hit selection in comparative screens can yield many hits, depending on the arbitrary hit selection threshold, of which only a few may be relevant for the research question at hand. Identifying and validating those relevant hits may be time-consuming, while there is no guarantee that a relevant hit will be identified. Unless the goal is to describe a general difference between the groups included in the screen, comparative screens have a risk of not yielding the desired results.

In forward screens, each sample will receive a unique treatment (e.g. knockout of a specific gene, treatment with a unique compound, etc.) compared to all other thousand or more samples, after which each sample is analyzed for an -often limited- set of readouts. These readouts may include viability or the expression of a certain protein. Some samples will deviate sufficiently from the other samples, as arbitrarily specified by the researcher, for their unique treatment to be considered hits. In follow up experiments the hits must be verified to ensure that the results observed in the screen can be replicated. Forward screens come in arrayed and pooled forms. In arrayed screens each sample is treated with a single compound, siRNA or CRISPR guide RNA, while in pooled screens a pool of these treatments is added to each well. Pooled screens therefore require additional steps to distinguish the individual treatments within a pool but have the advantage of a needing to measure fewer samples, which decreases inter-sample variability, the amount of work and the financial cost compared to arrayed screens. Importantly, causative relations are inherent to both types of forward screens as each outcome is linked to one unique

treatment.

Arrayed forward screening has been extensively applied in drug discovery where it involves the testing of a library of thousands of small drug-like molecules -synthesized in the lab or purified from biological samples- to identify lead compounds that may be developed into a treatment. This approach has led to drugs such as Dasatinib, which is now widely used in the treatment of Philadelphia chromosome-positive chronic myeloid leukemia (75–77). To uncover causal interactions that may occur naturally, libraries containing molecules found *in vivo,* such as metabolites, antibodies, or secreted proteins, can be applied. Screening libraries may also consist of agents that knockdown or knockout genes such as CRISPR-Cas9 guide RNAs which have been used to (further) dissect signaling pathways. Genome-wide genetic screens have led to the identification of regulators of MHCI (SPPL3) and MHCII (GTPase ARL14/ARF7) (78, 79).

Both comparative and forward screening enable the discovery of interactions that may not have been predicted by experts in a field and are therefore valuable tools to better understand communication in immunology.

Scope of this thesis

The scope of this thesis is to study immunological communication. **Chapter 2** of this thesis describes the generation of a conditioned medium-based secreted protein library containing 756 secreted proteins and the first application of such a library to find novel external signals that modulate viral infection. This screen identified fibroblast growth factor 16 as an inhibitor of viral replication independent of type I IFNs, thereby uncovering fibroblast growth factors as anti-viral signaling molecules. In **Chapter 3** the secreted protein library is applied to an *in vitro* model of B cells during a germinal center reaction to identify soluble proteins that drive B cell differentiation into antibody secreting cells. Type I IFNs induce differentiation into plasmablasts and plasma cells in both naive and memory B cells, but soluble FAS ligand stimulates plasmablast differentiation and antibody secretion only in memory B cells. In **Chapter 4** the original secreted protein library is almost doubled to include over 1200 secreted proteins. Using this extended library in a high-throughput setting, we search for novel factors and hereto-unknown functions of established secreted proteins that affect naive CD4$^+$ or CD8$^+$ T cell differentiation into effector and memory cells. Multiple secreted proteins, including type I interferons, affect granzyme B expression in CD8$^+$ T cells, yet only IL-21 induces granzyme B in CD4$^+$ T cells. In **Chapter 5** renal cell carcinoma (RCC) and paired non-tumorous kidney tissue digests are analyzed for their immune infiltration and cultured to expand tumor infiltrating lymphocytes (TILs). While T cells are increased in RCC and after expansion recognize autologous tumor digest, these expanded TILs do not have increased cytokine production, indicating that these TILs have not received the appropriate communication signals to exert their anti-tumor effector functions. The results of this thesis are summarized and discussed in **Chapter 6**.

References

1. Motran, C. C., L. Silvane, L. S. Chiapello, M. G. Theumer, L. F. Ambrosio, X. Volpini, D. P. Celias, and L. Cervi. 2018. Helminth infections: Recognition and modulation of the immune response by innate immune cells. *Front. Immunol.* 9: 1.

2. Chen, X., S. Liu, M. U. Goraya, M. Maarouf, S. Huang, and J. L. Chen. 2018. Host immune response to influenza A virus infection. *Front. Immunol.* 9.

3. Guzman, L. G. M., N. Keating, and S. E. Nicholson. 2020. Natural Killer Cells: Tumor Surveillance and Signaling. *Cancers (Basel).* 12.

4. Fajgenbaum, D. C., and C. H. June. 2020. Cytokine Storm. *N. Engl. J. Med.* 383: 2255–2273.

5. Ortega-Gómez, A., M. Perretti, and O. Soehnlein. 2013. Resolution of inflammation: an integrated view. *EMBO Mol. Med.* 5: 661–74.

6. Kumar, H., T. Kawai, and S. Akira. 2011. Pathogen recognition by the innate immune system. *Int. Rev. Immunol.* 30: 16–34.

7. Courtney, A. H., W.-L. Lo, and A. Weiss. 2018. TCR Signaling: Mechanisms of Initiation and Propagation. *Trends Biochem. Sci.* 43: 108–123.

8. Tanaka, S., and Y. Baba. 2020. B Cell Receptor Signaling. In *B Cells in Immunity and Tolerance* J.-Y. Wang, ed. Springer Singapore, Singapore. 23–36.

9. Cameron, M. J., and D. J. Kelvin. 2013. Cytokines, Chemokines and Their Receptors. .

10. Müller, E., W. Wang, W. Qiao, M. Bornhäuser, P. W. Zandstra, C. Werner, and T. Pompe. 2016. Distinguishing autocrine and paracrine signals in hematopoietic stem cell culture using a biofunctional microcavity platform. *Sci. Rep.* 6: 31951.

11. Worbs, T., S. I. Hammerschmidt, and R. Förster. 2017. Dendritic cell migration in health and disease. *Nat. Rev. Immunol.* 17: 30–48.

12. Petri, B., and M.-J. Sanz. 2018. Neutrophil chemotaxis. *Cell Tissue Res.* 371: 425–436.

13. Gong, T., L. Liu, W. Jiang, and R. Zhou. 2020. DAMP-sensing receptors in sterile inflammation and inflammatory diseases. *Nat. Rev. Immunol.* 20: 95–112.

14. Kato, H., S. Sato, M. Yoneyama, M. Yamamoto, S. Uematsu, K. Matsui, T. Tsujimura, K. Takeda, T. Fujita, O. Takeuchi, and S. Akira. 2005. Cell type-specific involvement of RIG-I in antiviral response. *Immunity* 23: 19–28.

15. Sadler, A. J., and B. R. G. Williams. 2008. Interferon-inducible antiviral effectors. *Nat. Rev. Immunol.* 8: 559–568.

16. Jego, G., A. K. Palucka, J.-P. Blanck, C. Chalouni, V. Pascual, and J. Banchereau. 2003. Plasmacytoid dendritic cells induce plasma cell differentiation through type I interferon and interleukin 6. *Immunity* 19: 225–34.

17. Fink, K., K. S. Lang, N. Manjarrez-Orduno, T. Junt, B. M. Senn, M. Holdener, S. Akira, R. M. Zinkernagel, and H. Hengartner. 2006. Early type I interferon-mediated signals on B cells specifically enhance antiviral humoral responses. *Eur. J. Immunol.* 36: 2094–105.

18. van Boxel-Dezaire, A. H. H., M. R. S. Rani, and G. R. Stark. 2006. Complex modulation of cell type-specific signaling in response to type I interferons. *Immunity* 25: 361–72.

19. Turner, M. W. 2003. The role of mannose-binding lectin in health and disease. *Mol. Immunol.* 40: 423–9.

20. Aderem, A., and D. M. Underhill. 1999. MECHANISMS OF PHAGOCYTOSIS IN MACROPHAGES. *Annu. Rev. Immunol.* 17: 593–623.

21. Lee, W. L., R. E. Harrison, and S. Grinstein. 2003. Phagocytosis by neutrophils. *Microbes Infect.* 5: 1299–1306.

22. Sivori, S., P. Vacca, G. Del Zotto, E. Munari, M. C. Mingari, and L. Moretta. 2019. Human NK cells: surface receptors, inhibitory checkpoints, and translational applications. *Cell. Mol. Immunol.* 16: 430–441.

23. de Greef, P. C., T. Oakes, B. Gerritsen, M. Ismail, J. M. Heather, R. Hermsen, B. Chain, and R. J. de Boer. 2020. The naive T-cell receptor repertoire has an extremely broad distribution of clone sizes. *Elife* 9.

24. Qi, Q., Y. Liu, Y. Cheng, J. Glanville, D. Zhang, J.-Y. Lee, R. A. Olshen, C. M. Weyand, S. D. Boyd, and J. J. Goronzy. 2014. Diversity and clonal selection in the human T-cell repertoire. *Proc. Natl. Acad. Sci.* 111: 13139–13144.

25. Liao, S., and P. Y. von der Weid. 2015. Lymphatic system: An active pathway for immune protection. *Semin. Cell Dev. Biol.* 38: 83–89.

26. Neefjes, J., M. L. M. Jongsma, P. Paul, and O. Bakke. 2011. Towards a systems understanding of MHC class I and MHC class II antigen presentation. *Nat. Rev. Immunol.* 11: 823–836.

27. Klein, L., B. Kyewski, P. M. Allen, and K. A. Hogquist. 2014. Positive and negative selection of the T cell repertoire: what thymocytes see (and don't see). *Nat. Rev. Immunol.* 14: 377–391.

28. Schumacher, T. N., W. Scheper, and P. Kvistborg. 2019. Cancer Neoantigens. *Annu. Rev. Immunol.* 37: 173–200.

29. Zheng, Y., Y. Zha, and T. F. Gajewski. 2008. Molecular regulation of T-cell anergy. *EMBO Rep.* 9: 50–55.

30. Boise, L. H., A. J. Minn, P. J. Noel, C. H. June, M. A. Accavitti, T. Lindsten, and C. B. Thompson. 1995. CD28 costimulation can promote T cell survival by enhancing the expression of Bcl-xL. *Immunity* 3: 87–98.

1

31. Savoldo, B., C. A. Ramos, E. Liu, M. P. Mims, M. J. Keating, G. Carrum, R. T. Kamble, C. M. Bollard, A. P. Gee, Z. Mei, H. Liu, B. Grilley, C. M. Rooney, H. E. Heslop, M. K. Brenner, and G. Dotti. 2011. CD28 costimulation improves expansion and persistence of chimeric antigen receptor-modified T cells in lymphoma patients. *J. Clin. Invest.* 121: 1822–1826.

32. Sharpe, A. H., and G. J. Freeman. 2002. The B7–CD28 superfamily. *Nat. Rev. Immunol.* 2: 116–126.

33. Harfuddin, Z., S. Kwajah, A. C. N. Sim, P. A. MacAry, and H. Schwarz. 2013. CD137L-stimulated dendritic cells are more potent than conventional dendritic cells at eliciting cytotoxic T-cell responses. *Oncoimmunology* 2: e26859.

34. Dharmadhikari, B., M. Wu, N. S. Abdullah, S. Rajendran, N. D. Ishak, E. Nickles, Z. Harfuddin, and H. Schwarz. 2015. CD137 and CD137L signals are main drivers of type 1, cell-mediated immune responses. *Oncoimmunology* 5: e1113367–e1113367.

35. Hintzen, R. Q., S. M. Lens, K. Lammers, H. Kuiper, M. P. Beckmann, and R. A. van Lier. 1995. Engagement of CD27 with its ligand CD70 provides a second signal for T cell activation. *J. Immunol.* 154.

36. Manetti, R., P. Parronchi, M. G. Giudizi, M.-P. Piccinni, E. Maggi, G. Trinchieri, and S. P. Omagnani. 1993. *Natural Killer Cell Stimulatory Factor (Interleukin 12 [11,12]) Induces T Helper Type 1 (Thl)-specific Immune Responses and Inhibits the Development of ID4-producing Th Cells,*. The Rockefeller University Press.

37. Reis e Sousa, C., S. Hieny, T. Scharton-Kersten, D. Jankovic, H. Charest, R. N. Germain, and A. Sher. 1997. In vivo microbial stimulation induces rapid CD40 ligand-independent production of interleukin 12 by dendritic cells and their redistribution to T cell areas. *J. Exp. Med.* 186: 1819–29.

38. Bromley, S. K., S. Y. Thomas, and A. D. Luster. 2005. Chemokine receptor CCR7 guides T cell exit from peripheral tissues and entry into afferent lymphatics. *Nat. Immunol.* 6: 895–901.

39. Braun, A., T. Worbs, G. L. Moschovakis, S. Halle, K. Hoffmann, J. Bölter, A. Münk, and R. Förster. 2011. Afferent lymph-derived T cells and DCs use different chemokine receptor CCR7-dependent routes for entry into the lymph node and intranodal migration. *Nat. Immunol.* 12: 879–887.

40. Von Andrian, U. H., and T. R. Mempel. 2003. Homing and cellular traffic in lymph nodes. *Nat. Rev. Immunol.* 3: 867–878.

41. Groom, J. R., and A. D. Luster. 2011. CXCR3 in T cell function. *Exp. Cell Res.* 317: 620–631.

42. Van Coillie, S., B. Wiernicki, and J. Xu. 2020. Molecular and Cellular Functions of CTLA-4. In *Regulation of Cancer Immune Checkpoints: Molecular and Cellular Mechanisms and Therapy* J. Xu, ed. Springer Singapore, Singapore. 7–32.

43. Ahmadzadeh, M., L. A. Johnson, B. Heemskerk, J. R. Wunderlich, M. E. Dudley, D. E. White, and S. A. Rosenberg. 2009. Tumor antigen-specific CD8 T cells infiltrating the tumor express high levels of PD-1 and are functionally impaired. *Blood* 114: 1537–1544.

44. Han, Y., D. Liu, and L. Li. 2020. PD-1/PD-L1 pathway: current researches in cancer. *Am. J. Cancer Res.* 10: 727–742.

45. Ishida, Y., Y. Agata, K. Shibahara, and T. Honjo. 1992. Induced expression of PD-1, a novel member of the immunoglobulin gene superfamily, upon programmed cell death. *EMBO J.* 11: 3887–3895.

46. Sharpe, A. H., E. J. Wherry, R. Ahmed, and G. J. Freeman. 2007. The function of programmed cell death 1 and its ligands in regulating autoimmunity and infection. *Nat. Immunol.* 8: 239–245.

47. Shevyrev, D., and V. Tereshchenko. 2020. Treg Heterogeneity, Function, and Homeostasis. *Front. Immunol.* 10: 3100.

48. Hoogeboom, R., and P. Tolar. 2016. Molecular Mechanisms of B Cell Antigen Gathering and Endocytosis. In *B Cell Receptor Signaling* T. Kurosaki, and J. Wienands, eds. Springer International Publishing, Cham. 45–63.

49. Song, W., and J. Craft. 2019. T follicular helper cell heterogeneity: Time, space, and function. *Immunol. Rev.* 288: 85–96.

50. Methot, S. P., and J. M. Di Noia. 2017. Molecular Mechanisms of Somatic Hypermutation and Class Switch Recombination. In *Advances in Immunology* vol. 133. Academic Press Inc. 37–87.

51. Lau, A. W., and R. Brink. 2020. Selection in the germinal center. *Curr. Opin. Immunol.* 63: 29–34.

52. Mesin, L., J. Ersching, and G. D. Victora. 2016. Germinal Center B Cell Dynamics. *Immunity* 45: 471–482.

53. Lu, L. L., T. J. Suscovich, S. M. Fortune, and G. Alter. 2018. Beyond binding: Antibody effector functions in infectious diseases. *Nat. Rev. Immunol.* 18: 46–61.

54. Lu, C., J. D. Klement, M. L. Ibrahim, W. Xiao, P. S. Redd, A. Nayak-Kapoor, G. Zhou, and K. Liu. 2019. Type i interferon suppresses tumor growth through activating the STAT3-granzyme B pathway in tumor-infiltrating cytotoxic T lymphocytes. *J. Immunother. Cancer* 7: 157.

55. Spaapen, R. M., M. Y. K. Leung, M. B. Fuertes, J. P. Kline, L. Zhang, Y. Zheng, Y.-X. Fu, X. Luo, K. S. Cohen, and T. F. Gajewski. 2014. Therapeutic Activity of High-Dose Intratumoral IFN-β Requires Direct Effect on the Tumor Vasculature. *J. Immunol.* 193: 4254–4260.

56. Gutterman, J. U. 1994. Cytokine therapeutics: lessons from interferon alpha. *Proc. Natl. Acad. Sci.* 91: 1198–1205.

57. Vedantham, S., H. Gamliel, and H. M. Golomb. 1992. Mechanism of Interferon Action in Hairy Cell Leukemia: A Model of Effective Cancer Biotherapy. *Cancer Res.* 52: 1056–66.

58. Randall, R. E., and S. Goodbourn. 2008. Interferons and viruses: An interplay between induction, signalling, antiviral responses and virus countermeasures. *J. Gen. Virol.* 89: 1–47.

59. Budhwani, M., R. Mazzieri, and R. Dolcetti. 2018. Plasticity of type I interferon-mediated responses in cancer therapy: From anti-tumor immunity to resistance. *Front. Oncol.* 8: 322.

60. Petersen, J. L., C. R. Morris, and J. C. Solheim. 2003. Virus Evasion of MHC Class I Molecule Presentation. *J. Immunol.* 171: 4473 LP – 4478.

61. Koutsakos, M., H. E. G. McWilliam, T. E. Aktepe, S. Fritzlar, P. T. Illing, N. A. Mifsud, A. W. Purcell, S. Rockman, P. C. Reading, J. P. Vivian, J. Rossjohn, A. G. Brooks, J. M. Mackenzie, J. D. Mintern, J. A. Villadangos, T. H. O. Nguyen, and K. Kedzierska. 2019. Downregulation of MHC class I expression by influenza A and B viruses. *Front. Immunol.* 10.

62. Cornel, A. M., I. L. Mimpen, and S. Nierkens. 2020. MHC class I downregulation in cancer: Underlying mechanisms and potential targets for cancer immunotherapy. *Cancers (Basel).* 12: 1–33.

63. Schönrich, G., and M. J. Raftery. 2019. The PD-1/PD-L1 axis and virus infections: A delicate balance. *Front. Cell. Infect. Microbiol.* 9: 207.

64. Dong, H., S. E. Strome, D. R. Salomao, H. Tamura, F. Hirano, D. B. Flies, P. C. Roche, J. Lu, G. Zhu, K. Tamada, V. A. Lennon, E. Celis, and L. Chen. 2002. Tumor-associated B7-H1 promotes T-cell apoptosis: A potential mechanism of immune evasion. *Nat. Med.* 8: 793–800.

65. Arneth, B. 2020. Tumor microenvironment. *Med.* 56.

66. Kruger, S., M. Ilmer, S. Kobold, B. L. Cadilha, S. Endres, S. Ormanns, G. Schuebbe, B. W. Renz, J. G. D'Haese, H. Schloesser, V. Heinemann, M. Subklewe, S. Boeck, J. Werner, and M. Von Bergwelt-Baildon. 2019. Advances in cancer immunotherapy 2019 - Latest trends. *J. Exp. Clin. Cancer Res.* 38: 268.

67. Sahin, U., P. Oehm, E. Derhovanessian, R. A. Jabulowsky, M. Vormehr, M. Gold, D. Maurus, D. Schwarck-Kokarakis, A. N. Kuhn, T. Omokoko, L. M. Kranz, M. Diken, S. Kreiter, H. Haas, S. Attig, R. Rae, K. Cuk, A. Kemmer-Brück, A. Breitkreuz, C. Tolliver, J. Caspar, J. Quinkhardt, L. Hebich, M. Stein, A. Hohberger, I. Vogler, I. Liebig, S. Renken, J. Sikorski, M. Leierer, V. Müller, H. Mitzel-Rink, M. Miederer, C. Huber, S. Grabbe, J. Utikal, A. Pinter, R. Kaufmann, J. C. Hassel, C. Loquai, and Ö. Türeci. 2020. An RNA vaccine drives immunity in checkpoint-inhibitor-treated melanoma. *Nature* 585: 107–112.

68. Ott, P. A., Z. Hu, D. B. Keskin, S. A. Shukla, J. Sun, D. J. Bozym, W. Zhang, A. Luoma, A. Giobbie-Hurder, L. Peter, C. Chen, O. Olive, T. A. Carter, S. Li, D. J. Lieb, T. Eisenhaure, E. Gjini, J. Stevens, W. J. Lane, I. Javeri, K. Nellaiappan, A. M. Salazar, H. Daley, M. Seaman, E. I. Buchbinder, C. H. Yoon, M. Harden, N. Lennon, S. Gabriel, S. J. Rodig, D. H. Barouch, J. C. Aster, G. Getz, K. Wucherpfennig, D. Neuberg, J. Ritz, E. S. Lander, E. F. Fritsch, N. Hacohen, and C. J. Wu. 2017. An immunogenic personal neoantigen vaccine for patients with melanoma. *Nature* 547: 217–221.

69. Ramasamy, M. N., A. M. Minassian, K. J. Ewer, A. L. Flaxman, P. M. Folegatti, D. R. Owens, M. Voysey, P. K. Aley, B. Angus, G. Babbage, S. Belij-Rammerstorfer, L. Berry, S. Bibi, M. Bittaye, K. Cathie, H. Chappell, S. Charlton, P. Cicconi, E. A. Clutterbuck, R. Colin-Jones, C. Dold, K. R. W. Emary, S. Fedosyuk, M. Fuskova, D. Gbesemete, C. Green, B. Hallis, M. M. Hou, D. Jenkin, C. C. D. Joe, E. J. Kelly, S. Kerridge, A. M. Lawrie, A. Lelliott, M. N. Lwin, R. Makinson, N. G. Marchevsky, Y. Mujadidi, A. P. S. Munro, E. Plested, J. Rand, T. Rawlinson, S. Rhead, H. Robinson, A. J. Ritchie, A. L. Ross-Russell, S. Saich, N. Singh, C. C. Smith, M. D. Snape, R. Song, R. Tarrant, Y. Themistocleous, K. M. Thomas, T. L. Villafana, S. C. Warren, M. E. E. Watson, A. D. Douglas, A. V. S. Hill, T. Lambe, S. C. Gilbert, S. N. Faust, A. J. Pollard, J. Aboagye, K. Adams, A. Ali, E. R. Allen, J. L. Allison, F. Andritsou, R. Anslow, E. H. Arbe-Barnes, M. Baker, N. Baker, P. Baker, I. Baleanu, D. Barker, E. Barnes, J. R. Barrett, K. Barrett, L. Bates, A. Batten, K. Beadon, R. Beckley, D. Bellamy, A. Berg, L. Bermejo, E. Berrie, A. Beveridge, K. Bewley, E. M. Bijker, G. Birch, L. Blackwell, H. Bletchly, C. L. Blundell, S. R. Blundell, E. Bolam, E. Boland, D. Bormans, N. Borthwick, K. Boukas, T. Bower, F. Bowring, A. Boyd, T. Brenner, P. Brown, C. Brown-O'Sullivan, S. Bruce, E. Brunt, J. Burbage, J. Burgoyne, K. R. Buttigieg, N. Byard, I. Cabera Puig, S. Camara, M. Cao, F. Cappuccini, M. Carr, M. W. Carroll, P. Cashen, A. Cavey, J. Chadwick, R. Challis, D. Chapman, D. Charles, I. Chelysheva, J. S. Cho, L. Cifuentes, E. Clark, S. Collins, C. P. Conlon, N. S. Coombes, R. Cooper, C. Cooper, W. E. M. Crocker, S. Crosbie, D. Cullen, C. Cunningham, F. Cuthbertson, B. E. Datoo, L. Dando, M. S. Datoo, C. Datta, H. Davies, S. Davies, E. J. Davis, J. Davis, D. Dearlove, T. Demissie, S. Di Marco, C. Di Maso, D. DiTirro, C. Docksey, T. Dong, F. R. Donnellan, N. Douglas, C. Downing, J. Drake, R. Drake-Brockman, R. E. Drury, S. J. Dunachie, C. J. Edwards, N. J. Edwards, O. El Muhanna, S. C. Elias, R. S. Elliott, M. J. Elmore, M. R. English, S. Felle, S. Feng, C. Ferreira Da Silva, S. Field, R. Fisher, C. Fixmer, K. J. Ford, J. Fowler, E. Francis, J. Frater, J. Furze, P. Galian-Rubio, C. Galloway, H. Garlant, M. Gavrila, F. Gibbons, K. Gibbons, C. Gilbride, H. Gill, K. Godwin, K. Gordon-Quayle, G. Gorini, L. Goulston, C. Grabau, L. Gracie, N. Graham, N. Greenwood, O. Griffiths, G. Gupta, E. Hamilton, B. Hanumunthadu, S. A. Harris, T. Harris, D. Harrison, T. C. Hart, B. Hartnell, L. Haskell, S. Hawkins, J. A. Henry, M. Hermosin Herrera, D. Hill, J. Hill, G. Hodges, S. H. C. Hodgson, K. L. Horton, E. Howe, N. Howell,

J. Howes, B. Huang, J. Humphreys, H. E. Humphries, P. Iveson, F. Jackson, S. Jackson, S. Jauregui, H. Jeffers, B. Jones, C. E. Jones, E. Jones, K. Jones, A. Joshi, R. Kailath, J. Keen, D. M. Kelly, S. Kelly, D. Kelly, D. Kerr, L. Khan, B. Khozoee, A. Killen, J. Kinch, L. D. W. King, T. B. King, L. Kingham, P. Klenerman, J. C. Knight, D. Knott, S. Koleva, G. Lang, C. W. Larkworthy, J. P. J. Larwood, R. Law, A. Lee, K. Y. N. Lee, E. A. Lees, S. Leung, Y. Li, A. M. Lias, A. Linder, S. Lipworth, S. Liu, X. Liu, S. Lloyd, L. Loew, R. Lopez Ramon, M. Madhavan, D. O. Mainwaring, G. Mallett, K. Mansatta, S. Marinou, P. Marius, E. Marlow, P. Marriott, J. L. Marshall, J. Martin, S. Masters, J. McEwan, J. L. McGlashan, L. McInroy, N. McRobert, C. Megson, A. J. Mentzer, N. Mirtorabi, C. Mitton, M. Moore, M. Moran, E. Morey, R. Morgans, S. J. Morris, H. M. Morrison, G. Morshead, R. Morter, N. A. Moya, E. Mukhopadhyay, J. Muller, C. Munro, S. Murphy, P. Mweu, A. Noé, F. L. Nugent, K. O'Brien, D. O'Connor, B. Oguti, V. Olchawski, C. Oliveira, P. J. O'Reilly, P. Osborne, L. Owen, N. Owino, P. Papageorgiou, H. Parracho, K. Parsons, B. Patel, M. Patrick-Smith, Y. Peng, E. J. Penn, M. P. Peralta-Alvarez, J. Perring, C. Petropoulos, D. J. Phillips, D. Pipini, S. Pollard, I. Poulton, D. Pratt, L. Presland, P. C. Proud, S. Provstgaard-Morys, S. Pueschel, D. Pulido, R. Rabara, K. Radia, D. Rajapaska, F. Ramos Lopez, H. Ratcliffe, S. Rayhan, B. Rees, E. Reyes Pabon, H. Roberts, I. Robertson, S. Roche, C. S. Rollier, R. Romani, Z. Rose, I. Rudiansyah, S. Sabheha, S. Salvador, H. Sanders, K. Sanders, I. Satti, C. Sayce, A. B. Schmid, E. Schofield, G. Screaton, C. Sedik, S. Seddiqi, R. R. Segireddy, B. Selby, I. Shaik, H. R. Sharpe, R. Shaw, A. Shea, S. Silk, L. Silva-Reyes, D. T. Skelly, D. J. Smith, D. C. Smith, N. Smith, A. J. Spencer, L. Spoors, E. Stafford, I. Stamford, L. Stockdale, D. Stockley, L. V. Stockwell, M. Stokes, L. H. Strickland, A. Stuart, S. Sulaiman, E. Summerton, Z. Swash, A. Szigeti, A. Tahiri-Alaoui, R. Tanner, I. Taylor, K. Taylor, U. Taylor, R. te Water Naude, A. Themistocleous, M. Thomas, T. M. Thomas, A. Thompson, K. Thompson, V. Thornton-Jones, L. Tinh, A. Tomic, S. Tonks, J. Towner, N. Tran, J. A. Tree, A. Truby, C. Turner, R. Turner, M. Ulaszewska, R. Varughese, D. Verbart, M. K. Verheul, I. Vichos, L. Walker, M. E. Wand, B. Watkins, J. Welch, A. J. West, C. White, R. White, P. Williams, M. Woodyer, A. T. Worth, D. Wright, T. Wrin, X. L. Yao, D. A. Zbarcea, and D. Zizi. 2020. Safety and immunogenicity of ChAdOx1 nCoV-19 vaccine administered in a prime-boost regimen in young and old adults (COV002): a single-blind, randomised, controlled, phase 2/3 trial. *Lancet* 396: 1979–1993.

70. Iwasaki, A., and S. B. Omer. 2020. Why and How Vaccines Work. *Cell* 183: 290–295.
71. Castelli, M. S., P. McGonigle, and P. J. Hornby. 2019. The pharmacology and therapeutic applications of monoclonal antibodies. *Pharmacol. Res. Perspect.* 7: e00535.
72. Rohaan, M. W., J. H. van den Berg, P. Kvistborg, and J. B. A. G. Haanen. 2018. Adoptive transfer of tumor-infiltrating lymphocytes in melanoma: a viable treatment option. *J. Immunother. cancer* 6: 102.
73. Kurata, M., K. Yamamoto, B. S. Moriarity, M. Kitagawa, and D. A. Largaespada. 2018. CRISPR/Cas9 library screening for drug target discovery. *J. Hum. Genet.* 63: 179–186.
74. Koch, C. M., S. F. Chiu, M. Akbarpour, A. Bharat, K. M. Ridge, E. T. Bartom, and D. R. Winter. 2018. A beginner's guide to analysis of RNA sequencing data. *Am. J. Respir. Cell Mol. Biol.* 59: 145–157.
75. Das, J., P. Chen, D. Norris, R. Padmanabha, J. Lin, R. V. Moquin, Z. Shen, L. S. Cook, A. M. Doweyko, S. Pitt, S. Pang, D. R. Shen, Q. Fang, H. F. De Fex, K. W. McIntyre, D. J. Shuster, K. M. Gillooly, K. Behnia, G. L. Schieven, J. Wityak, and J. C. Barrish. 2006. 2-Aminothiazole as a novel kinase inhibitor template. Structure-activity relationship studies toward the discovery of N-(2-chloro-6-methylphenyl)-2-[[6- [4-(2-hydroxyethyl)-1-piperazinyl]-2-methyl-4-pyrimidinyl]amino]-1, 3-thiazole-5-carboxamide (Dasatinib, BMS-354825) as a potent pan-Src kinase inhibitor. *J. Med. Chem.* 49: 6819–6832.
76. Padmanabha, R., Y. Z. Shu, L. S. Cook, J. A. Veitch, M. Donovan, S. Lowe, S. Huang, D. Pirnik, and S. P. Manly. 1998. 1-Methoxy-agroclavine from Penicillium sp. WC75209, a novel inhibitor of the Lck tyrosine kinase. *Bioorganic Med. Chem. Lett.* 8: 569–574.
77. MacArron, R., M. N. Banks, D. Bojanic, D. J. Burns, D. A. Cirovic, T. Garyantes, D. V. S. Green, R. P. Hertzberg, W. P. Janzen, J. W. Paslay, U. Schopfer, and G. S. Sittampalam. 2011. Impact of high-throughput screening in biomedical research. *Nat. Rev. Drug Discov.* 10: 188–195.
78. Paul, P., T. Van Den Hoorn, M. L. M. Jongsma, M. J. Bakker, R. Hengeveld, L. Janssen, P. Cresswell, D. A. Egan, M. Van Ham, A. Ten Brinke, H. Ovaa, R. L. Beijersbergen, C. Kuijl, and J. Neefjes. 2011. A genome-wide multidimensional RNAi screen reveals pathways controlling MHC class II antigen presentation. *Cell* 145: 268–283.
79. Jongsma, M. L. M., A. A. de Waard, M. Raaben, T. Zhang, B. Cabukusta, R. Platzer, V. A. Blomen, A. Xagara, T. Verkerk, S. Bliss, X. Kong, C. Gerke, L. Janssen, E. Stickel, S. Holst, R. Plomp, A. Mulder, S. Ferrone, F. H. J. Claas, M. H. M. Heemskerk, M. Griffioen, A. Halenius, H. Overkleeft, J. B. Huppa, M. Wuhrer, T. R. Brummelkamp, J. Neefjes, and R. M. Spaapen. 2020. The SPPL3-Defined Glycosphingolipid Repertoire Orchestrates HLA Class I-Mediated Immune Responses. *Immunity* 54.

1

CHAPTER 2

Secretome Screening Reveals Fibroblast Growth Factors as Novel Inhibitors of Viral Replication

Saskia D. van Asten, Matthijs Raaben, Benjamin Nota, Robbert M. Spaapen

Abstract

Cellular antiviral programs can efficiently inhibit viral infection. These programs are often initiated through signaling cascades induced by secreted proteins, such as type I interferons, interleukin-6 (IL-6), or tumor necrosis factor alpha (TNF-α). In the present study, we generated an arrayed library of 756 human secreted proteins to perform a secretome screen focused on the discovery of novel modulators of viral entry and/ or replication. The individual secreted proteins were tested for the capacity to inhibit infection by two replication-competent recombinant vesicular stomatitis viruses (VSVs) with distinct glycoproteins utilizing different entry pathways. Fibroblast growth factor 16 (FGF16) was identified and confirmed as the most prominent novel inhibitor of both VSVs and therefore of viral replication, not entry. Importantly, an antiviral interferon signature was completely absent in FGF16-treated cells. Nevertheless, the antiviral effect of FGF16 is broad, as it was evident on multiple cell types and also on infection by coxsackievirus. In addition, other members of the FGF family also inhibited viral infection. Thus, our unbiased secretome screen revealed a novel protein family capable of inducing a cellular antiviral state. This previously unappreciated role of the FGF family may have implications for the development of new antivirals and the efficacy of oncolytic virus therapy.

Introduction

In order to infect their host, enveloped viruses bind to cell surface receptors and enter target cells by using virus-encoded glycoproteins that drive membrane fusion. After fusion of the virus envelope with the cell's plasma membrane or endosomal membrane, the viral genome is delivered into the cytoplasm, where it can be transcribed and replicated. Replication of some viruses, such as lentiviruses and influenza viruses, requires translocation of the viral genome to the nucleus.

Cells are equipped with sophisticated programs to combat virus infections. These programs include antiviral signaling cascades downstream of ligand-activated receptors. Several ligands secreted locally or systemically convey antiviral activity. For example, tumor necrosis factor alpha (TNF-α), interleukin-6 (IL-6), IL-34, and IL-1β inhibit hepatitis B virus infection, IL-6$^{-/-}$ macrophages have been shown to be more vulnerable to herpes simplex virus 1 (HSV-1) infection, and IL-27 decreases shedding of HSV-1 in vitro (1–4). Yet the best-studied and most potent secreted antiviral proteins are alpha interferon (IFN-α) and IFN-β, also known as type I interferons (IFNs). Type I IFNs activate STAT signaling through the IFN-α/β receptor (IFNAR), leading to transcription of hundreds of interferon-stimulated genes (ISGs) (5). Only a small subset of the ISGs (e.g., myxovirus resistance protein 1 [MxA; also called MX1] and RNase L [RNASEL]) are direct antiviral effectors. MxA is located in the endoplasmic reticulum, where it can bind viral components, which leads to their inactivation (6–9). RNASEL is activated by 2′,5′-oligoadenylate synthetase 1 (OAS1), which recognizes double-stranded RNA. After its activation, RNASEL degrades the viral RNA (10, 11). Furthermore, the physiological importance of type I IFNs is demonstrated by the fact that most viruses are capable of counteracting the IFN pathway. Viruses have evolved to inhibit the production of IFNs, block the signaling downstream of IFNAR, and/or affect the synthesis of IFN effector molecules (12). Although several cytokines have been described to induce antiviral signaling programs, potential antiviral properties of most secreted proteins have not yet been explored.

Secretome libraries have successfully been employed to establish roles of secreted proteins in various biological systems (13, 14). For instance, secretome screens led to the identification of IL-34 as a promoter of monocyte viability and of pigment epitheliumderived factor as an inducer of human embryonic stem cell proliferation (15, 16). In the present study, we generated and employed a library containing 756 secreted proteins to perform a secretome screen for modulators of viral entry and/or replication. We specifically used recombinant vesicular stomatitis viruses expressing the glycoprotein from Lassa virus (VSV-LASV) or Ebola virus (VSV-EBOV), since the glycoproteins of these viruses initiate distinct entry pathways (17–19). This allowed for straightforward discrimination between modulators at the level of viral entry versus viral replication. Using this approach, we identified fibroblast growth factor 16 (FGF16) as a novel inhibitor of viral replication. Its antiviral activity was recapitulated in multiple cell lines and was not limited to VSV pseudotypes, as it also decreased infection by coxsackievirus. Treatment

with FGF16 induced an FGF-like transcriptional response, and several other members of the FGF family inhibited viral replication, indicating that the induction of FGF signaling represents a novel way to combat certain virus infections.

Materials and Methods

Cells and viruses

The HEK293T (provided by J. Neefjes, NKI, Amsterdam, The Netherlands; HLA-A and -B typed as a control for authenticity), HAP1 (Horizon Genomics), HepG2 (ATCC), U2OS (ATCC), and 2A14 (provided by M. Griffioen, LUMC, Leiden, The Netherlands) (52) cell lines were cultured in IMDM (Lonza) supplemented with 10% fetal calf serum (FCS) and 1% penicillin-streptomycin at 37°C and 5% $CO2$. VSV-LASV, VSV-EBOV, VSV-GTOV, VSV-MACV, and VSV-JUNV expressing EGFP as well as GFPexpressing coxsackievirus B3 (CV-B3-GFP; strain Nancy) were propagated as described previously (17, 18, 35, 36). A replication-incompetent lentivirus pseudotyped with the VSV glycoprotein (VSV-G) and expressing GFP was produced using the puc2CL6IPwo plasmid (kindly provided by H. Hanenberg) in combination with packaging constructs (53).

Recombinant secreted proteins

Plasmids for the secreted protein library were obtained from Origene and GE Healthcare. HEK293T cells (40,000) were plated in wells containing 0.5 ml medium in 24-well plates and incubated overnight. Transfection mixes were prepared by mixing 50 ng plasmid DNA with 1.5 µg polyethylenimine (Polysciences) in 50 µl serum-free medium per transfection, followed by 30 min of incubation at room temperature. Fifty microliters of transfection mix was added per well. After 6 h of incubation, the medium was replaced by 1 ml fresh medium. After three more days, conditioned medium for each individual transfection was collected and cleared of cells by multiple rounds of centrifugation. Levels of IFN-γ and TNF-α were determined by enzyme-linked immunosorbent assay (ELISA) according to the manufacturer's protocol (Sanquin). Purified recombinant human proteins IFN-α, FGF1, FGF5, FGF8b, FGF9, FGF10, FGF16, FGF20, and FGF21 were all from PeproTech. Anti-IFN-α clone M710 was obtained from Thermo Scientific, and anti-IFN-β was produced in-house. JAK inhibitor I was obtained from Calbiochem.

Viral infection assay.

Target cells were plated in black flat clear-bottomed 96-well tissue culture plates (Greiner). HAP1 and U2OS cells were plated at 15,000 cells/well, and other cell lines were plated at 20,000 cells/well. The next day, conditioned medium or purified recombinant proteins (at the indicated concentrations) were added. The final dilution of conditioned medium in the screen was 11x, as this dilution resulted in the maximal difference between empty vector and control IFNB1 samples in optimization experiments. Individual screening plates contained two control wells with IFNB1-conditioned medium and four control

wells with empty vector-conditioned media covering the different backbones of the secreted protein-encoding plasmids. After overnight incubation, cells were infected using a concentration of virus that enabled significant detection of inhibition and induction of viral infection, using a microplate reader for readout (Fig. 2B). After 5 to 7 h, cells were fixed using 4% formaldehyde for 30 min. Plates were washed twice with phosphate-buffered saline (PBS). Total GFP fluorescence per well was measured with a Clariostar microplate reader (BMG Labtech).

Screen analysis

The quality of an assay to be used for screening can be assessed by the Z-factor (20). The Z-factor for the viral infection assay was calculated from the GFP fluorescence intensities of the negative (empty vector) and positive (IFNB1) controls by using the following formula: $Z' = 1 - \frac{3(\sigma_{empty\ vector} + \sigma_{IFNB1})}{(\mu_{empty\ vector} - \mu_{IFNB1})}$ in which σ equals the standard deviation and μ equals the mean. GFP fluorescence intensities in the secretome screens were normalized per plate by B-score normalization in Excel (Microsoft), as described by Malo et al. (21). This method normalizes for plate and row confounding effects by iterative subtraction of median row and column values (excluding those for IFNB1 controls) from each individual well value. After this median polishing step, the B-score for each well was determined by a plate normalization using the median absolute deviation, as follows: MAD = median{|polished_well_va - median(polished_wells_plate)|}. Each virus screen was performed in duplicate. The final B-score for a condition was the mean of the two values. The cutoff for hit selection was set at 3 times the standard deviation for all conditions, excluding IFNB1 controls.

Fluorescence microscopy and flow cytometry

Imaging of infected cells (i.e., GFP-positive cells) was performed after visualizing cellular nuclei by use of 4=,6-diamidino-2-phenylindole (DAPI; Invitrogen) and a fluorescence microscope (Zeiss, Oberkochen, Germany). For lentivirus infections, HAP1 cells were inoculated with virus for 24 h before the GFP-positive cells could be determined by flow cytometry using an LSR flow cytometer (BD Biosciences). Data were analyzed using FlowJo VX (Treestar).

RNA-seq

HAP1 cells were plated at a density of 0.5 million cells/well of a 6-well plate. The following day, cells were treated with either medium or 6 μg/ml purified recombinant FGF16 (n = 3; total of six samples). After 24 h of incubation, cells were harvested and lysed in TRIzol reagent (Invitrogen). RNA libraries were prepared for sequencing using the standard manufacturer's protocols and sequenced on a HiSeq 2000 platform (Illumina). The single-read sequences were mapped against the human genome (hg38) by use of Tophat software. Read counts were determined using HTseq-count (22). In edgeR, counts per million were calculated from the read counts, and lowly expressed genes, with 1

cpm or less in three or more samples, were discarded. A multidimensional scaling (MDS) plot was made to confirm whether a paired analysis was appropriate. In limma, VOOM normalization was applied, and a linear model was fitted using a paired design (54, 55). The false-discovery rate (FDR) was used to correct for multiple testing, and adjusted *P* values of <0.05 were considered significant. For the significantly upregulated genes, enrichment of known transcription factor binding motifs in the transcription start site region of -400 to +100 was identified using the findMotifs.pl script of Homer (v4.9.1) (56; http://homer.ucsd.edu/homer/).

Statistics

P values were determined by the indicated statistical tests, using R. The following symbols are used to indicate statistical significance in the figures: *, P < 0.05; **, P < 0.01; ***, P < 0.001; ****, P < 0.0001; and n.s., not significant. IC50 values were calculated using the online IC50 calculator tool of AAT Bioquest (https://www.aatbio.com/tools/ic50-calculator).

Accession number(s)

The RNA-Seq data have been deposited in the Sequence Read Archive under accession no. SRP151416.

Results

Generation of a secreted protein library

To identify new secreted proteins that affect viral infection, we generated a large secretome library. To this end, we acquired a cDNA collection representing 756 different transcripts derived from 679 genes. Ninety-six percent of the transcripts in this collection encode established secreted proteins, while the rest of the encoded proteins are predicted to be secreted. Our secretome library covers a broad spectrum of physiological functions (Fig. 1A; see also Appendices: The Secreted Protein Library) and includes cytokines and chemokines but also peptide hormones, extracellular matrix proteins, neuropeptides, and enzymes. Each of these categories consists of a mix of broadly studied secreted proteins and proteins with hitherto undiscovered functions. Our library enables the discovery of new functions for well-described proteins as well as identification of the functions of less-well-explored proteins. To produce protein from each transcript within this secretome library, each individual cDNA was transfected into HEK293T cells, and cell-free conditioned medium was collected and stored for use in a separate viral infection assay (Fig.1B). Quantification of secreted proteins in the conditioned medium showed average levels of IFN-γ above 30 ng/ml, while TNF-α levels reached up to 1.4 µg/ml (Fig. 1C). The production was performed in seven rounds, for which the efficiency was monitored by separate transfections of IFN-γ and TNF-α cDNAs. The amounts of released cytokines in the medium were consistently within the same range, indicating that the transfection

performance was robust over time (Fig. 1C). Next to the secretion of IFN-γ and TNF-α, we observed secretion of biologically active concentrations of nine other proteins (our unpublished observations), indicating that we generated a functional secretome library that can be used for high-throughput screening.

Secretome screening reveals FGF16 as a novel modulator of viral replication

We next studied the effects of secreted proteins on viral infection by using enhanced green fluorescent protein (EGFP)-expressing VSV-LASV and VSV-EBOV. These two viruses have different modes of viral entry due to their respective glycoproteins, while they share the same cytoplasmic replication mechanism. The level of viral infection on HAP1 cells was determined by the total EGFP fluorescence intensity as quantified using a sensitive microplate reader. Using infections with and without preincubation with IFNB1-conditioned medium, a known inhibitor of VSV replication, we set up a reproducible assay which allowed us to detect inhibition and potentially also enhancement of viral infection (Fig. 2A and B). Notably, the Z-factor of this assay was higher than 0.5 for both VSV-LASV and VSV-EBOV, indicating that the dynamic range was large enough for effective high-throughput arrayed screening (Fig. 2C) (20).

This assay was then used to identify novel secreted proteins with the capacity to modulate viral infection. The total arrayed library of 756 cell-free conditioned media was tested and was controlled by 56 empty vector-conditioned media and 28 IFNB1-containing media
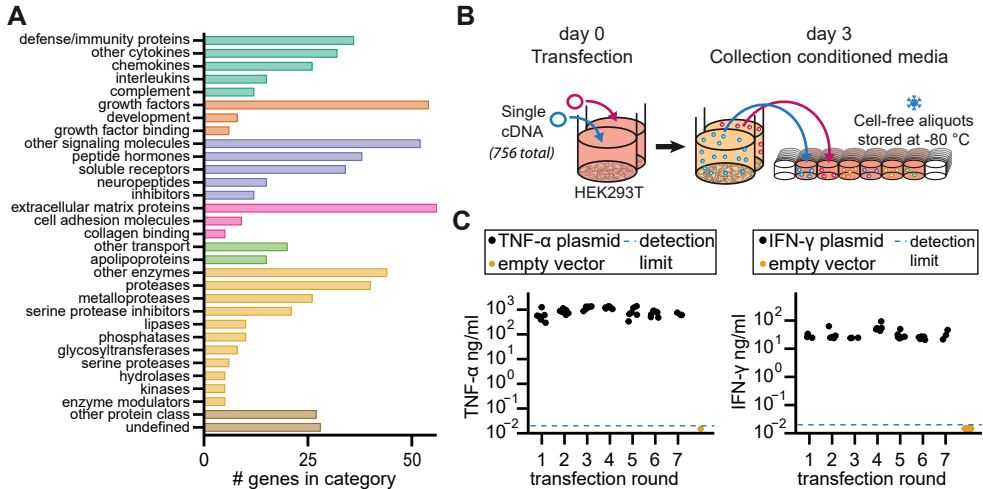
Figure 1. Generation of a secreted protein library covering broadly diverse physiological functions. (A) Our cDNA library consists of 679 genes encoding 756 transcripts. The 679 genes were categorized according to the Panther and Gene Ontology classification systems and additionally colored from top to bottom to belong to the supercategories immunology, development, signaling, extracellular matrix, transport, enzymes, and other/undefined (57–59). (B) Schematic overview of conditioned medium generation. HEK293T cells were plated, incubated overnight, and then transfected with single plasmid DNAs. The cell-free secreted protein-conditioned medium was collected at day 3. Aliquots were diluted 4x in medium and stored in ready-to-screen plates at -80°C. (C) Transfection consistency across different transfection rounds was determined by ELISA with control IFNγ and TNF-α-conditioned media. IFN-γ and TNF-α levels in empty vector-conditioned medium were below the detection limit of 20 pg/ml.
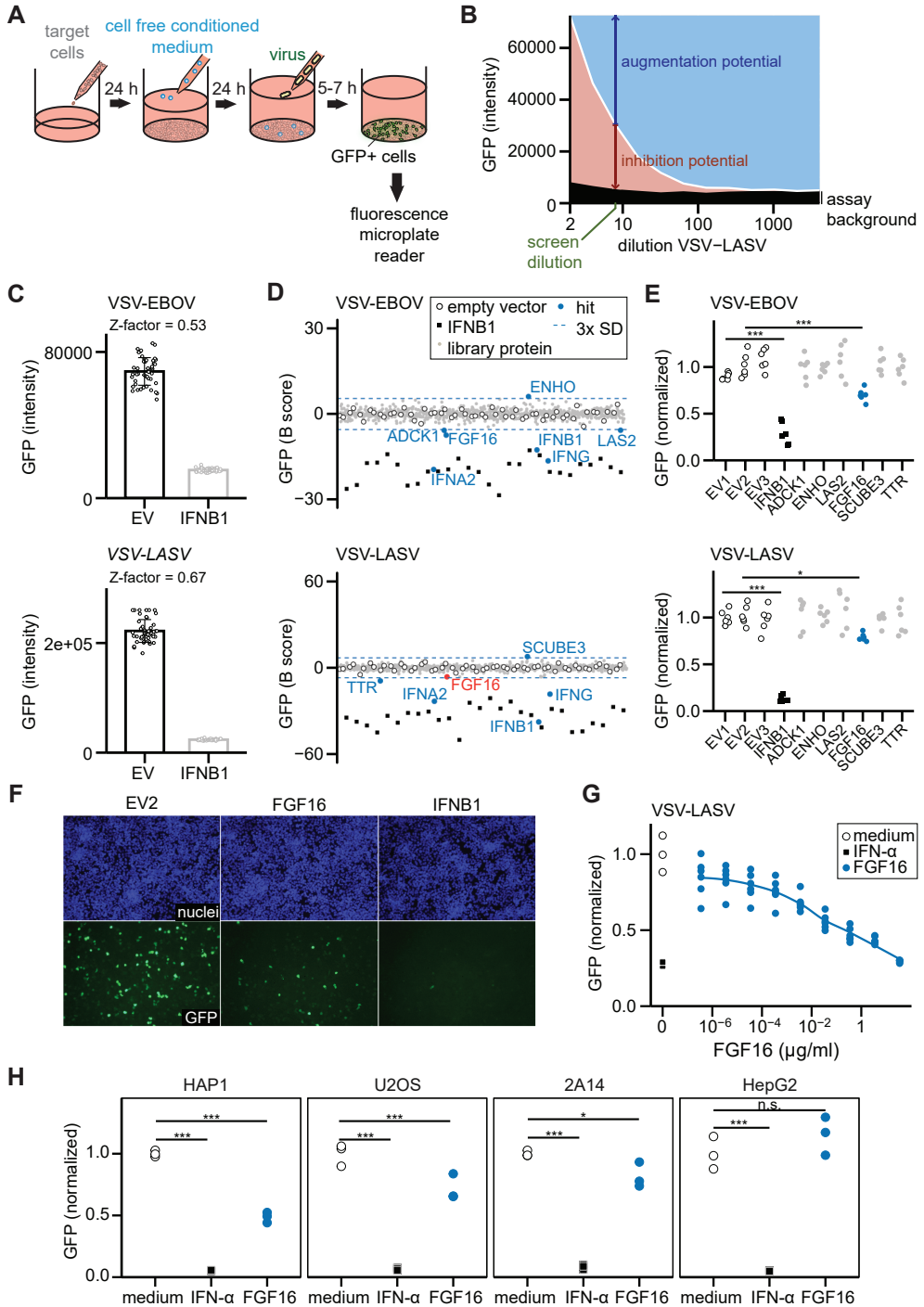
Figure 2. Secreted protein screening reveals FGF16 as an inhibitor of VSV-EBOV and VSV-LASV infection.
(A) Viral infection assay set-up. One day after HAP1 target cells were plated, they were exposed to different secreted proteins for another 24 h. Finally, cells were infected with VSV-EBOV or VSV-LASV for 5 or 6 h, respectively. GFP levels were detected using a fluorescence microplate reader. (B) HAP1 cells were pretreated

equally distributed over the library plates. The screens were performed independently with VSV-LASV and VSV-EBOV, both as biological duplicates. Data were normalized using the B-score, a method that is well suited for analysis of multiplate high-throughput screens (21). The majority of the conditioned medium treated wells had GFP levels similar to those of the empty vector controls for both viruses, whereas IFNB1-containing media showed clear inhibition (Fig. 2D). Importantly, this unbiased analysis highlighted known inhibitors of viral replication within our library (IFNA2, IFNB1, and IFNG) in both virus screens (Fig. 2D). The most significant novel infection inhibitors in either of the screens were ADCK1, FGF16, LAS2, and TTR, while SCUBE3 and ENHO2 seemed to enhance virus infectivity. Subsequently, we set out to validate these hits by using both VSV recombinants and found that only FGF16 reproducibly inhibited infection (Fig. 2E and F). Interestingly, FGF16 significantly inhibited both viruses, with the strongest inhibition against VSV-EBOV. Further analysis of the data from the VSV-LASV screen revealed that FGF16 was just below the stringent cutoff for hit selection (Fig. 2D), while nonvalidated hits were all within the single standard deviation (SD) range in the screen for the other VSV pseudotype. All these experiments were performed using FGF16-conditioned medium, in which the exact concentration of FGF16 was unknown. The FGF16-conditioned medium used for the screens may have contained a suboptimal concentration of FGF16. Consequently, we investigated the effect of commercially available purified recombinant FGF16 to determine its active concentration. More than 40% reductions in viral infection were detected at FGF16 concentrations of 35 ng/ml and higher, confirming the initial findings using conditioned medium (Fig. 2G). Moreover, at higher concentrations, FGF16 almost completely abolished infection, similar to recombinant IFN-α. To determine whether FGF16's inhibitory effect would apply broadly to cell types other than our model HAP1

Figure 2 Legend (continued)

with empty vector- or IFNB1-conditioned medium for 24 h. These cells were then infected with serial dilutions of VSV-LASV supernatant. IFNB1-treated cells nearly completely resisted infection. For the sake of simplicity, we therefore used the residual GFP signal in IFNB1-pretreated wells as the background of the assay. Medium treatment was plotted as a white line. We chose to use an 8x dilution of VSV-LASV in the screen because, at this dilution, the dynamic range to find potential inhibitors (blue arrow) or augmenters (red arrow) of viral infection seemed optimal. (C) HAP1cells were preincubated as described for panel A, followed by infection with either VSV-LASV or VSV-EBOV. Forty-eight wells were analyzed for each condition. The Z-factors for both assays were subsequently calculated. (D) The secretome screens were performed in this screen-compatible assay, including additional control empty vector- and IFNB1-conditioned media on each plate. Calculation of B-scores for the GFP levels is described in Materials and Methods. The averages for two replicates for each screen are depicted in readout order. Hits beyond three times the SD (dashed line) are shown in blue. FGF16 is colored red in the VSV-LASV screen because its value is below the threshold for hit selection here. (E) All hits were tested again, using new conditioned media. The statistical significance of the difference between each secreted protein and its corresponding empty vector (EV) was determined by analysis of variance (ANOVA) followed by Tukey's *post hoc* test. (F) Specified images of VSV-EBOV infections. Nuclei were stained with DAPI. (G) Target cells were treated with medium, 1 µg/ml IFN-α, or a serial dilution of commercially available purified recombinant FGF16, followed by infection with VSV-LASV. (H) HAP1, U2OS, 2A14, and HepG2 cells were pretreated with control medium, 1 µg/ml IFN-α, or 5 µg/ml FGF16 and infected with VSV-LASV. Statistically significant differences were identified by ANOVA followed by Tukey's *post hoc* test. For panels E, G, and H, GFP fluorescence intensities were normalized to the mean for all empty vector or medium controls. Data from a representative experiment of 2 (G) or 3 (H) experiments are shown. For panel H, background fluorescence intensities of noninfected cells were subtracted before normalization to improve the comparability between cell lines.
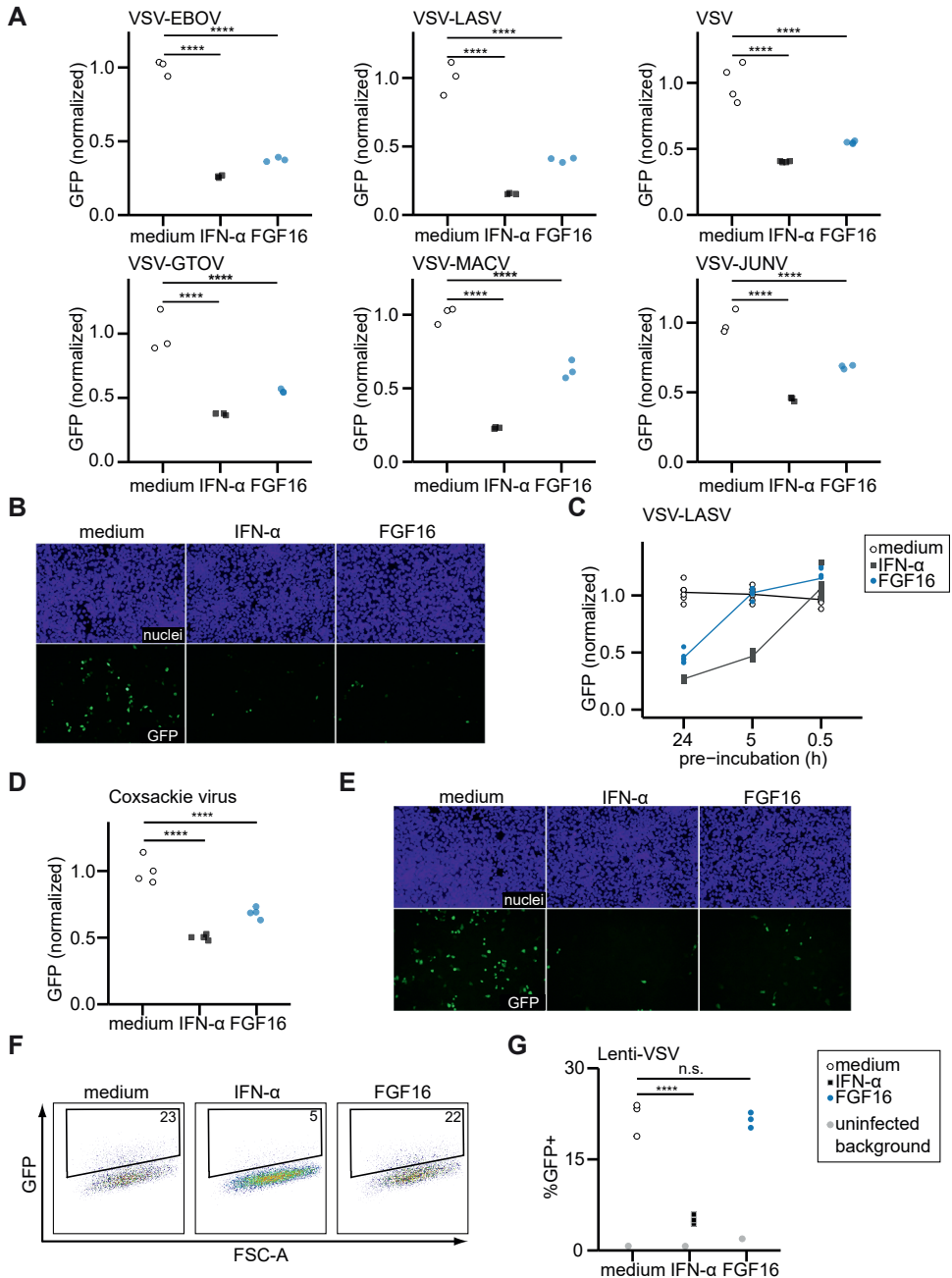
Figure 3. FGF16 inhibits replication of cytoplasmic viruses. (A) HAP1 cells were pretreated with medium, 1 µg/ml IFN-α, or 5 µg/ml FGF16, followed by infection with the indicated VSV pseudotypes. (B) Representative images of DAPI-stained cells after VSV infection. (C) HAP1 cells, pretreated for 24 h, 5 h, or 0.5 h, as indicated, were infected with VSV-LASV. (D) Infection of HAP1 cells with GFP-expressing coxsackie B3 virus for 5 h. (E) Representative images of coxsackie B3 virus-infected cells. (F) HAP1 cells were pretreated as described above, followed by infection with GFP-expressing Lenti-VSV for 24 h. Percentages of GFP+ cells were determined by flow cytometry. (G) Quantification of GFP cells. For panels A, C, and D, GFP intensities were normalized to the medium control. Statistical significance was determined by ANOVA followed by Tukey's post hoc test.

cell line, we additionally pretreated the osteosarcoma cell line U2OS, the uveal melanoma cell line 2A14, and the liver cancer cell line HepG2. FGF16 exhibited significant antiviral effects on U2OS and 2A14 cells but not on HepG2 cells, indicating that multiple—but not all—cell types can be protected against viral infection by FGF16 (Fig. 2H).

FGF16 inhibits replication of multiple cytosolic viruses

FGF16 apparently affected general VSV replication, since infection by both VSV-LASV and VSV-EBOV was inhibited. While the cell entry mechanisms of these viruses differ, their replication machineries are identical. To further confirm this notion, we analyzed the infectivity of VSV expressing its native glycoprotein or one of the glycoproteins of the New World arenaviruses Guanarito virus (VSV-GTOV), Machupo virus (VSV-MACV), and Junin virus (VSV-JUNV), which utilize yet another entry pathway. Indeed, next to inhibiting VSV-LASV and VSV-EBOV infection, FGF16 robustly inhibited infection by wild-type VSV and three other VSV pseudotypes (Fig. 3A and B). Furthermore, FGF16 did not seem to block a step in viral entry, as the antiviral activity of FGF16 was pronounced only after prolonged pretreatment (Fig. 3C). These data indicate that a downstream replication process, not viral entry, was inhibited by FGF16.

To gain more insight into the mechanism of the antiviral activity of FGF16, we tested whether the antiviral effect of FGF16 extended beyond the VSV replication machinery. Strikingly, coxsackievirus, a nonenveloped cytoplasmic RNA virus, was also inhibited by FGF16 treatment (Fig. 3D and E). Since both VSV and coxsackievirus replicate in the cytosol, we next wondered whether FGF16 targets only cytosolic viral replication. As a model virus for nuclear replication, we utilized a VSV-pseudotyped lentivirus (Lenti-VSV) which consequently has the same viral entry mechanism as wild-type VSV. Interestingly, Lenti-VSV infection was not inhibited by FGF16 (Fig. 3F and G), which further substantiated the notion that FGF16 does not inhibit viral entry. Taken together, these data suggest that FGF16 mainly affects cytosolic replication of multiple RNA viruses.

FGF signaling inhibits viral replication

We next hypothesized that the mechanism by which FGF16 inhibits viral replication may have similarities to that of type I IFN-mediated antiviral activity. To determine the expression signature of cells, we performed transcriptome sequencing (RNA-Seq) of FGF16-treated cells. Importantly, genes which have been shown to play a role in viral infection after type I IFN stimulation were not significantly upregulated after FGF16 stimulation, arguing for a distinct mechanism of action compared to that of type I IFN-mediated viral inhibition (Fig. 4A) (22). To confirm that FGF16's mechanism of action is indeed independent of the type I IFN pathway, we either neutralized type I IFNs by use of antibodies or inhibited IFNAR signaling by use of JAK inhibitor I (23, 24). As expected based on the transcriptome analysis, FGF16 inhibited viral infection regardless of type I IFN pathway interference, while the antiviral activity of IFN-α was significantly reduced (Fig.

2
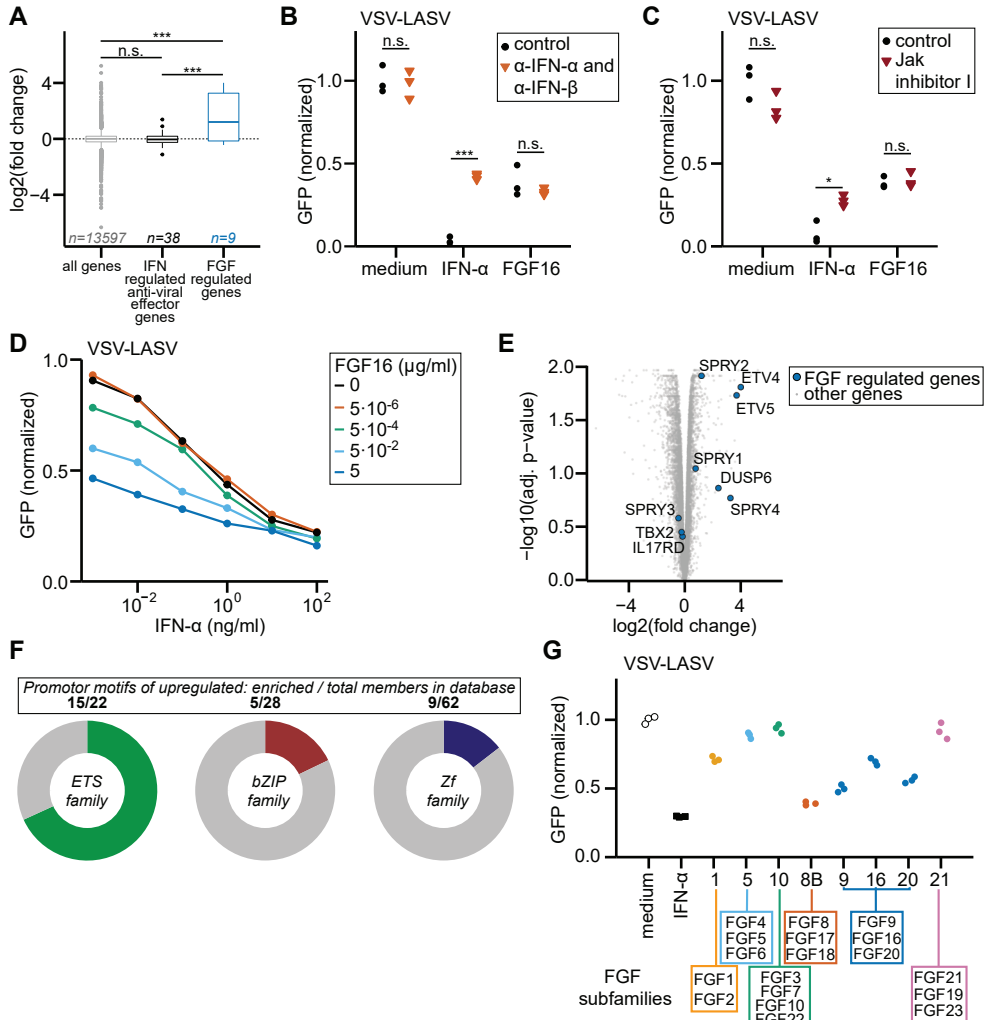
Figure 4. FGF signaling induces resistance to viral infection. (A) RNA-Seq was performed on three replicates of HAP1 cells that were treated with either medium or 6 µg/ml FGF16 for 24 h. Box plots show the log2-transformed ratios of gene expression of FGF16 over the medium control [$\log_2$(fold change)]. Data for genes that are induced by type I IFN or FGF signaling, according to the literature (22, 25, 26, 28–30, 60), were plotted in separate box plots. The data were analyzed by ANOVA followed by Tukey's *post hoc* test. (B and C) HAP1 cells were pretreated with 50 µg/ml anti-IFN-α and 50 µg/ml anti-IFN-β (B), 1 µM JAK inhibitor I (C), or medium (control) for 1 h before treatment with either medium, 5 µg/ml FGF16, or 1 µg/ml IFN-α for 24 h, followed by infection with VSV-LASV. The data were analyzed by two-way ANOVA followed by Tukey's *post hoc* test. (D) HAP1 cells were pretreated with the indicated concentrations of IFN-α together with FGF16 for 24 h before infection with VSV-LASV. (E) Volcano plot showing the expression change versus adjusted P value for each FGF signaling-induced gene (gray dots) as determined by the RNA-Seq analysis described for panel A. (F) The promoter region (-400 to +100) of the 949 significantly upregulated genes (P < 0.05) was further analyzed for enrichment of known transcription factor binding motifs by use of Homer (56). The 38 significant motifs (P < 0.05) are shown in Table S2 in the supplemental material. The pie charts depict, for each indicated family (top three families), the proportion of transcription factor motifs within the Homer database that were significantly enriched (colored) in the upregulated promoters. (G) HAP1 cells were pretreated with either medium, 1 µg/ml IFN-α, or 5 µg/ml of at least one FGF of each canonical and endocrine subfamily of FGFs. The corresponding subfamilies are depicted below each FGF (27). Data are shown for a representative experiment of two experiments. For panels B, C, D, and G, data were normalized to the medium control after subtraction of background fluorescence.

4B and C). Thus, the mechanism by which FGF16 inhibits viral infection is independent of type I IFN production or (IFN) signaling via JAK/STAT.

Since FGF16 and type I IFNs thus probably activate distinct antiviral pathways, their effects may be additive. To investigate this, we performed serial dilution of IFN-α in the presence of different concentrations of FGF16. FGF16 increased the inhibition of viral infection at suboptimal levels of IFN-α, arguing that FGF16 may act in conjunction with type I IFNs to inhibit viral replication (Fig. 4D). Note that the 50% inhibitory concentration (IC$_{50}$) for inhibition of VSV-LASV infection was 76.4 ng/ml (3.2 nM) for FGF16 and 0.15 ng/ml (6.7 pM) for IFN-α (calculated from the data in Fig. 2G and 4D, respectively).

We next analyzed the RNA-Seq data set for other obvious transcriptional signatures and found that —as could be expected after FGF16 stimulation— FGF receptor (FGFR)-regulated genes were significantly upregulated (Fig. 4A) (25, 26). These genes included those for the transcription factors ETV4 and ETV5, DUSP6, and SPRY family members, all of which are known targets of E26 transformation-specific (ETS) transcriptional activity downstream of FGFR signaling (Fig. 4E) (27). Moreover, in-depth analyses of all upregulated genes after FGF16 treatment showed that their promoter regions were significantly enriched for the ETS binding site motif (Fig. 4F; see Table S2 in the supplemental material) (28–31). Thus, the transcriptional profile of FGF16-treated cells suggests that inhibition of viral replication may be directed via signaling through FGFR. If general FGF signaling induces resistance to viral infection, then other FGFs may also cause this effect. To test this hypothesis, we pretreated cells with members of each of the five subfamilies of secreted FGFs, including FGF9 and FGF20 of the FGF16-containing subfamily. Subsequently, we inoculated these cells with virus and quantified the levels of infection. Similar to FGF16, both FGF9 and FGF20 strongly inhibited viral replication (Fig. 4G). Several other FGF subfamily members were also capable of inducing protection against viral infection, as illustrated by marked reductions of infection after preincubation with FGF1 and FGF8B (Fig. 4G). These results reinforce the notion that FGF signaling triggers an antiviral program.

Discussion

In the present study, we generated and employed a secreted protein library to discover novel cell-intrinsic pathways that can modulate viral infection. Using this unbiased and unique forward screening approach, we identified FGFs as a novel family of secreted proteins with antiviral properties. The major advantage of forward screening approaches is that hits have a causal relationship with the observed phenotype. In our screen, perturbations—consisting of hundreds of secreted proteins—were tested for their effect on the observed outcome—virus infection—leading to the discovery that FGFs can cause a cellular antiviral state. In the past, secretome screens have led to other fascinating discoveries, but to our knowledge, they have not been performed before to study viral infection (13–16).

FGFs are required for organ development and regeneration but are also involved

in metabolism (27). However, little is known about their role during viral infection. The human FGF family consists of 18 secreted and four intracellular FGFs, categorized into seven subfamilies (27). For each of the six secreted FGF subfamilies, we tested the antiviral capacity of a representative member and found that at least three subfamilies can induce an antiviral state in cells. The secreted subfamilies are known to signal via one or more of the four FGFRs, each also having several splice variants (32). The expression of FGFRs and downstream molecules differs between cell lines, which may have accounted for the difference in antiviral efficacy of FGF16 in the cell lines examined here. In addition, FGFR binding and downstream signaling may be enhanced by cofactors, such as heparin/heparan sulfate proteoglycans or the Klotho protein family, but these did not act synergistically with FGF16 (data not shown). We next analyzed the relationship between the antiviral activities of the FGF and type I IFN families. The transcriptional profile of FGF16-treated cells lacks upregulation of IFN antiviral effector molecules. Furthermore, neither neutralization of potentially produced type I IFNs nor inhibition of JAK/STAT signaling inhibited FGF16's antiviral capacity. These data indicate that the antiviral mechanism induced by FGF16 is distinct from that of IFNs. FGF signaling may therefore represent an innate strategy by which host cells can combat IFN-resistant viruses (12). It is still unclear which intracellular effector molecules exert the antiviral effect of FGF signaling, although the requirement for more than 5 h of preexposure to FGFs suggests that the antiviral effect induced by FGF16 covers a transcription activation program. A more detailed molecular investigation of the effectors targeting the viral replication cycle is required to further understand the FGF-induced antiviral pathway and to elucidate why infection by cytoplasmic but not nuclear RNA viruses is inhibited by FGF signaling.

Interestingly, HSV-1 specifically uses FGFRs for docking and entry (33), and blockade of FGFRs with the high-affinity ligand FGF2 can inhibit HSV-1 infection *in vitro* and *in vivo* (33, 34). Importantly, the antiviral effect of FGF16 is not through blockade of FGFRs, since FGFRs are not the entry receptors for the viruses that we tested (18, 35–37). Furthermore, a short preincubation with FGF16 before infection still allowed efficient viral infection, arguing for a mechanism that entails receptor-mediated signaling. Since the antiviral effect was established for several different viruses with diverse cell entry strategies, the mechanism is distinct from FGF-mediated inhibition of HSV-1 infection. In this study, the cytoplasmic viruses VSV and coxsackievirus, but not the nuclear virus Lenti-VSV, were inhibited by FGF16. Others have found that nuclear adenovirus type 2 is not inhibited by FGF2, supporting the notion that the antiviral activity of FGFs may be exerted in the cytoplasm (33). However, adenovirus type 2 is a DNA virus, as opposed to the RNA viruses studied here. It would be of considerable interest to investigate whether FGFs can also potentiate antiviral responses against DNA viruses, especially those with cytoplasmic replication, such as vaccinia virus (38).

Different members of the *Herpesviridae* as well as measles virus have been reported to induce expression of FGF2 (39). Transfection with a plasmid encoding the Epstein-Barr virus

latent membrane protein 1 leads to increased FGF2 expression (40). Higher levels of FGF2 have also been reported following herpes simplex virus 1 (HSV-1) infection in both mice and humans (41, 42). These data together suggest that FGFs may participate in the innate antiviral response. Although for many viral infections the induction of FGF expression has not been determined, it is clear that FGFs are expressed upon tissue damage to promote tissue regeneration. Our data suggest inhibition of viral replication as an added benefit of FGF expression. FGF signaling may therefore be harnessed to strengthen this effect. However, this requires further investigation of the pathways involved in this process in order to determine whether molecular determinants of FGF signaling may be a suitable therapeutic target.

Since the secretome library contains seven additional classical FGFs besides FGF16, we wondered why they were not identified as hits in the screens. Interestingly, these included five FGFs from the subfamilies that did not affect viral infection (FGF4, FGF7, FGF10, FGF21, and FGF23) (Fig. 4D), possibly explaining a lack of antiviral efficacy in the screen. Furthermore, subfamily members FGF1 and FGF2 in the library may not have been potent enough, since purified recombinant FGF1 only partially inhibited viral infection. Alternatively, it is possible that the FGFs in the library were not expressed at sufficient (bioactive) levels to inhibit viral replication, as the recombinant protein levels in the library conditioned media varied considerably (from nanograms per milliliter to micrograms per milliliter) (Fig. 1C and data not shown).

Recently, the excellent capacity of oncolytic viruses —such as VSV and coxsackievirus— to lyse cells and elicit a systemic immune response has been harnessed clinically for immunotherapy of cancer (43–45). However, intracellular antiviral signaling may inhibit successful infection of tumor cells by these viruses. Indeed, mice treated with IFN-α showed a weaker response to oncolytic alphavirus M1 treatment (46). These results may be extrapolated to FGFs, as the expression of various FGFs is upregulated in ovarian cancer, breast cancer, prostate cancer, and colon cancer (47–51). In tumor microenvironments with high FGF levels, replication of oncolytic VSV or coxsackievirus is possibly naturally inhibited. Such oncolytic virus therapy may benefit from additional inhibition of FGF signaling. Since in our experiments not all viruses are affected by FGFs, the use of FGF-resistant oncolytic viruses may be considered for cancers which highly express FGFs.

In conclusion, we identified FGFs as novel inhibitors of virus infection. This finding may have several implications: promoting FGF signaling may have potential for antiviral therapy, while inhibition of FGF signaling provides opportunities for the improvement of oncolytic viral therapy.

Acknowledgments

References

1. Isorce N, Testoni B, Locatelli M, Fresquet J, Rivoire M, Luangsay S, Zoulim F, Durantel D. 2016. Antiviral activity of various interferons and pro-inflammatory cytokines in non-transformed cultured hepatocytes infected with hepatitis B virus. Antiviral Res 130:36–45.

2. Cheng S-T, Tang H, Ren J-H, Chen X, Huang A-L, Chen J. 2017. Interleukin-34 inhibits hepatitis B virus replication in vitro and in vivo. PLoS One 12:e0179605.

3. Murphy EA, Davis JM, Brown AS, Carmichael MD, Ghaffar A, Mayer EP. 2008. Effect of IL-6 deficiency on susceptibility to HSV-1 respiratory infection and intrinsic macrophage antiviral resistance. J Interferon Cytokine Res 28:589–595.

4. Heikkilä O, Nygårdas M, Paavilainen H, Ryödi E, Hukkanen V. 2016. Interleukin-27 Inhibits Herpes Simplex Virus Type 1 Infection by Activating STAT1 and 3, Interleukin-6, and Chemokines IP-10 and MIG. J Interf Cytokine Res 36:617–629.

5. Rusinova I, Forster S, Yu S, Kannan A, Masse M, Cumming H, Chapman R, Hertzog PJ. 2013. Interferome v2.0: an updated database of annotated interferon-regulated genes. Nucleic Acids Res 41:D1040-1046.

6. Kochs G, Haller O. 1999. Interferon-induced human MxA GTPase blocks nuclear import of Thogoto virus nucleocapsids. Proc Natl Acad Sci U S A 96:2082–2086.

7. Accola MA, Huang B, Al Masri A, McNiven MA. 2002. The antiviral dynamin family member, MxA, tubulates lipids and localizes to the smooth endoplasmic reticulum. J Biol Chem 277:21829–21835.

8. Reichelt M, Stertz S, Krijnse-Locker J, Haller O, Kochs G. 2004. Missorting of LaCrosse virus nucleocapsid protein by the interferon-induced MxA GTPase involves smooth ER membranes. Traffic 5:772–784.

9. Kochs G, Janzen C, Hohenberg H, Haller O. 2002. Antivirally active MxA protein sequesters La Crosse virus nucleocapsid protein into perinuclear complexes. Proc Natl Acad Sci U S A 99:3153–3158.

10. Donovan J, Dufner M, Korennykh A. 2013. Structural basis for cytosolic double-stranded RNA surveillance by human oligoadenylate synthetase 1. Proc Natl Acad Sci U S A 110:1652–1657.

11. Dong B, Silverman RH. 1995. 2-5A-dependent RNase molecules dimerize during activation by 2-5A. J Biol Chem 270:4133–4137.

12. Randall RE, Goodbourn S. 2008. Interferons and viruses: An interplay between induction, signalling, antiviral responses and virus countermeasures. J Gen Virol 89:1–47.

13. Harbinski F, Craig VJ, Sanghavi S, Jeffery D, Liu L, Sheppard KA, Wagner S, Stamm C, Buness A, Chatenay-Rivauday C, Yao Y, He F, Lu CX, Guagnano V, Metz T, Finan PM, Hofmann F, Sellers WR, Porter JA, Myer VE, Graus-Porta D, Wilson CJ, Buckler A, Tiedt R. 2012. Rescue screens with secreted proteins reveal compensatory potential of receptor tyrosine kinases in driving cancer growth. Cancer Discov 2:948–959.

14. Liu T, Jia P, Ma H, Reed SA, Luo X, Larman HB, Schultz PG. 2017. Construction and Screening of a Lentiviral Secretome Library. Cell Chem Biol 24:767–771.e3.

15. Lin H, Lee E, Hestir K, Leo C, Huang M, Bosch E, Halenbeck R, Wu G, Zhou A, Behrens D, Hollenbaugh D, Linnemann T, Qin M, Wong J, Chu K, Doberstein SK, Williams LT. 2008. Discovery of a cytokine and its receptor by functional screening of the extracellular proteome. Science 320:807–811.

16. Gonzalez R, Jennings LL, Knuth M, Orth AP, Klock HE, Ou W, Feuerhelm J, Hull M V, Koesema E, Wang Y, Zhang J, Wu C, Cho CY, Su AI, Batalov S, Chen H, Johnson K, Laffitte B, Nguyen DG, Snyder EY, Schultz PG, Harris JL, Lesley S a. 2010. Screening the mammalian extracellular proteome for regulators of embryonic human stem cell pluripotency. Proc Natl Acad Sci U S A 107:3552–3557.

17. Takada A, Robison C, Goto H, Sanchez A, Murti KG, Whitt MA, Kawaoka Y. 1997. A system for functional analysis of Ebola virus glycoprotein. Proc Natl Acad Sci U S A 94:14764–14769.

18. Jae LT, Raaben M, Riemersma M, van Beusekom E, Blomen VA, Velds A, Kerkhoven RM, Carette JE, Topaloglu H, Meinecke P, Wessels MW, Lefeber DJ, Whelan SP, van Bokhoven H, Brummelkamp TR. 2013. Deciphering the glycosylome of dystroglycanopathies using haploid screens for lassa virus entry. Science 340:479–483.

19. Jae LT, Brummelkamp TR. 2015. Emerging intracellular receptors for hemorrhagic fever viruses. Trends Microbiol 23:392–400.

20. Jager M, Ksander BR, Zierhut M. 2002. Immunology of Ocular Tumors. Swetz & Zeitlinger Publishers: 119.

21. Staring J, von Castelmur E, Blomen VA, van den Hengel LG, Brockmann M, Baggen J, Thibaut HJ, Nieuwenhuis J, Janssen H, van Kuppeveld FJM, Perrakis A, Carette JE, Brummelkamp TR. 2017. PLA2G16 represents a switch between entry and clearance of Picornaviridae. Nature 541:412–416.

22. Raaben M, Jae LT, Herbert AS, Kuehne AI, Stubbs SH, Chou Y ying, Blomen VA, Kirchhausen T, Dye JM, Brummelkamp TR, Whelan SP. 2017. NRP2 and CD63 Are Host Factors for Lujo Virus Cell Entry. Cell Host Microbe 22:688–696.e5.

23. Nakano M, Kelly EJ, Wiek C, Hanenberg H, Rettie AE. 2012. CYP4V2 in Bietti's crystalline dystrophy: ocular localization, metabolism of ω-3-polyunsaturated fatty acids, and functional deficit of the p.H331P variant. Mol Pharmacol 82:679–686.

24. Zhang, Chung, Oldenburg. 1999. A Simple Statistical Parameter for Use in Evaluation and Validation of High Throughput Screening Assays. J Biomol Screen 4:67–73.

25. Malo N, Hanley JA, Cerquozzi S, Pelletier J, Nadon R. 2006. Statistical practice in high-throughput screening data analysis. Nat Biotechnol 24:167–75.

26. Smyth GK. 2004. Linear models and empirical bayes methods for assessing differential expression in microarray experiments. Stat Appl Genet Mol Biol 3:Article3.

27. Gentleman RC, Carey VJ, Bates DM, Bolstad B, Dettling M, Dudoit S, Ellis B, Gautier L, Ge Y, Gentry J, Hornik K, Hothorn T, Huber W, Iacus S, Irizarry R, Leisch F, Li C, Maechler M, Rossini AJ, Sawitzki G, Smith C, Smyth G, Tierney L, Yang JYH, Zhang J. 2004. Bioconductor: open software development for computational biology and bioinformatics. Genome Biol 5:R80.

28. Heinz S, Benner C, Spann N, Bertolino E, Lin YC, Laslo P, Cheng JX, Murre C, Singh H, Glass CK. 2010. Simple combinations of lineage-determining transcription factors prime cis-regulatory elements required for macrophage and B cell identities. Mol Cell 38:576–89.

29. Schoggins JW, Rice CM. 2011. Interferon-stimulated genes and their antiviral effector functions. Curr Opin Virol 1:519–525.

30. Darnell JE, Kerr IM, Stark GR. 1994. Jak-STAT pathways and transcriptional activation in response to IFNs and other extracellular signaling proteins. Science 264:1415–1421.

31. Müller M, Briscoe J, Laxton C, Guschin D, Ziemiecki A, Silvennoinen O, Harpur AG, Barbieri G, Witthuhn BA, Schindler C. 1993. The protein tyrosine kinase JAK1 complements defects in interferon-alpha/beta and -gamma signal transduction. Nature 366:129–135.

32. Yu T, Yaguchi Y, Echevarria D, Martinez S, Basson MA. 2011. Sprouty genes prevent excessive FGF signalling in multiple cell types throughout development of the cerebellum. Development 138:2957–2968.

33. Ekerot M, Stavridis MP, Delavaine L, Mitchell MP, Staples C, Owens DM, Keenan ID, Dickinson RJ, Storey KG, Keyse SM. 2008. Negative-feedback regulation of FGF signalling by DUSP6/MKP-3 is driven by ERK1/2 and mediated by Ets factor binding to a conserved site within the DUSP6/MKP-3 gene promoter. Biochem J 412:287–298.

34. Ornitz DM, Itoh N. 2015. The fibroblast growth factor signaling pathway. Wiley Interdiscip Rev Dev Biol 4:215–266.

35. Firnberg N, Neubüser A. 2002. FGF signaling regulates expression of Tbx2, Erm, Pea3, and Pax3 in the early nasal region. Dev Biol 247:237–250.

36. McCabe KL, McGuire C, Reh TA. 2006. Pea3 expression is regulated by FGF signaling in developing retina. Dev Dyn 235:327-335

37. Raible F, Brand M. 2001. Tight transcriptional control of the ETS domain factors Erm and Pea3 by Fgf signaling during early zebrafish development. Mech Dev 107:105–117.

38. Sharrocks AD, Brown AL, Ling Y, Yates PR. 1997. The ETS-domain transcription factor family. Int J Biochem Cell Biol 29:1371–1387.

39. Zhang X, Ibrahimi OA, Olsen SK, Umemori H, Mohammadi M, Ornitz DM. 2006. Receptor specificity of the fibroblast growth factor family. The complete mammalian FGF family. J Biol Chem 281:15694–15700.

40. Kaner RJ, Baird A, Mansukhani A, Basilico C, Summers BD, Florkiewicz RZ, Hajjar DP. 1990. Fibroblast growth factor receptor is a portal of cellular entry for herpes simplex virus type 1. Science 248:1410–1413.

41. Kim B, Lee S, Kaistha SD, Rouse BT. 2006. Application of FGF-2 to modulate herpetic stromal keratitis. Curr Eye Res 31:1021–1028.

42. Carette JE, Raaben M, Wong AC, Herbert AS, Obernosterer G, Mulherkar N, Kuehne AI, Kranzusch PJ, Griffin AM, Ruthel G, Dal Cin P, Dye JM, Whelan SP, Chandran K, Brummelkamp TR. 2011. Ebola virus entry requires the cholesterol transporter Niemann-Pick C1. Nature 477:340–343.

43. Schmid M, Speiseder T, Dobner T, Gonzalez RA. 2014. DNA virus replication compartments. J Virol 88:1404–1420.

44. Sundaram K, Senn J, Yuvaraj S, Rao DS, Reddy S V. 2009. FGF-2 stimulation of RANK ligand expression in Paget's disease of bone. Mol Endocrinol 23:1445–1454.

45. Wakisaka N, Murono S, Yoshizaki T, Furukawa M, Pagano JS. 2002. Epstein-barr virus latent membrane protein 1 induces and causes release of fibroblast growth factor-2. Cancer Res 62:6337–6344.

46. Jimenez-Sousa MA, Almansa R, De La Fuente C, Caro-Paton A, Ruiz L, Sanchez-Antolín G, Gonzalez JM, Aller R, Alcaide N, Largo P, Resino S, Ortiz De Lejarazu R, Bermejo-Martin JF. 2010. Increased Th1, Th17 and pro-fibrotic responses in hepatitis C-infected patients are down-regulated after 12 weeks of treatment with pegylated interferon plus ribavirin. Eur Cytokine Netw 21:84–91.

47. Gurung HR, Carr MM, Bryant K, Chucair-Elliott AJ, Carr DJ. 2018. Fibroblast growth factor-2 drives and

2

maintains progressive corneal neovascularization following HSV-1 infection. Mucosal Immunol 11:172–185.

48. Melzer MK, Lopez-Martinez A, Altomonte J. 2017. Oncolytic Vesicular Stomatitis Virus as a Viro-Immunotherapy: Defeating Cancer with a "Hammer" and "Anvil". Biomedicines 5.

49. Kim MK, Breitbach CJ, Moon A, Heo J, Lee YK, Cho M, Lee JW, Kim S-G, Kang DH, Bell JC, Park BH, Kirn DH, Hwang T-H. 2013. Oncolytic and immunotherapeutic vaccinia induces antibody-mediated complement-dependent cancer cell lysis in humans. Sci Transl Med 5:185ra63.

50. Breitbach CJ, Arulanandam R, De Silva N, Thorne SH, Patt R, Daneshmand M, Moon A, Ilkow C, Burke J, Hwang TH, Heo J, Cho M, Chen H, Angarita FA, Addison C, McCart JA, Bell JC, Kirn DH. 2013. Oncolytic vaccinia virus disrupts tumor-associated vasculature in humans. Cancer Res 73:1265–1275.

51. Ying L, Cheng H, Xiong XW, Yuan L, Peng ZH, Wen ZW, Ka LJ, Xiao X, Jing C, Qian TY, Liang GZ, Mei YG, Bo ZW, Liang P. 2017. Interferon alpha antagonizes the anti-hepatoma activity of the oncolytic virus M1 by stimulating anti-viral immunity. Oncotarget 8:24694–24705.

52. Sun Y, Fan X, Zhang Q, Shi X, Xu G, Zou C. 2017. Cancer-associated fibroblasts secrete FGF-1 to promote ovarian proliferation, migration, and invasion through the activation of FGF-1/FGFR4 signaling. Tumour Biol 39:1010428317712592.

53. Barron GA, Goua M, Wahle KWJ, Bermano G. 2017. Circulating levels of angiogenesis-related growth factors in breast cancer: A study to profile proteins responsible for tubule formation. Oncol Rep 38:1886–1894.

54. Feng S, Wang J, Zhang Y, Creighton CJ, Ittmann M. 2015. FGF23 promotes prostate cancer progression. Oncotarget 6:17291–17301.

55. Feng S, Dakhova O, Creighton CJ, Ittmann M. 2013. Endocrine fibroblast growth factor FGF19 promotes prostate cancer progression. Cancer Res 73:2551–2562.

56. Leushacke M, Spörle R, Bernemann C, Brouwer-Lehmitz A, Fritzmann J, Theis M, Buchholz F, Herrmann BG, Morkel M. 2011. An RNA interference phenotypic screen identifies a role for FGF signals in colon cancer progression. PLoS One 6:e23381.

57. Gene Ontology Consortium. 2015. Gene Ontology Consortium: going forward. Nucleic Acids Res 43:D1049-1056.

58. Ashburner M, Ball CA, Blake JA, Botstein D, Butler H, Cherry JM, Davis AP, Dolinski K, Dwight SS, Eppig JT, Harris MA, Hill DP, Issel-Tarver L, Kasarskis A, Lewis S, Matese JC, Richardson JE, Ringwald M, Rubin GM, Sherlock G. 2000. Gene ontology: tool for the unification of biology. The Gene Ontology Consortium. Nat Genet 25:25–29.

59. Mi H, Huang X, Muruganujan A, Tang H, Mills C, Kang D, Thomas PD. 2017. PANTHER version 11: expanded annotation data from Gene Ontology and Reactome pathways, and data analysis tool enhancements. Nucleic Acids Res 45:D183–D189.

60. Sadler AJ, Williams BRG. 2008. Interferon-inducible antiviral effectors. Nat Rev Immunol 8:559–568.t

Supplementary data

Table S2. Enriched transcription factor binding motifs in all significantly upregulated genes by FGF16 as determined by Homer software.

Rank	Motif	Name	Family	P-value	% Target sequences with motif	% Background with motif
1		Sp5	Zf	10^{-8}	65.80%	56.57%
2		ETS1	ETS	10^{-7}	41.81%	33.29%
3		Sp1	Zf	10^{-7}	41.40%	32.96%
4		Fli1	ETS	10^{-6}	50.89%	42.45%
5		Elk4	ETS	10^{-6}	43.17%	35.01%
6		KLF3	Zf	10^{-6}	40.56%	32.53%
7		KLF5	Zf	10^{-5}	64.55%	57.30%
8		Etv2	ETS	10^{-5}	33.89%	27.17%
9		ERG	ETS	10^{-5}	47.24%	40.03%
10		Elk1	ETS	10^{-5}	41.19%	34.18%
11		Chop	bZIP	10^{-4}	4.59%	2.31%
12		ETS	ETS	10^{-4}	27.53%	22.12%
13		GABPA	ETS	10^{-4}	39.83%	33.87%
14		ETV1	ETS	10^{-3}	48.18%	42.14%
15		EWS:FLI1-fusion	ETS	10^{-3}	24.09%	19.51%
16		EWS:ERG-fusion	ETS	10^{-3}	15.33%	11.63%
17		CEBP:AP1	bZIP	10^{-3}	11.57%	8.43%
18		ELF1	ETS	10^{-3}	36.39%	31.39%
19		Atf4	bZIP	10^{-3}	5.42%	3.37%
20		KLF6	Zf	10^{-3}	55.16%	50.00%
21		YY1	Zf	10^{-3}	8.55%	5.96%
22		BORIS	Zf	10^{-3}	13.03%	9.85%
23		KLF14	Zf	10^{-2}	73.10%	68.52%
24		Klf4	Zf	10^{-2}	21.48%	17.76%
25		STAT6	Stat	10^{-2}	9.59%	7.13%
26		HRE	HSF	10^{-2}	4.28%	2.67%
27		E2F4	E2F	10^{-2}	36.08%	31.82%

(Continued on next page)

Table S2 (continued)

Rank	Motif	Name	Family	P-value	% Target sequences with motif	% Background with motif
28		E2F	E2F	10^{-2}	5.74%	3.89%
29		IRF1	IRF	10^{-2}	3.75%	2.30%
30		PU.1	ETS	10^{-2}	13.87%	11.04%
31		EHF	ETS	10^{-2}	35.14%	31.16%
32		Ets1-distal	ETS	10^{-2}	7.09%	5.12%
33		HRE	HSF	10^{-2}	4.48%	3.00%
34		PR	NR	10^{-2}	28.99%	25.48%
35		Fra1	bZIP	10^{-2}	7.40%	5.50%
36		Tbx5	T-box	10^{-2}	50.78%	46.86%
37		Atf1	bZIP	10^{-2}	18.25%	15.37%
38		ISRE	IRF	10^{-2}	2.09%	1.15%

2

CHAPTER 3

Soluble FAS ligand enhances suboptimal CD40L/IL-21-mediated human memory B cell differentiation into antibody-secreting cells

Saskia D. van Asten, Peter-Paul Unger*, Casper Marsman*, Sophie Bliss, Tineke Jorritsma, Nicole M. Thielens, S. Marieke van Ham, Robbert M. Spaapen

* These authors contributed equally

Abstract

Differentiation of antigen-specific B cells into class-switched, high affinity antibody-secreting cells provides protection against invading pathogens but is undesired when antibodies target self-tissues in autoimmunity, beneficial non-self blood transfusion products or therapeutic proteins. Essential T cell factors have been uncovered that regulate T cell-dependent B cell differentiation. We performed a screen using a secreted protein library to identify novel factors that promote this process and may be used to combat undesired antibody formation. We tested the differentiating capacity of 756 secreted proteins on human naive or memory B cell differentiation in a setting with suboptimal T cell help *in vitro* (suboptimal CD40L and IL-21). High-throughput flow cytometry screening and validation revealed that type I IFNs and soluble FAS ligand (sFASL) induce plasmablast differentiation in memory B cells. Furthermore, sFASL induces robust secretion of IgG1 and IgG4 antibodies, indicative of functional plasma cell differentiation. Our data suggest a mechanistic connection between elevated sFASL levels and the induction of autoreactive antibodies, providing a potential therapeutic target in autoimmunity. Indeed, the modulators identified in this secretome screen are associated with systemic lupus erythematosus and may also be relevant in other autoimmune diseases and allergy.

Introduction

The immune response against a wide variety of pathogens is critically dependent on antigen-specific, high affinity antibodies generated upon natural infection or through vaccination. In contrast, antibodies are detrimental when induced against self-antigens in autoimmune disorders or against allergens, therapeutic proteins, blood products or transplants. Protective and pathogenic antibodies are produced by antibody-secreting plasmablasts or plasma cells (ASCs) that originate from B cells. T cell help consisting of CD40L/CD40 costimulation and the secretion of specific cytokines is essential for the generation of long-lived plasma cells that produce high-affinity, class switched antibodies. Short-lived plasmablasts differentiated from B cells without T cell help mostly secrete low-affinity antibodies.

T cell-dependent B cells differentiate in secondary lymphoid organs after being activated by their cognate antigen (1). Upon activation they migrate to the border of the B and T cell zones where they present antigen-derived peptides to activated T helper cells. After receiving T cell help, B cells migrate back into the B cell follicles while undergoing class switching. They initiate so called germinal center (GC) reactions by alternating between stages of proliferation in GC dark zones (DZ) and reacquisition of antigen to receive additional help from GC-resident antigen-specific follicular T helper (T_{FH}) cells in GC light zones (LZ) (2, 3). Expression of the chemokine receptor CXCR4 allows migration into the DZ, whereas absence of CXCR4 favors LZ localization. During this cycling process, somatic hypermutation of the B cell receptor (BCR) occurs followed by affinity maturation, where B cells with the highest affinity BCRs for the antigen selectively proliferate. Ultimately, these B cells differentiate into memory B cells (CD38⁻CD27⁺) and later into ASCs consisting of plasmablasts (CD38⁺CD27⁺CD138⁻) and terminally differentiated plasma cells (CD38⁺CD27⁺CD138⁺) (1, 4–7). A subset of memory B cells expresses CXCR3 to migrate into inflamed tissue, while others remain in lymphoid organs or circulates in the peripheral blood (8). Upon reinfection and antigen recall, memory B cells may reengage in GC reactions (8, 9). Plasma cell migration to the bone marrow for long-term survival is directed by CXCR4 (10).

Essential for driving B cell differentiation are membrane-bound interactions between receptor-ligand pairs on B cells and T_{FH}, such as CD40/CD40L (11–13). Furthermore, it is clear that soluble factors like T_{FH} cytokines IL-21 and IL-4 are key T_{FH} cytokines for effective B cell differentiation and that IFN-γ promotes, among other things, migration to inflamed tissue (11, 14, 15). Yet, several other secreted proteins such as IL-10 and type I IFNs affect B cell differentiation in humans, indicating that the role of soluble factors to modulate this process is underexplored (16–18).

To study B cell differentiation *in vitro*, T cell help may be mimicked using a CD40L-expressing cell line and recombinant IL-21 and IL-4. This system is well-suited to study which additional signals modulate differentiation of naive or memory B cells into ASCs. Here, we used a previously generated secreted protein library to identify soluble B cell

differentiation modulators (19). We designed the library to contain immune-related and non-immune human proteins including cytokines, growth factors, peptide hormones and enzymes, because factors from non-hematopoietic cells may also modulate B cell differentiation. Using this diverse library, we identified few additional factors affecting naive B cell differentiation but several molecules with a strong impact on memory B cell differentiation. More specifically, type I IFNs, MAp19 (mannan-binding lectin-associated protein of 19 kDa, transcript variant of complement enzyme MASP-2)(20) and soluble FASL (sFASL) induced plasmablast differentiation in IgG+ memory B cells. Moreover, sFASL promoted the secretion of substantial amounts of IgG1 and IgG4, showing that FASL drives the formation of ASCs. The different modulators identified in our screens improve the understanding of B cell differentiation and may represent new targets for modulation of B cells and antibody production during disease.

Methods

Generation of CD40L expressing 3T3 cell line

NIH3T3 fibroblast cells (3T3) cells were cultured in IMDM medium (Lonza, Basel, Switzerland) supplemented with 10% FCS (Bodinco, Alkmaar, The Netherlands), 100 U/ml penicillin (Thermo Fisher Scientific, Waltham, Massachusetts), 100 μg/ml streptomycin (Thermo Fisher Scientific), 2mM L-glutamine (Thermo Fisher Scientific) and 50 μM β-mercaptoethanol (Sigma Aldrich, St. Louis, Missouri). The 3T3 cells were transfected with Fsp I linearized CD40L plasmid (a kind gift from G. Freeman (21, 22)) and Pvu I linearized pcDNA3-Neomycin plasmid) using Lipofectamine 2000 Reagent (Thermo Fisher Scientific) according to manufacturer's protocol. Three days after transfection, the 3T3 culture medium was supplemented with 500 μg/ml G418 (Thermo Fisher Scientific) to select successfully transfected cells. The 3T3 cells were FACS sorted four times for expression of CD40L using an anti-CD40L antibody (clone TRAP1, BD Biosciences, San Jose, California). This resulted in a stable CD40L-expressing cell line that was cultivated in G418 containing selection media to maintain expression. The same batch of 3T3 CD40L-expressing cells was used for all experiments.

Secreted protein library

The arrayed secreted protein library was generated previously (19). Additional conditioned media were generated using the exact same protocol. In brief, HEK293T cells were individually transfected with plasmids encoding for secreted proteins (OriGene Technologies, Rockville, Maryland and GE Health Care, Chicago, Illinois) using polyethylenimine (Polysciences, Warrington, Pennsylvania). Six hours after transfection, medium was replaced with fresh medium (IMDM supplemented with 10% FCS, 100 U/ml penicillin and 100 μg/ml streptomycin). Three days after transfection, conditioned media were collected and stored in ready-to-screen 96 well plates at -80°C.

Isolation of human B cells

Buffy coats were obtained from healthy volunteers upon written informed consent in conformity with the protocol of the local institutional review board, the Medical Ethics Committee of Sanquin Blood Supply (Amsterdam, The Netherlands). PBMCs were isolated by density gradient centrifugation using Lymphoprep (Axis-Shield PoC AS, Oslo, Norway). CD19$^+$ cells were isolated from PBMCs using CD19 Pan B Dynabeads and DETACHaBEAD (Thermo Fisher Scientific) according to manufacturer's protocol with purity >99% and cryopreserved.

In vitro differentiation culture of human naive and IgG memory B cells

One day ahead of B cell culture, CD40L$^+$ 3T3 cells were irradiated with 30 Gy and plated at a density of 10,000 cells/well in a 96 flat-bottom plate (Nunc, Roskilde, Denmark) in B cell culture medium, which is RPMI-1640 without phenol-red (Thermo Fisher Scientific) supplemented with 5% FCS, 100 U/ml penicillin, 100 µg/ml streptomycin, 2mM L-glutamine, 50 µM β-mercapthoethanol and 20 µg/ml human apotransferrin (Sigma Aldrich, St. Louis, Missouri; depleted for human IgG with protein G sepharose). The following day thawed human B cells were stained with CD19-BV510 (clone 5J25C1, BD Biosciences), CD27-PE-Cy7 (clone 0323, Thermo Fisher Scientific) and IgG-DyLight 650 (clone MH16-1, Sanquin Reagents, Amsterdam, The Netherlands; conjugated using DyLight 650 NHS Ester (Thermo Fisher Scientific) according to manufacturer's protocol). CD19$^+$CD27$^+$IgG$^+$ memory or CD19$^+$CD27$^-$IgG$^-$ naive B cells were isolated using an Aria II sorter (BD Biosciences). The sorted B cells were then added to the irradiated CD40L$^+$ 3T3 cells at a density of 500-25000 cells/well, in the presence of 5 or 50 ng/ml IL-21 (Thermo Fisher Scientific) as indicated. Conditioned medium from the secreted protein library was added at a 1:12 dilution. For the screens, four wells of empty vector and two wells of IL-21 conditioned media were added to each of the 14 plates. Purified recombinant IFN-α, soluble FAS ligand (both PeproTech, London, United Kingdom) and MAp19 were added at indicated concentrations (23). After 9-10 days, B cells were analyzed by flow cytometry. The culture supernatants were used for ELISA.

Flow cytometry

B cells were stained with LIVE/DEAD fixable near-IR dye (Thermo Fisher Scientific), and CD19-BV510, CD27-PE-Cy7, CD38-V450 (clone HB7, BD Biosciences), CD138-FITC (clone MI15, BD Biosciences), or CD95-PE-CF594 (BD Biosciences) for 30 minutes at 4 °C. After staining, cells were washed twice with and taken up in PBS containing 1% BSA and 0.01% azide to be measured on an LSRII (BD Biosciences). Data was analyzed using FlowJo software (BD Biosciences).

ELISA

Levels of total IgG1 and IgG4 in culture supernatants were determined by sandwich

ELISA. Maxisorp ELISA plates (Nunc) were coated overnight with anti-IgG1 or anti-IgG4 (2 µg/ml clones MH161-1, MH161-1, MH164-4 respectively, Sanquin Reagents) in PBS. Plates were washed five times with 0.02% Tween-20 (Avantor, Radnor Township, Pennsylvania) in PBS (Fresenius Kabi, Bad Homburg, Germany), and incubated with culture supernatants (diluted in high-performance ELISA buffer, Sanquin Reagents). Plates were again washed five times and incubated for one hour with horseradish peroxidase-conjugated mouse-anti-human-IgG (1 µg/ml, clone MH16-1, Sanquin Reagents). After a final five-times wash, the ELISA was developed with 100 µg/ml tetramethylbenzidine (Interchim, Montluçon, France) in 0.11 mol/L sodium acetate (pH 5.5) containing 0.003% (v/v) H_2O_2 (all from Merck, Darmstadt, Germany). The reaction was stopped with 2M H_2SO_4 (Merck). IgG concentrations were determined from the 450 nm minus background 540 nm absorption (Synergy2; BioTek, Winooski, Vermont) in comparison to a serial diluted serum pool standard in each plate.

Screen analysis

The Z-factor (Z') can be calculated to determine whether an assay is suitable for high-throughput screening (24). The Z' for multiple parameters was calculated from empirical data of 27 replicates of negative (empty vector conditioned medium) and positive control (IL-21 conditioned medium) B cell cultures as indicated using the following formula: $Z' = 1 - \frac{3(\sigma_{\text{empty vector}} + \sigma_{\text{IL-21}})}{(\mu_{\text{empty vector}} - \mu_{\text{IL-21}})}$ in which σ represents the measured standard deviation, and µ the measured mean. For each parameter, the screen data were normalized per plate by B-score normalization using R as described by Malo *et al.* (25). This method normalizes for column and row confounding effects by three iterative subtractions of median row and column values (excluding IL-21 controls) from each individual well value. After performing this median polish, the B-score for each well was determined by division of the median absolute deviation (MAD = median {|well – median(plate)|}). The screen was performed twice, using B cells from two different healthy donors. The final B-score per secreted protein per condition was the mean of these two screens. The cut-off for hit selection was set at 3 times standard deviation of all conditions, excluding IL-21 controls.

Proliferation assay

Sorted B cells were washed twice with 10 ml PBS and resuspended to a concentration of 2×10^7 cells/ml in PBS. Cells and 40 µM CellTrace Yellow (Thermo Fisher Scientific) were mixed at a 1:1 ratio and incubated 15 minutes at RT in the dark, vortexing the tube every 5 minutes to ensure uniform staining. Cells were washed twice using a 10 times volume of cold culture medium to end labeling. Thereafter, B cells were cultured according to the protocol described above. At day 4 and day 10 of culture B cells were mixed with at least 2000 Cyto-Cal counting beads (Thermo Fisher Scientific) or CountBright Absolute counting beads (Thermo Fisher Scientific) and prepared for flow cytometry analysis as described above. Absolute B cell counts were determined according to the formula:

$$\frac{\text{\# Live CD19}}{\text{\# beads measured}} \times \text{\# beads added}.$$

Transcription factor staining

Transcription factor detection assays were performed as previously described (26). In short, at day 4 of culture in the B cell differentiation assay, B cells were harvested and stained with LIVE/DEAD fixable near-IR dye (Thermo Fisher Scientific), and CD19-BV510 (BD Biosciences), CD27-BUV395 (BD Biosciences) and CD38-FITC (Beckman Coulter) in 0.1% BSA in PBS for 15 minutes on ice. Cells were washed with 0.1% BSA in PBS, followed by fixation in Foxp3 fixation buffer (FoxP3 Transcription Factor staining buffer set, eBioscience) for 30 minutes at 4 °C. Cells were washed with permeabilization buffer (FoxP3 Transcription Factor staining buffer set) and stained with PAX5-PE (Biolegend), BLIMP1-AF647 (R&D) antibodies in permeabilization buffer for 30 minutes at 4 °C. The stained cells were again washed with permeabilization buffer before measurement on the BD FACSymphony (BD Biosciences).

Statistics

Statistical analysis was performed using R and GraphPad prism 8.2.1 (GraphPad Software, San Diego, California). *P*-values were determined by indicated statistical tests and depicted using the following symbols: $p < 0.05$ = *, $p < 0.01$ = **, $p < 0.001$ = ***, n.s. = not significant.

Results

An in vitro assay allows for unbiased large-scale evaluation of factors required for B cell differentiation into plasmablasts

Because CD40 stimulation and IL-21 signaling seem to be minimal requirements to induce differentiation into antibody secreting cells (27), we set out to identify soluble factors that cooperate or act in synergy with these T_{FH} signals. To discover new soluble factors that coregulate human B cell differentiation into antibody-secreting cells, we set up *in vitro* B cell cultures suitable for arrayed secreted protein screening. IgG$^+$ memory B cells or naive B cells were cultured with irradiated CD40L-expressing cells in the presence of IL-21 (Fig. 1A). After nine days, the B cell differentiation state was analyzed by flow cytometry using antibodies against CD27, CD38, CD138 and surface-bound IgG (gating in Fig. S1A). The chemokine receptors CXCR3 and CXCR4 were included in the analysis as they are essential for LZ-DZ cycling and migration to inflamed tissue or bone marrow (Fig. S1A). The B cell differentiation factor IL-21 was titrated to minimize memory and naive B cell differentiation into CD27$^+$CD38$^+$ ASCs and IgG$^+$ B cells respectively, while still supporting B cell survival (Fig. 1B and C). Comparison of the effects of different B cell starting numbers on the efficacy of differentiation into IgG$^+$ B cells and CD27$^+$CD38$^+$ ASCs demonstrated similar trajectories of the IL-21 titration curves (Fig. 1B and C, right panels). Culture initiation with

500 memory B cells per well yielded too few cells for reliable endpoint measurements. Therefore, we chose to start the ensuing differentiation cultures with 1000 memory B cells per well in presence of 5 ng/ml IL-21. For naive B cells, culture initiation with 10,000 cells and 5 ng/ml of IL-21 provided sufficient survival signal for the nine-day culture period, while inducing only few cells to class switch to IgG (Fig. 1C).

The screen was executed using a library of arrayed conditioned media each enriched for a single soluble protein secreted by cDNA-transfected HEK293T cells (19). This library contains 756 secreted proteins with a broad variety of biological functions, such as neuropeptides, hormones, growth factors and cytokines. To determine the optimal dilution of the library to use in the B cell differentiation screen, we generated IL-21 and empty vector conditioned positive and negative control media respectively. Titrations of both
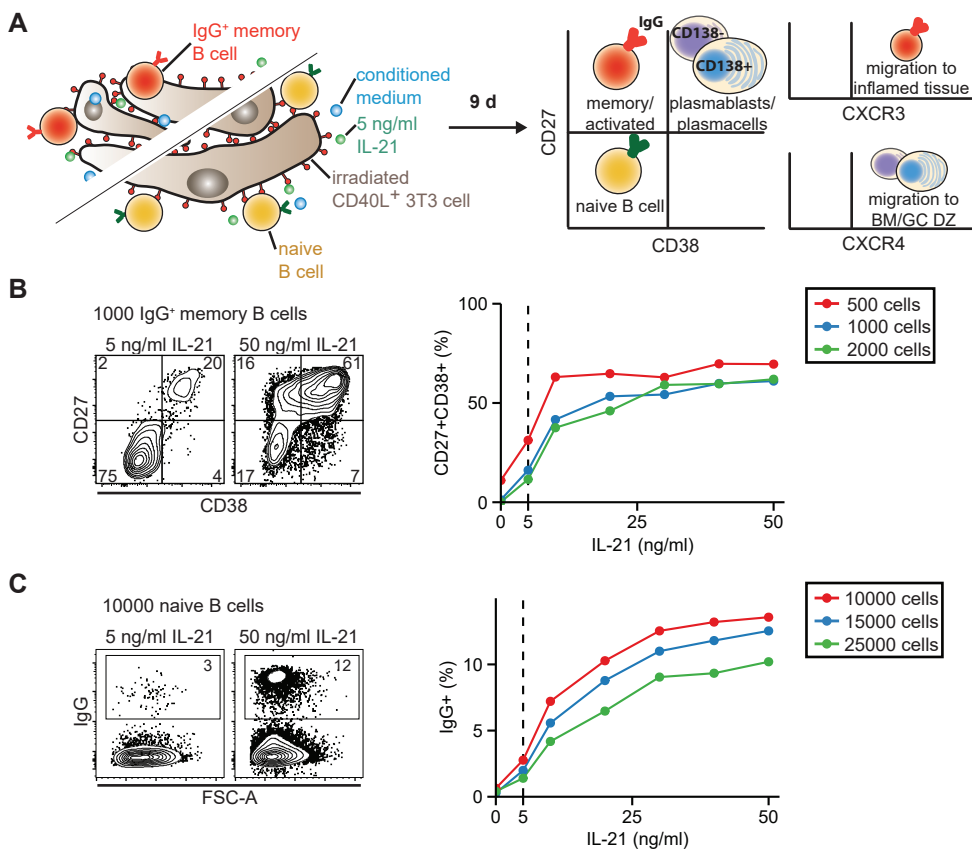
Figure 1. Setup of a suitable assay for arrayed secreted protein screening. (A) Schematic overview of the B cell differentiation assay used in Figures 2-5. Isolated CD27+IgG+ memory B cells or CD27-IgG- naive B cells were cultured for nine days in the presence of irradiated 3T3 cells, 5 ng/ml IL-21 (see B and C) and the individual conditioned media of the secreted protein library. B cells were analyzed by flow cytometry for expression of CD27, CD38, CD138, surface IgG (red), CXCR3 and CXCR4. (B and C) Determination of a suboptimal concentration of IL-21 to culture different indicated starting amounts of memory (B) or naive (C) B cells (n=1). Left panels contain example flow cytometry plots of CD27/CD38 (B) and IgG (C) at the indicated concentrations. Right panels show quantification of the percentage of positive cells in the depicted gates. Dashed line indicates 5 ng/ml IL-21. BM = bone marrow, GC DZ= germinal center dark zone.

control media showed that the IL-21 conditioned medium was more effective at inducing CD27$^+$CD38$^+$ ASC differentiation from IgG$^+$ memory B cells at lower concentrations, possibly because of supra-optimal IL-21 levels in the conditioned medium (Fig. S1B). While the IL-21 concentration in the supernatant was in the mg/ml range as determined by ELISA (data not shown), we previously found that several other conditioned media in the library contained lower (functional) levels of secreted protein (19). For naive B cells, the optimal IL-21 conditioned medium dilution to promote IgG class switching was 1:12 (Fig. S1C). For the library screen on naive and memory B cells, a 1:12 dilution was subsequently used, as it induced no measurable background signal with empty vector (EV) and was sufficient to distinguish IL-21 differentiation effects (Fig. S1B, C dashed line). Finally, we analyzed whether this optimized assay was applicable for screening by determining the dynamic range between 48 negative and positive controls. We found that for several parameters (including the CD27$^+$CD38$^+$ population and CXCR4 expression) Z' was higher than zero, indicating that the assay was suitable for large scale screening (Fig. S1D, E).

IFN-γ induces CXCR3 expression in naive and memory B cells

After setting up a suitable assay, the complete secreted protein library was screened for factors that alter chemokine receptor expression or induce differentiation of B cells. Data from two screens using two different healthy donors were averaged after per plate B-score normalization, which accounts for row and column effects within a single plate as well as variation between plates. Most conditioned media resulted in similar phenotypes compared to empty conditioned media with a B score close to zero (Fig. 2). Positive control IL-21 conditioned medium significantly altered surface CXCR3 and CXCR4 expression in memory B cells and CXCR4 in naive B cells, showing that the library IL-21 conditioned medium was biologically active (Fig. 2A, E, G). The threshold for hit selection was set at three times standard deviation of all conditioned media except the IL-21 positive control (Fig. 2). IFN-γ conditioned medium was the strongest CXCR3 inducer in both memory and naive B cell screens (Fig. 2A-D), in line with previous reports (14). In memory B cells, CXCR3 expression was also upregulated by IFN-β1, but not by IFN-α2 (Fig. 2A). Both type I IFNs failed to induce CXCR3 expression in naive B cells (Fig. 2C). In addition, sFASL, FGF5, RLN2, IL15RA and MMP24 conditioned media led to slightly increased CXCR3 levels in memory B cells. None of the conditioned media clearly reduced CXCR4 expression in memory B cells compared to EV (Fig. 2E), yet naive B cells exposed to IFNs, C8B, NRG1, EBI3 and SERPINF1 had lower CXCR4 levels compared to EV (Fig. 2G). HPR, CLC and IL-2 led to marginally enhanced CXCR4 upregulation in memory B cells, and sFASL in both memory and naive B cells (Fig. 2E-H).

Type I IFNs induce plasmablast differentiation

We next analyzed the capacity of individual secreted proteins to differentiate B cells into CD27$^+$CD38$^+$ ASCs. Control conditioned medium containing biologically active IL-21 (see

Fig. 2) did not greatly induce CD27⁺CD38⁺ ASCs, possibly because of supra-optimal IL-21 levels similar as found during the screen set up (Fig. S1B). Type I IFNs, MAp19 and sFASL all induced memory B cell differentiation into CD27⁺CD38⁺ ASCs, with IFN-α2 and IFN-β1 being the strongest hits (Fig. 3A-C). In addition, naive B cells cultured with type I IFNs differentiated into CD27⁻CD38⁺ B cells (35%), while hardly any CD27⁺ B cells were formed (Fig. 3D-G). The naive B cell differentiation into CD27⁺ B cells was stimulated by IL-2, HPR, CLC, ADAMTS10 and FGF5 conditioned media, but these conditioned media largely failed to drive CD38⁺ plasmablast differentiation.

Since type I IFNs were the most potent inducers of B cell differentiation in our screens,
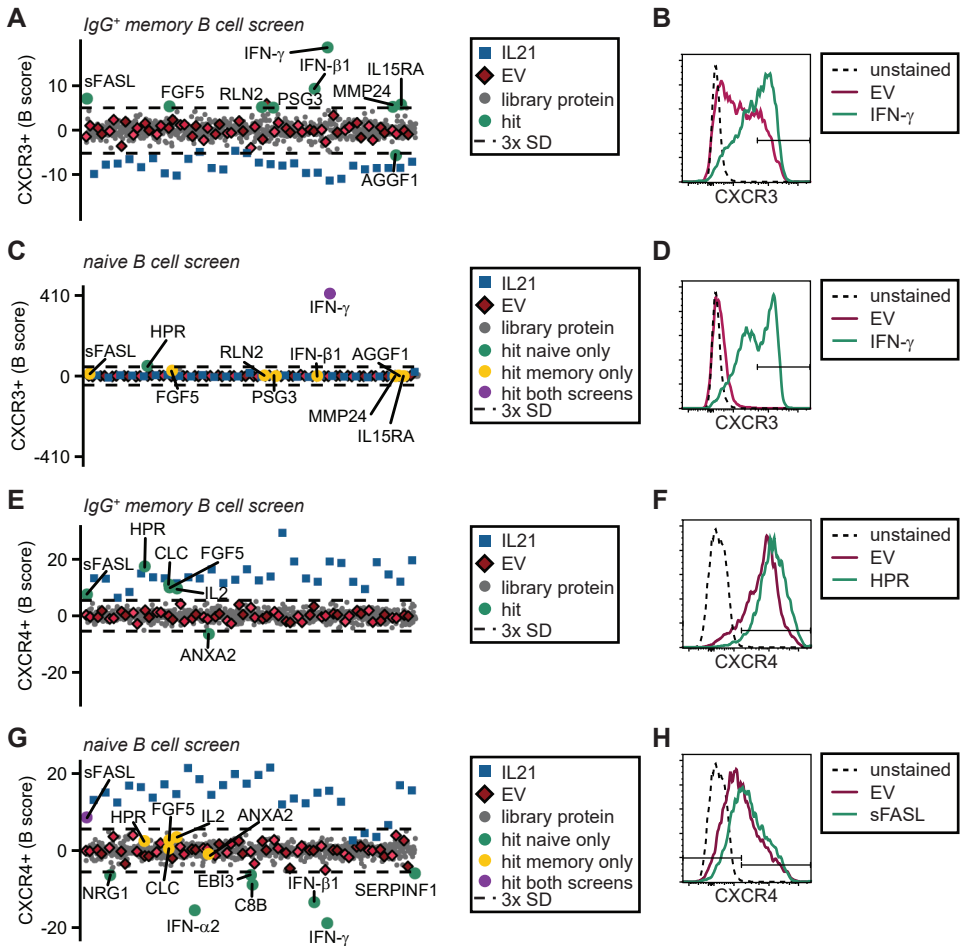
Figure 2. The secreted protein screen identifies several proteins to affect the chemokine receptors CXCR3 and CXCR4. The entire secreted protein library was screened on B cells of two healthy donors. (A-D) Data of CXCR3 expression on IgG⁺ memory (A and B) and naive B cells (C and D). (E-H) Data of CXCR4 expression on IgG⁺ memory (E and F) and naive B cells (G and H). (A, C, E and G) Pooled B score normalized percentages of each phenotype were averaged. For each readout the threshold for hit selection was set at three times SD (dashed line). Controls, hits and other secreted proteins are annotated in the legend boxes. EV is empty vector. (B, D, F and H) Example histograms of the secreted proteins inducing the highest indicated receptor expression on IgG⁺ memory and naive B cells.
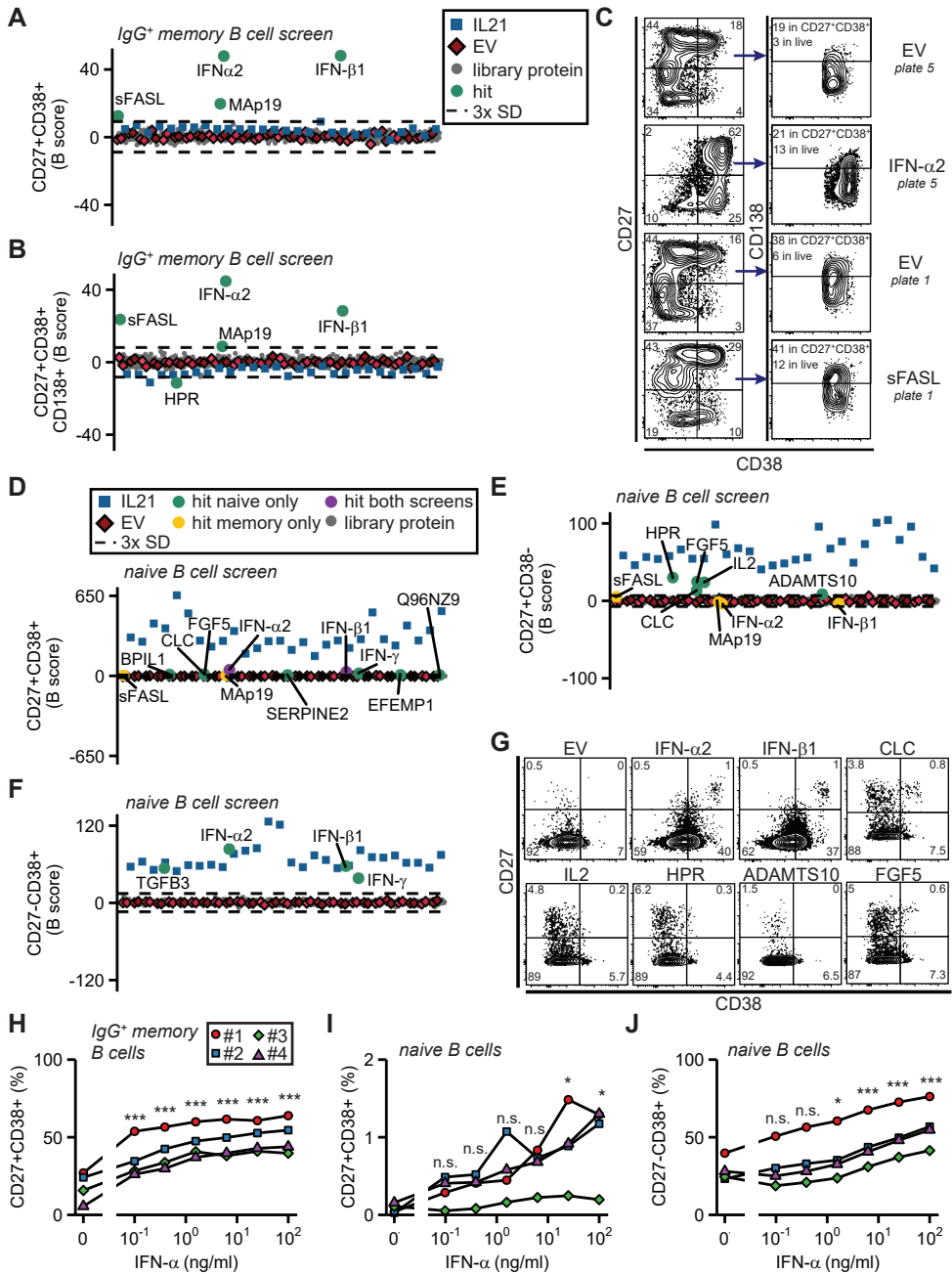
Figure 3. Secretome screening reveals multiple plasmablast differentiation inducing factors. (A, B, and D-F) Mean B scores of screen readouts for various differentiation stages of IgG+ memory and naive B cells from two healthy donors. Legend boxes contain annotation of controls, hits and other secreted proteins. EV is empty vector. Differentiation stage was based on CD27, CD38 and CD138 expression as indicated and gated as shown in the contour plots in (C and G) for controls and the most prominent hits (hit threshold is three times SD; dashed lines). IgG+ memory (H) or naive (I and J) B cells from four different healthy donors were cultured as in Figure 1A using serial dilutions of purified recombinant IFN-α instead of conditioned medium. Significance compared to 0 ng/ml IFN-α is shown as determined by ANOVA with Tukey's post hoc test.

we validated these findings using serial dilutions of recombinant purified IFN-α. At all tested concentrations (starting at 0.1 ng/ml), IFN-α significantly directed IgG$^+$ memory B cells towards CD27$^+$CD38$^+$ ASCs (Fig. 3H). IFN-α was also effective in inducing CD38 and CD27 expression in naive B cells, suggesting that the capacity of type I IFN signaling is similar between naive and memory B cells (Fig. 2I-J). Together, our screens reveal that a variety of secreted proteins can stimulate B cell differentiation and support the fact that naive B cells require different signals compared to memory B cells to differentiate into ASCs.

sFASL induces ASC differentiation

Our screens identified known and unknown secreted proteins to drive naive and memory B cells into various stages of differentiation. As the largest effects were witnessed upon differentiation of memory B cells, we validated these results for two additional donors using newly generated conditioned media. These confirmed that IFN-α2, IFN-β1, MAp19 and sFASL conditioned media induced plasmablast differentiation from memory B cells (Fig. S2A). We further continued investigating MAp19 and sFASL, because to our knowledge these factors were unknown to promote B cell differentiation. MAp19 is a splice variant of MASP-2 (28). The function of MAp19 is unknown as it lacks the MASP-2 catalytic domain which is responsible for activating complement by cleaving C2 and C4 and may not be sufficiently expressed to compete with MASP-2 for binding to mannan-binding lectin (20). FASL is known as an inducer of apoptosis in many (embryonic) developmental and immunological processes (29, 30). In addition, occasional reports have described cell death independent functions of FASL (31). The FASL cDNA in our library encodes for a membrane-bound protein, which may be cleaved to obtain soluble FASL (sFASL) (32). As we used the conditioned medium of FASL transfected cells, we hypothesized that sFASL was present in the conditioned media.

Our validation assays showed that the conditioned media containing MAp19 or sFASL significantly induced CD27$^+$CD38$^+$ B cells in IgG$^+$ memory B cells from four different donors (Fig. 4A). To further pinpoint the activity of these proteins, we repeated the assay with purified recombinant MAp19 or sFASL. MAp19 failed to reproduce the conditioned medium effect on B cell differentiation (Fig. 4B). In contrast, sFASL induced B cell differentiation into CD27$^+$CD38$^+$ B cells starting at 10 ng/ml (Fig. 4C).

FASL signals via the FAS receptor, also known as CD95. During germinal center reactions, B cells express this receptor due to stimulation with CD40L (33). In line with these data, the vast majority of B cells in our B cell differentiation assay express FAS after one day of culture in the presence of CD40L costimulation (Fig. S2B). The broad FAS receptor upregulation on B cells in our culture system is therefore not correlated with sFASL-mediated differentiation of a fraction of these B cells.

There are multiple possible explanations for sFASL-driven plasmablast differentiation. sFASL may cause the death of non-differentiating cells, it could encourage the

proliferation of differentiating cells or finally, sFASL could drive differentiation into ASCs. To gain more insight into the mechanism, we analyzed the effect of sFASL on cell survival and proliferation by flow cytometry four days after culture initiation (gating in Fig. S3A). sFASL-treated B cells were still in an early stage of ASC differentiation, and had proliferated at a similar speed as the control without sFASL. Similar B cell numbers were present in sFASL-stimulated cultures compared to the control on both day 4 and day 10, indicating that sFASL does not promote plasmablast differentiation by affecting B cell apoptosis or proliferation (Fig. 5A-C).

Differentiation of B cells into ASCs is regulated by multiple transcription factors including the key molecules PAX5 and BLIMP-1 (34). Accordingly, PAX5 was downregulated in the presence of high amounts of IL-21 at day 4 of differentiation into ASCs, while expression of BLIMP-1 was increased (Fig. 5D). sFASL also induced more cells with a BLIMP-1$^+$PAX5^{low} phenotype compared to the control condition without sFASL (Fig. 5D), suggesting that sFASL supports B cell differentiation in a similar manner as IL-21. To investigate if these differentiated B cells could secrete antibodies, we measured the amounts of IgG1 and IgG4 in the culture supernatants. sFASL induced secretion of IgG1 and IgG4 in a concentration-dependent manner (normalized data in Fig. 5E, absolute values in S3C-S3D). The levels of produced IgG1 and IgG4 corresponded with the degree of CD27$^+$CD38$^+$ cell differentiation

3
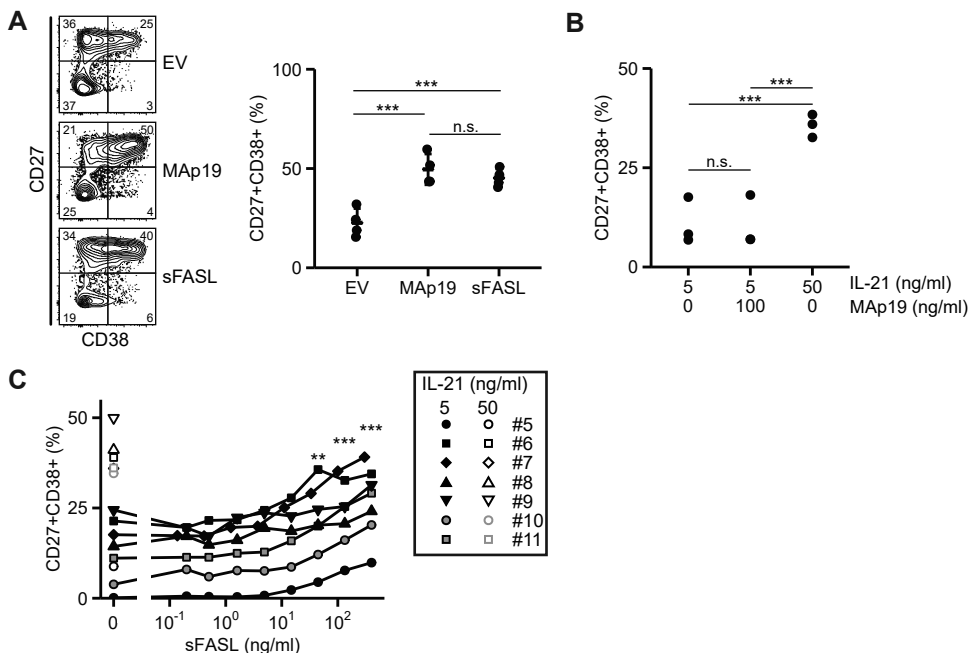
Figure 4. sFASL induces differentiation into ASCs. (A) Newly prepared conditioned media for MAp19 and sFASL were tested for CD27$^+$CD38$^+$ ASC induction potential on IgG$^+$ memory B cells of four different healthy donors (two are the same as in Fig. S2). (B and C) IgG$^+$ memory B cell differentiation into CD27$^+$CD38$^+$ ASCs in the presence of purified recombinant MAp19 (n=3) (B) or a serial dilution of commercially available recombinant sFASL (n=7) (C). Statistical significance was determined by ANOVA with Tukey's post hoc test. In panel only C statistical significance compared to 0 ng/mL FASL is shown.
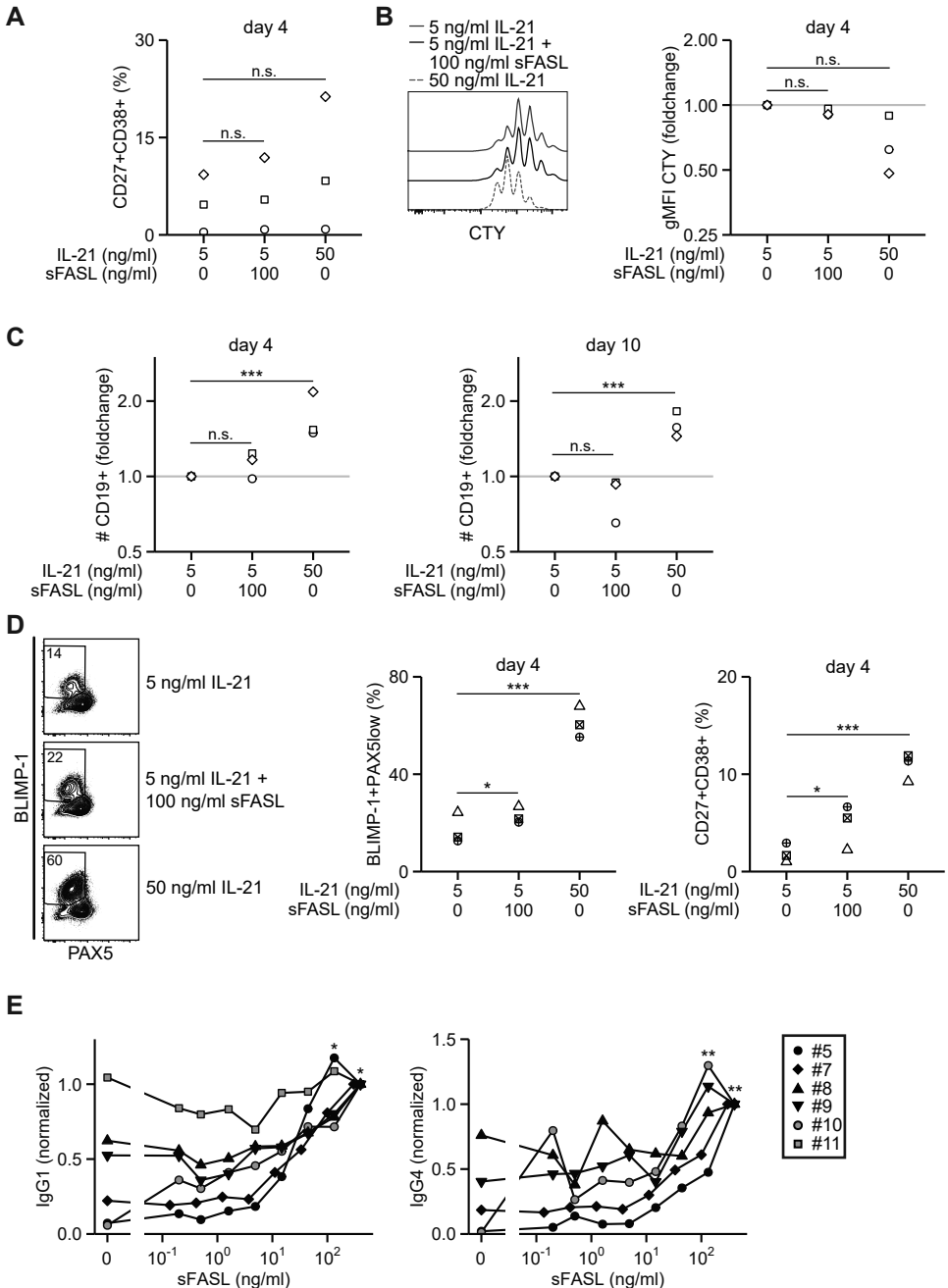
Figure 5. sFASL affects differentiation and not proliferation into IgG1- and IgG4-secreting cells. (A) CD27^{+}CD38^{+} expression analysis at day 4 of IgG^{+} memory B cell culture in the presence of purified recombinant sFASL (n=3). (B) Histogram of cell trace yellow (CTY) dilution at day 4 after labeling (left panel) and geometric mean fluorescence intensity quantification of CTY dilution from three healthy donors (right panel) (n=3). (C) Counting bead normalized amount of CD19^{+} B cells after 4-day (left panel) and 10-day (right panel) culture of IgG^{+} memory B cells with indicated conditions (n=3). (D) PAX5^{low}BLIMP-1^{+} and CD27^{+}CD38^{+} analysis at day 4 (n=3). (E) IgG1 (n=6) and IgG4 (n=5) levels were determined by ELISA in the culture supernatants obtained

for each donor (Fig. 4C, S3C-S3D). In conclusion, sFASL induced differentiation of IgG$^+$ memory B cells into antibody-secreting CD27$^+$CD38$^+$ cells.

Discussion

The germinal center reaction is a dynamic process where activated B cells differentiate into ASCs upon receiving the appropriate signals. By employing a secreted protein library, we successfully identified multiple proteins that promote T cell-dependent differentiation of naive or memory B cells in the presence of to CD40L and IL-21.

The strongest inducers of B cell differentiation in our screens are the well-studied type I IFNs. These multipotent proinflammatory cytokines signal through the Interferon-alpha/beta receptor (IFNAR) to inhibit viral replication by inducing an anti-viral state in non-immune cells and by activating immune cells including B cells. Type I IFNs induce upregulation of CD69, CD86 and CD40 in murine B cells, promote antibody secretion during influenza infection in mice, and can induce antibody secretion in human B cells *in vitro* (18, 35–38). Although the pro-inflammatory effects of type I IFNs are beneficial during viral infection, type I IFNs may also promote auto-reactive B cells in autoimmune diseases such as systemic lupus erythematosus (SLE) as reviewed by Kiefer *et al* (39).

While IFN-α and sFASL directly stimulate differentiation of memory B cells into CD27$^+$CD38$^+$CD138$^+$ plasma cells, purified MAp19 does not. A possible explanation as to why MAp19 conditioned medium induces B cell differentiation and its purified form does not may be that MAp19 stimulates HEK293T cells to secrete another protein or metabolic products. Alternatively, there may be structural differences between the freshly secreted and purified MAp19. Currently MAp19 has no known function (20), yet the fact that it is a spliced variant of the complement factor MASP-2 warrants future research on potential regulation of B cell differentiation through the complement system .

It is relevant to consider physiological concentrations when using soluble proteins in *in vitro* systems. Nonetheless, many soluble proteins have higher local than systemic concentrations, for example when they are secreted in immunological synapses. Such soluble proteins include the cytokine IL-21 (here used at 50 ng/mL for optimal B cell differentiation) and sFASL. In both of these cases, the physiological concentration is difficult to determine. Still, the role of IL-21 in B cell differentiation is beyond question because of the overwhelming amount of physiological relevance generated over the last years (e.g. using IL-21$^{-/-}$ mice) (40–42). We here provide the first data that in principle sFASL can play a role in human B cell differentiation.

Figure 5 Legend (continued)

at the end of IgG$^+$ memory B cell cultures in the presence of serial dilutions of sFASL. Data were normalized to the highest sFASL concentration per donor. Donor numbers (#) correspond to Figure 4C. For donor 11 IgG4 levels were below detection for all conditions including 50 ng/mL IL-21, therefore these data were excluded from analysis. Raw data are plotted in Fig. S3. Statistical significance was determined by ANOVA with Tukey's post hoc test for panels A-D. In E the Friedman test followed by Dunn's posttest was applied to determine statistical significance between 0 ng/ml sFASL and the individual serial dilutions of sFASL.

FASL is well-known for its apoptosis-inducing capacity. For example, membrane-bound FASL is expressed by activated T cells to kill infected or malignant target cells by binding to and oligomerizing its receptor FAS present on these cells. Apoptosis plays a central role in selection of B cells during affinity maturation. CD40 ligation stimulates FAS expression and sensitizes B cells for FAS-mediated apoptosis, although IL-4 protects B cells from cell death (43, 44). Yet, in vivo studies showed that FAS signaling is dispensable for GC B cell selection in mice (45, 46).

The function of sFASL is still under debate as it is less effective in inducing apoptosis than membrane-bound FASL. sFASL may compete with membrane-bound FASL for FAS-binding thereby blocking apoptosis and even promoting proliferation (32, 47). We did not observe a role of sFASL in the induction of apoptosis. Our results rather highlight a novel function of sFASL, which is to directly induce differentiation of CD40-activated memory B cells into ASCs.

sFASL may partake in the pathogenesis of several autoimmune diseases. Increased sFASL levels have been found in the serum of SLE patients and saliva of Sjögren's syndrome patients compared to healthy individuals. In addition, patients with more severe rheumatoid arthritis have higher sFASL levels in synovial fluid compared to those with less severe pathology (48–50). These autoimmune diseases are all characterized by the presence of autoantibodies, produced by ASCs originating from self-reactive B cells. So far, it remains unclear if the relationship between sFASL levels and autoimmunity is causal. Our data now demonstrates a direct role for sFASL in promoting B cell differentiation. It therefore opens the way for novel research exploring if sFASL initiates or worsens immune-mediated diseases by promoting differentiation of detrimental, autoreactive B cells.

References

1. Mesin, L., J. Ersching, and G. D. Victora. 2016. Germinal Center B Cell Dynamics. *Immunity* 45: 471–482.
2. Roco, J. A., L. Mesin, S. C. Binder, C. Nefzger, P. Gonzalez-Figueroa, P. F. Canete, J. Ellyard, Q. Shen, P. A. Robert, J. Cappello, H. Vohra, Y. Zhang, C. R. Nowosad, A. Schiepers, L. M. Corcoran, K. M. Toellner, J. M. Polo, M. Meyer-Hermann, G. D. Victora, and C. G. Vinuesa. 2019. Class-Switch Recombination Occurs Infrequently in Germinal Centers. *Immunity* 51: 337-350.e7.
3. Bannard, O., R. M. Horton, C. D. C. Allen, J. An, T. Nagasawa, and J. G. Cyster. 2013. Germinal center centroblasts transition to a centrocyte phenotype according to a timed program and depend on the dark zone for effective selection. *Immunity* 39: 912–924.
4. Kräutler, N. J., D. Suan, D. Butt, K. Bourne, J. R. Hermes, T. D. Chan, C. Sundling, W. Kaplan, P. Schofield, J. Jackson, A. Basten, D. Christ, and R. Brink. 2017. Differentiation of germinal center B cells into plasma cells is initiated by high-affinity antigen and completed by Tfh cells. *J. Exp. Med.* 214: 1259–1267.
5. Lau, A. W., and R. Brink. 2020. Selection in the germinal center. *Curr. Opin. Immunol.* 63: 29–34.
6. Bannard, O., and J. G. Cyster. 2017. Germinal centers: programmed for affinity maturation and antibody diversification. *Curr. Opin. Immunol.* 45: 21–30.
7. Weisel, F. J., G. V. Zuccarino-Catania, M. Chikina, and M. J. Shlomchik. 2016. A Temporal Switch in the Germinal Center Determines Differential Output of Memory B and Plasma Cells. *Immunity* 44: 116–130.
8. McHeyzer-Williams, L. J., C. Dufaud, and M. G. McHeyzer-Williams. 2017. Do Memory B Cells Form Secondary Germinal Centers? Impact of Antibody Class and Quality of Memory T-Cell Help at Recall. *Cold Spring Harb. Perspect. Biol.* 16: a029116.
9. Riedel, R., R. Addo, M. Ferreira-Gomes, G. A. Heinz, F. Heinrich, J. Kummer, V. Greiff, D. Schulz, C. Klaeden, R. Cornelis, U. Menzel, U. Stervbo, R. Köhler, C. Haftmann, S. Kühnel, K. Lehmann, P. Maschmeyer, M. McGrath, S. Naundorf, S. Hahne, Ö. Sercan-Alp, F. Siracusa, J. Stefanowski, M. Weber, K. Westendorf, J. Zimmermann, A. E. Hauser, S. T. Reddy, P. Durek, H.-D. Chang, M.-F. Mashreghi, and A. Radbruch. 2020. Discrete populations of isotype-switched memory B lymphocytes are maintained in murine spleen and bone marrow. *Nat. Commun.* 11: 2570.
10. Hauser, A. E., G. F. Debes, S. Arce, G. Cassese, A. Hamann, A. Radbruch, and R. A. Manz. 2002. Chemotactic responsiveness toward ligands for CXCR3 and CXCR4 is regulated on plasma blasts during the time course of a memory immune response. *J. Immunol.* 169: 1277–82.
11. Ding, B. B., E. Bi, H. Chen, J. J. Yu, and B. H. Ye. 2013. IL-21 and CD40L Synergistically Promote Plasma Cell Differentiation through Upregulation of Blimp-1 in Human B Cells. *J. Immunol.* 190: 1827–1836.
12. Liu, D., H. Xu, C. Shih, Z. Wan, X. Ma, W. Ma, D. Luo, and H. Qi. 2015. T-B-cell entanglement and ICOSL-driven feed-forward regulation of germinal centre reaction. *Nature* 517: 214–218.
13. Good-Jacobson, K. L., C. G. Szumilas, L. Chen, A. H. Sharpe, M. M. Tomayko, and M. J. Shlomchik. 2010. PD-1 regulates germinal center B cell survival and the formation and affinity of long-lived plasma cells. *Nat. Immunol.* 11: 535–542.
14. Muehlinghaus, G., L. Cigliano, S. Huehn, A. Peddinghaus, H. Leyendeckers, A. E. Hauser, F. Hiepe, A. Radbruch, S. Arce, and R. A. Manz. 2005. Regulation of CXCR3 and CXCR4 expression during terminal differentiation of memory B cells into plasma cells. *Blood* 105: 3965–3971.
15. Gonzalez, D. G., C. M. Cote, J. R. Patel, C. B. Smith, Y. Zhang, K. M. Nickerson, T. Zhang, S. M. Kerfoot, and A. M. Haberman. 2018. Nonredundant Roles of IL-21 and IL-4 in the Phased Initiation of Germinal Center B Cells and Subsequent Self-Renewal Transitions. *J. Immunol.* 201: 3569–3579.
16. Laidlaw, B. J., Y. Lu, R. A. Amezquita, J. S. Weinstein, J. A. Vander Heiden, N. T. Gupta, S. H. Kleinstein, S. M. Kaech, and J. Craft. 2017. Interleukin-10 from CD4+ follicular regulatory T cells promotes the germinal center response. *Sci. Immunol.* 2.
17. Guthmiller, J. J., A. C. Graham, R. A. Zander, R. L. Pope, and N. S. Butler. 2017. Cutting Edge: IL-10 Is Essential for the Generation of Germinal Center B Cell Responses and Anti- Plasmodium Humoral Immunity . *J. Immunol.* 198: 617–622.
18. Jego, G., A. K. Palucka, J.-P. Blanck, C. Chalouni, V. Pascual, and J. Banchereau. 2003. Plasmacytoid dendritic cells induce plasma cell differentiation through type I interferon and interleukin 6. *Immunity* 19: 225–34.
19. van Asten, S. D., M. Raaben, B. Nota, and R. M. Spaapen. 2018. Secretome Screening Reveals Fibroblast Growth Factors as Novel Inhibitors of Viral Replication. *J. Virol.* 92: JVI.00260-18.
20. Degn, S. E., S. Thiel, O. Nielsen, A. G. Hansen, R. Steffensen, and J. C. Jensenius. 2011. MAp19, the alternative splice product of the MASP2 gene. *J. Immunol. Methods* 373: 89–101.
21. Urashima, M., D. Chauhan, H. Uchiyama, G. J. Freeman, and K. C. Anderson. 1995. CD40 ligand triggered interleukin-6 secretion in multiple myeloma. *Blood* 85: 1903–12.
22. Schultze, J. L., A. A. Cardoso, G. J. Freeman, M. J. Seamon, J. Daley, G. S. Pinkus, J. G. Gribben, and L. M. Nadler. 1995. Follicular lymphomas can be induced to present alloantigen efficiently: A conceptual model

3

to improve their tumor immunogenicity. *Proc. Natl. Acad. Sci. U. S. A.* 92: 8200–8204.

23. Thielens, N. M., S. Cseh, S. Thiel, T. Vorup-Jensen, V. Rossi, J. C. Jensenius, and G. J. Arlaud. 2001. Interaction Properties of Human Mannan-Binding Lectin (MBL)-Associated Serine Proteases-1 and -2, MBL-Associated Protein 19, and MBL. *J. Immunol.* 166: 5068–5077.

24. Zhang, J., T. D. Y. Chung, and K. R. Oldenburg. 1999. A Simple Statistical Parameter for Use in Evaluation and Validation of High Throughput Screening Assays. *J. Biomol. Screen.* 4: 67–73.

25. Malo, N., J. A. Hanley, S. Cerquozzi, J. Pelletier, and R. Nadon. 2006. Statistical practice in high-throughput screening data analysis. *Nat. Biotechnol.* 24: 167–75.

26. Marsman, C., T. Jorritsma, A. ten Brinke, and S. M. van Ham. 2020. Flow Cytometric Methods for the Detection of Intracellular Signaling Proteins and Transcription Factors Reveal Heterogeneity in Differentiating Human B Cell Subsets. *Cells* 9: 2633.

27. Tangye, S. G., and C. S. Ma. 2020. Regulation of the germinal center and humoral immunity by interleukin-21. *J. Exp. Med.* 217.

28. Takahashi, M., Y. Endo, T. Fujita, and M. Matsushita. 1999. A truncated form of mannose-binding lectin-associated serine protease (MASP)-2 expressed by alternative polyadenylation is a component of the lectin complement pathway. *Int. Immunol.* 11: 859–863.

29. French, L. E., M. Hahne, I. Viard, G. Radlgruber, R. Zanone, K. Becker, C. Müller, and J. Tschopp. 1996. Fas and Fas ligand in embryos and adult mice: ligand expression in several immune-privileged tissues and coexpression in adult tissues characterized by apoptotic cell turnover. *J. Cell Biol.* 133: 335–43.

30. Waring, P., and A. Müllbacher. 1999. Cell death induced by the Fas/Fas ligand pathway and its role in pathology. *Immunol. Cell Biol.* 77: 312–317.

31. Suzuki, I., and P. J. Fink. 2000. The dual functions of Fas ligand in the regulation of peripheral CD8+ and CD4+ T cells. *Proc. Natl. Acad. Sci. U. S. A.* 97: 1707–1712.

32. Schneider, P., N. Holler, J.-L. Bodmer, M. Hahne, K. Frei, A. Fontana, and J. Tschopp. 1998. Conversion of Membrane-bound Fas(CD95) Ligand to Its Soluble Form Is Associated with Downregulation of Its Proapoptotic Activity and Loss of Liver Toxicity. *J. Exp. Med.* 187: 1205–1213.

33. Schattner, E. J., K. B. Elkon, D. H. Yoo, J. Tumang, P. H. Krammer, M. K. Crow, and S. M. Friedman. 1995. CD40 ligation induces apo-1/fas expression on human B lymphocytes and facilitates apoptosis through the apo-1/fas pathway. *J. Exp. Med.* 182: 1557–1565.

34. Nutt, S. L., N. Taubenheim, J. Hasbold, L. M. Corcoran, and P. D. Hodgkin. 2011. The genetic network controlling plasma cell differentiation. *Semin. Immunol.* 23: 341–349.

35. Coro, E. S., W. L. W. Chang, and N. Baumgarth. 2006. Type I IFN receptor signals directly stimulate local B cells early following influenza virus infection. *J. Immunol.* 176: 4343–51.

36. Braun, D., I. Caramalho, and J. Demengeot. 2002. IFN-alpha/beta enhances BCR-dependent B cell responses. *Int. Immunol.* 14: 411–9.

37. Peters, M., L. Ambrus, A. Zheleznyak, J. A. Y. H. Hoofnaglel, and F. Washington. 1986. Effect of interferon-alpha on immunoglobulin synthesis by human B cells. *J. Immunol.* 137: 3153–3157.

38. Klarquist, J., R. Cantrell, M. A. Lehn, K. Lampe, C. M. Hennies, K. Hoebe, and E. M. Janssen. 2020. Type I IFN Drives Experimental Systemic Lupus Erythematosus by Distinct Mechanisms in CD4 T Cells and B Cells. *ImmunoHorizons* 4: 140–152.

39. Kiefer, K., M. A. Oropallo, M. P. Cancro, and A. Marshak-Rothstein. 2012. Role of type i interferons in the activation of autoreactive B cells. *Immunol. Cell Biol.* 90: 498–504.

40. Zotos, D., J. M. Coquet, Y. Zhang, A. Light, K. D'Costa, A. Kallies, L. M. Corcoran, D. I. Godfrey, K.-M. Toellner, M. J. Smyth, S. L. Nutt, and D. M. Tarlinton. 2010. IL-21 regulates germinal center B cell differentiation and proliferation through a B cell-intrinsic mechanism. *J. Exp. Med.* 207: 365–78.

41. Ozaki, K., R. Spolski, C. G. Feng, C.-F. Qi, J. Cheng, A. Sher, H. C. Morse, C. Liu, P. L. Schwartzberg, and W. J. Leonard. 2002. A critical role for IL-21 in regulating immunoglobulin production. *Science* 298: 1630–4.

42. Ozaki, K., R. Spolski, R. Ettinger, H.-P. Kim, G. Wang, C.-F. Qi, P. Hwu, D. J. Shaffer, S. Akilesh, D. C. Roopenian, H. C. Morse, P. E. Lipsky, and W. J. Leonard. 2004. Regulation of B Cell Differentiation and Plasma Cell Generation by IL-21, a Novel Inducer of Blimp-1 and Bcl-6. *J. Immunol.* 173: 5361–5371.

43. Garrone, P., E. M. Neidhardt, E. Garcia, L. Galibert, C. Van Kooten, and J. Banchereau. 1995. Fas ligation induces apoptosis of CD40-activated human B lymphocytes. *J. Exp. Med.* 182: 1265–1273.

44. Nakanishi, K., K. Matsui, S. Kashiwamura, Y. Nishioka, J. Nomura, Y. Nishimura, N. Sakaguchi, S. Yonehara, K. Higashino, and S. Shinka. 1996. IL-4 and anti-CD40 protect against Fas-mediated B cell apoptosis and induce B cell growth and differentiation. *Int. Immunol.* 8: 791–8.

45. Butt, D., T. D. Chan, K. Bourne, J. R. Hermes, A. Nguyen, A. Statham, L. A. O'Reilly, A. Strasser, S. Price, P. Schofield, D. Christ, A. Basten, C. S. Ma, S. G. Tangye, T. G. Phan, V. K. Rao, and R. Brink. 2015. FAS Inactivation Releases Unconventional Germinal Center B Cells that Escape Antigen Control and Drive IgE and Autoantibody Production. *Immunity* 42: 890–902.

46. Smith, K. G. C., G. J. V. Nossal, and D. M. Tarlinton. 1995. FAS is highly expressed in the germinal center but is not required for regulation of the B-cell response to antigen. *Proc. Natl. Acad. Sci. U. S. A.* 92: 11628–11632.

47. Audo, R., F. Calmon-Hamaty, L. Papon, B. Combe, J. Morel, and M. Hahne. 2014. Distinct Effects of Soluble and Membrane-Bound Fas Ligand on Fibroblast-like Synoviocytes From Rheumatoid Arthritis Patients. *Arthritis Rheumatol.* 66: 3289–3299.

48. Vincent, F. B., R. Kandane-Rathnayake, R. Koelmeyer, J. Harris, A. Y. Hoi, F. MacKay, F. MacKay, and E. F. Morand. 2020. Associations of serum soluble Fas and Fas ligand (FasL) with outcomes in systemic lupus erythematosus. *Lupus Sci. Med.* 7: 375.

49. Nakamura, H., A. Kawakami, M. Izumi, T. Nakashima, Y. Takagi, H. Ida, T. Nakamura, T. Nakamura, and K. Eguchi. 2005. Detection of the soluble form of Fas ligand (sFasL) and sFas in the saliva from patients with Sjögren's syndrome. *Clin. Exp. Rheumatol.* 23: 915.

50. Hashimoto, H., M. Tanaka, T. Suda, T. Tomita, K. Hayashida, E. Takeuchi, M. Kaneko, H. Takano, S. Nagata, and T. Ochi. 1998. Soluble fas ligand in the joints of patients with rheumatoid arthritis and osteoarthritis. *Arthritis Rheum.* 41: 657–662.

3

Supplementary figures
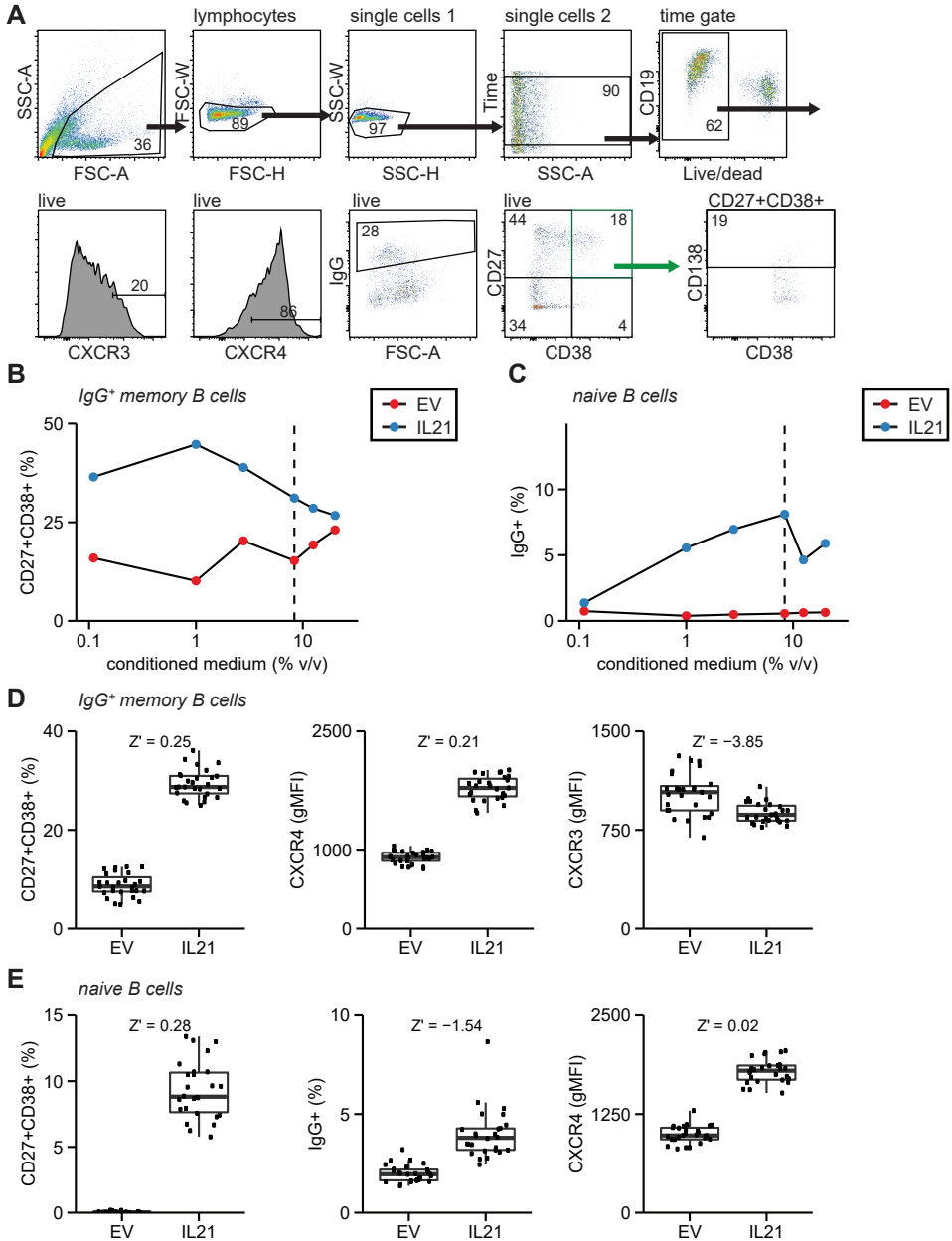
Figure S1. Optimization of B cell differentiation assay for arrayed screening. (A) Strategy at the end of the B cell differentiation assay to gate live, single CD19+ B cells. Markers of interest within these B cells include CXCR3, CXCR4, IgG and also CD27/CD38 to allow gating on plasmablasts and plasma cells. Plasma cells were identified by gating for CD138 within CD27+CD38+ B cells. Percentages of CD27+CD38+CD138+ cells were calculated within live B cells. (B and C) IgG+ memory (B) and naive B cells (C) were cultured as depicted in Figure 1A in the presence of a serial dilution of conditioned medium derived from empty vector (EV) or IL-21 cDNA transfected HEK293T cells in addition to 5 ng/ml IL-21. 1:12 (8.3 % v/v) was chosen as the preferred conditioned medium dilution for

(Continued on next page)

3

Figure S1 Legend (continued)
the secreted protein screen, here indicated with a dashed line. (D-E) 24 replicates of control empty vector and IL-21 conditioned media were assayed according to the optimized conditions. Depicted parameters were readout at the end of IgG⁺ memory (D) and naive B cell (E) cultures. Z' scores are shown, Z'>0 indicates suitability of the assay for arrayed screening.

A

B
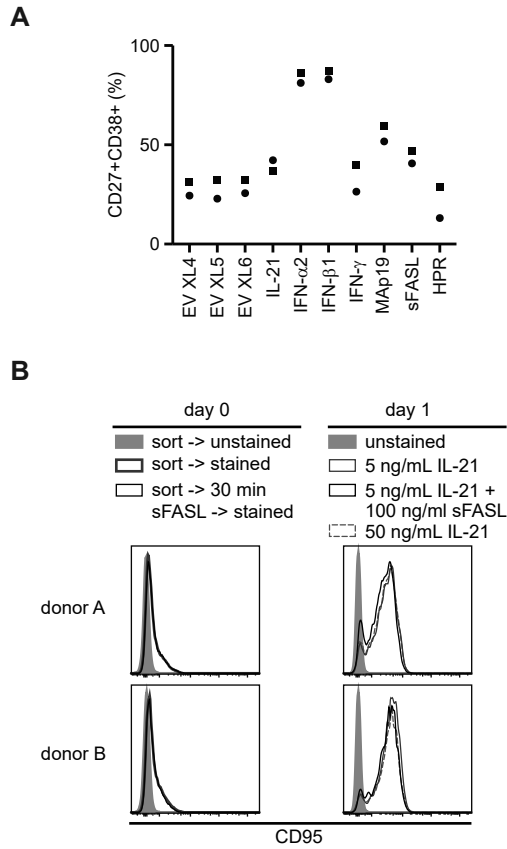
Figure S2. Type I IFNs, sFASL and MAp19 induce the formation of CD27⁺CD38⁺ ASCs. (A) Newly prepared conditioned media from indicated cDNAs and empty vectors (XL4, XL5 and XL6 backbones) were tested for CD27⁺CD38⁺ ASC induction potential on IgG⁺ memory B cells of two different healthy donors (part of the data is also included in Fig. 4A). (B) IgG⁺ memory B cells from two donors were stained for CD95 immediately after the sort (left panel), after 30 minutes of incubation with sFASL (left panel) or after 1 day in the B cell differentiation assay (right panel).
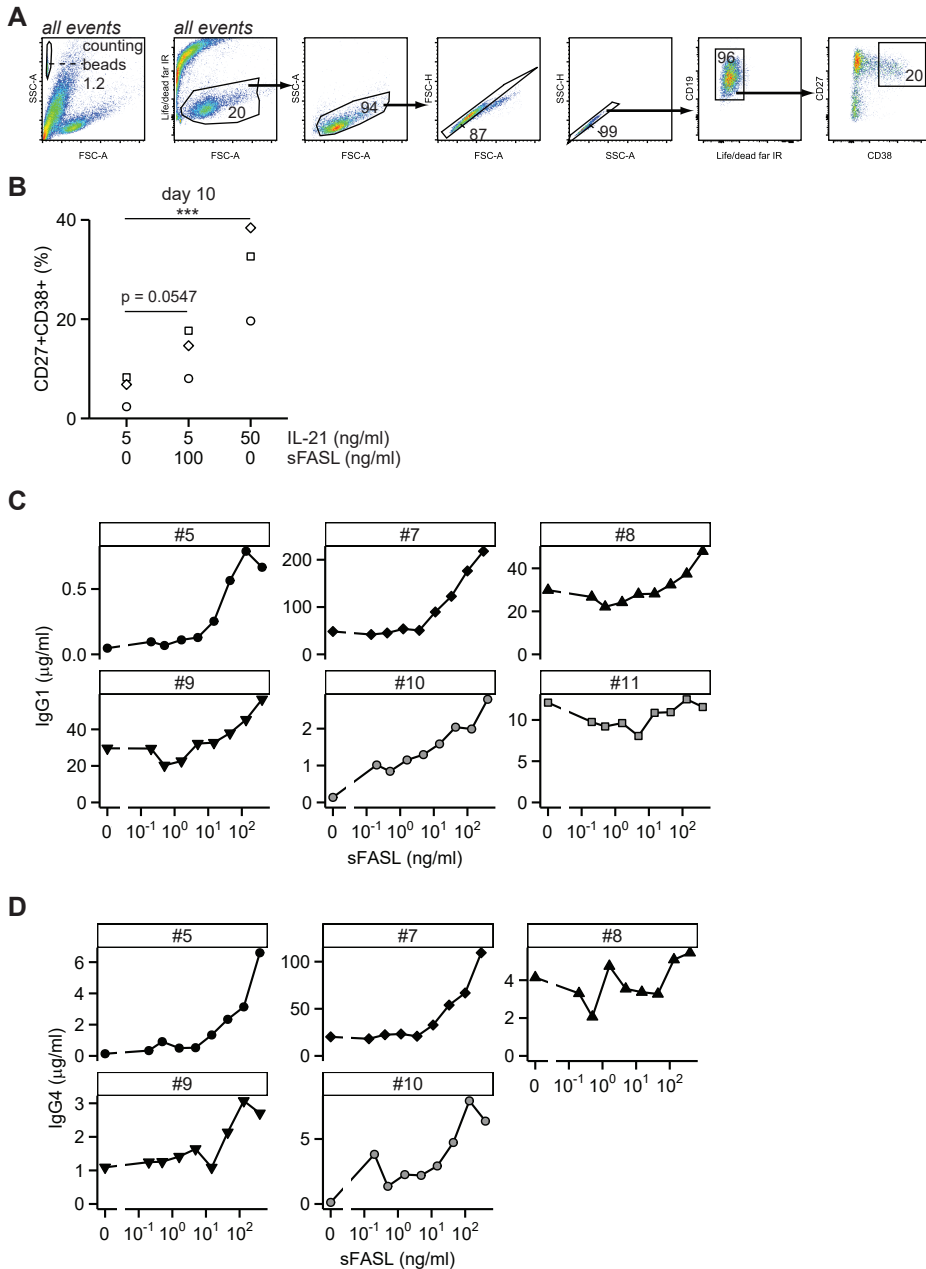
Figure S3. Gating strategy of B cell proliferation assay. (A) Strategy to gate on counting beads, CD19+ live cells and CD27+CD38+ ASCs on both day 4 and day 10 of the proliferation assay. (B) Quantification of CD27+CD38+ ASCs within live CD19+ B cells on day 10. Statistical significance was determined by ANOVA with Tukey's post hoc test. (C and D) IgG1 (C) and IgG4 (D) levels in culture supernatants of IgG+ memory B cells cultured in the presence of sFASL serial dilutions.

CHAPTER 4

Secreted protein library screen uncovers IL-21 as an inducer of granzyme B expression in activated CD4+ T cells

Saskia D. van Asten, Sophie Bliss, Natasja Kragten, Derk Amsen, Monika C. Wolkers, Klaas van Gisbergen, Robbert M. Spaapen

Abstract

T cells stimulate the immune response and kill target cells in viral infections, cancer, and autoimmune diseases. Activated T cells can promote immune responses through expression of cell-surface ligands and receptors, secretion of pro-inflammatory cytokines or killing of target cells after differentiation into one of the effector T cell subtypes. A subset of T cells can become memory T cells that remain after pathogen clearance to readily reactivate upon secondary challenge. T cell receptor signaling, co-stimulation by membrane-bound molecules and cytokines collectively drive T cell differentiation into effector and memory subtypes. Comprehension of how T cells differentiate into this diverse set of functional states is vital for our understanding of how they combat pathogens. In an effort to improve our understanding of T cell differentiation, we screened over 1200 secreted proteins to determine new factors that affect differentiation of T cells. We measured a comprehensive set of markers and cytokines to broadly study T cell differentiation status in activated CD4$^+$ and CD8$^+$ T cells separately. While multiple factors affected T cell differentiation, the most pronounced effect was the induction of granzyme B expression by type I interferons, IL-21, and TGF-β. Strikingly, IL-21 also induced granzyme B in CD4$^+$ T cells, which indicates that these CD4$^+$ T cells either have a cytotoxic or inhibitory profile. These findings reveal that locally secreted IL-21 can drive CD4$^+$ T cells towards a differentiation state that may have a specific function during viral infections, cancer, and autoimmunity.

Introduction

T cells are key players in the clearance of pathogens and tumor cells through direct cytotoxicity and through support of the activation of other immune cells. Naïve T cells differentiate into functional effector cells after recognition of their cognate antigen and exposure to appropriate costimulatory signals. After the successful clearance of a pathogen or tumor the activated T cell population contracts while a subset remains to form immunological memory (1). Upon secondary exposure, memory T cells exert their effector functions more rapidly than naive T cells because they require less costimulatory signals to become activated. Consequently, a secondary challenge will be resolved more rapid than the primary one.

The diversity of T cell functionality has inspired the designation of numerous subtypes. T cells are classified based on the expression of T cell receptor (TCR) co-receptors CD4 or CD8, on their differentiation status and on their effector capacity. There are multiple memory subtypes. Central memory T cells (T_{CM}) patrol lymph nodes and the peripheral circulation in search for their cognate antigen, effector memory T cells (T_{EM}) patrol the peripheral circulation and tissues, while tissue resident memory T cells (T_{RM}) remain in tissues to stand guard for a potential secondary infection (2). Together these memory T cell subtypes, distinguishable by expression of CD27, CCR7, CD69 and CD103, survey different compartments for reappearance of their cognate antigen. Cytokines such as IL-15, IL-7 and IL-21 but also TCR signaling strength can skew or maintain memory differentiation towards stem cell or central memory, yet the process of memory T cell differentiation is not fully understood (3–5).

Activated T cells, derived from naive or memory T cells, can be classified by a diverse set of functions. CD8 T cells, also known as cytotoxic cells (T_C), can kill target cells through intracellular delivery of granzymes, such as granzyme B, by perforin, through ligand-mediated death receptor crosslinking (e.g. FASL-FAS), or via the secretion of cytotoxic cytokines such as IFN-γ and TNF-α (6–9). Historically, CD4 T cells have been described as helper T_H cells providing cytokine and membrane-bound ligand support to differentiation and effector functions of other immune cells, such as CD8 T cells, B cells and macrophages. But CD4 T cells possess MHC class II restricted cytolytic activity, while CD8 T cells may secrete "helper" cytokines such as IL-4 and IL-17 (10–15). IFN-γ induces differentiation towards T_H1/T_C1 cells which secrete IL-2, IFN-γ and TNF-α in the defense against tumors and viral infections. The IL-4, IL-5 and IL-13 secreting T_H2/T_C2 cells, induced by IL-4, promote humoral immunity. A mix of cytokines including TGF-β and IL-6 promote T_H17/T_C17 differentiation. T_H17/T_C17 cells, involved in combatting fungal and bacterial infections, secrete IL-17 as their hallmark cytokine. T_H9/T_C9 are induced by IFN-γ, TGF-β, IL-4 and IL-2 and preferentially secrete IL-9. T_H9 cells are reported to aid in the clearance of parasitic worms, while both T_H9 and T_C9 cells have been described to inhibit tumor growth (12, 16–19). T follicular helper cells (T_{FH}) secrete IL-21 to promote B cell differentiation into antibody secreting cells in secondary lymphoid organs (20). In addition to this non-

4

exhaustive list of pro-inflammatory subtypes, induced T regulatory cells suppress the immune system using various methods, including through secretion of TGF-β and IL-10, to prevent unwanted activation and to resolve an inflammation.

The mechanisms of T cell differentiation induction have not been fully elucidated. While multiple polarizing cytokines have been identified, they may exert unknown effects in particular cell types or situations. In addition, the effect of non-cytokine secreted proteins on T cell differentiation is underexplored. We previously generated a library of 756 secreted proteins to find novel inhibitors of viral replication (21). In this study, we extended this library to include up to 1222 secreted proteins in total to find novel modulators of T cell differentiation into effector and memory subtypes. Of these, 66 secreted proteins modulated differentiation and effector function in our screens using T cells from two healthy donors. The most pronounced finding was that IL-21 induced the differentiation of granzyme B expressing CD4+ T cells. As granzyme B has both pro- and anti-inflammatory functions, its expression by CD4+ T cells should be further explored to elucidate its exact effects in autoimmune diseases, infections and cancer.

Methods

Primary cells and cell lines

Apheresis material and buffy coats were obtained from healthy volunteers (Sanquin Blood Supply) upon informed consent. Lymphocytes were isolated from apheresis material using the Elutra cell separation system (Gambro, Lakewood, USA) and cryopreserved (Elutra lymphocytes). PBMCs were isolated from the buffycoats by density gradient centrifugation using Lymphoprep (Axis-Shield PoC AS) and cryopreserved. The HEK293T cell line was kindly provided by Dr. J. Neefjes (NKI, Amsterdam; HLA-A, -B typed as control for authenticity). All cells were cultured in IMDM (Lonza) supplemented with 10% FCS and 1% penicillin-streptomycin (medium) at 37°C 5% CO_2.

Antibodies for flow cytometry

CD8-BV605 (clone RPA-T8), CD45RA-PE-Cy7 (clone HI100), CD4-PerCp-Cy5.5 (clone SK3), CD69-BUV395 (clone FN50), Granzyme B-AF700 (clone GB11), IFN-γ-PE (clone B27), IL-4-Percp-Cy5.5 (clone 8D4-8), IL-21-BV421 (clone 3A3-N2) and IL-2-BV510 (clone MQ1-17H12) were all from BD. PD1-PE-Cy7 (clone EH12.2H7), CCR7-BV510 (clone 6043H7), IL17a-FITC (eBio64DEC17), TNF-α-APC (clone Mab11) and IL-9-PE-Cy7 (clone MH9A4) were all from Biolegend. The near-IR Live/dead dye was from Life Technologies, CD45-ECD (clone A07784) from Beckman Coulter, CD27-FITC (clone CLB-27/1, 9F4) from Sanquin.

Recombinant secreted proteins

The first sets of plasmids within the secreted protein library (SPL) were obtained from Origene and GE Health Care. The second set of plasmids was a kind gift of Dr. R. Beijersbergen. The transfections were performed as described previously (21). HEK293T

cells were plated in 24-well plates and incubated overnight. Transfection mixes were prepared by mixing 50 ng plasmid DNA with 1.5 µg polyethylenimine (Polysciences) in 50 µl serum-free medium per transfection, followed by 30 min incubation at room temperature. 50 µl transfection mix was added per well. After 6 h incubation medium was replaced by 1 ml fresh medium. After three more days, conditioned medium for each individual transfection was collected and cleared of cells by multiple rounds of centrifugation and collection of the supernatants. The collected conditioned media were stored in ready-to-screen plates at -80 °C. Levels of IFN-γ were determined by ELISA according to manufacturer's protocol (Sanquin). Purified recombinant human IL-21 was from Life technologies, IL-15 from Peprotech.

T cell differentiation assay

Thawed elutra lymphocytes (screen and validation) or PBMCs (other experiments) were stained with CD4-PerCp-Cy5.5, CD8-BV605, CD45RA-PE-Cy7 and CD27-FITC in 0.1% BSA in PBS (PBS-BSA) for 30 minutes on ice. Cells were washed twice with PBS-BSA and centrifuged as before. Any clumps were removed using tubes with cell strainer caps (Corning). Naive CD4 T cells (CD4⁺CD8⁻CD45RA⁺CD27⁺) and naive CD8 T cells (CD4⁻CD8⁺CD45RA⁺CD27⁺) were sorted using an Aria II sorter (BD). Naive CD4 and CD8 T cells were separately cultured in the presence of 0.1 µg/ml αCD3 (clone 1XE, Sanquin), 0.1 µg/ml αCD28 (clone CLB.CD28/1, Sanquin) and 50 IU/ml IL-2 (Proleukin, Novartis) at a density of 1 million cells/well in a 24 well plate for three days. At day three, T cells were washed twice with medium, plated at a density of 2500-5000 cells/well in a 96 well plate, with 1/12 dilution of SPL conditioned medium and 20 ng/ml IL-15 (Peprotech). After seven days, the content of each well was split in two. The first half was transferred to V bottom 96 well plates for staining with flow cytometry panel 1, the second half was returned to the incubator. After o/n incubation, these cells were restimulated with 0.1 µg/ml PMA, 1 µg/ml ionomycin and 10 µg/ml Brefeldin A (all Sigma). After 5h restimulation cells were stained with flow cytometry panel 2.

Flow cytometry

For flow cytometry panel 1, CD4 and CD8 T cells treated with the same conditioned medium were pooled before staining. The pooled cells were centrifuged 1800 rpm for 2 minutes. Cell pellets were stained with CD8-BV605, CD27-FITC, CCR7-BV510, CD69-BUV395, CD103-PE and far-IR live dead dye in stain buffer (0.5% BSA, 0.01% azide in PBS) for 30 min at RT. Cells were washed with stain buffer, and then fixed with the fixation solution of the FoxP3 stain kit (eBioscience) for 30 min. Next the fixated cells were stained intracellularly with Granzyme-B-AF700 in Perm/Wash buffer of the FoxP3 stain kit for 30 min. After staining cells were washed twice with Perm/Wash buffer and taken up in stain buffer for measurement on an LSR Fortessa (BD).

For flow cytometry panel 2, CD4 and CD8 T cells were stained extracellularly separately.

Figure 1. Set-up of the secreted protein library screen in naïve CD4+ and CD8+ T cells. (A) The cDNA library used to generate our secreted protein library contains 1222 transcripts derived from 1080 genes. The genes were categorized using Panther and Gene Ontology databases and colored according to the super categories immunology, signaling, development, extra cellular matrix, transport, enzymes, and other/undefined (colored groups from left to right) (82–84). (B) cDNAs of the secreted protein library were individually transfected into HEK-293T cells followed by collection of the conditioned media at day 3. Each production batch included an IFN-γ control cDNA, of which the production was determined by ELISA. Part A contains the first set of cDNAs

CD4 cells were stained with CD45-ECD and near-IR live/dead dye in stain buffer, while CD8 T cells were stained solely with the live/dead dye for 30 min on ice. Cells were washed twice with stain buffer. CD4 and CD8 T cells treated with the same conditioned medium were then pooled before intracellular staining. The T cells were stained with IL-9-PE-Cy7, IFN-γ-PE, TNF-α-APC, IL-17A-FITC, IL-4-PerCp-Cy5.5, IL-21-BV421 and IL-2-BV510 in saponin buffer (0.25% saponin, 0.1% Azide, 1% BSA in PBS; 0.4 µm filtered) for 30 min on ice. After staining cells were washed thrice with stain buffer before measurement on an LSR Fortessa.

Screen analysis

The quality of an assay to be used for screening can be assessed by the Z-factor (24). The Z-factor for the T cell differentiation infection assay was calculated from data the negative (empty vector) and positive controls (IFNB1 or TGFB1) using the following formula: $Z' = 1-(3*(\sigma_{empty\ vector} + \sigma_{positive\ control})/(|\mu_{empty\ vector} - \mu_{positive\ control}|))$, in which σ equals standard deviation, and µ equals mean.

All readout values of the secretome screens were normalized per plate by B-score normalization using R as described by Malo et al. (25). This method normalizes for plate and row confounding effects by iterative subtraction of median row and column values within a plate (excluding IFNB1 controls) from each individual well value. After performing this median polish, the median absolute deviation (MAD) was calculated for each plate: MAD = median {|polished_well – median(polished_wells_plate)|}. The B-score is calculated by dividing the polished value of each well by the MAD of the plate they were on. A positive B-score indicates that a sample has a higher value for the indicated readout compared to the median of all screen conditions (excluding IFNB1 controls), while a negative B-score indicates a decrease. The absolute B-score is dependent on the raw value of both individual datapoints as well as the variance across all samples for a single readout.

Statistics

P-values were determined by indicated statistical tests using R. The following symbols are used to indicate statistical significance: $p<0.05 = *$, $p<0.01 = **$, $p<0.001 = ***$, $p<0.0001 = ****$, n.s. = not significant.

Results

We previously generated a secreted protein library of 756 different conditioned media harvested from cDNA transfected HEK293T cells. The library contains a multitude of

Figure 1 Legend (continued)

generated previously (21). 466 additional cDNAs were now included in the library (part B). (C) Schematic of the T cell differentiation assay and flow cytometry panels. (D) CD8⁺ T cells cultured and stained with the T = 10 panel as in C (gating strategy in Fig. S1A), cultured with either empty vector (EV), TGFB1 or IFNB1 conditioned media. Statistical significance was determined by ANOVA followed by Dunnett's test. A Z' > 0 indicates that the difference between the indicated two conditions is sufficiently large enough for screening.

secreted proteins, some of which may modulate T cell differentiation or effector function. We have now extended this library with 466 secreted proteins, creating a secreted protein library (SPL) with a highly diverse content (Fig 1A). The SPL contains many immunological proteins such as cytokines and components of the complement system, but also hundreds of enzymes, protein hormones, growth factors and other secreted proteins including proteins of unknown function (Fig. 1A and Appendices: The Secreted Protein Library). The transfections were performed in multiple rounds, each of which included IFNG cDNA to monitor production efficiency. IFN-γ levels in these conditioned control media of the second set of the library (part B) were in the same range as the first (part A, Fig 1B), validating the consistent production of recombinant proteins in the library. Collected conditioned media were stored in aliquots for use in multiple screens.

To screen for novel modulators of T cell differentiation and function the following assay was used. First, activated FACS sorted human naive CD4$^+$ (CD4$^+$CD8$^-$CD45RA$^+$CD27$^+$) or naive CD8$^+$ (CD8$^+$CD4$^-$CD45RA$^+$CD27$^+$) T cells were cultured for three days with IL-2 and a suboptimal dose of αCD3 and αCD28 (Fig. 1C). The activated T cells were then exposed to the individual empty vector conditioned media in the presence of IL-15 to ensure cell viability. After seven days, half of the T cells were stained with the first flow cytometry panel to assess their memory differentiation state, while the other half was incubated o/n to be restimulated the next day with PMA/ionomycin in order to evaluate their cytokine production capacity using the second flow cytometry panel. CD4$^+$ and CD8$^+$ T cells treated with the same secreted protein were combined after culture for staining with two different antibody panels. Because PMA/ionomycin stimulation decreases expression of CD4 and CD8, we prelabeled CD4$^+$ but not CD8$^+$ T cells with anti-CD45 antibodies (Fig. 1C) (22) in order to distinguish both subsets. We then assessed the influence of each secreted protein on the differentiation, memory, and activation status of T cells by FACS analysis of the various markers as outlined in Figure 1C.

To determine the suitability of this assay for screening, we analyzed reproducibility using CD8$^+$ T cells stimulated with either control empty vector (EV), IFNB1 or TGFB1 conditioned media (Fig 1D, S1), with the first flow cytometry panel as readouts. In concordance with previous reports, IFNB1 significantly induced expression of CD69 and GZMB compared to EV, while TGFB1 induced expression of CD103 (23–26). Suitability of an assay for screening is generally determined by the calculation of the Z', a factor describing variability in relation to the effect size between negative and positive controls (27). For CD103, CD69 and GZMB we found a $0 < Z' < 0.5$ (see methods section), meaning the assay was sufficiently suitable for screening for these readouts. The variability of the other readouts was within the same range (Fig. S1), therefore small alterations in expression are likely to be detected in an assay with many conditions. Thus, the assay is suitable for screening.

The T cell differentiation screen was performed for all 1222 secreted proteins using IFNB1 and EV controls evenly spread over all 23 screen plates. Each conditioned media was tested in T cells from two donors, out of a total of three donors. We then searched

for screening hits based on individual and combined marker expression, which was subjected to B-score (gating in supplementary Fig. S2; Fig. S3-S5). The B-score calculation

Figure 2. Secretome screening reveals that type I IFNs affect T cells in 30% of all readouts. (A) Genes are considered hits in the secretome screens when meeting one of the two depicted criteria for at least one parameter, which depend on the deviation of measured values compared to the other genes in the screen. (B) Heatmap displaying for each hit for which parameter it was considered a hit (increase, red; decrease, blue).

consists of two phases which are executed for each readout separately. In the first phase each value is normalized across each row and column of a 96 well plate, called a median polish, to account for within-plate variability, while in the second phase the polished values are normalized to the absolute median of all conditions excluding IFNB1 controls to minimize between-plate variability. Positive B-scores indicate that a sample has a relatively high value for a readout compared to all other conditions, a negative B-score indicates a relatively low value. We then determined the expression difference between a single conditioned medium and all other conditioned media, as expressed by the number of standard deviations (SD) of all conditioned media excluding IFNB controls. For individual conditioned media to be selected for validation experiments, it needed to meet one of two selection criteria for at least one of the read-out parameters (Fig 2A). Replicates should either deviate at least 1 SD in one donor and 2.5 SD in the same direction in the other donor or deviate at least 4 SD in one of the two donors to be considered a hit. This hit selection procedure identified 66 conditioned media as hits, corresponding to 5% of the SPL (Fig. 2B). The hits and all of the measured parameters were hierarchically clustered. 15 conditioned media contained type I interferons (IFNs), of which 13 clustered together based on their similar broad effect on T cells (Fig. 2B). The IFNs in this cluster each altered expression of 18 to 56 readout parameters, including their previously described effect on expression of CD69, PD1 and GZMB (28–30). In contrast, 28 secreted proteins affected only one parameter, and eight proteins affected two parameters. Thus while type I IFNs affect a relatively large number of readouts in accordance with the study by Lin *et al.*, most secreted proteins induced a relatively specific phenotype (31).

TGFB3 and some of the type I IFNs induced CD27$^+$CCR7$^+$ double expression, a hallmark of T$_{cm}$ memory cells, only in CD8$^+$ T cells, while IL-2 negatively affected this phenotype only in CD4$^+$ T cells (Fig 2B). No soluble proteins were found to induce CD103$^+$CD69$^+$ co-expression in this specific T cell differentiation assay (Fig. 2B). Similarly, none of the secreted proteins substantially increased expression of IL-17 or IL-9, the expression of all other markers was altered by one or more secreted proteins (Fig. 2B). IL-4 induced IFN-γ expression in both CD4$^+$ and CD8$^+$ T cells, GHRH and CRISP2 in CD4$^+$ T cells only, while LCN8 promoted IFN-γ expression solely in CD8$^+$ T cells (Fig. 2B). Most IFNs reduced TNF-α and IL-2 expression in CD4$^+$ T cells, while only IFNA7, IFNA13 and IFNA21 induced both TNF-α and IL-2 in CD8$^+$ T cells. This indicates that while overall IFNs induced similar results, there are differences between IFNs conditioned media, which may be due to differences in concentration. In contrast, expression of CD69, CD103, PD-1 and IL-4 were increased in CD4$^+$ and/or CD8$^+$ T cells by either TGFB3 and/or multiple IFNs (Fig. 2B). IL-4, NXPH2 and SEMG1 reduced CD69 expression in CD8$^+$ T cells only. Finally, expression of GZMB and IL-21 were induced by IL-21 and multiple IFNs. GZMB expression in CD4$^+$ T cells was only promoted by IL-21 and IL-10 (Fig. 2B).

To prioritize which hits should be investigated further, for 54 hits new conditioned media were prepared and tested in a third donor. Only three out of 15 type I interferons

were repeated to avoid redundancy (IFNA2, IFNB1 and IFNW1). Most effects observed in the screen were not reproduced in this validation experiment, possibly because the biological effect size in the original screen donors of many of these hits was limited, while donor- or technical variation may have resulted in some conditioned media being hits in one donor and not in the other (Fig. S6). Still 11 out of 54 conditioned media did
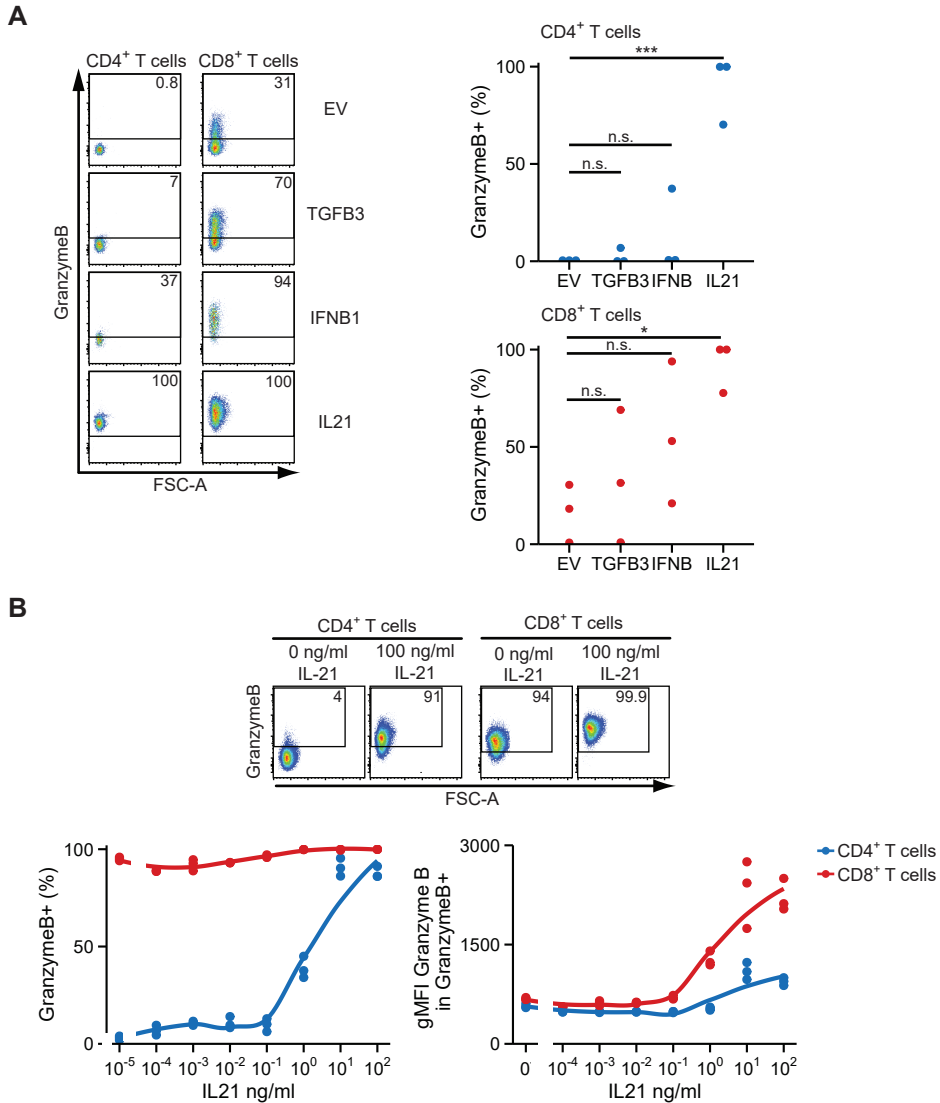
Figure 3. IL-21 promotes GZMB expression in CD4⁺ and CD8⁺ T cells. (A) Naive CD4⁺ and CD8⁺ T cells of three donors were cultured as in Fig. 1B in the presence of the depicted conditioned media followed by GZMB expression analysis by FACS. Example FACS plots (left panel) and quantified percentage of GZMB positive population in CD4⁺ and CD8⁺ T cells (right panels). Statistical significance was determined by ANOVA followed by Dunnett's test. (B) GZMB expression in terms of percentage (example FACS plots upper panel, quantified in bottom left panel) or geometric MFI (gMFI; bottom right panel) in T cells cultured as in A, replacing conditioned media for a serial dilution of commercially obtained purified recombinant IL-21. Three replicates of one donor.

alter marker expression, of which IL-21, TGFB3 and all three type I IFNs strongly induced expression of GZMB in CD8^{+} T cells, while only IL-21 induced GZMB in CD4^{+} T cells (Fig. S6). To further investigate these effects on GZMB expression, the same IFNB1, TGFB3 and Il-21 conditioned media were tested again in T cells from two other donors (Fig. 3A). IFNB1 and IL-21 induced GZMB expression in varying levels in CD8^{+} T cells in all three donors, TGFB3 only in two out of three donors. Yet only IL21 consistently induced GZMB expression in CD8^{+} and CD4^{+} T cells. A serial dilution showed that IL-21 impacted GZMB expression from 1 ng/ml onwards in both CD4^{+} and CD8^{+} T cells (Fig. 3B). Although almost all CD8^{+} T cells expressed GZMB in the absence of IL-21 in this donor, the expression per cell was consistently increased by IL-21. In contrast, CD4^{+} T cells did not express GZMB in the absence of IL-21, yet almost all CD4^{+} T cells were GZMB^{+} after stimulation with 100 ng/ ml IL21. The expression level per cell of granzyme B was lower in CD4^{+} T cells compared to CD8^{+} T cells. Importantly, we show here that IL-21 not only induces GZMB in CD8+ T cells, as reported previously, but also in CD4^{+} T cells.

Discussion

Comprehension of the extracellular signals which determine T cell differentiation will enable intervention in cases where the T cell immune response is lacking or deficient. In this study, we used an extensive library of secreted protein containing culture media to identify novel modulators that drive T cell activation or differentiation. This forward screening approach enables the discovery of (direct) causal relationships between a secreted protein and the observed differentiation state. Strikingly, all of the validated hits were immunology-associated proteins, while non-immunological proteins comprise over three quarters of the SPL. This outcome suggests that T cell differentiation is influenced by a limited set of secreted proteins. However, it does not imply a lack of interaction between immune- and non-immune cells as the secretion of these immunological proteins is not limited to immune cells. For example, fibroblasts can secrete multiple cytokines and chemokines, a feat which especially compromises T cell activity in tumors (32).

IL-21 strongly induced GZMB expression by CD4^{+} T cells. This cytokine is mainly produced by CD4^{+} T cells and NKT cells (33, 34). In CD4^{+} T cells IL-21 is described to support differentiation into Th17 cells, although there are varying reports whether this requires the presence of TGF-β or whether it can exert this effect in conjunction with αCD3 and αCD28 alone (35–38). In our culture system, IL-21 conditioned medium failed to induce IL-17 expression in either CD4^{+} or CD8^{+} T cells, indicating that the GZMB expression by CD4+ T cells is independent of a Th17 or Tc17 differentiation in our culture system. Variations in the exact culture conditions, such as how T cells are activated, whether full PBMCs or sorted naïve CD4^{+} T cells are used, what the timing and concentration of IL-21 is, and whether other cytokines are present, may very well explain the discrepancies between the aforementioned studies. The GZMB-inducing effects of IL-21 have been reported for CD8^{+} T cells, NK cells, B cells, and plasmacytoid dendritic cells (pDCs) (39–43). Yet, while

many studied the effects of IL-21 on CD4⁺ T cells, to our knowledge no one described an induction of GZMB in this cell type by IL-21.

GZMB is a well-known serine protease. NK cells, CD8⁺ and CD4⁺ cytotoxic T cells kill target cells by secreting perforin which creates pores in the membrane of the target cell, allowing a multitude of cytotoxic molecules including GZMB to enter the target cell. GZMB can cleave caspases, as well as the caspase targets BID and ICAD, leading to an induction of apoptosis (44–48). In addition, granzymes cleave viral and host proteins involved in viral replication (49, 50). The MHC class II restricted CD4⁺ cytotoxic T cells can kill cells presenting viral peptides, such as macrophages and dendritic cells, as well as tumor cells (11, 15, 51–55). Induction of cytotoxic CD4⁺ T cells can be beneficial under these pathological conditions, which may be promoted by IL-21. Yet, GZMB requires concerted perforin secretion to exert its cytotoxic effect. We were unable to successfully stain perforin in either CD8⁺ or CD4⁺ T cells, but as of writing we are investigating the cytotoxicity of CD4⁺ T cells by using target cells expressing membrane bound anti-CD3. Thus, it is unclear whether activated CD4⁺ T cells are indeed cytotoxic after culture with IL-21.

The proteolytic effects of GZMB are not solely pro-inflammatory, as it can also suppress T cell activity through different mechanisms. Anti-BCR and IL-21 stimulated B cells suppress T cell proliferation by cleaving the TCR-ζ chain intracellularly using GZMB, a mechanism which may be relevant in HIV where CD4⁺ T cells express insufficient CD40L, causing B cells to express GZMB resulting in further inhibition of T cell function (56–58). T cells internalize GZMB secreted by pDCs resulting in suppressed proliferation *in vitro* (40, 59). As both GZMB expressing pDCs and B cells are reported to lack perforin expression, it is unclear how GZMB enters T cells although alternative mechanisms are suggested (39, 59–61). Tregs suppress effector T cells using GZMB, yet the proposed mechanism here is cell death induction supported by perforin (62–64). Thus, GZMB can suppress T cells through different mechanisms, indicating that granzyme B expressing CD4⁺ T cells induced by IL-21 may suppress other T cells.

Both IL-21 and GZMB levels, or the cells that produce them, are increased in multiple autoimmune diseases, including Systemic Lupus Erythematosus (SLE), celiac disease, primary Sjögren's, and rheumatoid arthritis (65, 66, 75, 67–74). These proteins are associated with disease severity, yet a link between the two is underexplored in these diseases (76, 77). Nonetheless, granzyme B expressing CD8⁺ T cells correlate with active SLE (78). The granzyme B-inducing effect of IL-21 on multiple cell types, including CD4⁺ T cells as we now show, should be further explored in autoimmune disease to determine whether IL-21 is responsible for GZMB induction in these patients, and if the currently explored anti-IL-21 therapies affect GZMB producing cells (79–81).

In the current study we show IL-21 capable of inducing GZMB expression in CD4⁺ T cells. Further research should reveal whether IL-21 stimulated CD4⁺ T cells become cytotoxic or suppressive. Understanding how CD4⁺ T cells become cytotoxic or suppressive is relevant

4

for many immune related diseases, including viral infections, cancer, and autoimmunity.

Acknowledgments

References

1. Chang, J. T., E. J. Wherry, and A. W. Goldrath. 2014. Molecular regulation of effector and memory T cell differentiation. *Nat. Immunol.* 15: 1104–1115.
2. Jameson, S. C., and D. Masopust. 2018. Understanding Subset Diversity in T Cell Memory. *Immunity* 48: 214–226.
3. Cieri, N., B. Camisa, F. Cocchiarella, M. Forcato, G. Oliveira, E. Provasi, A. Bondanza, C. Bordignon, J. Peccatori, F. Ciceri, M. T. Lupo-Stanghellini, F. Mavilio, A. Mondino, S. Bicciato, A. Recchia, and C. Bonini. 2013. IL-7 and IL-15 instruct the generation of human memory stem T cells from naive precursors. *Blood* 121: 573–584.
4. Santegoets, S. J. A. M. a M., A. W. Turksma, M. M. Suhoski, A. G. M. M. Stam, S. M. Albelda, E. Hooijberg, R. J. Scheper, A. J. M. M. van den Eertwegh, W. R. Gerritsen, D. J. Powell, C. H. June, and T. D. de Gruijl. 2013. IL-21 promotes the expansion of CD27+ CD28+ tumor infiltrating lymphocytes with high cytotoxic potential and low collateral expansion of regulatory T cells. *J. Transl. Med.* 11: 37.
5. Li, K. P., B. H. Ladle, S. Kurtulus, A. Sholl, S. Shanmuganad, and D. A. Hildeman. 2020. T-cell receptor signal strength and epigenetic control of Bim predict memory CD8+ T-cell fate. *Cell Death Differ.* 27: 1214–1224.
6. Lopez, J. A., O. Susanto, M. R. Jenkins, N. Lukoyanova, V. R. Sutton, R. H. P. Law, A. Johnston, C. H. Bird, P. I. Bird, J. C. Whisstock, J. A. Trapani, H. R. Saibil, and I. Voskoboinik. 2013. Perforin forms transient pores on the target cell plasma membrane to facilitate rapid access of granzymes during killer cell attack. *Blood* 121: 2659–2668.
7. Ritter, A. T. T., Y. Asano, J. C. C. Stinchcombe, N. M. G. M. G. Dieckmann, B.-C. C. Chen, C. Gawden-Bone, S. van Engelenburg, W. Legant, L. Gao, M. W. W. Davidson, E. Betzig, J. Lippincott-Schwartz, G. M. M. Griffiths, S. van Engelenburg, W. Legant, L. Gao, M. W. W. Davidson, E. Betzig, J. Lippincott-Schwartz, and G. M. M. Griffiths. 2015. Actin Depletion Initiates Events Leading to Granule Secretion at the Immunological Synapse. *Immunity* 42: 864–876.
8. Shustov, A., P. Nguyen, F. Finkelman, K. B. Elkon, and C. S. Via. 1998. Differential expression of Fas and Fas ligand in acute and chronic graft-versus-host disease: up-regulation of Fas and Fas ligand requires CD8+ T cell activation and IFN-gamma production. *J. Immunol.* 161: 2848–55.
9. Ashkenazi, A., and V. M. Dixit. 1998. Death receptors: Signaling and modulation. *Science (80-.).* 281: 1305–1308.
10. Mucida, D., M. M. Husain, S. Muroi, F. van Wijk, R. Shinnakasu, Y. Naoe, B. S. Reis, Y. Huang, F. Lambolez, M. Docherty, A. Attinger, J.-W. Shui, G. Kim, C. J. Lena, S. Sakaguchi, C. Miyamoto, P. Wang, K. Atarashi, Y. Park, T. Nakayama, K. Honda, W. Ellmeier, M. Kronenberg, I. Taniuchi, and H. Cheroutre. 2013. Transcriptional reprogramming of mature CD4+ helper T cells generates distinct MHC class II-restricted cytotoxic T lymphocytes. *Nat. Immunol.* 14: 281–9.
11. Quezada, S. A., T. R. Simpson, K. S. Peggs, T. Merghoub, J. Vider, X. Fan, R. Blasberg, H. Yagita, P. Muranski, P. A. Antony, N. P. Restifo, and J. P. Allison. 2010. Tumor-reactive CD4(+) T cells develop cytotoxic activity and eradicate large established melanoma after transfer into lymphopenic hosts. *J. Exp. Med.* 207: 637–50.
12. Vargas, T. R., and L. Apetoh. 2018. The Secrets of T Cell Polarization. In *Oncoimmunology* L. Zitvogel, and G. Kroemer, eds. 69–95.
13. Croft, M., L. Carter, S. L. Swain, and R. W. Dutton. 1994. Generation of Polarized Antigen-specific CD8 Effector Populations: Reciprocal Action of Interleukin (IL)-4 and IL-12 in Promoting Type 2 versus Type 1 Cytokine Profiles. *J. Exp. Med.* 180: 1715–1728.
14. Yen, H.-R., T. J. Harris, S. Wada, J. F. Grosso, D. Getnet, M. V. Goldberg, K.-L. Liang, T. C. Bruno, K. J. Pyle, S.-L. Chan, R. A. Anders, C. L. Trimble, A. J. Adler, T.-Y. Lin, D. M. Pardoll, C.-T. Huang, and C. G. Drake. 2009. Tc17 CD8 T Cells: Functional Plasticity and Subset Diversity. *J. Immunol.* 183: 7161–7168.

15. Spaapen, R. M., H. M. Lokhorst, K. Den Van Oudenalder, B. E. Otterud, H. Dolstra, M. F. Leppert, M. C. Minnema, A. C. Bloem, and T. Mutis. 2008. Toward targeting B cell cancers with CD4 + CTLs: Identification of a CD19-encoded minor histocompatibility antigen using a novel genome-wide analysis. *J. Exp. Med.* 205: 2863–2872.

16. Licona-Limón, P., J. Henao-Mejia, A. U. Temann, N. Gagliani, I. Licona-Limón, H. Ishigame, L. Hao, D. R. Herbert, and R. A. Flavell. 2013. Th9 Cells Drive Host Immunity against Gastrointestinal Worm Infection. *Immunity* 39: 744–57.

17. Purwar, R., C. Schlapbach, S. Xiao, H. S. Kang, W. Elyaman, X. Jiang, A. M. Jetten, S. J. Khoury, R. C. Fuhlbrigge, V. K. Kuchroo, R. A. Clark, and T. S. Kupper. 2012. Robust tumor immunity to melanoma mediated by interleukin-9-producing T cells. *Nat. Med.* 18: 1248–53.

18. Lu, Y., S. Hong, H. Li, J. Park, B. Hong, L. Wang, Y. Zheng, Z. Liu, J. Xu, J. He, J. Yang, J. Qian, and Q. Yi. 2012. Th9 cells promote antitumor immune responses in vivo. *J. Clin. Invest.* 122: 4160–71.

19. Lu, Y., B. Hong, H. Li, Y. Zheng, M. Zhang, S. Wang, J. Qian, and Q. Yi. 2014. Tumor-specific IL-9-producing CD8+ Tc9 cells are superior effector than type-I cytotoxic Tc1 cells for adoptive immunotherapy of cancers. *Proc. Natl. Acad. Sci. U. S. A.* 111: 2265–70.

20. Shinnakasu, R., and T. Kurosaki. 2017. Regulation of memory B and plasma cell differentiation. *Curr. Opin. Immunol.* 45: 126–131.

21. van Asten, S. D., M. Raaben, B. Nota, and R. M. Spaapen. 2018. Secretome Screening Reveals Fibroblast Growth Factors as Novel Inhibitors of Viral Replication. *J. Virol.* 92: JVI.00260-18.

22. O'Neil-Andersen, N. J., and D. A. Lawrence. 2002. Differential modulation of surface and intracellular protein expression by T cells after stimulation in the presence of monensin or brefeldin A. *Clin. Diagn. Lab. Immunol.* 9: 243–250.

23. Newby, B. N., T. M. Brusko, B. Zou, M. A. Atkinson, M. Clare-Salzler, and C. E. Mathews. 2017. Type 1 interferons potentiate human cd8+ t-cell cytotoxicity through a stat4-and granzyme b-dependent pathway. *Diabetes* 66: 3061–3071.

24. Urban, S. L., L. J. Berg, and R. M. Welsh. 2016. Type 1 interferon licenses naïve CD8 T cells to mediate anti-viral cytotoxicity. *Virology* 493: 52–59.

25. Hadley, G. A., E. A. Rostapshova, D. M. Gomolka, B. M. Taylor, S. T. Bartlett, C. I. Drachenberg, and M. R. Weir. 1999. Regulation of the epithelial cell-specific integrin, CD103, by human CD8+ cytolytic T lymphocytes. *Transplantation* 67: 1418–1425.

26. Robertson, H., W. Keong Wong, D. Talbot, A. D. Burt, and J. A. Kirby. 2001. Tubulitis after renal transplantation: Demonstration of an association between CD103+ T cells, transforming growth factor β1 expression and rejection grade. *Transplantation* 71: 306–313.

27. Zhang, J., T. D. Y. Chung, and K. R. Oldenburg. 1999. A Simple Statistical Parameter for Use in Evaluation and Validation of High Throughput Screening Assays. *J. Biomol. Screen.* 4: 67–73.

28. Sun, S., X. Zhang, D. F. Tough, and J. Sprent. 1998. Type I Interferon-mediated Stimulation of T Cells by CpG DNA. *J. Exp. Med.* 188: 2335–2342.

29. Terawaki, S., S. Chikuma, S. Shibayama, T. Hayashi, T. Yoshida, T. Okazaki, and T. Honjo. 2011. IFN-α Directly Promotes Programmed Cell Death-1 Transcription and Limits the Duration of T Cell-Mediated Immunity. *J. Immunol.* 186: 2772–2779.

30. Curtsinger, J. M., J. O. Valenzuela, P. Agarwal, D. Lins, and M. F. Mescher. 2005. Cutting Edge: Type I IFNs Provide a Third Signal to CD8 T Cells to Stimulate Clonal Expansion and Differentiation. *J. Immunol.* 174: 4465–4469.

31. Lin, H., E. Lee, K. Hestir, C. Leo, M. Huang, E. Bosch, R. Halenbeck, G. Wu, A. Zhou, D. Behrens, D. Hollenbaugh, T. Linnemann, M. Qin, J. Wong, K. Chu, S. K. Doberstein, and L. T. Williams. 2008. Discovery of a cytokine and its receptor by functional screening of the extracellular proteome. *Science* 320: 807–811.

32. Monteran, L., and N. Erez. 2019. The dark side of fibroblasts: Cancer-associated fibroblasts as mediators of immunosuppression in the tumor microenvironment. *Front. Immunol.* 10: 1835.

33. Coquet, J. M., K. Kyparissoudis, D. G. Pellicci, G. Besra, S. P. Berzins, M. J. Smyth, and D. I. Godfrey. 2007. IL-21 Is Produced by NKT Cells and Modulates NKT Cell Activation and Cytokine Production. *J. Immunol.* 178: 2827–2834.

34. Parrish-Novak, J., S. R. Dillon, A. Nelson, A. Hammond, C. Sprecher, J. A. Gross, J. Johnston, K. Madden, W. Xu, J. West, S. Schrader, S. Burkhead, M. Heipel, C. Brandt, J. L. Kuijper, J. Kramer, D. Conklin, S. R. Presnell, J. Berry, F. Shiota, S. Bort, K. Hambly, S. Mudri, C. Clegg, M. Moore, F. J. Grant, C. Lofton-Day, T. Gilbert, F. Raymond, A. Ching, L. Yao, D. Smith, P. Webster, T. Whitmore, M. Maurer, K. Kaushansky, R. D. Holly, and D. Foster. 2000. Interleukin 21 and its receptor are involved in NK cell expansion and regulation of lymphocyte function. *Nature* 408: 57–63.

35. Kastirr, I., S. Maglie, M. Paroni, J. S. Alfen, E. Nizzoli, E. Sugliano, M.-C. Crosti, M. Moro, B. Steckel, S. Steinfelder, K. Stölzel, C. Romagnani, F. Botti, F. Caprioli, M. Pagani, S. Abrignani, and J. Geginat. 2014. IL-21 is a central

4

memory T cell-associated cytokine that inhibits the generation of pathogenic Th1/17 effector cells. *J. Immunol.* 193: 3322–31.

36. Yang, L., D. E. Anderson, C. Baecher-Allan, W. D. Hastings, E. Bettelli, M. Oukka, V. K. Kuchroo, and D. A. Hafler. 2008. IL-21 and TGF-β are required for differentiation of human T H17 cells. *Nature* 454: 350–352.

37. Tian, Y., C. Yuan, D. Ma, Y. Zhang, Y. Liu, W. Zhang, F. Hou, and B. Cui. 2011. IL-21 and IL-12 Inhibit Differentiation of Treg and T H 17 Cells and Enhance Cytotoxicity of Peripheral Blood Mononuclear Cells in Patients With Cervical Cancer. *Int. J. Gynecol. Cancer* 21.

38. Liu, Z., L. Yang, Y. Cui, X. Wang, C. Guo, Z. Huang, Q. Kan, Z. Liu, and Y. Liu. 2009. IL-21 enhances NK cell activation and cytolytic activity and induces Th17 cell differentiation in inflammatory bowel disease. *Inflamm. Bowel Dis.* 15: 1133–1144.

39. Hagn, M., E. Schwesinger, V. Ebel, K. Sontheimer, J. Maier, T. Beyer, T. Syrovets, Y. Laumonnier, D. Fabricius, T. Simmet, and B. Jahrsdörfer. 2009. Human B Cells Secrete Granzyme B When Recognizing Viral Antigens in the Context of the Acute Phase Cytokine IL-21. *J. Immunol.* 183: 1838–1845.

40. Karrich, J. J., L. C. M. Jachimowski, M. Nagasawa, A. Kamp, M. Balzarolo, M. C. Wolkers, C. H. Uittenbogaart, S. M. Van Ham, and B. Blom. 2013. IL-21–stimulated human plasmacytoid dendritic cells secrete granzyme B, which impairs their capacity to induce T-cell proliferation. *Blood* 121: 3103–3111.

41. Zeng, R., R. Spolski, S. E. Finkelstein, S. Oh, P. E. Kovanen, C. S. Hinrichs, C. A. Pise-Masison, M. F. Radonovich, J. N. Brady, N. P. Restifo, J. A. Berzofsky, and W. J. Leonard. 2005. Synergy of IL-21 and IL-15 in regulating CD8 + T cell expansion and function. *J. Exp. Med.* 201: 139–148.

42. Sutherland, A. P. R., N. Joller, M. Michaud, S. M. Liu, V. K. Kuchroo, and M. J. Grusby. 2013. IL-21 Promotes CD8 + CTL Activity via the Transcription Factor T-bet . *J. Immunol.* 190: 3977–3984.

43. Skak, K., K. S. Frederiksen, and D. Lundsgaard. 2008. Interleukin-21 activates human natural killer cells and modulates their surface receptor expression. *Immunology* 123: 575–583.

44. Darmon, A. J., D. W. Nicholson, and R. C. Bleackley. 1995. Activation of the apoptotic protease CPP32 by cytotoxic T-cell-derived granzyme B. *Nature* 377: 446–448.

45. Barry, M., J. A. Heibein, M. J. Pinkoski, S.-F. Lee, R. W. Moyer, D. R. Green, and R. C. Bleackley. 2000. Granzyme B Short-Circuits the Need for Caspase 8 Activity during Granule-Mediated Cytotoxic T-Lymphocyte Killing by Directly Cleaving Bid. *Mol. Cell. Biol.* 20: 3781–3794.

46. Thomas, D. A., C. Du, M. Xu, X. Wang, and T. J. Ley. 2000. DFF45/ICAD can be directly processed by granzyme B during the induction of apoptosis. *Immunity* 12: 621–632.

47. Sharif-Askari, E., A. Alam, E. Rhéaume, P. J. Beresford, C. Scotto, K. Sharma, D. Lee, W. E. DeWolf, M. E. Nuttall, J. Lieberman, and R. P. Sékaly. 2001. Direct cleavage of the human DNA fragmentation factor-45 by granzyme B induces caspase-activated DNase release and DNA fragmentation. *EMBO J.* 20: 3101–3113.

48. Adrain, C., B. M. Murphy, and S. J. Martin. 2005. Molecular ordering of the caspase activation cascade initiated by the cytotoxic T lymphocyte/natural killer (CTL/NK) protease granzyme B. *J. Biol. Chem.* 280: 4663–4673.

49. van Domselaar, R., and N. Bovenschen. 2011. Cell death-independent functions of granzymes: Hit viruses where it hurts. *Rev. Med. Virol.* 21: 301–314.

50. Romero, V., and F. Andrade. 2008. Non-apoptotic functions of granzymes. *Tissue Antigens* 71: 409–416.

51. Sacha, J. B., J. P. Giraldo-Vela, M. B. Buechler, M. A. Martins, N. J. Maness, W. Chung, L. T. Wallace, E. J. Leóna, T. C. Friedrich, N. A. Wilson, A. Hiraoka, and D. I. Watkins. 2009. Gag- and Nef-specific CD4+ T cells recognize and inhibit SIV replication in infected macrophages early after infection. *Proc. Natl. Acad. Sci. U. S. A.* 106: 9791–9796.

52. Wahid, R., M. J. Cannon, and M. Chow. 2005. Virus-Specific CD4 + and CD8 + Cytotoxic T-Cell Responses and Long-Term T-Cell Memory in Individuals Vaccinated against Polio . *J. Virol.* 79: 5988–5995.

53. Marshall, N. B., and S. L. Swain. 2011. Cytotoxic CD4 T cells in antiviral immunity. *J. Biomed. Biotechnol.* 2011.

54. Oh, D. Y., S. S. Kwek, S. S. Raju, T. Li, E. McCarthy, E. Chow, D. Aran, A. Ilano, C. C. S. Pai, C. Rancan, K. Allaire, A. Burra, Y. Sun, M. H. Spitzer, S. Mangul, S. Porten, M. V. Meng, T. W. Friedlander, C. J. Ye, and L. Fong. 2020. Intratumoral CD4+ T Cells Mediate Anti-tumor Cytotoxicity in Human Bladder Cancer. *Cell* 181: 1612-1625. e13.

55. Spaapen, R. M., R. W. J. Groen, K. van den Oudenalder, T. Guichelaar, M. van Elk, T. Aarts-Riemens, A. C. Bloem, G. Storm, A. C. Martens, H. M. Lokhorst, and T. Mutis. 2010. Eradication of medullary multiple myeloma by CD4+ cytotoxic human T lymphocytes directed at a single minor histocompatibility antigen. *Clin. Cancer Res.* 16: 5481–8.

56. Lindner, S., K. Dahlke, K. Sontheimer, M. Hagn, C. Kaltenmeier, T. F. E. Barth, T. Beyer, F. Reister, D. Fabricius, R. Lotfi, O. Lunov, G. U. Nienhaus, T. Simmet, R. Kreienberg, P. Moller, H. Schrezenmeier, and B. Jahrsdorfer. 2013. Interleukin 21-induced granzyme b-expressing b cells infiltrate tumors and regulate t cells. *Cancer Res.* 73: 2468–2479.

57. Kaltenmeier, C., A. Gawanbacht, T. Beyer, S. Lindner, T. Trzaska, J. A. van der Merwe, G. Härter, B. Grüner,

D. Fabricius, R. Lotfi, K. Schwarz, C. Schütz, M. Hönig, A. Schulz, P. Kern, M. Bommer, H. Schrezenmeier, F. Kirchhoff, and B. Jahrsdörfer. 2015. CD4 + T Cell–Derived IL-21 and Deprivation of CD40 Signaling Favor the In Vivo Development of Granzyme B–Expressing Regulatory B Cells in HIV Patients. *J. Immunol.* 194: 3768–3777.

58. Wieckowski, E., G.-Q. Wang, B. R. Gastman, L. A. Goldstein, and H. Rabinowich. 2002. Granzyme B-mediated degradation of T-cell receptor zeta chain. *Cancer Res.* 62: 4884–9.

59. Jahrsdörfer, B., A. Vollmer, S. E. Blackwell, J. Maier, K. Sontheimer, T. Beyer, B. Mandel, O. Lunov, K. Tron, G. Ulrich Nienhaus, T. Simmet, K. M. Debatin, G. J. Weiner, and D. Fabricius. 2010. Granzyme B produced by human plasmacytoid dendritic cells suppresses T-cell expansion. *Blood* 115: 1156–1165.

60. Froelich, C. J., K. Orth, J. Turbov, P. Seth, R. Gottlieb, B. Babior, G. M. Shah, R. C. Bleackley, V. M. Dixit, and W. Hanna. 1996. New paradigm for lymphocyte granule-mediated cytotoxicity: Target cells bind and internalize granzyme B, but an endosomolytic agent is necessary for cytosolic delivery and subsequent apoptosis. *J. Biol. Chem.* 271: 29073–29079.

61. Gross, C., W. Koelch, A. DeMaio, N. Arispe, and G. Multhoff. 2003. Cell Surface-bound Heat Shock Protein 70 (Hsp70) Mediates Perforin-independent Apoptosis by Specific Binding and Uptake of Granzyme B. *J. Biol. Chem.* 278: 41173–41181.

62. Loebbermann, J., H. Thornton, L. Durant, T. Sparwasser, K. E. Webster, J. Sprent, F. J. Culley, C. Johansson, and P. J. Openshaw. 2012. Regulatory T cells expressing granzyme B play a critical role in controlling lung inflammation during acute viral infection. *Mucosal Immunol.* 5: 161–172.

63. Sun, B., M. Liu, M. Cui, and T. Li. 2020. Granzyme B-expressing treg cells are enriched in colorectal cancer and present the potential to eliminate autologous T conventional cells. *Immunol. Lett.* 217: 7–14.

64. Cao, X., S. F. Cai, T. A. Fehniger, J. Song, L. I. Collins, D. R. Piwnica-Worms, and T. J. Ley. 2007. Granzyme B and Perforin Are Important for Regulatory T Cell-Mediated Suppression of Tumor Clearance. *Immunity* 27: 635–646.

65. Tak, P. P., L. Spaeny-Dekking, M. C. Kraan, F. C. Breedveld, C. J. Froelich, and C. E. Hack. 1999. The levels of soluble granzyme A and B are elevated in plasma and synovial fluid of patients with rheumatoid arthritis (RA). *Clin. Exp. Immunol.* 116: 366–70.

66. Spaeny-Dekking, E. H. A., W. L. Hanna, A. M. Wolbink, P. C. Wever, A. J. Kummer, A. J. G. Swaak, J. M. Middeldorp, H. G. Huisman, C. J. Froelich, and C. E. Hack. 2009. Extracellular granzymes A and B in humans: Detection of native species during CTL responses in vitro and in vivo. *J. Immunol.* 182: 5152.1-5152.

67. Augustin, M. T., J. Kokkonen, R. Karttunen, and T. J. Karttunen. 2005. Serum granzymes and CD30 are increased in children's milk protein sensitive enteropathy and celiac disease. *J. Allergy Clin. Immunol.* 115: 157–62.

68. Kok, H. M., L. L. van den Hoogen, J. A. G. van Roon, E. J. M. Adriaansen, R. D. E. Fritsch-Stork, T. Q. Nguyen, R. Goldschmeding, T. R. D. J. Radstake, and N. Bovenschen. 2017. Systemic and local granzyme B levels are associated with disease activity, kidney damage and interferon signature in systemic lupus erythematosus. *Rheumatology* 56: 2129–2134.

69. Dolff, S., W. H. Abdulahad, J. Westra, B. Doornbos-van der Meer, P. C. Limburg, C. G. M. Kallenberg, and M. Bijl. 2011. Increase in IL-21 producing T-cells in patients with systemic lupus erythematosus. *Arthritis Res. Ther.* 13: R157.

70. Nakou, M., E. D. Papadimitraki, A. Fanouriakis, G. K. Bertsias, C. Choulaki, N. Goulidaki, P. Sidiropoulos, and D. T. Boumpas. Interleukin-21 is increased in active systemic lupus erythematosus patients and contributes to the generation of plasma B cells. *Clin. Exp. Rheumatol.* 31: 172–9.

71. Fina, D., M. Sarra, R. Caruso, G. Del Vecchio Blanco, F. Pallone, T. T. MacDonald, and G. Monteleone. 2008. Interleukin 21 contributes to the mucosal T helper cell type 1 response in coeliac disease. *Gut* 57: 887–92.

72. Gottenberg, J.-E., J.-M. Dayer, C. Lukas, B. Ducot, G. Chiocchia, A. Cantagrel, A. Saraux, P. Roux-Lombard, and X. Mariette. 2012. Serum IL-6 and IL-21 are associated with markers of B cell activation and structural progression in early rheumatoid arthritis: results from the ESPOIR cohort. *Ann. Rheum. Dis.* 71: 1243–1248.

73. Liu, R., Q. Wu, D. Su, N. Che, H. Chen, L. Geng, J. Chen, W. Chen, X. Li, and L. Sun. 2012. A regulatory effect of IL-21 on T follicular helper-like cell and B cell in rheumatoid arthritis. *Arthritis Res. Ther.* 14: R255.

74. Ma, J., C. Zhu, B. Ma, J. Tian, S. E. Baidoo, C. Mao, W. Wu, J. Chen, J. Tong, M. Yang, Z. Jiao, H. Xu, L. Lu, and S. Wang. 2012. Increased Frequency of Circulating Follicular Helper T Cells in Patients with Rheumatoid Arthritis. *Clin. Dev. Immunol.* 2012: 1–7.

75. Papp, G., E. Gyimesi, K. Szabó, É. Zöld, and M. Zeher. 2016. Increased IL-21 Expression Induces Granzyme B in Peripheral CD5 + B Cells as a Potential Counter-Regulatory Effect in Primary Sjögren's Syndrome. *Mediators Inflamm.* 2016: 1–8.

76. Dinesh, P., and M. Rasool. 2018. Multifaceted role of IL-21 in rheumatoid arthritis: Current understanding and future perspectives. *J. Cell. Physiol.* 233: 3918–3928.

77. Long, D., Y. Chen, H. Wu, M. Zhao, and Q. Lu. 2019. Clinical significance and immunobiology of IL-21 in

autoimmunity. *J. Autoimmun.* 99: 1–14.

78. Blanco, P., V. Pitard, J.-F. Viallard, J.-L. Taupin, J.-L. Pellegrin, and J.-F. Moreau. 2005. Increase in activated CD8+ T lymphocytes expressing perforin and granzyme B correlates with disease activity in patients with systemic lupus erythematosus. *Arthritis Rheum.* 52: 201–211.

79. Ignatenko, S., B. K. Skrumsager, and U. Mouritzen. 2016. Safety, PK, and PD of recombinant anti-interleukin-21 monoclonal antibody in a first-in-human trial. *Int. J. Clin. Pharmacol. Ther.* 54: 243–52.

80. von Herrath, M., S. C. Bain, B. Bode, J. O. Clausen, K. Coppieters, L. Gaysina, J. Gumprecht, T. K. Hansen, C. Mathieu, C. Morales, O. Mosenzon, S. Segel, G. Tsoukas, T. R. Pieber, and Anti-IL-21–liraglutide Study Group investigators and contributors. 2021. Anti-interleukin-21 antibody and liraglutide for the preservation of β-cell function in adults with recent-onset type 1 diabetes: a randomised, double-blind, placebo-controlled, phase 2 trial. *lancet. Diabetes Endocrinol.* 9: 212–224.

81. Hussaini, A., R. Mukherjee, D. M. Berdieva, C. Glogowski, R. Mountfield, and P. T. C. Ho. 2020. A Double-Blind, Phase I, Single Ascending Dose Study to Assess the Safety, Pharmacokinetics, and Pharmacodynamics of BOS161721 in Healthy Subjects. *Clin. Transl. Sci.* 13: 337–344.

82. Gene Ontology Consortium. 2015. Gene Ontology Consortium: going forward. *Nucleic Acids Res.* 43: D1049-1056.

83. Ashburner, M., C. A. Ball, J. A. Blake, D. Botstein, H. Butler, J. M. Cherry, A. P. Davis, K. Dolinski, S. S. Dwight, J. T. Eppig, M. A. Harris, D. P. Hill, L. Issel-Tarver, A. Kasarskis, S. Lewis, J. C. Matese, J. E. Richardson, M. Ringwald, G. M. Rubin, and G. Sherlock. 2000. Gene ontology: tool for the unification of biology. The Gene Ontology Consortium. *Nat. Genet.* 25: 25–29.

84. Mi, H., X. Huang, A. Muruganujan, H. Tang, C. Mills, D. Kang, and P. D. Thomas. 2017. PANTHER version 11: expanded annotation data from Gene Ontology and Reactome pathways, and data analysis tool enhancements. *Nucleic Acids Res.* 45: D183–D189.

Supplementary figures

A
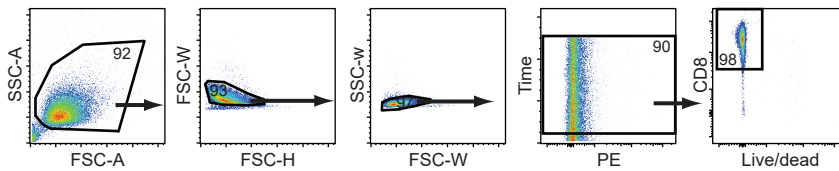
B
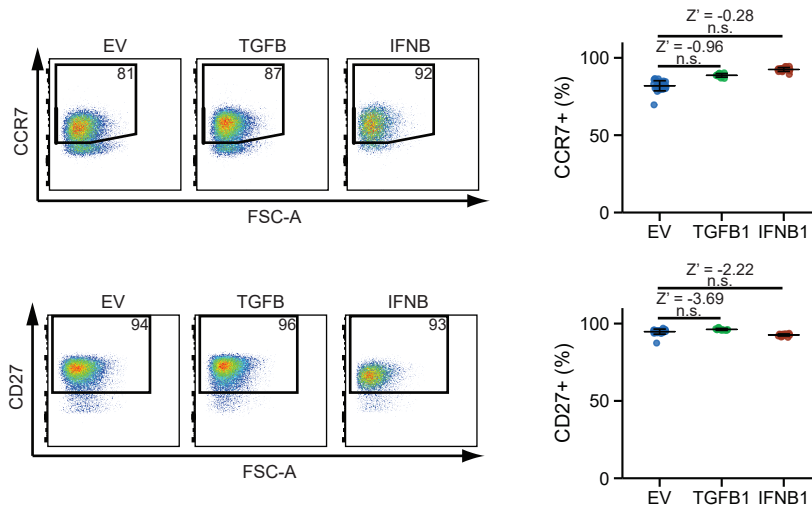
Figure S1. TGFB1 nor IFNB1 strongly affect CCR7 or CD27 expression in CD8+ T cells. CD8+ T cells were cultured in the presence of empty vector (EV), TGFB1 or IFNB1 conditioned medium and analyzed by FACS (same experiments as in Fig. 1D). (A) Gating strategy to include only live CD8+ T cells, and to exclude debris and doublets. (B) Expression of CCR7 and CD27 in CD8+ T cells. Statistical significance was determined by ANOVA followed by Dunnett's test. A Z' > 0 indicates that the difference between the indicated two conditions is sufficiently large enough for screening.

4

Figure S2. Gating strategy for the secreted protein library screen on T cell differentiation. (A) At day 10 of culture, half of the separately cultured CD4+ and CD8+ T cells treated with the same conditions were combined in one well for staining and flow cytometry analysis (see schematic overview in Fig. 1C). For each sample, events were included based on forward and side scatter (single cells) and absence of disturbances in flow over time. CD8+ T cells were identified as CD8+ and negative for the live/dead marker, CD4+ T cells as CD8- and negative for the live/dead marker. Further gates were set separately for both T cell subsets as indicated. (B) After 5h stimulation with PMA/ionomycin and brefeldin A on day 11, CD4+ T cells were stained for CD45. Then, CD4+ and CD8+ T cells of matching conditions were combined for further staining and flow cytometry analysis. Events were included based on forward and side scatter (single cells) and absence of irregularities in flow over time. CD4+ T cells were identified as CD45+, CD8+ T cells as CD45-, both negative for the live/dead marker. Further gates were set separately for both T cell subsets as indicated.

A
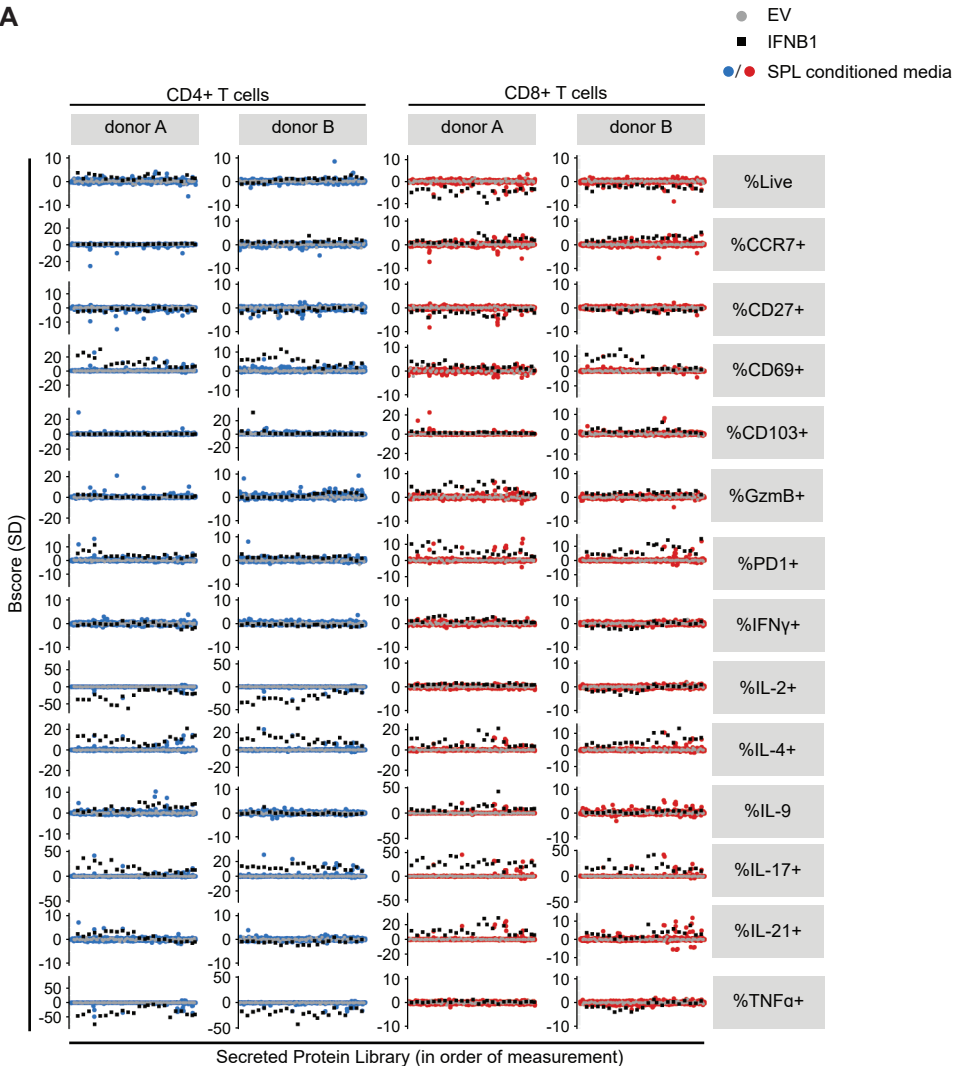
Figure S3. Secreted protein library screen reveals that several individual conditioned media affect the readout parameters (annotated in Fig. 2B). Each individual conditioned medium of the secreted protein library was tested for the ability to affect differentiation in T cells of two healthy donors following the protocol shown in Fig. 1C. Each value per parameter value (percentage of positive cells (A), normalized geometric MFI (gMFI) (B) and percentage of positive cells for combinations of two or three related parameters (C)) was normalized per plate using B-score normalization. Plots show for every individual parameter the number of standard deviations each conditioned media deviates from the entire screen B-score median (excluding IFNB1 controls).

(Continued on next page)

B

CD4+ T cells — donor A, donor B; CD8+ T cells — donor A, donor B

Legend: EV; IFNB1; SPL conditioned media

Markers: gMFI CD69, gMFI PD1, gMFI CD103, gMFI CCR7, gMFI GzmB, gMFI CD27, gMFI PD1+, gMFI GzmB+, gMFI CD103+, gMFI CD69+, gMFI TNFα, gMFI IL-2, gMFI IFNγ, gMFI IFNγ+, gMFI IL-4, gMFI IL-21

B score (SD)

Secreted Protein Library (in order of measurement)
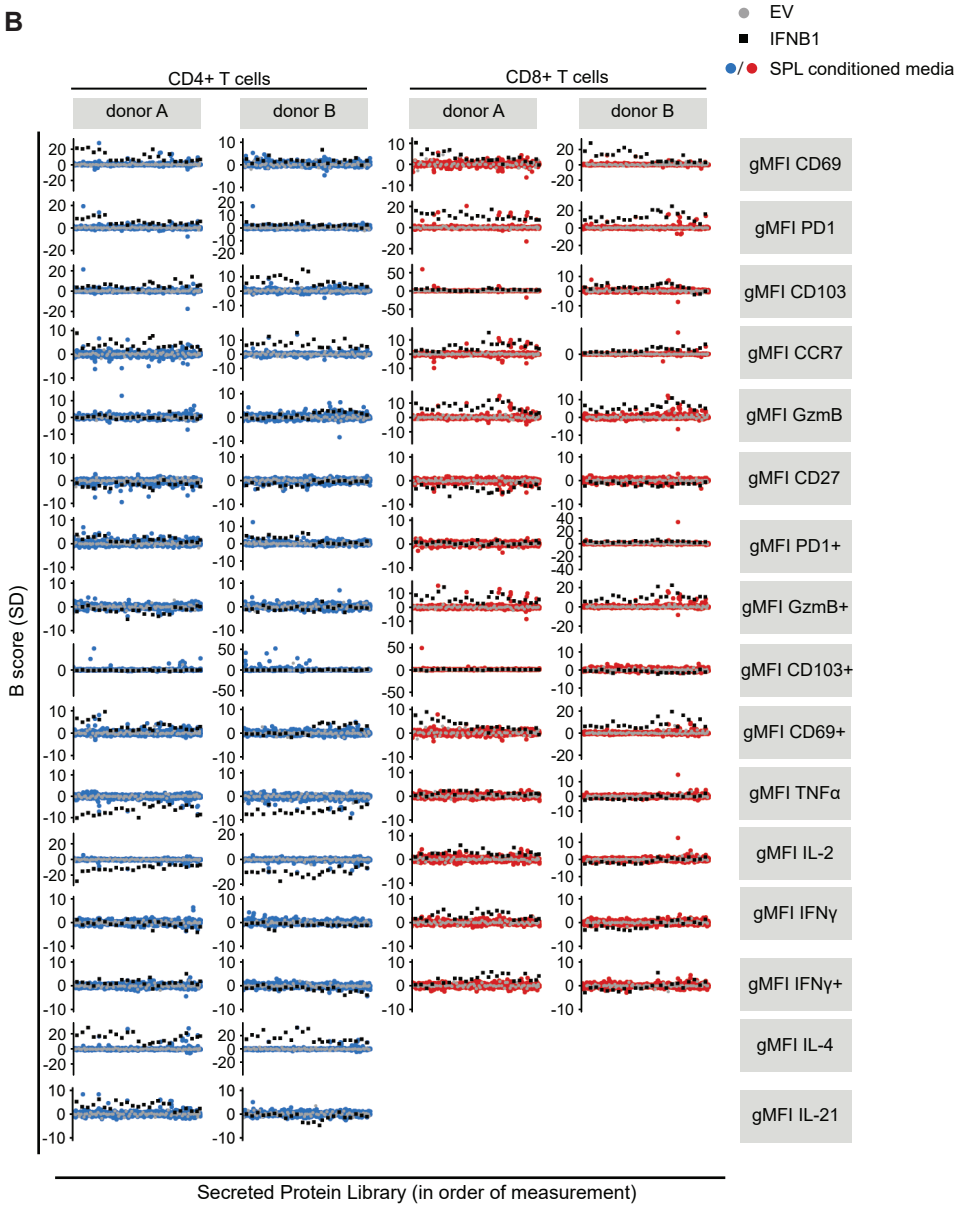
(Continued on next page)

C
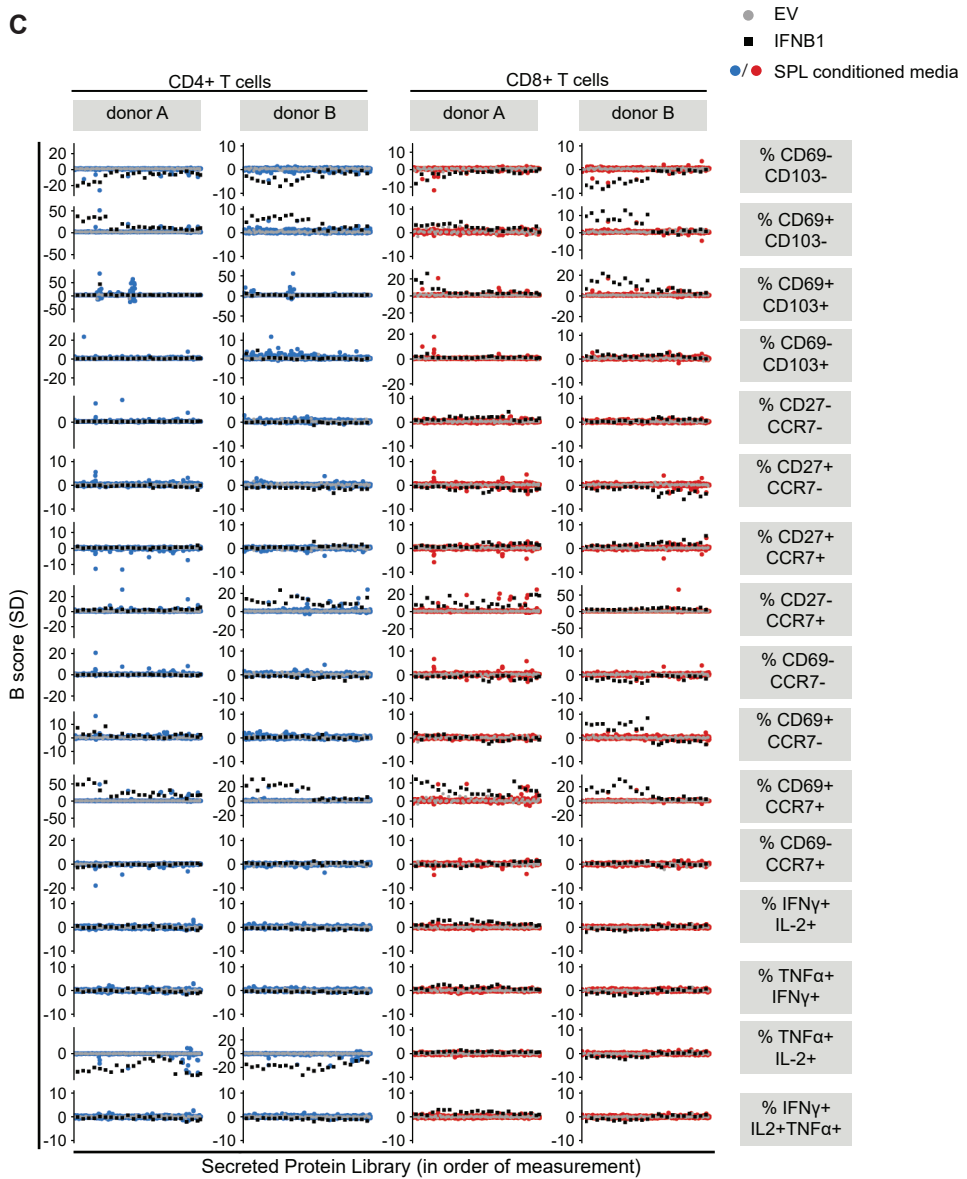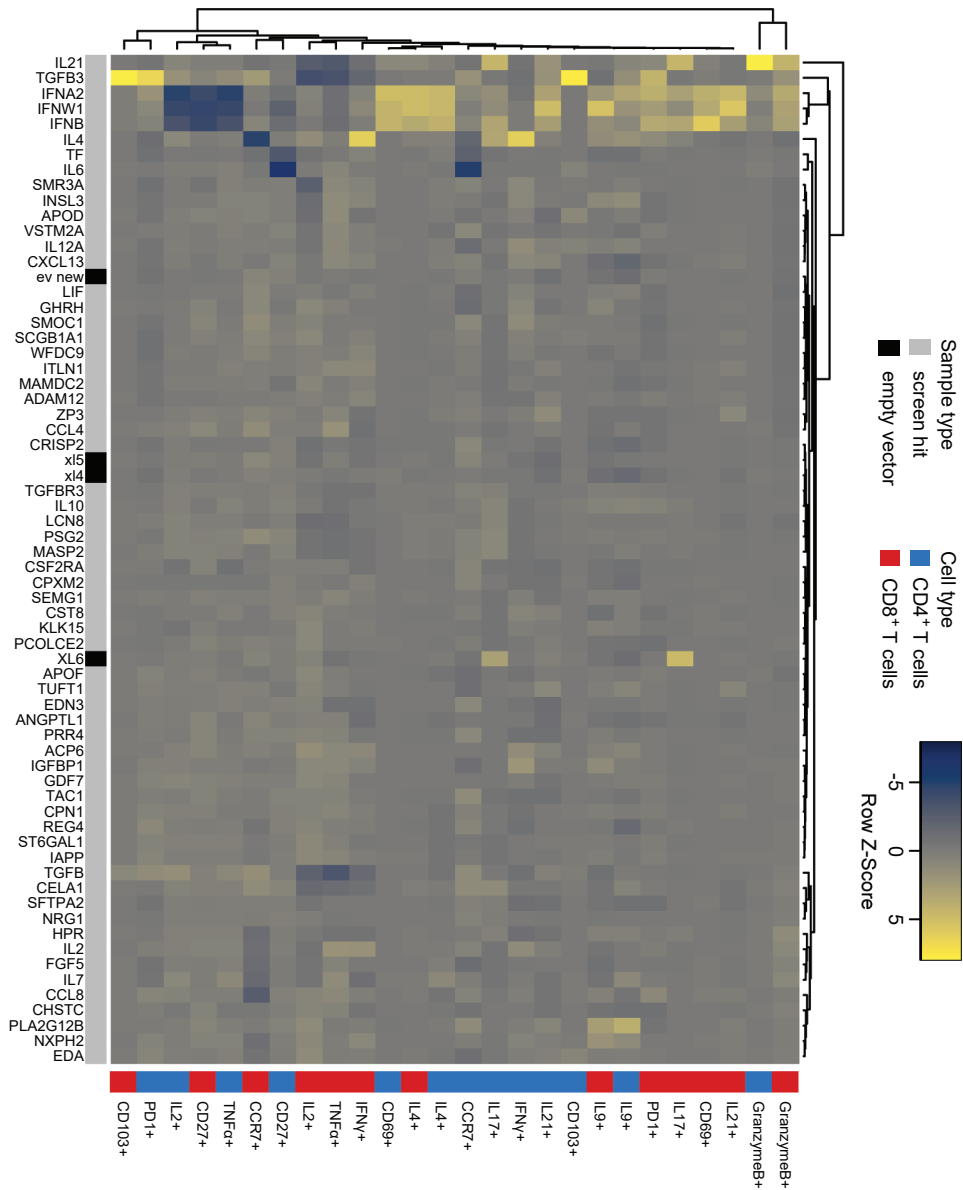
Figure S4. GZMB expression in CD4+ and CD8+ T cells is affected by multiple conditioned media. CD4+ and CD8+ T cells were assayed as in Fig. 1C, using the conditioned media displayed on the x-axis of the heatmap. Each parameter on the y-axis is shown separately for CD4+ (blue) and CD8+ (red) T cells. The flow cytometry obtained values for each parameter in CD4+ or CD8+ T cells were z-score normalized and shown as heatplot following the in-figure legend.

4

CHAPTER 5

T cells expanded from renal cell carcinoma display tumor-specific CD137 expression but lack significant IFN-γ, TNF-α or IL-2 production

Saskia D. van Asten[#], Rosa de Groot[#], Marleen M. van Loenen, Suzanne M. Castenmiller, Jeroen de Jong, Kim Monkhorst, John B.A.G. Haanen, Derk Amsen, Axel Bex, Robbert M. Spaapen[$], Monika C. Wolkers[$]

[#/$] *These authors contributed equally*

Abstract

Metastatic renal cell carcinoma (RCC) has a poor prognosis. Recent advances have shown beneficial responses to immune checkpoint inhibitors, such as anti-PD-1/PD-L1 antibodies. As only a subset of RCC patients respond, alternative strategies should be explored. Patients refractory to anti-PD-1 therapy may benefit from autologous tumor infiltrating lymphocyte (TIL) therapy. Even though efficient TIL expansion was reported from RCC lesions, it is not well established how many RCC TIL products are tumor-reactive, how well they produce pro-inflammatory cytokines in response to autologous tumors, and whether their response correlates with the presence of specific immune cells in the tumor lesions.

We here compared the immune infiltrate composition of RCC lesions with that of autologous kidney tissue of 18 RCC patients. T cell infiltrates were increased in the tumor lesions, and CD8$^+$ T cell infiltrates were primarily of effector memory phenotype. Nine out of 16 (56%) tested TIL products we generated were tumor-reactive, as defined by CD137 upregulation after exposure to autologous tumor digest. Tumor reactivity was found in particular in TIL products originating from tumors with a high percentage of infiltrated T cells compared to autologous kidney, and increased CD25 expression on CD8$^+$ T cells. Importantly, although TIL products had the capacity to produce the key effector cytokines IFN-γ, TNF-α or IL-2, they failed to produce significant amounts in response to autologous tumor digests. In conclusion, TIL products from RCC lesions contain tumor-reactive T cells. Their restricted tumor-specific cytokine production requires further investigation of immunosuppressive factors in RCC and subsequent optimization of RCC-derived TIL culture conditions.

Introduction

Patients with metastatic renal cell carcinoma (RCC) have a poor 5-year survival rate.[1] Several lines of evidence suggest that RCC patients may benefit from immunotherapy.[1, 2] In the past, treatment with high dose IL-2 resulted in partial responses. However, severe acute toxicities were common.[3–5] Allogeneic stem cell transplantation also elicited complete responses in several RCC patients,[6, 7] a finding that could not be reproduced by others.[8–10] Whilst the degree of T cell infiltration in RCC inversely correlated with the patient's survival, recent advances with checkpoint inhibitors to reinvigorate T cell responses yielded robust response rates in RCC patients.[11, 12] Antibodies directed against PD-1 or its ligands PD-L1 and PD-L2 in combination with anti-CTLA-4 or axitinib, a VEGFR tyrosine kinase inhibitor, resulted in 50% objective response rates of metastatic clear-cell RCC patients, and led to complete responses in 10% of the patients.[13, 14] This combination therapy has therefore replaced anti-VEGF targeted therapy as the new standard of care for treatment of naïve RCC patients.

Another emerging immunotherapeutic treatment is the administration of *ex vivo* reprogrammed tumor infiltrating lymphocytes (TILs). This adoptive TIL therapy induced objective responses in almost half of treated metastatic melanoma patients, and complete responses in 15-20% of patients.[15–17] Furthermore, TIL infusion yielded an objective response rate of 38% in melanoma patients that were refractory to anti-PD-1 therapy, indicating that TIL therapy represents an alternative treatment for patients who fail to respond to immune checkpoint blockade.[18] The success rate of TIL therapy to treat metastatic melanoma has sparked the interest to develop TIL therapy for other solid tumors, such as ovarian, colon, liver, breast and non-small cell lung cancers.[19–24] TIL products have also been generated from RCC lesions.[25–28] Although the expansion rate of RCC-derived TILs was comparable to that of melanoma-derived TILs, the *in vitro* response rates to autologous tumors were highly variable,[25–28] a characteristic that is not well understood. It would be useful to be able to predict from the composition of the initial tumor infiltrate which TIL products will be tumor-reactive. However biomarkers that allow such prediction have not been identified. Furthermore, it is unclear whether those RCC-derived TIL products that respond to tumors contain T cells that co-produce multiple effector molecules in response to autologous tumors. Such polyfunctionality is considered a prerequisite for successful anti-tumor T cell responses as well as for TIL therapy.[29, 30]

In this study, we characterized the patient-specific RCC immune cell composition compared to autologous non-tumor kidney tissue. Irrespective of high inter-patient variation, we found that T cells, especially of the effector memory subtype, constituted the major immune cell type in the RCC tumors, that were predominantly of the clear cell subtype. RCC-derived T cells responded to the autologous tumor digest by CD137 upregulation in 9 out of 16 (56%) patients. Higher frequencies of tumor-reactive T cells were found in TIL products generated from tumor lesions with high T cell infiltrates, in particular when CD8$^+$ T cells expressed high levels of CD25. However, even though

expanded TILs had the capacity to produce all key cytokines upon PMA/ionomycin stimulation, they lacked significant production in response to autologous tumor tissue.

Methods

Materials and solutions

Several solutions were used in sample processing. Collection medium consisted of 50µg/ml gentamycin (Sigma-Aldrich), 2% Penicillin-Streptomycin (P/S), 12.5µg/ml Fungizone (Amphotericin B, Gibco) and 20% fetal calf serum (FCS) (Bodego) in RPMI 1640 (Gibco). Digestion medium consisted of 30 IU/ml collagenase IV (Worthington), 1% FCS and 12.5µg/ml DNAse (Roche) in IMDM (Gibco). Washing medium consisted of RPMI 1640 supplemented with 2% FCS and 2% P/S. FACS buffer contained 2% FCS and 2mM EDTA in PBS. Red blood cell lysis buffer consisted of 155 mM NH4Cl, 10 mM KHCO3 and 0.1 mM EDTA (pH 7.4) in PBS. T cell culture medium consisted of 5% human serum (Sanquin), 5% FCS, 50 µg/ml gentamycin and 1.25 µg/ml fungizone in 20/80 T cell mixed media (Miltenyi Biotech). Freezing medium consisted of 10% DMSO (Corning) and 30% FCS in IMDM.

Sampling of tumor and non-tumor kidney tissue

Tumor and spatially distant non-tumor kidney tissue were collected from 20 RCC patients undergoing a nephrectomy from April 2016 to March 2018. Patient 08 was excluded from this study as the collected tumor piece proved too small for isolation of sufficient cell numbers for *ex vivo* analysis. A patient with oncocytoma (patient 11) was excluded from all analysis because we aimed to analyze malignant material only. From patient 05 we could only collect tumor tissue. This patient was therefore excluded from non-tumor and tumor paired comparisons. For patients 19 and 20, blood accompanying the resected kidney was collected from the transport vehicle. The patient characteristics of the 18 included patients are shown in Table 1. The cohort included 5 female and 13 male patients. 14 Tumors were classified as clear cell carcinoma, three as chromophobe and one as not otherwise specified (NOS). The tumor diameters ranged from 5.2 cm to 16.5 cm. The patient age at time of surgery ranged from 51 to 79, with a mean age of 63. Seven patients were smokers. The study was performed according to the Declaration of Helsinki (seventh revision, 2013), and executed with approval of the Institutional Review Board of the Dutch Cancer Institute (NKI), Amsterdam, the Netherlands (study number CFMPB317). All subjects provided written informed consent for ex vivo analyses of resected tumor material.

The tissue was obtained directly after surgery, stored in collection medium, weighed, and completely processed within 5 hours, except for patients 12 and 13, which were processed within 18 hours. Of note, viability and immune cell composition of tumor and kidney digests of these two patients was within range of all other tissue digests.

Table 1. Patient and tumor characteristics

Patient	Sex (M/F)	Age at surgery	Smoker	Pretreatment	RCC type	Fuhrman grade	Max tumor diameter (cm)	# tumors within kidney	PD-L1 TC (%)	PD-L1 IC (IC0-3)
01	M	61	yes	sunitinib	ccRCC	3	9	1	0	IC1
02	M	59			chRCC	NA	13	2	60	IC1
03	M	66		sunitinib	ccRCC	2	9	1	0	IC2
04	M	75		sunitinib	ccRCC, metastasis adrenal gland	2	8.5	1	ND	ND
05	F	71			ccRCC	2	8.5	2	0	IC0
06	M	59			ccRCC	3	8	2	0	IC0
07	M	55	yes		NOS, metastasis adrenal gland	NA	13	1	1	IC0
09	M	54	yes	axitinib + avelumab	ccRCC, metastatic	3	7	1	90	IC2
10	F	61			ccRCC	1	14	1	0	IC0
12	F	78			ccRCC	4	5.5	1	10	IC0
13	M	80			chRCC	NA	7	1	0	IC0
14	M	57			ccRCC	2	4.5	1	1	IC2
15	M	61	yes		ccRCC	3	9.2	1	0	IC2
16	M	57			ccRCC	3	8.5	1	0	IC1
17	M	63		pazopanib	chRCC metastatic	4	16.5	1	0	IC2
18	F	64		sunitinib	ccRCC	3	9.5	1	0	IC1
19	F	65	yes		chRCC	2	8.5	1	30	IC0
20	M	52	yes	sunitinib	ccRCC, metastatic	1	7	1	0	IC2

Abbreviations: M = male, F = female, ccRCC = clear cell RCC, chRCC = chromophobe RCC, NOS = not otherwise specified, NA = not applicable, ND = not determined, TC = tumor cell, IC = immune cell, IC0-3 = PD-L1 immune cell score 0-3

5

Isolation & digestion

We used our standardized isolation, digestion and TIL culture procedures as described before(21). In short, the tissues were chopped into small pieces of ~1mm³ and incubated for 45 minutes at 37°C in 5 ml digestion medium/g tissue. After digestion, cell suspensions were centrifuged for 10 min at 360 g. The pellets were washed with washing medium. After removal of the washing medium by centrifugation, cell pellets were vigorously suspended in FACS buffer to loosen the cells from the tissue. The cell suspensions were filtered over an autoclaved tea filter, followed by filtering over a 100 μm cell strainer (Falcon). The pelleted flow-through was treated with Red blood cell lysis buffer for 15 minutes at 4°C. The cell suspensions were again washed with FACS buffer before counting. The cells were manually counted in trypan blue solution (Sigma). 1-2 million live cells were used per flow cytometry panel (2-4 million total), 1 million live cells for TIL cultures, and the remaining cells were cryo preserved.

Ex vivo flow cytometry

Cells were stained at 4°C in FACS buffer for 30 minutes in U-bottom 96-well plates at 1-2 million cells per panel. For the immune cell subset analysis, the staining mix included the following antibodies: CD11c PerCP-Cy5.5, CD15 BV605, CD3 BV510, CD11B BV421, CD274 PE (all Biolegend), anti-HLA-DR FITC, CD45 BUV805, CD19 BUV737, CD20 BUV737, CD16 BUV496, CD1a BUV395, CD33 AF700 (all BD Biosciences), CD14 PE-Cy7 (eBioscience) and LIVE/DEAD™ Fixable Near-IR Stain (Invitrogen) (Table S1). For phenotypic analysis of T cells, the staining mix included the following antibodies: CD3 PerCP-Cy5.5, PD-1 FITC, CD56 BV605, CD27 BV510, CCR7 BV421, CD103 PE-Cy7, CD25 PE (all Biolegend), CD8 BUV805, CD45RA BUV737, CD4 BUV496, CD69 BUV395 (all BD Biosciences) and LIVE/DEAD™ Fixable Near-IR Stain (Table S1). After antibody incubation at RT degrees for 20 min, cells were centrifuged for 4 min at 350 g. Cell pellets were washed twice with FACS buffer. Cells were fixed using the fixation solution of the anti-human FoxP3 staining Kit (BD Biosciences). After fixation for 30 minutes, cells were washed twice with FACS buffer, and then once with the permeabilization buffer of the anti-human FoxP3 staining kit. For immune cell subset analysis, cells were stained with CD68 APC and for the T cell phenotype analysis with anti-FOXP3 AF647 in permeabilization buffer for 30 minutes (Table S1). Cell suspensions were washed twice with permeabilization buffer, taken up in FACS buffer and filtered using Filcon Syringe-Type 50 μm filters (BD biosciences) right before measurement. Samples from patients 01–09 were measured on a LSRFortessa flow cytometer and samples from patients 10–20 on a FACSymphony (both BD Biosciences).

Immunohistochemistry

Formalin-fixed, paraffin-embedded tumor tissue samples were stained for PD-L1 (clone 22C3, Agilent) using the Ventana Benchmark Ultra. Membranous PD-L1 expression of any intensity on viable tumor cells was scored as a percentage of at least 100 tumor cells. The

percentage of PD-L1 positive immune cells was scored as the proportion of tumor area that is occupied by PD-L1 staining of immune cells of any intensity and categorized as follows: 0% = IC0, 0% > IC1 < 5% > IC2 < 10% < IC3.

TIL culture

Freshly isolated live cells were cultured in 24 well plates (10^6 cells per well) in T cell culture medium supplemented with 6000 IU/ml IL-2 for ~2 weeks at 37°C 5% CO_2. Medium was refreshed approximately every 4 days. Wells were split when a monolayer of cells was observed in the entire well. After this initial culture period, cells were cultured using a standard rapid expansion protocol (REP) for another two weeks: the culture medium was replaced with T cell culture medium supplemented with 3000 IU/ml IL-2 and anti-CD3 (clone OKT3; Miltenyi Biotech), also containing 8-10 x 10^6 irradiated (40 Gray) PBMCs pooled from 10 healthy donors. Of note, comparison of the use of allogeneic versus autologous feeder cells during the TIL expansion phase revealed that both have a similar risk of emergence of new TCR clonotypes.[31] Cells were passaged when multiple clusters of dividing T cells were observed, which was usually once or twice during the two-week REP culture period. The expanded T cells were cryo-preserved in freezing medium.

Tumor reactivity assay

Expanded T cells were thawed in RPMI containing 2% FCS at 37°C. Cells were washed twice with T cell culture medium and centrifugation at 350 g for 5 min. The number of living trypan blue negative cells was determined using a hemocytometer. Cells were pre-stained in FACS buffer containing CD8 BUV805, CD4 BUV496 and CD3 BUV395 (clone SK7, BD biosciences) for 30 min at 4°C, washed twice and taken up in T cell culture medium (Table S1). 100,000 expanded live cells were assayed in T cell culture medium alone (= medium control) or co-cultured with either thawed tumor or kidney digest containing 50,000 to 100,000 living cells or exposed to PMA/ionomycin (10 ng/ml PMA, 1 μg/ml ionomycin). After one hour, Brefeldin A (1:1000, Invitrogen) and 1:1000 monensin (eBioscience) were added. After six hours, cells were washed with FACS buffer before staining with anti-PD-1 BV421 (BD biosciences), CD154 BV510 (Biolegend)[32, 33] and LIVE/DEAD™ Fixable Near-IR Stain for 30 minutes followed by centrifugation for 4 min at 350 g. Cell pellets were washed twice with FACS buffer. Cells were fixed using fixation solution (BD, FoxP3 staining kit) for 30 min and washed twice using FACS buffer. Cells were kept overnight at 4°C, washed with permeabilization buffer and stained with anti-TNF-α AF488, CD137 PE-Cy7[34], anti-IFN-γ PE (all Biolegend) and anti-IL-2 APC (Invitrogen) in permeabilization buffer for 30 min. Cells were washed twice with permeabilization buffer and analyzed in FACS buffer on a BD FACSymphony. Cytokine and activation marker expression levels were only included in the analysis when the cell population of interest contained at least 200 events.

5

Analysis

Flowjo version 10.1 (Tree Star) was used to analyze flow cytometry data. Further analysis of the percentages of the stated phenotypes, data transformations, generation of figures and statistical calculations were all performed in R. *P*-values were determined by indicated statistical tests and depicted using the following symbols: p<0.05 = *, p<0.01 =**, p<0.001 = ***, n.s. = not significant.

Results

Clear cell RCC lesions are highly infiltrated by T cells

To determine the composition of immune cells infiltrating RCC lesions, we collected both tumor and non-tumor sections from resected kidneys of 18 RCC patients, ranging from Fuhrman grade 1 to 4 and with varying PD-L1 expression on tumor and immune cells (IC) (Table 1). Roughly half of the patients had received pretreatment with protein tyrosine kinase inhibitors, while the other half was treatment naive (Table 1). The non-tumor section (hereafter referred to as kidney tissue) was dissected as spatially distant as possible from the tumor. Single cell suspensions were generated from the collected tissue by physical disruption and digestion with DNAase and collagenase IV. After extensive filtration, the number of live cells was determined. The yield of cells per mg tissue derived from tumor lesions and kidney tissue was similar (Fig. 1A).

We next quantified the immune infiltrates by flow cytometry. We measured T cells, monocytes, macrophages, neutrophils, NK cells, B cells, dendritic cells (DCs) and NKT cells (gating in Fig. S1). To determine whether the identified immune cells were contaminants from peripheral blood, we compared the immune cell content of tissue digests from two patients side-by-side with paired blood samples. This analysis revealed that the immune cell composition in tumor and kidney tissue digests was clearly distinct from that of blood (Fig. S2B), thus validating our analysis of tumor-infiltrating cells. Overall, higher numbers of immune cells were found in tumor lesions compared to paired kidney tissue (Fig. 1A). Similar to the kidney tissue, T cells constituted the major immune cell subset in RCC lesions, with an average of 48 ± 27% of the immune infiltrate (Fig. 1B; Fig. S2A). Also, monocytes and macrophages were >20% present in the infiltrate in tumor tissue of 6 and 5 patients respectively (Fig. 1B). The tumor infiltrates contained on average less than 5% of neutrophils, NK cells, B cells, DCs and NKT cells (Fig. 1B). Interestingly, tumors of the four patients with the lowest percentages of T cells (patient 02, 09, 13, and 19) also contained the highest percentages of macrophages (Fig. S2C). Of note, three of these patients were diagnosed with chromophobe RCC (Fig. S2C). B cells, DCs, monocytes, macrophages and a subset of T cells expressed HLA-DR, albeit with varying levels (Fig. S2D).

The high proportion of T cells in the tumor lesions led us to further explore these immune cell subsets (gating in Fig. S3A). Overall, CD8+ T cells were more abundant in tumor lesions than CD4+ conventional (conv) T cells (Fig. 1C). FOXP3+ CD25hi T cells contributed on

average 2.4 ± 3.2% to the total T cell population in RCC lesions (Fig 1C). These percentages of FOXP3$^+$ T cells are substantially lower than those measured in melanoma or ovarian cancer lesions (~15% of CD3$^+$ T cells).(21)
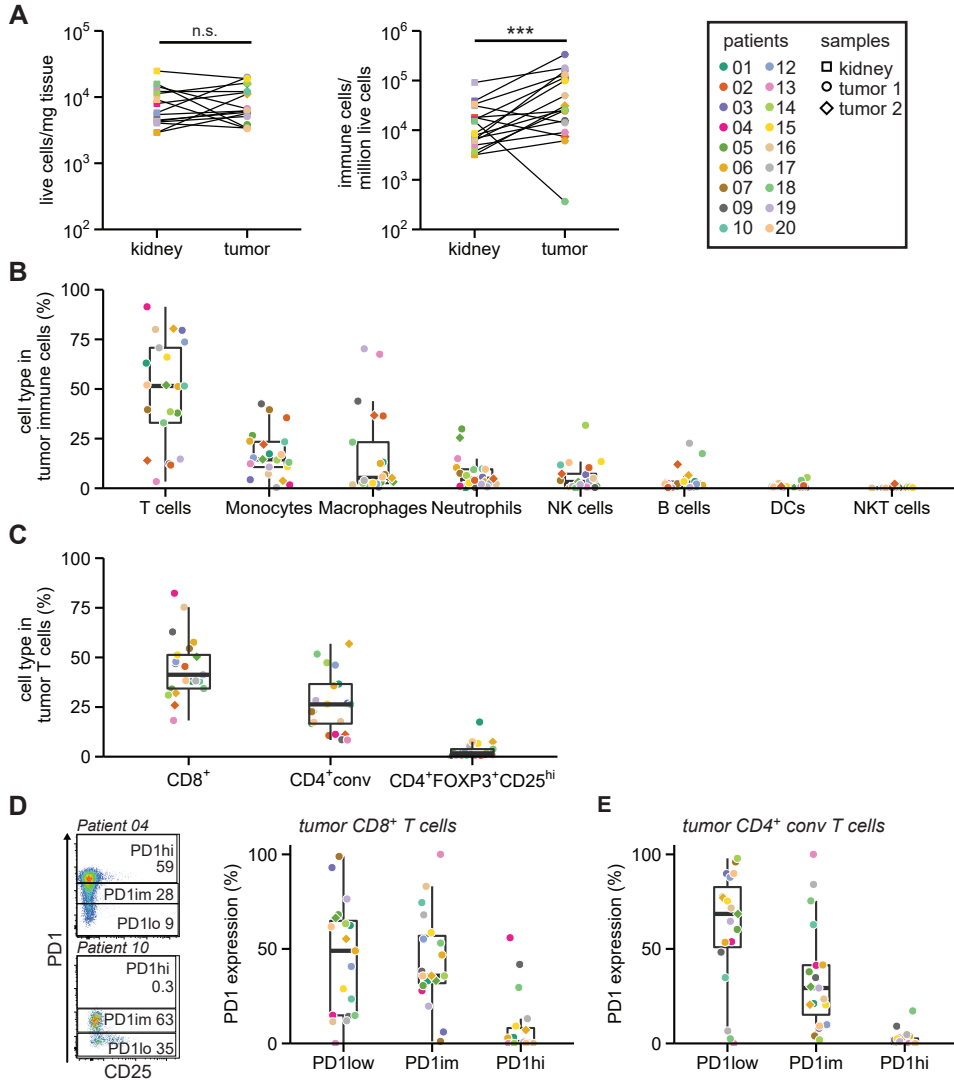
Figure 1. T cells are enriched in RCC lesions. (A) Tissue from RCC lesions and distal non-tumor kidney tissue was collected from 18 RCC patients. The number of living cells in single cell suspensions were determined using trypan blue (left panel). The number of T cells, monocytes, macrophages, neutrophils, natural killer (NK) cells, B cells, dendritic cells (DCs) and NKT cells were determined by flow cytometry. Collectively these cell types are defined as immune cells (middle panel). Statistical significance was determined by Wilcoxon signed-rank test. Right panel: Patient color coding and sample shape coding, which is used throughout all figures. (B) Percentage of indicated immune cell subsets of the total immune cells in tumor digests. No events were excluded for these ex vivo analyses. (C) T cell subsets as a percentage of total CD3$^+$ T cells in the tumor digest as determined by flow cytometry. CD4$^+$ conventional (conv) T cells are defined as non-FOXP3$^+$CD25^{hi} (see Fig. S3). (D) Gating strategy (left panel) of two representative patients to define high (hi), intermediate (im) and low (lo) PD-1 expression in tumor-infiltrating CD8$^+$ T cells and summary (right panel). (E) Similar gating was used for CD4$^+$ conv T cells (E).

High expression levels of PD-1 (PD-1hi) on CD8$^+$ T cells in solid tumors is reportedly often indicative for tumor reactivity.(35) RCC tumors are enriched for checkpoint inhibitor-expressing T cells compared to paired PBMC or adjacent kidney tissue in RCC.(36–38) Most RCC infiltrating CD8$^+$ and CD4$^+$ conv T cells showed low (PD-1low) or intermediate PD-1 (PD-1im) expression (Fig. 1D, E). Nevertheless, 6 tumors contained more than 5% PD-1hi CD8$^+$ T cells, which in 2 cases (patients 09 and 18) coincided with the presence of PD-1hi CD4$^+$ conv T cells. In conclusion, high percentages of CD8$^+$ and CD4$^+$ conv T cells with variable PD-1 expression levels are present in clear cell RCC lesions.

RCC infiltrating T cells display an effector memory phenotype

We next determined the differentiation and activation status of tumor infiltrating T cells compared to T cells from paired kidney tissue. We analyzed the expression of CD45RA, CD27, CCR7, CD103 and CD69 to differentiate between naïve, effector and memory subtypes, and of CD25 and PD-1 to define T cell activation and exhaustion (gating in Fig. S3B). To prevent the inclusion of unreliable data, all populations included in the PCA contained at least 200 cells. We visualized the relationship between different patient samples and within patients by applying principal component analysis (PCA) on the percentage of T cell subtypes and the percentage of activation/exhaustion marker expression within these T cell subsets (Fig. 2A and B). Distances between T cells from tumor and kidney samples of individual patients seemed limited (Fig. 2A), suggesting that TILs resemble T cells from the corresponding kidney more than TILs from other patients. Nonetheless, PC2 potently separated T cells from tumor and kidney sample groups (Fig. 2B). We therefore examined which variables contributed most to PC2. Samples with a high PC2 score were enriched for CD27$^-$CD45RA$^-$ and CCR7$^-$CD45RA$^-$ expressing CD8$^+$ and CD4$^+$ conv effector memory T cells (T$_{EM}$) compared to samples with a low PC2 score, which contained more naïve (CD27$^+$CD45RA$^+$ and CCR7$^+$CD45RA$^+$) expressing CD8$^+$ and CD4$^+$ conv T cells (Fig. 2C). Specific analyses of these parameters showed that both CD8$^+$ and CD4$^+$ conv T cells in tumor tissue were enriched for the T$_{EM}$ phenotype (CD27$^-$CD45RA$^-$) compared to kidney T cells (Fig. 2D and E), in line with the findings of Attig *et al.* and Kawashima *et al.* (39, 40). Also, naïve CD8$^+$ T cells (CD27$^+$CD45RA$^+$) were significantly reduced in tumors compared to CD8$^+$ T cells in the kidney (Fig. 2D). In addition, samples with a low PC2 score were enriched for CD25 expressing CD8$^+$ and CD4$^+$ conv T cells (Fig. 2C). Indeed, tumor-derived CD8$^+$ T cells and CD4$^+$ conv T cells (which predominantly exhibit relatively high PC2 scores) had lower percentages of CD25 expression than T cells present in the kidney tissue (Fig. 2F and G). Although high CD25 expression is a hallmark of FOXP3$^+$ Tregs, the overall percentage of infiltrated FOXP3$^+$ CD25hi T cells did not significantly differ between tumor and kidney tissue (Fig. 2H).(41) In conclusion, tumor-infiltrating T cells are enriched for a T$_{EM}$ phenotype but have lower CD25 levels compared to T cells isolated from paired kidney tissue.

Figure 2. RCC-derived T cells are phenotypically different from kidney T cells. (A-B). The activation and memory profiles of CD8+, CD4+ conv T cells and CD4+FOXP3+CD25hi cells were determined by flow cytometry in the populations of interest exceeding 200 events. These profiles included three PD-1 levels (low, intermediate, high), CD25 expression, CD103+CCR7-, CD103-CCR7-, and all combinations of CD27/CD45RA, CCR7/CD45RA and CD103/CD69 (see Fig. S3). Dimensions of these data were reduced using principal component analysis (PCA). The first two principal components (PC) are shown as colored by patient (A) and by sample type (B). (C) The ten phenotypes that contributed most to variance in PC2. Colors indicate whether a phenotype was observed in CD4+ conv T cells (red) or CD8+ T cells (blue). (D) Left panel: gating for memory phenotypes in CD8+ T cells. Middle and right panels: effector memory and naïve T cell percentages within CD8+ T cells. (E) As in D, but then for CD4+ conv T cells. (F) CD25 expression gating (left panel) and quantification (right panel) for CD8+ T cells. (G) As in F, for CD4+ conv T cells. (H) Percentage of CD4+FOXP3+CD25hi cells in CD3+ T cells. For D-H only paired samples were plotted. Statistical significance in panels A and D-H was determined by Wilcoxon signed-rank test.

Figure 3. Expanded RCC TILs are capable cytokine producers. Tumor and kidney digests were cultured for two weeks in 6000 IU/ml IL-2, followed by two weeks of REP. (A) Fold change of number of T cells post-REP compared to ex vivo. (B) Fraction of CD8+ and CD4+ T cells from kidney (left panel) and RCC (right panel) ex vivo and post-REP (individual datapoints in Fig. S4B). (C-E) Post-REP TILs were re-stimulated with PMA/ionomycin for 6 h and analyzed for expression of intracellular CD137 and surface CD154 (C), expression of intracellular cytokines in CD8+ T cells (D) and in CD4+ T cells in (E). Statistical significance was determined by Wilcoxon signed-rank test for panels A and B and by ANOVA with Tukey's post hoc test for panels C-E.

Effective expansion of functionally active RCC TILs

To determine the expansion capacity of RCC TILs, we cultured tumor digests with 6000 IU/ml IL-2 for 14 days, followed by a 14 day rapid expansion protocol (REP)(42) using soluble anti-CD3 antibodies and 3000 IU/ml IL-2. For comparison, we also expanded T cells isolated from kidney tissue. The expansion rates were similar between kidney- and tumor-derived T cells, suggesting that immunomodulatory factors that were potentially present in the tumor digest did not substantially affect the T cell proliferation potential in vitro (Fig. 3A, S4A). On average, the ratio of CD4$^+$ to CD8$^+$ T cells did not alter significantly upon T cell expansion (Fig. 3B; gating in Fig. S4B). Nonetheless, this ratio was altered in individual patients during culture (Fig. S4C).

Next, we measured the activation potential of the expanded TIL products. We stimulated TILs with PMA/ionomycin for 6h and measured the expression of the activation markers CD137/4-1BB, and of CD154/CD40L, two markers that indicate T cell receptor-dependent activation.(34, 43, 44) In particular, the expression of CD137 was substantially induced in expanded CD8$^+$ and CD4$^+$ T cells generated from both kidney and tumor tissue (Fig. 3C; gating in Fig. S4B and D). Furthermore, the key pro-inflammatory cytokines IFN-γ, TNF-α and IL-2 were effectively produced by both kidney and tumor tissue-derived CD8$^+$ and CD4$^+$ T cells (Fig. 3D and E; gating in Fig. S4E). In conclusion, TILs from RCC lesions could be effectively expanded and were generally able to produce inflammatory cytokines in response to pharmacological stimulation.

Expanded TILs are tumor-reactive

We next tested the tumor reactivity of expanded TILs from 16 RCC lesions and -when available- from kidney tissue. We co-cultured the TIL products with autologous tumor digests for 6h and measured the induction of CD137 and CD154. To define the base line CD137 and CD154 expression, we cultured the expanded TILs in medium alone and exposed them to autologous kidney digests. Induction of CD154 expression on CD4$^+$ T cells was scarce in any of the culture conditions (Fig. 4A and S4F). Conversely, CD137 expression was significantly increased upon co-culture with tumor digest, in particular in CD8$^+$ T cells generated from both tumor and kidney tissue (Fig. 4A and S4F-G). In fact, in 9 out of 15 analyzed individual patients (60%), the CD137 expression on TILs was higher upon coculture with tumor tissue digest than with the autologous kidney tissue digest (Fig. 4B; kidney digest was lacking for patient 05). This finding indicates that RCC TIL products specifically responded to tumor tissue digests.

Because tumor reactivity was not detected in all TIL products (Fig. 4B), we asked whether the presence of tumor reactivity correlated with a particular *ex vivo* immune signature. Therefore, we compared the tumor immune cell composition to that of the kidney tissue (Fig. S5A). Even though the immune composition between digests greatly varied between patients, we detected significant differences in T cell, monocyte, neutrophil, DC and NKT cell content between tumor and kidney tissues (Fig. S5A). The most prominent of these

5
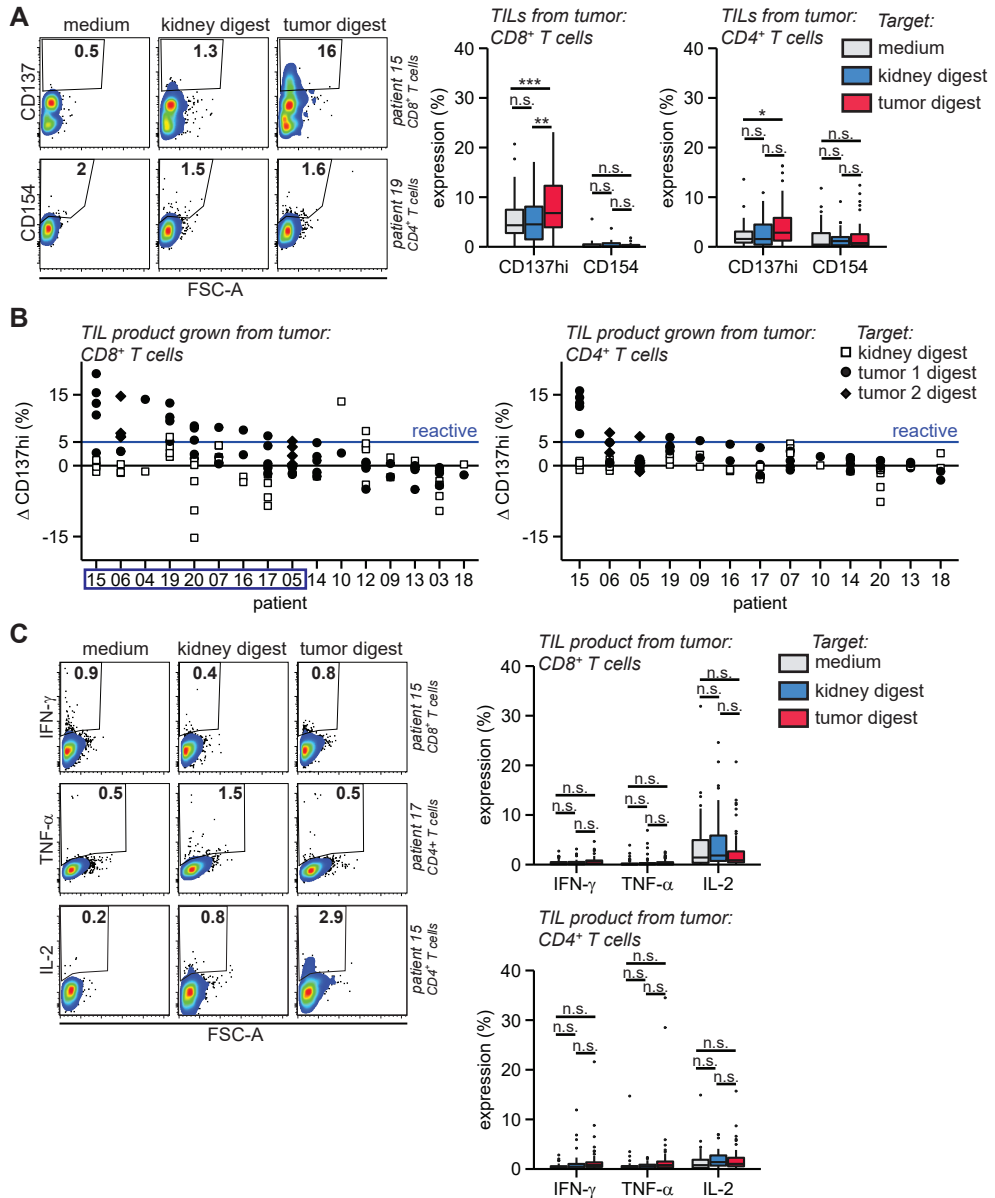
Figure 4. RCC TILs are tumor-reactive but do not produce key cytokines. Post-REP tumor derived TIL products were first stained for CD3, CD4 and CD8, then cultured in medium with or without autologous kidney or autologous tumor digests and analyzed by flow cytometry for CD137, CD154, IFN-γ, TNF-α or IL-2 after 6h of coculture. (A) Intracellular CD137 and surface CD154 expression, representative examples (left panels) and summary of quantifications (right panels). (B) The difference (Δ, Delta) in high CD137 (CD137hi) expression between co-culture of tumor-derived TILs with tissue digest and medium control (tissue digest – medium). TIL products with ΔCD137hi > 5% (blue line) in CD8+ T cells against tumor digests were considered tumor-reactive. Patients from which tumor-reactive TIL products were produced according to these criteria are enframed.

(C) Intracellular IFN-γ, TNF-α or IL-2 expression, representative examples (left panels) and summary of quantifications (right panels). Cytokine and activation marker expression levels were only analyzed in cell populations containing at least 200 events. Statistical significance was determined by ANOVA with Tukey's post hoc test for panels A and C. Replicates are separately cultured and tested TIL products.

differences was the reduced relative abundance of neutrophils in tumor digests (Fig. S5A). Because of the substantial variation and thus patient-specific immune landscape in RCC and kidney tissue, we calculated the difference between immune infiltrates in tumor and kidney digest and correlated that to the tumor reactivity of TIL products. Tumor reactivity was defined as follows: at least one of the individual TIL cultures from a patient showed >5% CD137 expression difference in CD8$^+$ T cells comparing coculture with tumor digest versus medium control (ΔCD137hi) (Fig. 4B, blue line). TIL products with a ΔCD137^{hi} <5% were considered 'not reactive'. We then correlated the reactive and non-reactive groups to changes in immune cell infiltration between tumor and kidney tissue. We found that tumor-reactive TIL products were more often derived from tumor tissues that contained increased infiltrates of T cells, NKT cells, B cells, and/or a loss of neutrophils (Fig. S5B). Of note, the percentages of these immune subsets just in tumor digests (Fig. 1B) lacked a significant correlation with tumor reactivity (Fig. S5C). Likewise, the percentage of tumor-infiltrating CD8$^+$ T cells, CD4$^+$ conv T cells, FOXP3$^+$ CD25hi T cells (Fig. 1C), the percentage of PD-1hi T cells (Fig. 1D and E) and the tumor or immune cell PD-L1 expression (Table 1) did not correlate with tumor reactivity (Fig. S6A-C).

As the PCA of T cell infiltrates derived from tumor and kidney tissue showed key differences in the memory phenotype and the percentage of CD25 expressing CD8$^+$ and CD4$^+$ conv T cells (Fig. 2A-G), we also investigated whether these parameters correlated with the tumor reactivity of TIL products. The differentiation status of CD8$^+$ and CD4$^+$ conv T cells in tumor digests, whether or not in relation to kidney tissue, did not correlate with tumor reactivity of the in vitro expanded TIL product (Fig. S7A and B). The percentage of CD25 expressing T cells correlated with tumor reactivity of the TIL product only within the tumor-infiltrating CD8$^+$ T cell population (Fig. S7C and D). Thus, increased T cell numbers that include CD25-expressing CD8$^+$ T cells in the tumor tissue indicated an increased likelihood of generating tumor-reactive TIL products.

Expanded tumor-reactive TILs show very limited cytokine production

Because effective TIL therapy requires cytokine-producing TIL products,(29) we examined whether expanded TILs also had the capacity to produce the key pro-inflammatory cytokines IFN-γ, TNF-α, and IL-2 when exposed to tumor tissue digest. Strikingly, even though PMA/ionomycin activation of TIL products showed the capacity of TIL products to produce high levels of IFN-γ, TNF-α, and IL-2 (Fig. 3D), and even though CD137 expression was clearly induced in CD8$^+$ and/or CD4$^+$ T cells in TIL products from 10 out of 16 patients when exposed to autologous tumor digest (Fig. 4A and B), the detection of tumor-specific production of these three cytokines was only incidental (Fig. 4C). In conclusion, even though tumor-reactive T cells in RCC lesions can be effectively expanded and produce cytokines after stimulation with pharmacological reagents, they show little- if any- production of pro-inflammatory cytokines in response to tumor digests.

5

Discussion

In this study, we show that TILs from RCC lesions can be effectively expanded with a standard REP. From 9 out of 16 patients (56%), TIL products contained tumor-reactive T cells as defined by the induction of tumor-specific CD137 expression. Our results are in the same range as seen in previous studies with RCC tumor lesions, although comparisons are complicated because of study-specific differences in methodology.(25–27) Previous paired analyses of primary and metastatic RCC lesions specified that the percentage of infiltrated T cells was similar.(45) Even though our results using primary material may not directly translate to the expansion potential from metastatic lesions, at least from primary lesions T cell expansions reach clinically relevant numbers. Before clinical translation the growth of tumor-reactive (and polyfunctional) TIL products from resectable metastatic lesions requires further investigation. The patient group we analyzed here contained RCC lesions from pretreated and treatment-naive patients. While the study group is too small for firm conclusions, a clear relation between patient pretreatment and TIL expansion or tumor reactivity of the TIL product was absent.

Whether a tumor-reactive TIL product can be developed may depend on the composition of the tumor immune infiltrate. The comparison of the tumor immune landscape with that of non-tumor tissue from the same patient allowed us to identify tumor-specific infiltrations. Here we show that an enrichment of T cells in RCC compared to autologous kidney tissue positively correlated with the presence of tumor-reactive T cells in the TIL products. This is in apparent accordance with data in colon and ovarian tumors showing a positive association between high tumor T cell infiltration and clinical outcome.(46–48) In addition, high expression of the activation markers PD-1, CD69 and CD25 on primary TILs is an important indicator for the percentage of tumor-reactive T cells and therapeutic response in NSCLC.(21, 35) In the current study, we only found that the presence of CD25-expressing CD8+ TILs correlated with tumor reactivity of expanded TILs. Pre-selection of these CD8+ TILs, or alternatively PD-1+ or CD137+ TILs before expansion may therefore be a useful strategy to increase outgrowth of tumor-reactive T cells.(49, 50)

Also, an increased presence of B cells in tumor lesions compared to paired kidney tissue associated with the occurrence of tumor-reactive T cells in TIL products. B cells are indicative for the presence of tertiary lymphoid structures, which are thought to drive anti-tumor immunity.(51) In line with this, B cell signatures are enriched in responders to immune checkpoint blockade compared to non-responders in RCC, sarcoma and melanoma.(51, 52) Finally, a reduction of neutrophils in RCC lesions compared to paired kidney tissue correlated with increased tumor reactivity of expanded TIL products. Although only present in small numbers, it is tempting to speculate that neutrophils interfere with the functional potential of tumor-reactive T cells, especially because low neutrophil to lymphocyte ratios in RCC positively correlate with clinical anti-PD-1 therapy responses.(53) Overall, we show that the composition of the tumor specific immune infiltrate in all likelihood determines the potential to generate a TIL product containing

tumor-reactive T cells.

Although we found CD137-expressing tumor-reactive T cells, they generally failed to produce cytokines after stimulation with autologous RCC. Other pioneering studies reporting tumor reactivity of expanded RCC TILs showed low cytokine production and lacked thorough polyfunctional analyses.(25–27) Differences between these and our studies are likely caused by the specific isolation and stimulation protocols. Intriguingly, with the identical protocol we used here, we generated clinical-grade melanoma TILs at our facilities that readily produce effector cytokines against autologous tumor digest for seven out of seven patients.(42, 54) Similarly, 76% of our NSCLC-derived TIL products showed tumor-specific cytokine responses to autologous tumors, of which 25% was even polyfunctional.(21) Thus, the restricted tumor-specific cytokine production we observed for RCC-derived TIL products is tumor-type specific. The relative absence of tumor-specific cytokine production could not be attributed to an overall inability to produce these cytokines, as the RCC TILs produced ample amounts upon stimulation with PMA/ionomycin. Hence, what are the underlying mechanisms for the lack of cytokine production by RCC-derived TILs in response to tumor digests? A lack of cytokine production may have been imposed during the tumor reactivity assay by immune cells that include suppressive T cell populations or myeloid-derived suppressor cells (MDSCs). Even though we did not find a significant correlation of *ex vivo* $CD4^+FOXP3^+CD25^{hi}$ cells with tumor reactivity, this T cell subset could be strongly suppressive.(55, 56) Alternatively, RCC-resident CD25-expressing $CD4^+FOXP3^-$ T cells can produce IL-10 and correlate with worse patient survival.(57) In addition, abundantly present MDSCs in RCC negatively affect TIL outgrowth, and potentially interfere with immunotherapy.(28) Furthermore, non-immune cells such as tumor cells or stromal cells often harbor the capacity to suppress functional T cell responses to tumor digest.(58) For example, surface PD-L1 is one of the known key molecules to suppress anti-tumor recognition, and was expressed by tumor cells in some RCC lesions in this study. Alternatively, an immunosuppressive environment could hinder the re-programming of dysfunctional T cells to gain a pro-inflammatory profile. Because PMA/ionomycin activation induced strong responses, we consider this possibility unlikely. Nevertheless, it is conceivable that signaling nodules engaged upon TCR-HLA complex interaction that are required for cytokine production, but not for CD137 induction, may not have been completely rewired during the TIL cultures. Further investigations should reveal whether the generation of RCC-derived TIL products would benefit from the upfront removal of any or all of these immune suppressive cells.

In addition to the conclusions of other pioneering studies on opportunities of TIL therapy for the treatment of RCC,(25–27) we recommend that TIL generation from RCC first requires a thorough mechanistic understanding of the RCC TIL dysfunction before application to patients. Moreover, the restricted functionality of RCC TILs may have contributed to the failure of their clinical application in the late 90s.(59) As of writing, we could only find one active TIL clinical trial for RCC in the ClinicalTrials.gov database.(60) In

5

contrast, multiple checkpoint inhibitor trials are ongoing, further emphasizing the current relative lack of knowledge to design effective TIL therapy for RCC.(61–63)

In conclusion, we successfully expanded tumor-reactive TILs from RCC patients, but further elucidation of molecular and cellular suppressive pathways in RCC is needed to restore their tumor-specific cytokine production.

Acknowledgments

References

1. Hsieh, J. J., M. P. Purdue, S. Signoretti, C. Swanton, L. Albiges, M. Schmidinger, D. Y. Heng, J. Larkin, and V. Ficarra. 2017. Renal cell carcinoma. *Nat. Rev. Dis. Prim.* 3: 17009.
2. Andersen, R., M. Donia, M. C. W. Westergaard, M. Pedersen, M. Hansen, and I. M. Svane. 2015. Tumor infiltrating lymphocyte therapy for ovarian cancer and renal cell carcinoma. *Hum. Vaccines Immunother.* 2790–2795.
3. McDermott, D. F., M. M. Regan, J. I. Clark, L. E. Flaherty, G. R. Weiss, T. F. Logan, J. M. Kirkwood, M. S. Gordon, J. A. Sosman, M. S. Ernstoff, C. P. G. Tretter, W. J. Urba, J. W. Smith, K. A. Margolin, J. W. Mier, J. A. Gollob, J. P. Dutcher, and M. B. Atkins. 2005. Randomized Phase III Trial of High-Dose Interleukin-2 Versus Subcutaneous Interleukin-2 and Interferon in Patients With Metastatic Renal Cell Carcinoma. *J. Clin. Oncol.* 23: 133–141.
4. Fyfe, G., R. I. Fisher, S. A. Rosenberg, M. Sznol, D. R. Parkinson, and A. C. Louie. 1995. Results of treatment of 255 patients with metastatic renal cell carcinoma who received high-dose recombinant interleukin-2 therapy. *J. Clin. Oncol.* 13: 688–696.
5. Buchbinder, E. I., J. P. Dutcher, G. A. Daniels, B. D. Curti, S. P. Patel, S. G. Holtan, G. P. Miletello, M. N. Fishman, R. Gonzalez, J. I. Clark, J. M. Richart, C. D. Lao, S. S. Tykodi, A. W. Silk, and D. F. McDermott. 2019. Therapy with high-dose Interleukin-2 (HD IL-2) in metastatic melanoma and renal cell carcinoma following PD1 or PDL1 inhibition. *J. Immunother. cancer* 7: 49.
6. Childs, R., A. Chernoff, N. Contentin, E. Bahceci, D. Schrump, S. Leitman, E. J. Read, J. Tisdale, C. Dunbar, W. M. Linehan, N. S. Young, A. J. Barrett, D. Epperson, V. Mayo, and A. J. Barrett. 2000. Regression of metastatic renal-cell carcinoma after nonmyeloablative allogeneic peripheral-blood stem-cell transplantation. *N. Engl. J. Med.* 343: 750–8.
7. Bregni, M., A. Dodero, J. Peccatori, A. Pescarollo, M. Bernardi, I. Sassi, C. Voena, A. Zaniboni, C. Bordignon, and P. Corradini. 2002. Nonmyeloablative conditioning followed by hematopoietic cell allografting and donor lymphocyte infusions for patients with metastatic renal and breast cancer. *Blood* 99: 4234–6.
8. Artz, A. S., M. Kocherginsky, and K. Van Besien. 2006. Order of patient entry influences outcome for metastatic renal cell cancer after non-myeloablative allogeneic stem cell transplantation. *Br. J. Haematol.* 132: 747–54.
9. Artz, A. S., K. Van Besien, T. Zimmerman, T. F. Gajewski, B. I. Rini, H. S. Hu, W. M. Stadler, and N. J. Vogelzang. 2005. Long-term follow-up of nonmyeloablative allogeneic stem cell transplantation for renal cell carcinoma: The University of Chicago Experience. *Bone Marrow Transplant.* 35: 253–260.
10. Rini, B. I., S. Halabi, R. Barrier, K. A. Margolin, D. Avigan, T. Logan, W. M. Stadler, P. L. McCarthy, C. A. Linker, E. J. Small, Cancer and Leukemia Group B, Eastern Cooperative Oncology Group, and Southwestern Oncology Group. 2006. Adoptive Immunotherapy by Allogeneic Stem Cell Transplantation for Metastatic Renal Cell Carcinoma: A CALGB Intergroup Phase II Study. *Biol. Blood Marrow Transplant.* 12: 778–785.
11. Geissler, K., P. Fornara, C. Lautenschläger, H.-J. Holzhausen, B. Seliger, and D. Riemann. 2015. Immune signature of tumor infiltrating immune cells in renal cancer. *Oncoimmunology* 4: e985082.
12. Nakano, O., M. Sato, Y. Naito, K. Suzuki, S. Orikasa, M. Aizawa, Y. Suzuki, I. Shintaku, H. Nagura, and H. Ohtani. 2001. Proliferative activity of intratumoral CD8(+) T-lymphocytes as a prognostic factor in human renal cell carcinoma: clinicopathologic demonstration of antitumor immunity. *Cancer Res.* 61: 5132–6.
13. Motzer, R. J., N. M. Tannir, D. F. McDermott, O. Arén Frontera, B. Melichar, T. K. Choueiri, E. R. Plimack, P.

Barthélémy, C. Porta, S. George, T. Powles, F. Donskov, V. Neiman, C. K. Kollmannsberger, P. Salman, H. Gurney, R. Hawkins, A. Ravaud, M.-O. Grimm, S. Bracarda, C. H. Barrios, Y. Tomita, D. Castellano, B. I. Rini, A. C. Chen, S. Mekan, M. B. McHenry, M. Wind-Rotolo, J. Doan, P. Sharma, H. J. Hammers, B. Escudier, and CheckMate 214 Investigators. 2018. Nivolumab plus Ipilimumab versus Sunitinib in Advanced Renal-Cell Carcinoma. *N. Engl. J. Med.* 378: 1277–1290.

14. Rini, B. I., E. R. Plimack, V. Stus, R. Gafanov, R. Hawkins, D. Nosov, F. Pouliot, B. Alekseev, D. Soulières, B. Melichar, I. Vynnychenko, A. Kryzhanivska, I. Bondarenko, S. J. Azevedo, D. Borchiellini, C. Szczylik, M. Markus, R. S. McDermott, J. Bedke, S. Tartas, Y.-H. Chang, S. Tamada, Q. Shou, R. F. Perini, M. Chen, M. B. Atkins, T. Powles, and KEYNOTE-426 Investigators. 2019. Pembrolizumab plus Axitinib versus Sunitinib for Advanced Renal-Cell Carcinoma. *N. Engl. J. Med.* 380: 1116–1127.

15. Besser, M. J., R. Shapira-Frommer, O. Itzhaki, A. J. Treves, D. B. Zippel, D. Levy, A. Kubi, N. Shoshani, D. Zikich, Y. Ohayon, D. Ohayon, B. Shalmon, G. Markel, R. Yerushalmi, S. Apter, A. Ben-Nun, E. Ben-Ami, A. Shimoni, A. Nagler, and J. Schachter. 2013. Adoptive Transfer of Tumor-Infiltrating Lymphocytes in Patients with Metastatic Melanoma: Intent-to-Treat Analysis and Efficacy after Failure to Prior Immunotherapies. *Clin. Cancer Res.* 19: 4792–4800.

16. Rosenberg, S. A., J. C. Yang, R. M. Sherry, U. S. Kammula, M. S. Hughes, G. Q. Phan, D. E. Citrin, N. P. Restifo, P. F. Robbins, J. R. Wunderlich, K. E. Morton, C. M. Laurencot, S. M. Steinberg, D. E. White, and M. E. Dudley. 2011. Durable complete responses in heavily pretreated patients with metastatic melanoma using T-cell transfer immunotherapy. *Clin. Cancer Res.* 17: 4550–4557.

17. Andersen, R., M. Donia, E. Ellebaek, T. H. Borch, P. Kongsted, T. Z. Iversen, L. R. Hölmich, H. W. Hendel, Ö. Met, M. H. Andersen, P. thor Straten, and I. M. Svane. 2016. Long-Lasting Complete Responses in Patients with Metastatic Melanoma after Adoptive Cell Therapy with Tumor-Infiltrating Lymphocytes and an Attenuated IL2 Regimen. *Clin. Cancer Res.* 22: 3734–3745.

18. Sarnaik, A., N. I. Khushalani, J. A. Chesney, H. M. Kluger, B. D. Curti, K. D. Lewis, S. S. Thomas, E. D. Whitman, O. Hamid, J. Lutzky, A. C. Pavlick, J. S. Weber, J. M. G. Larkin, D. Barton, L. Yung, S. Suzuki, M. Fardis, and J. M. Kirkwood. 2019. Safety and efficacy of cryopreserved autologous tumor infiltrating lymphocyte therapy (LN-144, lifileucel) in advanced metastatic melanoma patients who progressed on multiple prior therapies including anti-PD-1. *J. Clin. Oncol.* 37: 2518.

19. Deniger, D. C., A. Pasetto, P. F. Robbins, J. J. Gartner, T. D. Prickett, B. C. Paria, P. Malekzadeh, L. Jia, R. Yossef, M. M. Langhan, J. R. Wunderlich, D. N. Danforth, R. P. T. Somerville, and S. A. Rosenberg. 2018. T-cell Responses to *TP53* "Hotspot" Mutations and Unique Neoantigens Expressed by Human Ovarian Cancers. *Clin. Cancer Res.* 24: 5562–5573.

20. Ben-Avi, R., R. Farhi, A. Ben-Nun, M. Gorodner, E. Greenberg, G. Markel, J. Schachter, O. Itzhaki, and M. J. Besser. 2018. Establishment of adoptive cell therapy with tumor infiltrating lymphocytes for non-small cell lung cancer patients. *Cancer Immunol. Immunother.* 67: 1221–1230.

21. De Groot, R., M. M. Van Loenen, A. Guislain, B. P. Nicolet, J. J. Freen-Van Heeren, O. J. H. M. Verhagen, M. M. Van Den Heuvel, J. De Jong, P. Burger, C. E. Van Der Schoot, R. M. Spaapen, D. Amsen, J. B. A. G. Haanen, K. Monkhorst, K. J. Hartemink, and M. C. Wolkers. 2019. Polyfunctional tumor-reactive T cells are effectively expanded from non-small cell lung cancers, and correlate with an immune-engaged T cell profile. *Oncoimmunology* 8: e1648170.

22. Tran, E., S. Turcotte, A. Gros, P. F. Robbins, Y.-C. Lu, M. E. Dudley, J. R. Wunderlich, R. P. Somerville, K. Hogan, C. S. Hinrichs, M. R. Parkhurst, J. C. Yang, and S. a Rosenberg. 2014. Cancer immunotherapy based on mutation-specific CD4+ T cells in a patient with epithelial cancer. *Science* 344: 641–5.

23. Tran, E., P. F. Robbins, Y.-C. Lu, T. D. Prickett, J. J. Gartner, L. Jia, A. Pasetto, Z. Zheng, S. Ray, E. M. Groh, I. R. Kriley, and S. A. Rosenberg. 2016. T-Cell Transfer Therapy Targeting Mutant KRAS in Cancer. *N. Engl. J. Med.* 375: 2255–2262.

24. Zacharakis, N., H. Chinnasamy, M. Black, H. Xu, Y.-C. Lu, Z. Zheng, A. Pasetto, M. Langhan, T. Shelton, T. Prickett, J. Gartner, L. Jia, K. Trebska-McGowan, R. P. Somerville, P. F. Robbins, S. A. Rosenberg, S. L. Goff, and S. A. Feldman. 2018. Immune recognition of somatic mutations leading to complete durable regression in metastatic breast cancer. *Nat. Med.* 24: 724–730.

25. Andersen, R., M. C. W. Westergaard, J. W. Kjeldsen, A. Müller, N. W. Pedersen, S. R. Hadrup, Ö. Met, B. Seliger, B. Kromann-Andersen, T. Hasselager, M. Donia, and I. M. Svane. 2018. T-cell Responses in the Microenvironment of Primary Renal Cell Carcinoma-Implications for Adoptive Cell Therapy. *Cancer Immunol. Res.* 6: 222–235.

26. Markel, G., T. Cohen-Sinai, M. J. Besser, K. Oved, O. Itzhaki, R. Seidman, E. Fridman, A. J. Treves, Y. Keisari, Z. Dotan, J. Ramon, and J. Schachter. 2009. Preclinical evaluation of adoptive cell therapy for patients with metastatic renal cell carcinoma. *Anticancer Res.* 29: 145–54.

27. Baldan, V., R. Griffiths, R. E. Hawkins, and D. E. Gilham. 2015. Efficient and reproducible generation of tumour-infiltrating lymphocytes for renal cell carcinoma. *Br. J. Cancer* 112: 1510–8.

28. Guislain, A., J. Gadiot, A. Kaiser, E. S. Jordanova, A. Broeks, J. Sanders, H. van Boven, T. D. de Gruijl, J. B. A.

5

G. Haanen, A. Bex, and C. U. Blank. 2015. Sunitinib pretreatment improves tumor-infiltrating lymphocyte expansion by reduction in intratumoral content of myeloid-derived suppressor cells in human renal cell carcinoma. *Cancer Immunol. Immunother.* 64: 1241–50.

29. Donia, M., J. W. Kjeldsen, R. Andersen, M. C. W. Westergaard, V. Bianchi, M. Legut, M. Attaf, B. Szomolay, S. Ott, G. Dolton, R. Lyngaa, S. R. Hadrup, A. K. Sewell, and I. M. Svane. 2017. PD-1+ Polyfunctional T Cells Dominate the Periphery after Tumor-Infiltrating Lymphocyte Therapy for Cancer. *Clin. Cancer Res.* 23: 5779–5788.

30. Wimmers, F., E. H. J. G. Aarntzen, T. Duiveman-deBoer, C. G. Figdor, J. F. M. Jacobs, J. Tel, and I. J. M. de Vries. 2016. Long-lasting multifunctional CD8 + T cell responses in end-stage melanoma patients can be induced by dendritic cell vaccination. *Oncoimmunology* 5: e1067745.

31. Poschke, I. C., J. C. Hassel, A. Rodriguez-Ehrenfried, K. A. M. Lindner, I. Heras-Murillo, L. M. Appel, J. Lehmann, T. Lövgren, S. L. Wickström, C. Lauenstein, J. Roth, A. K. König, J. B. A. G. Haanen, J. van den Berg, R. Kiessling, F. Bergmann, M. Flossdorf, O. Strobel, and R. Offringa. 2020. The Outcome of Ex Vivo TIL Expansion Is Highly Influenced by Spatial Heterogeneity of the Tumor T-Cell Repertoire and Differences in Intrinsic In Vitro Growth Capacity between T-Cell Clones. *Clin. Cancer Res.* 26: 4289–4301.

32. Lee, B. O., L. Haynes, S. M. Eaton, S. L. Swain, and T. D. Randall. 2002. The biological outcome of CD40 signaling is dependent on the duration of CD40 ligand expression: Reciprocal regulation by interleukin (IL)-4 and IL-12. *J. Exp. Med.* 196: 693–704.

33. Ford, G. S., B. Barnhart, S. Shone, and L. R. Covey. 1999. Regulation of CD154 (CD40 ligand) mRNA stability during T cell activation. *J. Immunol.* 162: 4037–44.

34. Wolfl, M., J. Kuball, W. Y. Ho, H. Nguyen, T. J. Manley, M. Bleakley, and P. D. Greenberg. 2007. Activation-induced expression of CD137 permits detection, isolation, and expansion of the full repertoire of CD8+ T cells responding to antigen without requiring knowledge of epitope specificities. *Blood* 110: 201–10.

35. Thommen, D. S., V. H. Koelzer, P. Herzig, A. Roller, M. Trefny, S. Dimeloe, A. Kiialainen, J. Hanhart, C. Schill, C. Hess, S. Savic Prince, M. Wiese, D. Lardinois, P.-C. Ho, C. Klein, V. Karanikas, K. D. Mertz, T. N. Schumacher, and A. Zippelius. 2018. A transcriptionally and functionally distinct PD-1+ CD8+ T cell pool with predictive potential in non-small-cell lung cancer treated with PD-1 blockade. *Nat. Med.* 24: 994–1004.

36. Giraldo, N. A., E. Becht, Y. Vano, F. Petitprez, L. Lacroix, P. Validire, R. Sanchez-Salas, A. Ingels, S. Oudard, A. Moatti, B. Buttard, S. Bourass, C. Germain, X. Cathelineau, W. H. Fridman, and C. Sautes-Fridman. 2017. Tumor-infiltrating and peripheral blood T-cell immunophenotypes predict early relapse in localized clear cell renal cell carcinoma. *Clin. Cancer Res.* 23: 4416–4428.

37. Li, X., R. Wang, P. Fan, X. Yao, L. Qin, Y. Peng, M. Ma, N. Asley, X. Chang, Y. Feng, Y. Hu, Y. Zhang, C. Li, G. Fanning, S. Jones, C. Verrill, D. Maldonado-Perez, P. Sopp, C. Waugh, S. Taylor, S. Mcgowan, V. Cerundolo, C. Conlon, A. McMichael, S. Lu, X. Wang, N. Li, and T. Dong. 2019. A Comprehensive Analysis of Key Immune Checkpoint Receptors on Tumor-Infiltrating T Cells From Multiple Types of Cancer. *Front. Oncol.* 9: 1066.

38. Zelba, H., J. Bedke, J. Hennenlotter, S. Mostböck, M. Zettl, T. Zichner, A. Chandran, A. Stenzl, H. G. Rammensee, and C. Gouttefangeas. 2019. PD-1 and LAG-3 dominate checkpoint receptor-mediated T-cell inhibition in renal cell carcinoma. *Cancer Immunol. Res.* 7: 1891–1899.

39. Attig, S., J. Hennenlotter, G. Pawelec, G. Klein, S. D. Koch, H. Pircher, S. Feyerabend, D. Wernet, A. Stenzl, H. G. Rammensee, and C. Gouttefangeas. 2009. Simultaneous infiltration of polyfunctional effector and suppressor T cells into renal cell carcinomas. *Cancer Res.* 69: 8412–8419.

40. Kawashima, A., T. Kanazawa, K. Goto, M. Matsumoto, A. Morimoto-Okazawa, K. Iwahori, A. Ujike, A. Nagahara, K. Fujita, M. Uemura, N. Nonomura, and H. Wada. 2018. Immunological classification of renal cell carcinoma patients based on phenotypic analysis of immune check-point molecules. *Cancer Immunol. Immunother.* 67: 113–125.

41. Fontenot, J. D., M. A. Gavin, and A. Y. Rudensky. 2003. Foxp3 programs the development and function of CD4+CD25+ regulatory T cells. *Nat. Immunol.* 4: 330–336.

42. Rohaan, M. W., J. H. van den Berg, P. Kvistborg, and J. B. A. G. Haanen. 2018. Adoptive transfer of tumor-infiltrating lymphocytes in melanoma: a viable treatment option. *J. Immunother. cancer* 6: 102.

43. Ye, Q., D.-G. Song, M. Poussin, T. Yamamoto, A. Best, C. Li, G. Coukos, and D. J. Powell. 2014. CD137 Accurately Identifies and Enriches for Naturally Occurring Tumor-Reactive T Cells in Tumor. *Clin. Cancer Res.* 20: 44–55.

44. Frentsch, M., O. Arbach, D. Kirchhoff, B. Moewes, M. Worm, M. Rothe, A. Scheffold, and A. Thiel. 2005. Direct access to CD4+ T cells specific for defined antigens according to CD154 expression. *Nat. Med.* 11: 1118–1124.

45. Baine, M. K., G. Turcu, C. R. Zito, A. J. Adeniran, R. L. Camp, L. Chen, H. M. Kluger, and L. B. Jilaveanu. 2015. Characterization of tumor infiltrating lymphocytes in paired primary and metastatic renal cell carcinoma specimens. *Oncotarget* 6: 24990–25002.

46. Mlecnik, B., G. Bindea, H. K. Angell, P. Maby, M. Angelova, D. Tougeron, S. E. Church, L. Lafontaine, M. Fischer, T. Fredriksen, M. Sasso, A. M. Bilocq, A. Kirilovsky, A. C. Obenauf, M. Hamieh, A. Berger, P. Bruneval, J.-J. Tuech, J.-C. Sabourin, F. Le Pessot, J. Mauillon, A. Rafii, P. Laurent-Puig, M. R. Speicher, Z. Trajanoski, P. Michel,

R. Sesboüe, T. Frebourg, F. Pagès, V. Valge-Archer, J.-B. Latouche, and J. Galon. 2016. Integrative Analyses of Colorectal Cancer Show Immunoscore Is a Stronger Predictor of Patient Survival Than Microsatellite Instability. *Immunity* 44: 698–711.

47. Zhang, L., J. R. Conejo-Garcia, D. Katsaros, P. A. Gimotty, M. Massobrio, G. Regnani, A. Makrigiannakis, H. Gray, K. Schlienger, M. N. Liebman, S. C. Rubin, and G. Coukos. 2003. Intratumoral T cells, recurrence, and survival in epithelial ovarian cancer. *N. Engl. J. Med.* 348: 203–13.

48. Bindea, G., B. Mlecnik, M. Tosolini, A. Kirilovsky, M. Waldner, A. C. Obenauf, H. Angell, T. Fredriksen, L. Lafontaine, A. Berger, P. Bruneval, W. H. Fridman, C. Becker, F. Pagès, M. R. Speicher, Z. Trajanoski, and J. Galon. 2013. Spatiotemporal dynamics of intratumoral immune cells reveal the immune landscape in human cancer. *Immunity* 39: 782–95.

49. Parkhurst, M., A. Gros, A. Pasetto, T. Prickett, J. S. Crystal, P. Robbins, and S. A. Rosenberg. 2017. Isolation of T-cell receptors specifically reactive with mutated tumor-associated antigens from tumor-infiltrating lymphocytes based on CD137 expression. *Clin. Cancer Res.* 23: 2491–2505.

50. Gros, A., P. F. Robbins, X. Yao, Y. F. Li, S. Turcotte, E. Tran, J. R. Wunderlich, A. Mixon, S. Farid, M. E. Dudley, K. I. Hanada, J. R. Almeida, S. Darko, D. C. Douek, J. C. Yang, and S. A. Rosenberg. 2014. PD-1 identifies the patient-specific CD8+ tumor-reactive repertoire infiltrating human tumors. *J. Clin. Invest.* 124: 2246–2259.

51. Helmink, B. A., S. M. Reddy, J. Gao, S. Zhang, R. Basar, R. Thakur, K. Yizhak, M. Sade-Feldman, J. Blando, G. Han, V. Gopalakrishnan, Y. Xi, H. Zhao, R. N. Amaria, H. A. Tawbi, A. P. Cogdill, W. Liu, V. S. LeBleu, F. G. Kugeratski, S. Patel, M. A. Davies, P. Hwu, J. E. Lee, J. E. Gershenwald, A. Lucci, R. Arora, S. Woodman, E. Z. Keung, P.-O. Gaudreau, A. Reuben, C. N. Spencer, E. M. Burton, L. E. Haydu, A. J. Lazar, R. Zapassodi, C. W. Hudgens, D. A. Ledesma, S. Ong, M. Bailey, S. Warren, D. Rao, O. Krijgsman, E. A. Rozeman, D. Peeper, C. U. Blank, T. N. Schumacher, L. H. Butterfield, M. A. Zelazowska, K. M. McBride, J. Kalluri, J. Allison, F. Petitprez, W. H. Fridman, C. Sautès-Fridman, N. Hacohen, K. Rezvani, P. Sharma, M. T. Tetzlaff, L. Wang, and J. A. Wargo. 2020. B cells and tertiary lymphoid structures promote immunotherapy response. *Nature* 577: 549–555.

52. Petitprez, F., A. de Reyniès, E. Z. Keung, T. W. W. Chen, C. M. Sun, J. Calderaro, Y. M. Jeng, L. P. Hsiao, L. Lacroix, A. Bougoüin, M. Moreira, G. Lacroix, I. Natario, J. Adam, C. Lucchesi, Y. Laizet, M. Toulmonde, M. A. Burgess, V. Bolejack, D. Reinke, K. M. Wani, W. L. Wang, A. J. Lazar, C. L. Roland, J. A. Wargo, A. Italiano, C. Sautès-Fridman, H. A. Tawbi, and W. H. Fridman. 2020. B cells are associated with survival and immunotherapy response in sarcoma. *Nature* 577: 556–560.

53. Jeyakumar, G., S. Kim, N. Bumma, C. Landry, C. Silski, S. Suisham, B. Dickow, E. Heath, J. Fontana, and U. Vaishampayan. 2017. Neutrophil lymphocyte ratio and duration of prior anti-angiogenic therapy as biomarkers in metastatic RCC receiving immune checkpoint inhibitor therapy. *J. Immunother. cancer* 5: 82.

54. Van Den Berg, J. H., B. Heemskerk, N. Van Rooij, R. Gomez-Eerland, S. Michels, M. Van Zon, R. De Boer, N. A. M. Bakker, A. Jorritsma-Smit, M. M. Van Buuren, P. Kvistborg, H. Spits, R. Schotte, H. Mallo, M. Karger, J. A. Van Der Hage, M. W. J. M. Wouters, L. M. Pronk, M. H. Geukes Foppen, C. U. Blank, J. H. Beijnen, B. Nuijen, T. N. Schumacher, and J. B. A. G. Haanen. 2020. Tumor infiltrating lymphocytes (TIL) therapy in metastatic melanoma: Boosting of neoantigen-specific T cell reactivity and long-term follow-up. *J. Immunother. Cancer* 8.

55. Asma, G., G. Amal, M. Raja, D. Amine, C. Mohammed, and B. A. E. Amel. 2015. Comparison of circulating and intratumoral regulatory T cells in patients with renal cell carcinoma. *Tumour Biol.* 36: 3727–34.

56. Zhu, G., L. Pei, H. Yin, F. Lin, X. Li, X. Zhu, W. He, and X. Gou. 2019. Profiles of tumor-infiltrating immune cells in renal cell carcinoma and their clinical implications. *Oncol. Lett.* 18: 5235–5242.

57. Siddiqui, S. A., X. Frigola, S. Bonne-Annee, M. Mercader, S. M. Kuntz, A. E. Krambeck, S. Sengupta, H. Dong, J. C. Cheville, C. M. Lohse, C. J. Krco, W. S. Webster, B. C. Leibovich, M. L. Blute, K. L. Knutson, and E. D. Kwon. 2007. Tumor-Infiltrating Foxp3-CD4+CD25+ T Cells Predict Poor Survival in Renal Cell Carcinoma. *Clin. Cancer Res.* 13: 2075–2081.

58. Errarte, P., G. Larrinaga, and J. I. López. 2020. The role of cancer-associated fibroblasts in renal cell carcinoma. An example of tumor modulation through tumor/non-tumor cell interactions. *J. Adv. Res.* 21: 103–108.

59. Figlin, R. A., J. A. Thompson, R. M. Bukowski, N. J. Vogelzang, A. C. Novick, P. Lange, G. D. Steinberg, and A. S. Belldegrun. 1999. Multicenter, randomized, phase III trial of CD8(+) tumor-infiltrating lymphocytes in combination with recombinant interleukin-2 in metastatic renal cell carcinoma. *J. Clin. Oncol.* 17: 2521–9.

60. ClinicalTrials.gov. Identifier NCT02926053, TIL Therapy for Metastatic Renal Cell Carcinoma.t

61. ClinicalTrials.gov. Identifier NCT03229278, Trigriluzole With Nivolumab and Pembrolizumab in Treating Patients With Metastatic or Unresectable Solid Malignancies or Lymphoma.

62. ClinicalTrials.gov. Identifier NCT03549000, A Phase I/Ib Study of NZV930 Alone and in Combination With PDR001 and /or NIR178 in Patients With Advanced Malignancies.

63. ClinicalTrials.gov. Identifier NCT03311334, A Study of DSP-7888 Dosing Emulsion in Combination With Immune Checkpoint Inhibitors in Adult Subjects With Advanced Solid Tumors.

5

Supplementary data
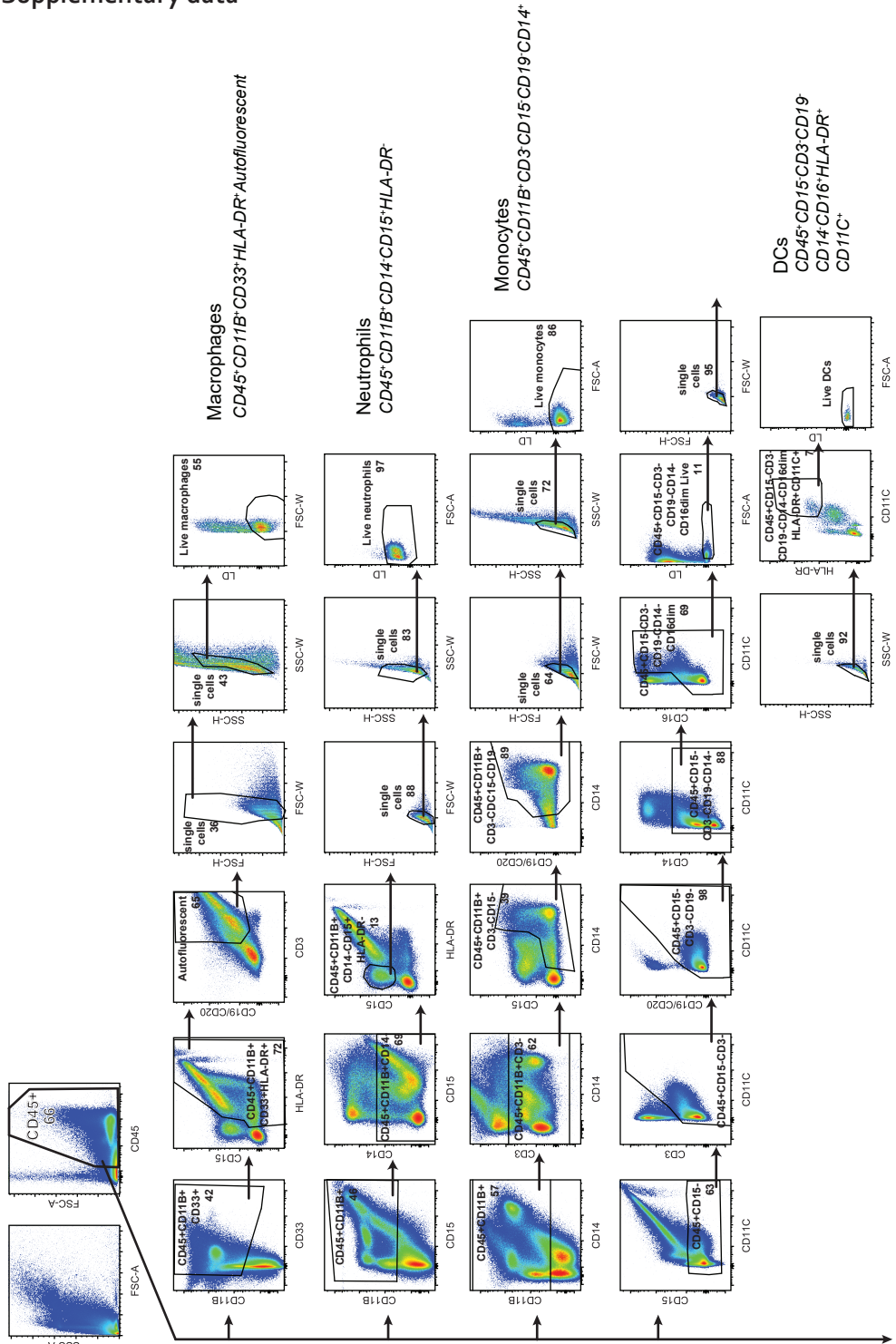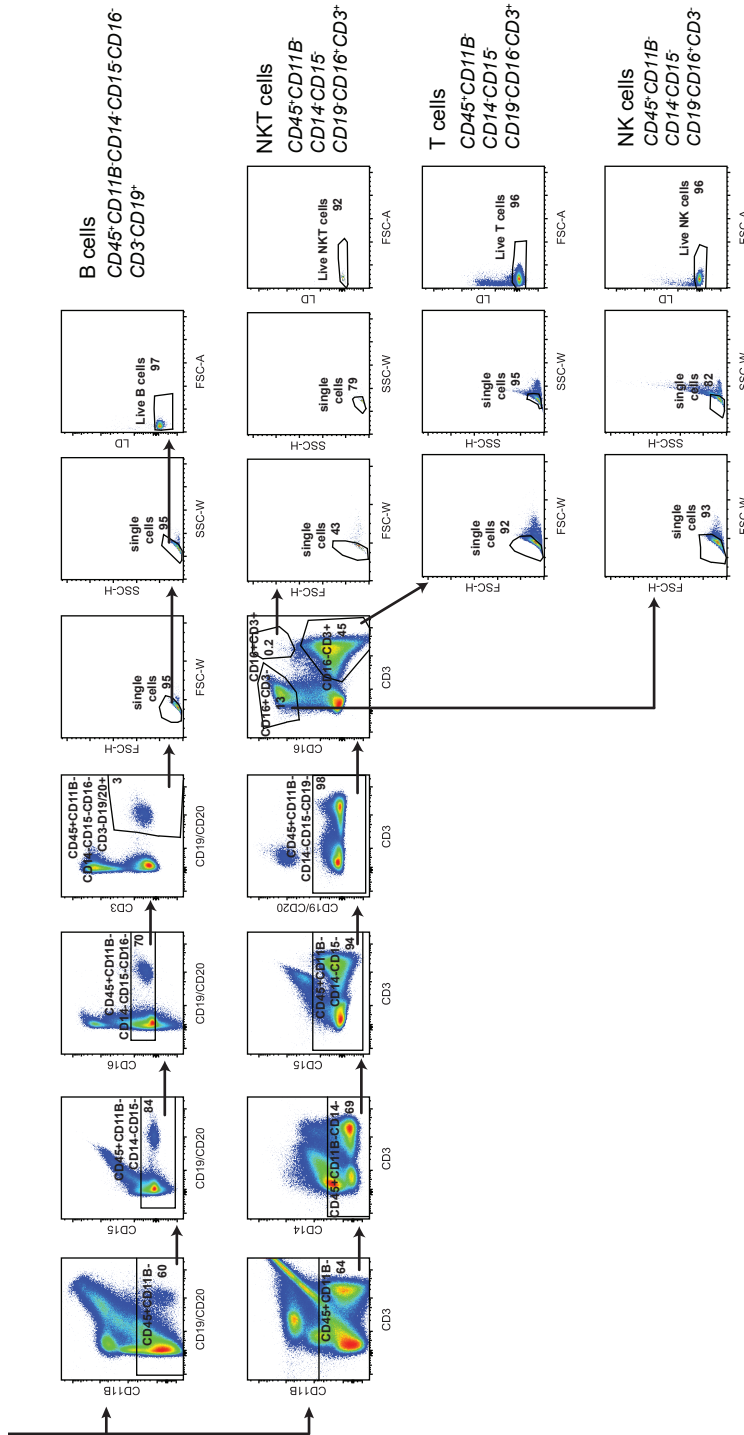
Figure S1. Gating strategy immune cell subsets. Gating strategy to determine the major immune subsets as quantified in Fig. 1. All subsets were first gated positively for CD45. Macrophages were gated positively for CD11b, HLA-DR, autofluorescence, followed by doublet exclusion and dead cell exclusion. This macrophage subset includes potential myeloid derived suppressor cells (MDSCs), for which no specific markers were included in the antibody panel. Neutrophils were gated positively for CD11b, negatively for CD14, CD15$^+$HLA-DR$^-$, followed by doublet exclusion and dead cell exclusion. Monocytes were gated positively for CD3, CD15$^+$CD14$^-$ cells were excluded, then gated positively for CD14, followed by exclusion of doublets and dead cells. Dendritic cells (DCs) were gated negatively for CD15, CD3, CD19/CD20 and CD14. CD16$^+$CD11C$^-$ cells, dead cells and doublets were excluded. Finally, DCs were identified as CD11C$^+$HLA-DR$^+$. B cells were gated negatively for CD11b, CD15, CD16, and positively for CD19/CD20. Doublets and dead cells were excluded. T cells and NK(T) cells had a similar gating strategy. They were gated negatively for CD11B, CD14, CD15 and CD19/CD20. Next NK cells were identified as CD3$^-$CD16$^+$ and T cells as CD3$^+$CD16$^-$. NKT cells were identified as CD3$^+$CD16$^+$, NKT cells as CD3$^+$CD16$^+$ and T cells as CD3$^+$CD16$^-$. Doublets and dead cells were excluded.

A

B

C

D
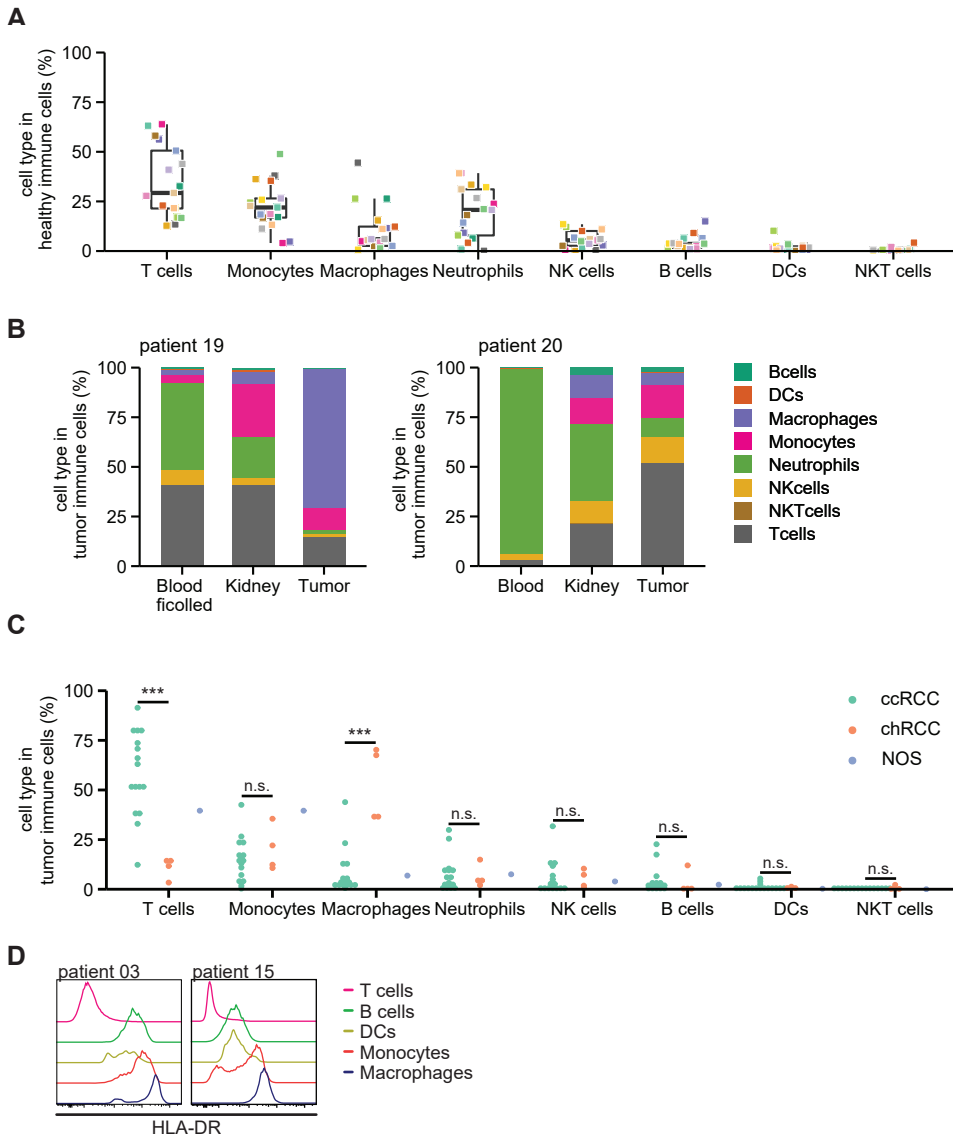
Figure S2. Immune subsets in kidney and in tumor per RCC subtype. (A-C) Immune subsets as a percentage of total immune cells in kidney digest (A), paired blood, kidney- and tumor digest (B) and in tumor digest per RCC type (C). No events were excluded for these ex vivo analyses. (D) HLA-DR expression in immune cells isolated from tumor digests. ccRCC = clear cell RCC, chRCC = chromophobe RCC, NOS = not otherwise specified. Aligned ranks transformation two-way ANOVA, Tukey's post hoc test.
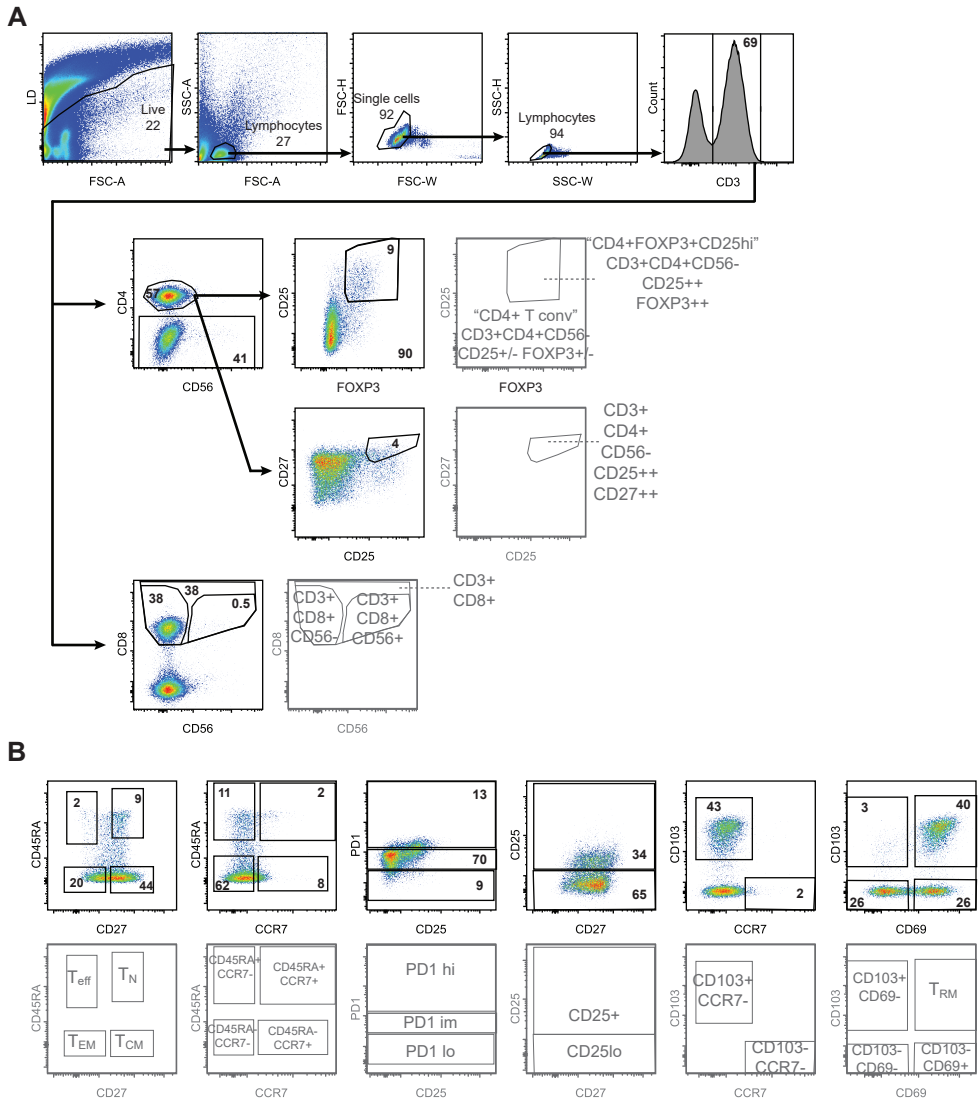
Figure S3. Gating strategy of the T cell focused antibody panel. (A) Lymphocytes were first gated negatively for the life/dead stain, then gated based on cell size, followed by exclusion of doublets. T cells were identified as CD3+. Within the CD8+ T cell population, CD8+CD56- and CD8+CD56+ subpopulations were identified. The CD4+ T cell population was split into FOXP3+CD25hi and non-FOXP3+CD25hi (CD4+ conv) subpopulations. The CD25hiCD27hi cells of the CD4+ T cell population were separately gated. (B) Gating strategy for the determination of various memory and activation phenotypes. This gating strategy was applied to all populations defined in A. The percentages of all different populations were used for the principle component analysis (Fig. 2A-C). In addition, this antibody panel was used in Figs. 1C-D, 2D-H, S6 and S7.

5
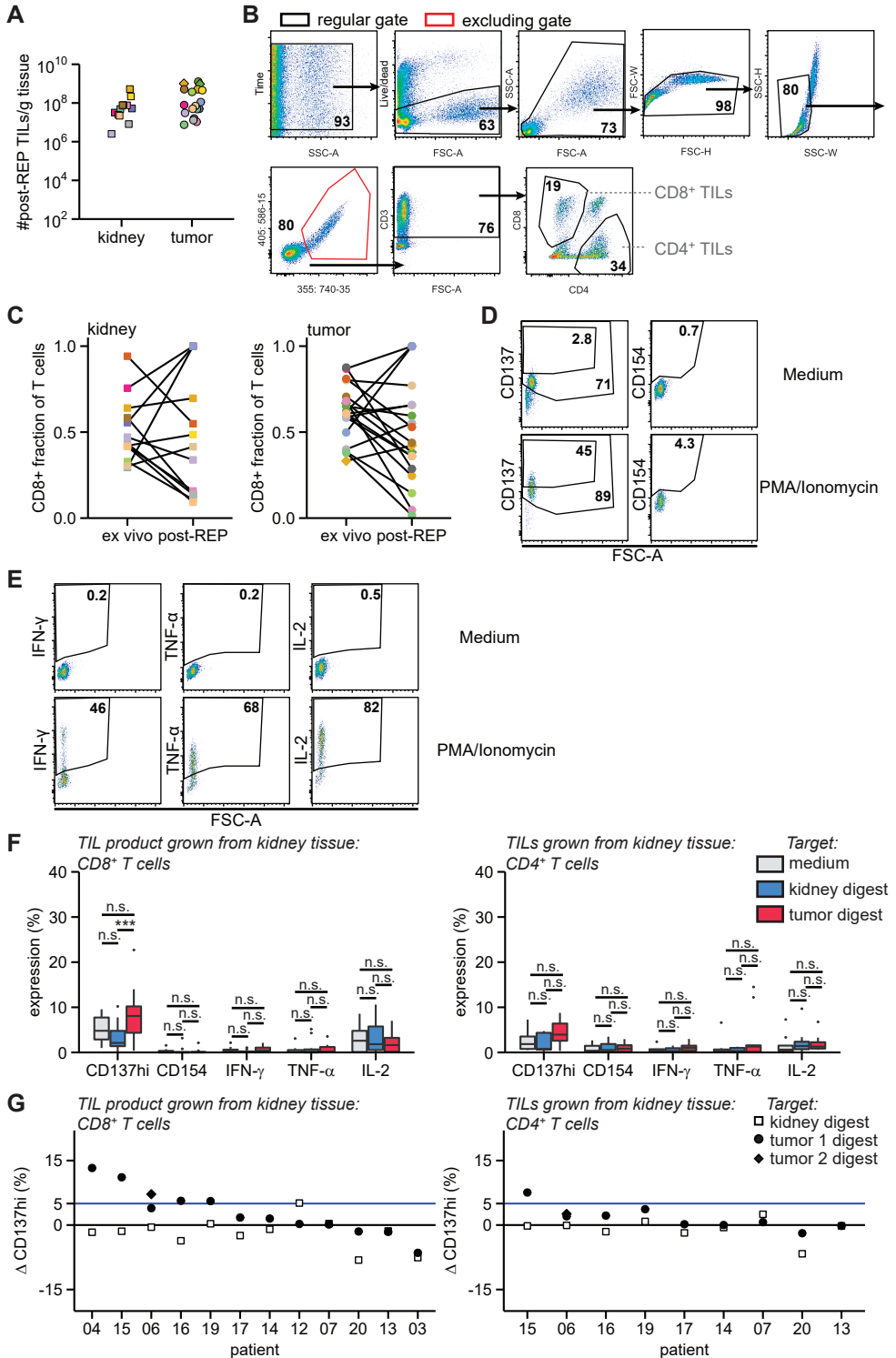
Figure S4. Gating strategy tumor reactivity assay and tumor reactivity TIL products from kidney.

5

Figure S4 Legend (continued)

(A) Number of post-REP TILs per gram of tissue from which they were derived. (B) Gating strategy for the tumor reactivity assay after TIL culture. Any obstructions in the flow of the cytometer were gated out using a time gate. Next, dead cells were excluded, cells were gated based on size followed by doublet exclusion. Tumor and kidney digests often contained autofluorescent cells. These cells were removed by excluding cells positive in two empty channels. Finally, TILs were identified by expression of CD3, and CD4 or CD8. (C) Fraction of CD8+ T cells within total T cells per patient (corresponds to Fig. 3B). (D) Gates for the activation markers CD137 and CD154 were based on medium control samples. The CD137+ gate was set starting at the positive population in the medium control sample, and the CD137hi gate above the first positive population. The CD154+ gate was set above the events in the medium control sample. (E) Example gating strategies for the cytokines IFN-γ, TNF-α or IL-2. (F-G) TIL products grown from kidney digests were cultured in medium with or without autologous tumor or kidney digest for 6 h. Extracellular CD154 and intracellular high CD137 (CD137hi), IFN-γ, TNF-α or IL-2 expression per stimulation (F) and per patient delta CD137hi (Δ; tissue digest – medium) reactivity of TIL products (G).
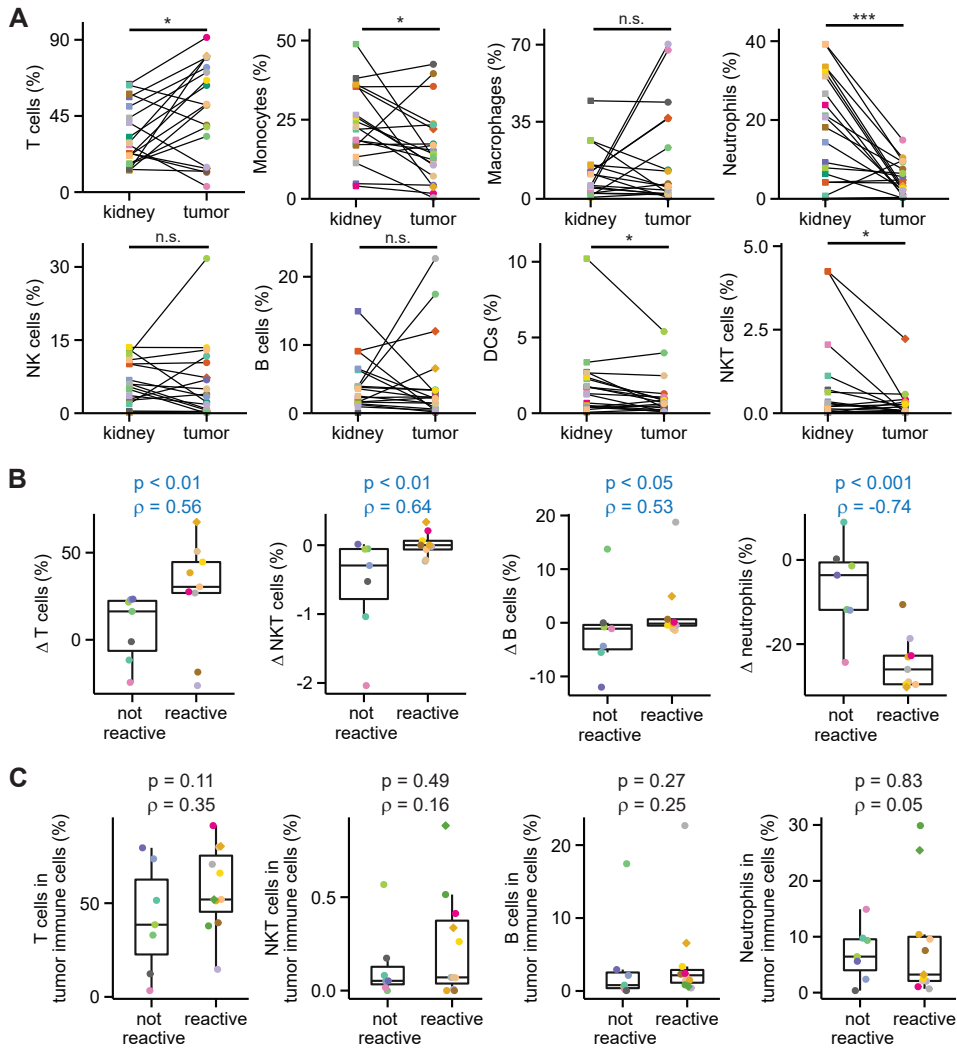
Figure S5. T cell infiltration correlates with tumor reactivity. (A) Ex vivo immune subsets as a percentage of total immune cells for paired kidney and tumor samples (data from Fig. 1B and S2A). Statistical significance was determined by Wilcoxon signed-rank test. (B) Delta (Δ) ex vivo immune cell subsets (tumor – kidney) were correlated with post-REP tumor reactivity of TIL products (Fig. 4B) using Spearman's correlation. (C) Spearman's correlation between the percentage of immune subsets in the ex vivo RCC samples (Fig. 1B) and post-REP tumor reactivity (Fig. 4B). For C and D p values and Spearman's rho (ρ) are shown above each panel. Significant (p < 0.05) correlations are colored blue, nonsignificant correlations black.
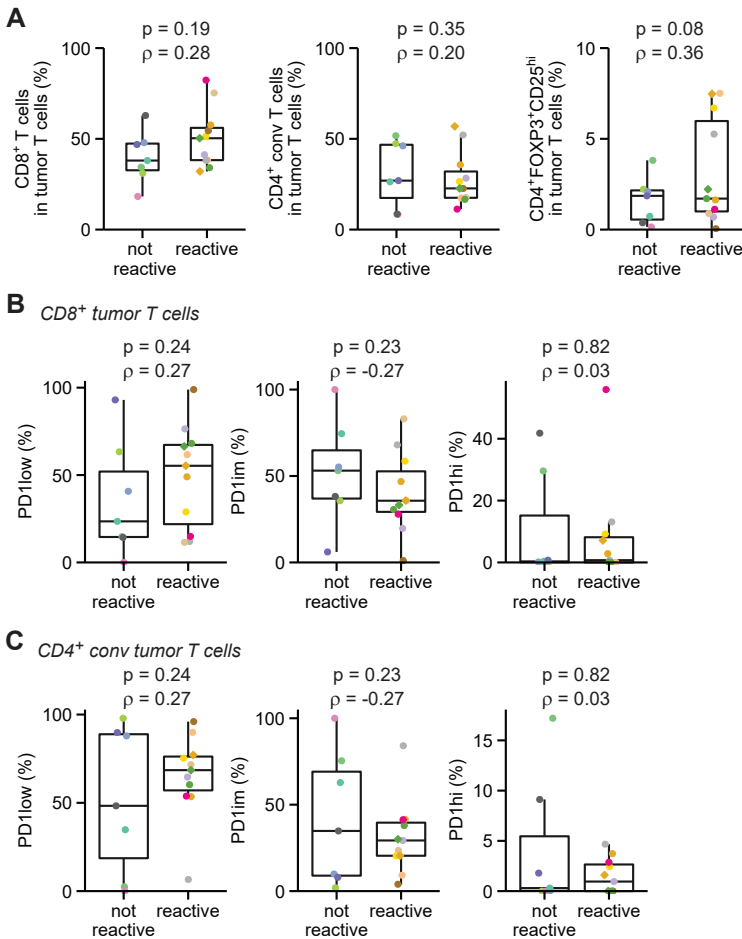
Figure S6. T cell subsets nor T cell PD-1 expression correlate with tumor reactivity. (A) Spearman's correlation between ex vivo T cell subpopulations (Fig. 1C) and post-REP tumor reactivity of TIL products (Fig. 4B). (B-C) Spearman's correlation between PD-1 expression levels in CD8+T cells (Fig. 1D) (B) or CD4+T cells (Fig. 1E) (C) and post-REP tumor reactivity (Fig. 4B). P values and Spearman's rho (ρ) are shown above each panel. Significant correlations (p < 0.05) are colored blue, nonsignificant correlations black.

5
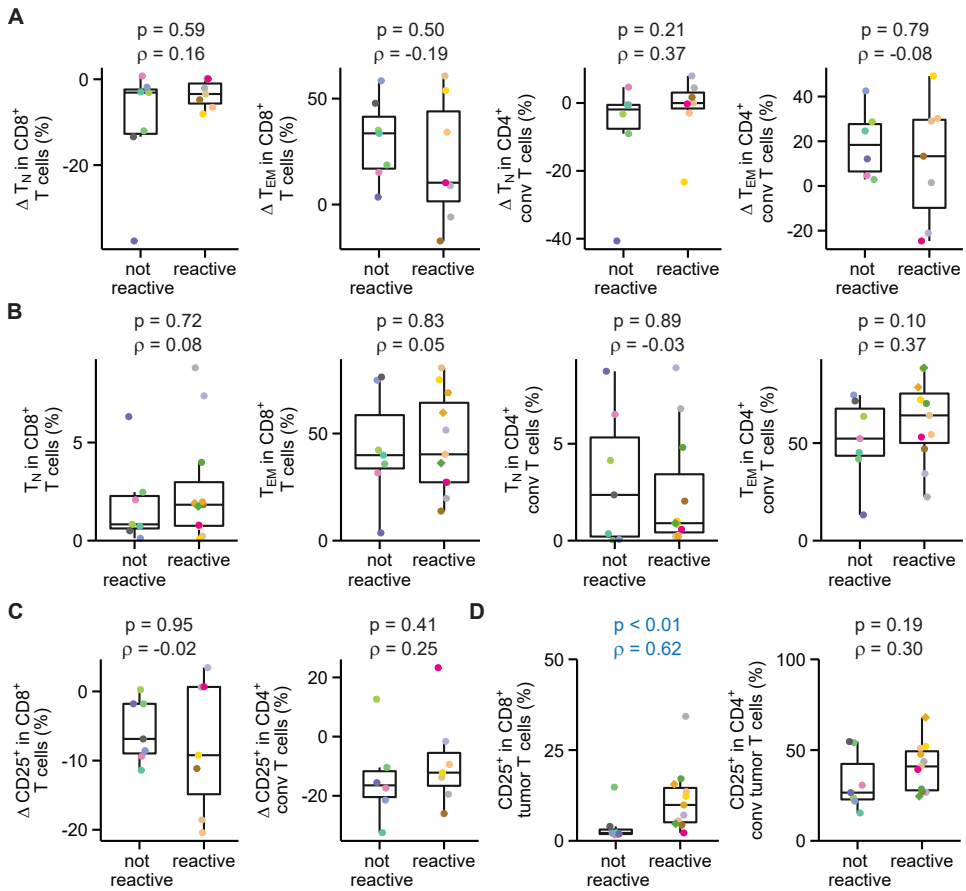
Figure S7. CD25 expression in ex vivo tumor CD8+ T cells correlates with tumor reactivity. (A-B) Ex vivo naïve (CD45RA+CD27+) and effector memory (CD45RA-CD27-) populations within CD8+ and CD4+ conv T cells (Fig. 2D and E) were correlated with post-REP tumor reactivity of TIL products (Fig. 4B) using Spearman's correlation. Correlation of the difference in infiltration between tumor and kidney (Δ; tumor - kidney) and tumor reactivity is shown in A, the correlation between tumor T cell subsets and tumor reactivity in B. (C-D) Ex vivo CD25 expression in CD8+ and CD4+ conv T cells (Fig. 2F and G) correlated with post-REP tumor reactivity (Fig. 4B). Delta CD25 expression (tumor – kidney) is shown in C, tumor CD25 expression in D. P values and Spearman's rho (ρ) are shown above each panel. Significant correlations ($p < 0.05$) are colored blue, nonsignificant correlations black.

Table S1. Flow cytometry panels

Antigen	Fluorochrome	Clone	Source
Immune cell subset panel			
CD11C	PerCp-Cy5.5	3.9	Biolegend
HLA-DR	FITC	L243 (G46-6)	BD Biosciences
CD15	BV605	W6D3	Biolegend
CD3	BV510	OKT3	Biolegend
CD11b	BV421	ICRF44	Biolegend
CD45	BUV805	HI30	BD Biosciences
CD19	BUV 737	SJ25C1	BD Biosciences
CD20	BUV 737	2H7	BD Biosciences
CD16	BUV 496	3G8	BD Biosciences
CD1a	BUV 395	HI149	BD Biosciences
LIVE/DEAD™ Fixable Stain	Near-IR		Invitrogen (Thermo Fisher Scientific)
CD33	Alexa Fluor 700	WM53	BD Biosciences
CD68	APC	Y1/82A	Biolegend
CD14	PECy7	61D3	eBioscience
CD274 / PD-L1	PE	29E.2A3	Biolegend
T cell panel			
CD3	PerCp-Cy5.5	SK7	Biolegend
PD-1	FITC	EH12-2H7	Biolegend
CD56	BV605	HCD56	Biolegend
CD27	BV510	O323	Biolegend
CCR7	BV421	G042H7	Biolegend
CD8	BUV805	SK1	BD Biosciences
CD45RA	BUV 737	HI100	BD Biosciences
CD4	BUV 496	SK3	BD Biosciences
CD69	BUV395	FN50	BD Biosciences
LIVE/DEAD™ Fixable Stain	Near-IR		Invitrogen (Thermo Fisher Scientific)
FOXP3	Alexa Fluor 647	259 D	Biolegend
CD103	PE-Cy7	B-Ly7	Biolegend
CD25	PE	2A3	Biolegend
Tumor reactivity panel			
CD8	BUV805	SK1	BD Biosciences
CD4	BUV496	SK3	BD Biosciences
CD3	BUV395	SK7	BD Biosciences
PD-1	BV421	EH12.1	BD Biosciences
CD154	BV510	24-31	Biolegend
LIVE/DEAD™ Fixable Stain	Near-IR		Invitrogen (Thermo Fisher Scientific)
TNF-α	Alexa Fluor 488	Mab11	Biolegend
CD137	PE-Cy7	4B4-1	Biolegend
IFN-γ	PE	4S.B3	Biolegend
IL-2	APC	MQ1-17H12	Invitrogen

5

CHAPTER 6

General discussion

General discussion

Effective immunological communication ensures that the appropriate components of the immune system are active in the desired immune response and only lead to the appropriate type of immune cell differentiation. Unfortunately, incorrect or suboptimal activation of immune cells is associated with many diseases, including, autoimmune diseases, cancer and chronic infections. Improved understanding of the mediators of immunological communication may support therapy development for these diseases. In this thesis we successfully applied high-throughput screening as a tool to uncover hereto unknown effects of known secreted signaling proteins.

Arrayed screening requires extensive preparation

The research described in **chapters 2-4** of this thesis were based on so-called forward arrayed screens. In arrayed screening the same in vitro assay is performed for many samples, with each sample receiving distinct treatment. This distinct treatment may be knockout of a unique gene in each sample, or treatment of each sample with a unique compound. The source of the different treatments stems from a library which may contain hundreds or even thousands of different CRISPR/Cas9 guide RNAs, small drug-like molecules, or conditioned media containing different secreted proteins (1–3). Both the library and the assay are chosen based on the biological question at hand and both will determine which hits can be identified.

The secreted protein library was developed with technical limitations

In this thesis we used a library of secreted proteins to uncover unknown effects of these proteins in immunological communication. We included secreted proteins both with a known or unknown immunological role. Initially the library contained 756 conditioned media, but as it is estimated that the entire human secretome contains over 3000 proteins we aimed to expand this library to include over 1200 conditioned media (listed in the Appendices) (4). The full secreted protein library as used in **chapter 4** can therefore still be expanded for a more comprehensive coverage of the full human secretome. A further expansion could be addition of heterodimeric secreted proteins, which are more difficult to produce as they require the producing cell to contain and translate both transcripts and achieve correct protein folding.

The library described here was prepared by individual transfection of cDNAs encoding for secreted proteins into HEK293T cells, followed by harvesting of the conditioned media three days later. This method was practically and financially feasible in our lab, yet there are several potential caveats inherent to this approach. In the ideal case every conditioned medium contains a biologically active concentration of the intended secreted protein. Yet in practice, not every transfection is equally efficient and not every protein is produced or secreted to a similar extent by the HEK293T cells (chapter 2, Fig. 1C). For example, in **chapter 3** the IL-21 conditioned medium did not clearly improve memory B cell

differentiation into antibody secreting cells (ASCs) (chapter 3, Fig. 3A), which may be due to a supra-optimal concentration of IL-21. Furthermore, TGFB1 conditioned media did not promote CD103 expression in the T cell differentiation screen (chapter 4, Fig. S3), while it did in the screen assay optimization experiments (chapter 4, Fig. 1D).

In addition, a successfully produced secreted protein may also induce secondary effects in the producing cells, including altered production or secretion of other proteins and/or an altered metabolism, all of which may affect the outcome of the final assay. This is a potential explanation for the discrepancy between MAp19 conditioned medium and purified MAp19 in **chapter 3**, as MAp19 conditioned medium clearly induced memory B cell differentiation into ASCs (chapter 3, Fig. 4A), yet purified recombinant MAp19 did not (chapter 3, Fig. 4B). As we did not quantify every secreted protein in our library (due to time and cost-constraints) this library cannot be used to analyze which secreted proteins can be ruled out to affect the readouts of each screen. Instead, transfection controls were used in every production round to monitor overall transfection efficiency.

Finally, conditioned media can affect cells in the screen assay as it is used media from HEK293T cells, meaning certain ingredients of the culture medium are depleted while other (metabolic) compounds are introduced by the HEK293T cells. To minimize these conditioned media-related effects we only used diluted conditioned media in our assays, which means that we also diluted any secreted protein of interest. Due to all the shortcomings of the secreted protein library only hits inducing an effect were selected for further analysis and validation experiments were performed using purified secreted proteins, while no conclusions can be drawn on conditioned media that did not alter the outcome of an assay (chapter 2-4). This library could be improved by purifying each secreted protein and determining the concentration.

All potential sources of external variation must be minimized to obtain an assay suitable for high-throughput screening

Arrayed screening is a very laborious process, as hundreds up to thousands of samples must be processed without introducing technical variation that may mask any biological effects. The lessons that we learned in setting up the multiple screens in this thesis fuel the following recommendations.

6

1. It is crucial to have a reproducible assay for arrayed screening. While the assays used in this thesis were already established, each assay needed to be optimized for high throughput screening as this approach includes many more samples than regular lab experiments requiring more reagents, cells, sample handling, and sophisticated data analysis. To accomplish this, we recommend that several titrations are performed to allow the use of limited resources (e.g. primary cells such as naive or IgG$^+$ memory B cells in chapter 3, Fig. 1B-C), minimize the use of expensive reagents (e.g. fluorochrome-labeled antibodies), and to ensure a large dynamic range between positive and negative controls (e.g. titration of IL-21 in chapter 3, Fig. 1B-C).

2. Ideally the assay has already been run many times in the lab before using it in a high-throughput screen so that any potential technical sources of variation are already identified so they can be mitigated, and both the negative control (baseline, e.g. empty vector conditioned medium or a non-targeting control) and the positive control (which induces a clear change from baseline) have been determined. In general, the less variation between replicates of each control, the more sensitive the eventual screen will be to identify conditions that have a more limited biological impact. This can be especially important, because screen conditions are usually not optimal for the individual hits, as we have seen after titrating FGF16 (chapter 2, Fig. 2G). We recommend introduction of a pilot screen, a small version of the eventual screen, as it can tell whether the assay itself is appropriate for screening and should preferably use reagents and cells of the same lot or donor as intended for the final screen. This pilot screen sensibly includes multiple replicates of both the positive and negative controls to calculate the Z-factor (Box 1) and may also consist of a few plates of the library. The latter was not done for any of the screens in this thesis but doing so may highlight issues with the placement of controls and samples on a plate.

3. Once an assay has successfully gone through a pilot screen there are still some points we recommend before performing the full screen. The pilot screen is still relatively small compared to the full screen. The increase in the number of conditions in the full screen can lead to unwanted effects. For example, handling more plates increases the time to perform each step of the protocol, leading to one plate being processed earlier after incubation compared to another plate, which may increase the variation between plates. Alternatively, the full screen can be split across multiple rounds, although this may lead to significant variation between rounds as was observed in the T cell differentiation screen (Fig. 1A, left panel), or a pipetting robot can be employed, although setting up a robot requires assay optimization as well. Importantly, we recommend that every plate in both pilot and full screens contains all controls to be able to monitor between-plate differences and to (have the option to) apply certain types of normalization.

Box 1. Z-factor calculation

The Z-factor (Z'), not to be confused with the Z-score, can be calculated to determine whether the effect size between negative and positive controls is sufficient for screening (1):

$$Z'=1- (3(\sigma_p + \sigma_n))/(|\mu_p - \mu_n|)$$

In which the measured means (μ) and standard deviations (σ) of both the positive (p) and negative controls (n) are considered. A perfect screen has a Z' of 1, yet any value above 0 means the assay is appropriate for high-throughput screening. All high-throughput screens described in this thesis were prefaced with a pilot experiment in which the Z' was determined as a final quality control.

---

4. Within plate effects may occur due to the fact that outer wells have slightly different CO_2 and O_2 levels, and different evaporation rate compared to inner wells, or that the used multichannel pipettes a slightly smaller volume in some channels compared to others causing one well to receive more of a certain compound than another. In the viral infection screen of **chapter 2** the plates had to be incubated in a specific incubator for safety reasons during the viral infection step of the protocol. The plates were stacked due to limited space, which led to significant within-plate effects: a gradient of fluorescence across both columns and rows (Fig. 1B, left panel). Some causes of within-plate effects can be minimized, making it essential to consider all sources of within-plate effects caused by increasing experiment size. For example, in the screens of **chapter 3** and **4** multiple incubators were reserved specifically for screening to prevent the necessity of stacking plates.

5. External sources of variation may be corrected using normalization. Between-plate variation can be correct by normalizing each sample to the controls or to all samples of their plate. Within-plate variation may also be normalized for, yet this depends on the plate-layout. Within-plate-variation can only be detected when the majority of samples in a plate are not hits, meaning their phenotype is at or close to baseline. The
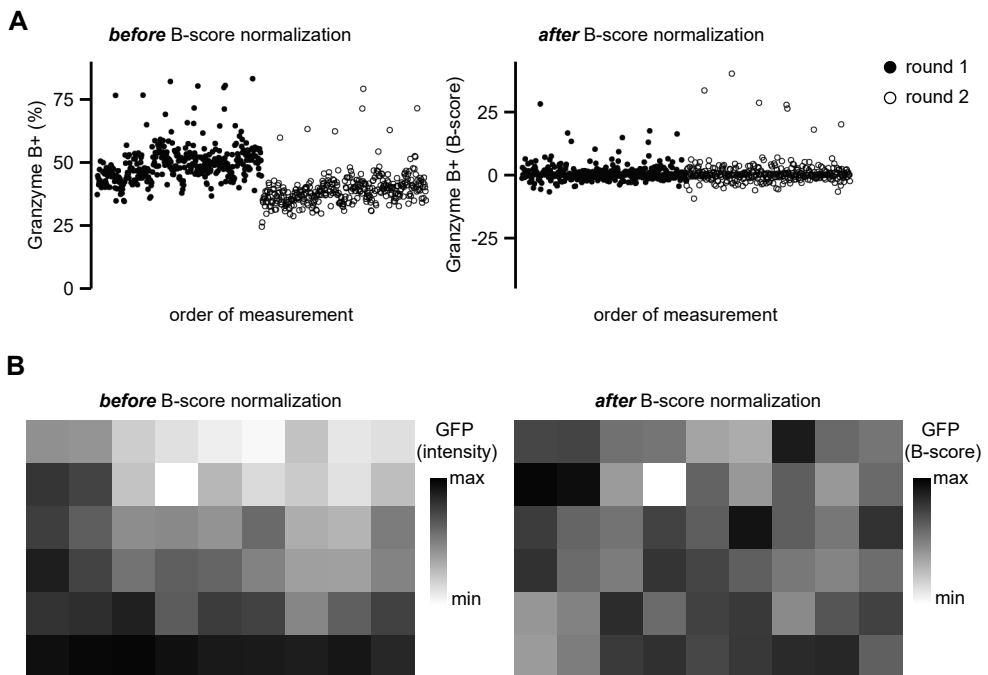
Figure 1. B-score normalization corrects for within- and between plate effects. (A) The T cell differentiation screen in chapter 4 was split across multiple rounds. Left panel shows GZMB as a percentage of CD8$^+$ T cells at day 10 of the T cell differentiation assay (see chapter 4, Fig. 1C for the assay) for the first two rounds, the right panel shows the same data after B-score normalization. (B) Heatmap of GFP fluorescence intensity of target cells after infection with VSV-LASV (see chapter 2, Fig. 2A for the assay). The left panel shows the plate before B-score normalization, the right panel shows the same plate after B-score normalization.

secreted protein library used in this thesis met this condition as each plate contained only a few hits at most, also because secreted proteins from the same family (e.g. type I interferons) were spread across multiple plates. We could therefore apply B-score normalization which performs a median polish across rows and columns consecutively to remove any row-wise and column-wise effects in a plate (Fig. 1A, B) (5). We recommend following a similar procedure. After considering how to tackle the different sources of between and within plate variation can the full screen be performed, and results normalized.

Hit selection is an arbitrary process

Once the data of a full screen have been normalized, hits can be selected. There are different methods for selecting hits. As conditions often have only one or two replicates in high-throughput screening, p-values often cannot be calculated. Instead, an arbitrary cutoff is set to separate hits from non-hits. This cutoff may for example be the top 100 conditions with the highest increase/decrease in a specific readout, or those samples which deviate a certain number of standard deviations from the rest. A more stringent cutoff results in less conditions to test in follow-up validation experiments, yet it may exclude potentially interesting hits. The number of hits selected may also depend on the resources a scientist is willing to spend on any follow up experiments. In **chapters 2-4** we based our cutoffs on the number of standard deviations each sample deviated from the full screen median. For the viral infection and B cell differentiation screens this was three standard deviations in either direction for every readout separately. In **chapter 4** we took between-donor variation into account, due to the discordance between the results of the different donors. The strongest hits for either donor were selected, as well as hits that were weaker but consistent in the screens of both donors. Both approaches led to interesting hits to validate, yet more hits may still be worth further investigation as weaker hits may induce a stronger effect once the purified protein instead of the conditioned medium is used as discussed above. The selected hits can be tested in multiple validation experiments repeating the same assay to ensure the effect observed in the screen can be replicated, which is especially important when the screen contained few replicates of each hit as was the case for the screens in this thesis. Hits that pass the validation experiments can be further studied in other assays, for example to determine the biological mechanism or clinical relevance.

Culture conditions determine which discoveries can be made

The details of the assay used in a high-throughput screen determine which hits can be discovered, yet the identified hits may only induce the observed function in the conditions imposed by the assay. In the virus screen, cells were pretreated with conditioned media for one day before addition of virus. In later experiments, it became apparent that FGF16 required this preincubation to act as an inhibitor of viral replication (chapter 2, Fig. 3C).

If we would have added the conditioned media simultaneously with the virus, the FGFs would not have been identified as hits. In the B cell differentiation screen (**chapter 3**), all conditioned media were added to a baseline of T cell derived stimulatory molecules CD40L and suboptimal IL-21. The assay could also have included agonistic anti-BCR, toll like receptor ligands such as CpG, or other cytokines known to affect B cell differentiation such as IL-10 or IL-4. The assay used in the B cell differentiation screen was insufficient for promoting naive B cells differentiation towards ASCs, and our aim was to identify if any the conditioned media of the library could render ASCs differentiation under these conditions. Current research in the lab identified other factors that support ACS-differentiation, and a new screen would possibly lead to new leads that further aid this process. In the T cell assay, naïve T cells were first activated for three days with anti-CD3 and anti-CD28 in the presence of IL-2, before washing and addition of IL-15 to sustain memory T cells, and the individual conditioned media of the library. Just as with the B cell screen, many variations on the assay can be imagined. For example, the conditioned media could have been added at another or multiple timepoints, IL-2 and IL-15 could have been replaced or supported by other cytokines such as IL-7 or IL-12, the strength of the initial stimulation could have been either increased or lowered. All these variations might have led to very different results compared to how the screens were run in **chapter 2-3**. This also implies that we probably missed yet unknown effects of certain secreted proteins, because we did not provide the necessary signals at the right time, which may explain why we did not observe increased IL-9 or IL-10 expression in any of the screen conditions.

The importance of culture conditions is not reserved to high-throughput screens. In **chapter 5**, tumor infiltrating lymphocytes (TILs) were cultured with high-dose IL-2 for two weeks before starting a rapid expansion protocol which included the addition of irradiated pooled-PBMCs and agonistic anti-CD3 antibodies. Unfortunately, after four weeks of TIL culture these T cells had very little cytokine expression after culture with autologous tumor digest. The reason for this lack of cytokine expression is up for speculation. As all cells in the tumor digests were put into culture, these cultures could contain suppressive cells which may have affected T cell functionality indirectly through inhibition during the four weeks of culture, or directly by inhibiting cytokine production during the tumor reactivity assay. If such suppressive cells can be identified they may either be removed through cell sorting at the start of culture or their inhibitory function may be negated through the addition of antibodies directed against the expressed inhibitory signaling molecules.

6

This thesis uncovers the presence of novel functional signaling pathways for cell-cell communication

The secreted protein library screens and the validation experiments thereof described in this thesis led to the identification of multiple new modulators of viral infection, B and T cell differentiation (Fig. 2). Follow up experiments highlighted the presence of signaling pathways that link these hits to the observed phenotype, although these pathways
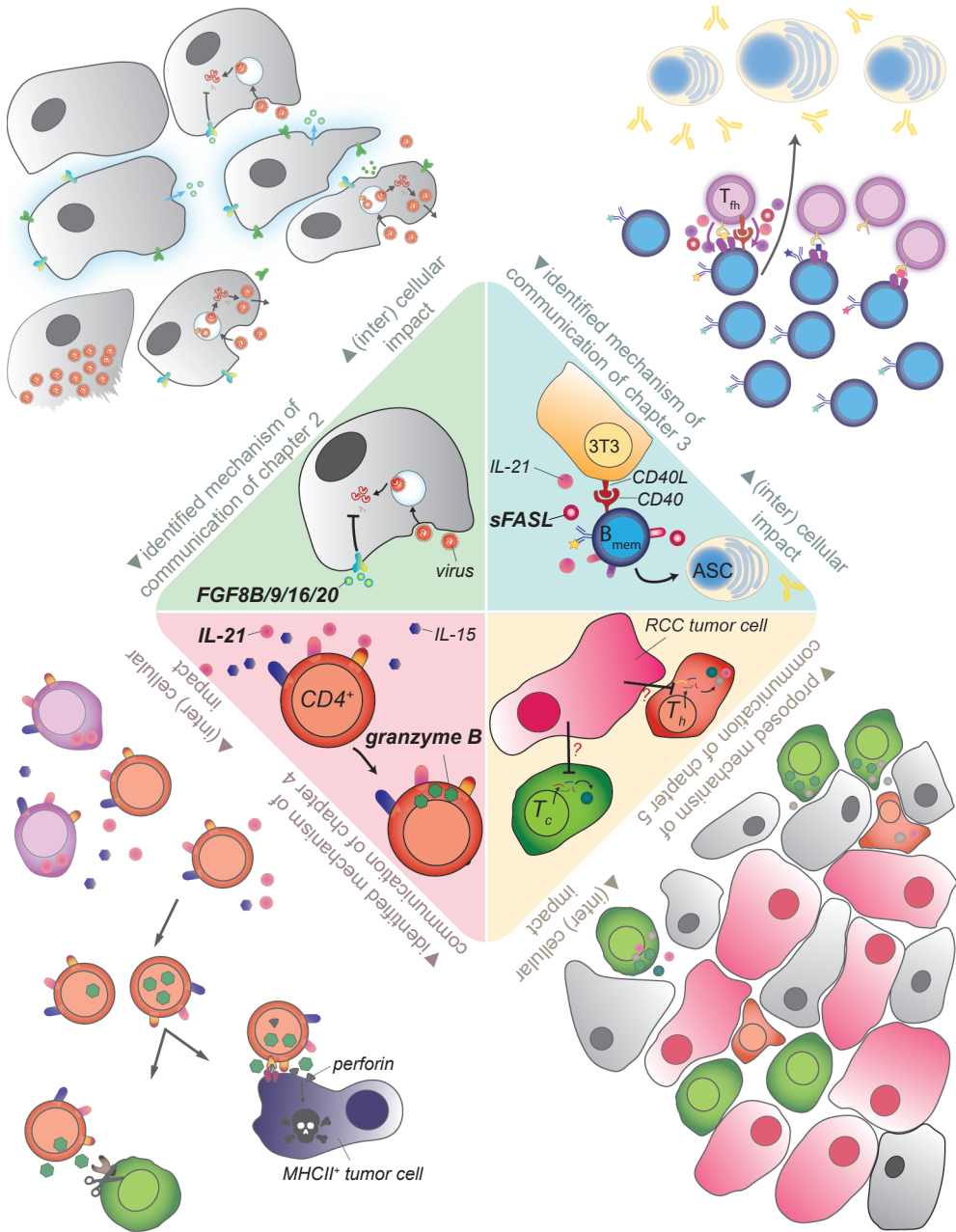
Figure 2. Secreted proteins facilitate intercellular communication. Each of the four research chapters of this thesis was centered around a mechanism of communication as depicted in the central diamond. The potential impact of each signaling moment is shown in the outer corners. (upper left quadrant) Several FGF family members can induce an antiviral state in target cells, consequently preventing viral replication. FGFs can be produced during viral infections to promote tissue repair but may also thwart viral infection directly. (upper right quadrant) sFASL enhances memory B cell differentiation into antibody secreting cells (ASC) when CD40L and IL-21 are present. During germinal center reactions sFASL may be present to exert this effect. (lower left quadrant) IL-21 promotes granzyme B (GZMB) expression in CD4+ T cells. The effects of CD4+ T cell derived

(Continued on next page)

require further elucidation.

The anti-viral effect of FGFs may be mediated by FGFR3c

Prior treatment of multiple cell lines with FGF16 was found to inhibit infection with vesicular stomatitis virus (VSV) or coxsackie virus in **chapter 2** (Fig. 2, upper left quadrant). The canonical FGFS are categorized in multiple subfamilies. Each subfamily is named after one of its members and include the FGF1, FGF4, FGF7, FGF9 (which includes FGF16) and FGF8 subfamilies. Multiple FGF family members showed inhibition of infection with VSV (chapter 2, Fig. 4G). However, through which FGF receptor(s) (FGFR) these FGFs were signaling were not uncovered, nor the downstream events that led to inhibition of viral replication. There are four FGF receptors for which the individual FGF subfamilies have varying affinity. The FGFs that inhibited VSV infection, including FGF16, FGF8b, FGF9, and FGF20, were from the FGF8 and FGF9 subfamilies which both have the highest relative affinity for FGFR3c (6). A recent study showed that FGF7 and FGF10, which both belong to the FGF7 subfamily, inhibited the anti-viral effect of type I IFNs in keratinocytes (7). Interestingly, FGF16 and IFN-α had an additive anti-viral effect in our assay, while FGF10 did not reduce infection with VSV (FGF7 was not tested in this assay) (chapter 2, Fig. 4D, G). This opposite effect of either promoting or inhibiting infection may be explained by the difference in FGFR type affinity as the FGF7 subfamily have affinity for FGFR2b and 1b. These data suggest that the anti-viral effect of FGF16 and its close FGF family members may be through FGFR3c. To test this hypothesis, we performed experiments to knock out the individual FGF receptors in our model HAP1 cell line and to visualize the different FGF receptors with flow cytometry. There was no clear FGFR staining with the antibodies used, yet other antibody clones could be tested in future experiments to study whether there is indeed a difference in signaling between the different FGFR types. Which specific cellular changes induced by FGF treatment leading to inhibition of viral replication remain a mystery at this moment. The effector molecules normally upregulated by type I IFNs to inhibit viral replication were not induced by FGF16, ruling out a type I IFN related mechanism (chapter 2, Fig. 4A). Viruses depend upon the machinery of host cells to replicate. FGFs might alter expression or functionality of any of these components, causing the viruses that critically depend on that component to become incapable of replicating. A CRISPR-Cas9 screen may uncover whether knockout of a single gene in FGF16 treated HAP1 cells negates the FGF-induced resistance to viral infection to shed some light on the mechanism. The antiviral effect of FGFs may already play a role during infections as increased levels of FGF2 have been reported for *Herpesviridae* and measles virus infections (8, 9). For the development of antiviral medicines, drugs or therapies, it would be interesting to uncover

6

Figure 2 Legend (continued)
GZMB is yet to be uncovered but may include the inhibition of other immune cells as well as the killing of tumor cells. (lower right quadrant) Expanded renal cell carcinoma (RCC) cells had poor cytokine production when co-cultured with autologous tumor digest. While the mechanism behind this poor in vitro cytokine production is not yet uncovered, this same mechanism may play a role in RCC tumors rendering T cells ineffective in mounting an anti-tumor response.

the antiviral effector mechanism induced by FGFs and investigate more broadly which viruses depend upon this component or these components.

Pro-apoptotic signaling through FAS is flipped towards anti-apoptotic signaling by FLIP

We uncovered that soluble FASL (sFASL) promotes the differentiation of memory B cells into antibody secreting cells (ASCs) in an assay that also contained CD40L and suboptimal IL-21 (**chapter 3**). As FASL is expressed in germinal centers this mechanism may also occur *in vivo* (Fig. 2, upper left quadrant) (10, 11). FASL comes in a membrane bound form (mFASL) which can be cleaved by different enzymes such as ADAM10 and metalloproteinases 3 and 7 to produce sFASL (12–14). Both forms bind the FAS receptor (FAS). mFASL binding to FAS promotes FAS clustering, thereby enabling FAS to recruit FADD which cleaves caspase-8 and caspase-10 (15). The subsequent activation of other members of the caspase family by caspase-8 and 10 leads to apoptosis. Varying reports exist whether sFASL can also induce cell death, as in some assays it promotes cell death, while in others it does not (14, 16, 17). The lack of oligomerization of sFASL with FAS has been used to explain why sFASL does not induce cell death in specific cells, yet this does not explain why in other cells sFASL can induce cell death. Regardless of potential differences in mFASL and sFASL signaling strength and pathways, cells can be resistant to FAS-mediated cell death through expression of cellular FLICE-inhibitory protein (c-FLIP; FLICE is an alternative name for caspase-8). c-FLIP can form a complex with caspase 8, this complex can bind the IKK complex, which frees NF-κB to move to the nucleus to promote proliferation (18). FLIP expression can be induced by BCR and CD40 signaling, although in mice BCR signaling is required to make B cells resistant to FAS mediated cell death, while human CD38⁻CD80⁻ tonsil B cells became resistant to FAS mediated cell death through CD40 signaling alone in an *in vitro* assay (19–21). Since in **chapter 3** B cells were stimulated with CD40L, CD40 ligation may have induced c-FLIP expression, thereby making B cells resistant to FASL mediated cell death. Inhibition of c-FLIP with siRNAs or small molecule inhibitors can reveal whether c-FLIP is indeed a key player in the differentiation induced by sFASL in our assay may, which may be the focus of future research (22). Another intriguing question is whether both mFASL and sFASL can promote B cell differentiation. Ideally, the culture system to test this hypothesis has similar CD40L expression as the one used in **chapter 3**, as different levels of CD40 ligation may render the B cells less resistant to FASL-mediated apoptosis. Transduction of the CD40L expressing 3T3 cell-line used in **chapter 3** with FASL would meet that goal. In addition, cleavage of mFASL can be prevented through inhibition of enzymes that cleave FAS extracellularly. Unfortunately, CD40L⁺ 3T3 cells transduced with the same human FASL used to generate sFASL for the secreted protein library were not viable, suggesting that these 3T3s are sensitive to FASL mediated cell death (data not shown). While we were unable to test this hypothesis in an assay with minimal deviation from the one used in **chapter 3**, future research could engineer HEK293T cells to express both CD40L and FASL, as this cell line did not show

a clear difference in viability after transfection with sFASL suggesting that it is resistant to FASL mediated cell death. A CD40L expressing HEK293T cell line may therefore be an alternative to the 3T3 model.

IL-21 and IL-15 may improve tumor infiltrating lymphocyte culture for renal cell carcinoma

IL-21 induces granzyme B (GZMB) not only in CD8$^+$ T cells, but also in CD4$^+$ T cells (**chapter 4** and Fig. 2 lower left quadrant). IL-21 is an important cytokine in the germinal center reaction produced by follicular T helper cells (T$_{fh}$), which suggests that T$_{fh}$ also express GZMB. However, the GZMB locus is methylated in T$_{fh}$ cells preventing GZMB expression, while T$_{h1}$ cells with their unmethylated GZMB locus can express this serine protease (23, 24). GZMB expression in T$_{fh}$ cells is not desirable as B cells that interact with T$_{fh}$ cells through MHC-I/TCR receptor signaling should be supported in their differentiation towards memory cells or ASCs, not killed. On the other hand, GZMB expression by Th1 cells may be beneficial in the tumor microenvironment, provided that GZMB is used to kill tumor cells and not used to inhibit other pro-inflammatory immune cells.

Ex vivo T cell expansion for adoptive transfer has traditionally been supported by high-dose IL-2. We used this established protocol to expand renal cell carcinoma (RCC) tumor infiltrating lymphocytes (TILs) in **chapter 5**, yet expanded TILs had poor cytokine production upon re-exposure to autologous tumor digest (Fig. 2, bottom right quadrant and chapter 5, Fig. 4C). However, as IL-2 stimulates terminal differentiation of conventional T cells as well as expansion of T regulatory cells (T$_{regs}$), IL-21 as well as the combination of IL-21 and IL-15 have been tested as a replacement for IL-2 by others (25–27). The expansion of Tregs in the RCC TIL cultures of **chapter 5** was not determined but could be an explanation for the suboptimal anti-tumor cytokine production. As we found in **chapter 4**, IL-15 combined with IL-21 may have an additional benefit of promoting the cytotoxicity of expanded TILs through induction of GZMB expression in both CD4$^+$ and CD8$^+$ T cells. IL-21 alone may not be the best culture supplement to promote cytokine production in T cells. IL-21 is regarded as a T$_{h1}$ differentiation inhibitor as it reduces IFN-γ expression (28, 29). Yet, Luo *et al*. found that T cells cultured with both IL-21 and IL-15 contained increased percentages of IFN-γ, TNF-α and IL-2 expressing cells compared to before culture, indicating that the combination of IL-21 and IL-15 can support T$_{h1}$ cells (26). Future RCC TIL culture experiments may test the combination of IL-21 and IL-15 in comparison to IL-2 for the expansion of TILs, while monitoring the proliferation of suppressive cells such as T$_{regs}$.

6

References

1. Agrotis A, Ketteler R. 2015. A new age in functional genomics using CRISPR/Cas9 in arrayed library screening. Front Genet 6:300.
2. Markossian S, Ang KK, Wilson CG, Arkin MR. 2018. Small-Molecule Screening for Genetic Diseases. Annu Rev Genomics Hum Genet 19:263–288.
3. Ding M, Tegel H, Sivertsson Å, Hober S, Snijder A, Ormö M, Strömstedt P-E, Davies R, Holmberg Schiavone L. 2020. Secretome-Based Screening in Target Discovery. SLAS Discov Adv Sci Drug Discov 25:535–551.
4. Uhlén M, Fagerberg L, Hallström BM, Lindskog C, Oksvold P, Mardinoglu A, Sivertsson Å, Kampf C, Sjöstedt E, Asplund A, Olsson I, Edlund K, Lundberg E, Navani S, Szigyarto CA-K, Odeberg J, Djureinovic D, Takanen JO, Hober S, Alm T, Edqvist P-H, Berling H, Tegel H, Mulder J, Rockberg J, Nilsson P, Schwenk JM, Hamsten M, von Feilitzen K, Forsberg M, Persson L, Johansson F, Zwahlen M, von Heijne G, Nielsen J, Pontén F. 2015. Tissue-based map of the human proteome. Science 347:1260419.
5. Malo N, Hanley JA, Cerquozzi S, Pelletier J, Nadon R. 2006. Statistical practice in high-throughput screening data analysis. Nat Biotechnol 24:167–75.
6. Ornitz DM, Itoh N. 2015. The fibroblast growth factor signaling pathway. Wiley Interdiscip Rev Dev Biol 4:215–266.
7. Maddaluno L, Urwyler C, Rauschendorfer T, Meyer M, Stefanova D, Spörri R, Wietecha M, Ferrarese L, Stoycheva D, Bender D, Li N, Strittmatter G, Nasirujjaman K, Beer H-D, Staeheli P, Hildt E, Oxenius A, Werner S. 2020. Antagonism of interferon signaling by fibroblast growth factors promotes viral replication. EMBO Mol Med 12:e11793.
8. Kaner RJ, Baird A, Mansukhani A, Basilico C, Summers BD, Florkiewicz RZ, Hajjar DP. 1990. Fibroblast growth factor receptor is a portal of cellular entry for herpes simplex virus type 1. Science 248:1410–1413.
9. Kim B, Lee S, Kaistha SD, Rouse BT. 2006. Application of FGF-2 to modulate herpetic stromal keratitis. Curr Eye Res 31:1021–1028.
10. Verbeke CS, Wenthe U, Zentgraf H. 1999. Fas ligand expression in the germinal centre. J Pathol 189:155–160.
11. Hao Z, Duncan GS, Seagal J, Su Y-W, Hong C, Haight J, Chen N-J, Elia A, Wakeham A, Li WY, Liepa J, Wood GA, Casola S, Rajewsky K, Mak TW. 2008. Fas Receptor Expression in Germinal-Center B Cells Is Essential for T and B Lymphocyte Homeostasis. Immunity 29:615–627.
12. Schulte M, Reiss K, Lettau M, Maretzky T, Ludwig A, Hartmann D, de Strooper B, Janssen O, Saftig P. 2007. ADAM10 regulates FasL cell surface expression and modulates FasL-induced cytotoxicity and activation-induced cell death. Cell Death Differ 14:1040–1049.
13. Mitsiades N, Yu WH, Poulaki V, Tsokos M, Stamenkovic I. 2001. Matrix metalloproteinase-7-mediated cleavage of Fas ligand protects tumor cells from chemotherapeutic drug cytotoxicity. Cancer Res 61:577–581.
14. Powell WC, Fingleton B, Wilson CL, Boothby M, Matrisian LM. 1999. The metalloproteinase matrilysin proteolytically generates active soluble Fas ligand and potentiates epithelial cell apoptosis. Curr Biol CB 9:1441–1447.
15. Yamada A, Arakaki R, Saito M, Kudo Y, Ishimaru N. 2017. Dual Role of Fas/FasL-Mediated Signal in Peripheral Immune Tolerance. Front Immunol 8:403.
16. Suda T, Hashimoto H, Tanaka M, Ochi T, Nagata S. 1997. Membrane Fas Ligand Kills Human Peripheral Blood T Lymphocytes, and Soluble Fas Ligand Blocks the Killing. J Exp Med 186:2045–2050.
17. Hohlbaum AM, Moe S, Marshak-Rothstein A. 2000. Opposing Effects of Transmembrane and Soluble FAS Ligand Expression on Inflammation and Tumor Cell Survival. J Exp Med 191:1209–1220.
18. Golks A, Brenner D, Krammer PH, Lavrik IN. 2006. The c-FLIP–NH2 terminus (p22-FLIP) induces NF-κB activation. J Exp Med 203:1295–1305.
19. Rathmell JC, Townsend SE, Xu JC, Flavell RA, Goodnow CC. 1996. Expansion or elimination of B cells in vivo: dual roles for CD40- and Fas (CD95)-ligands modulated by the B cell antigen receptor. Cell 87:319–29.
20. Wang J, Lobito AA, Shen F, Hornung F, Winoto A, Lenardo MJ. 2000. Inhibition of Fas-mediated apoptosis by the B cell antigen receptor through c-FLIP. Eur J Immunol 30:155–163.
21. Hennino A, Berard M, Casamayor-Pallejà M, Krammer PH, Defrance T. 2000. Regulation of the Fas Death Pathway by FLICE-Inhibitory Protein in Primary Human B Cells. J Immunol 165:3023–3030.
22. Safa AR, Pollok KE. 2011. Targeting the Anti-Apoptotic Protein c-FLIP for Cancer Therapy. Cancers 3:1639–1671.
23. Xie MM, Fang S, Chen Q, Liu H, Wan J, Dent AL. 2019. Follicular regulatory T cells inhibit the development of granzyme B-expressing follicular helper T cells. JCI Insight 4:128076.
24. Hale JS, Youngblood B, Latner DR, Mohammed AUR, Ye L, Akondy RS, Wu T, Iyer SS, Ahmed R. 2013. Distinct Memory CD4+ T Cells with Commitment to T Follicular Helper- and T Helper 1-Cell Lineages Are Generated after Acute Viral Infection. Immunity 38:805–817.

25. Santegoets SJAM a M, Turksma AW, Suhoski MM, Stam AGMM, Albelda SM, Hooijberg E, Scheper RJ, van den Eertwegh AJMM, Gerritsen WR, Powell DJ, June CH, de Gruijl TD. 2013. IL-21 promotes the expansion of CD27+ CD28+ tumor infiltrating lymphocytes with high cytotoxic potential and low collateral expansion of regulatory T cells. J Transl Med 11:37.
26. Luo X-H, Meng Q, Liu Z, Paraschoudi G. 2020. Generation of high-affinity CMV-specific T cells for adoptive immunotherapy using IL-2, IL-15, and IL-21. Clin Immunol 217:108456.
27. Huarte E, Fisher J, Turk MJ, Mellinger D, Foster C, Wolf B, Meehan KR, Fadul CE, Ernstoff MS. 2009. Ex vivo expansion of tumor specific lymphocytes with IL-15 and IL-21 for adoptive immunotherapy in melanoma. Cancer Lett 285:80–88.
28. Wurster AL, Rodgers VL, Satoskar AR, Whitters MJ, Young DA, Collins M, Grusby MJ. 2002. Interleukin 21 Is a T Helper (Th) Cell 2 Cytokine that Specifically Inhibits the Differentiation of Naive Th Cells into Interferon γ–producing Th1 Cells. J Exp Med 196:969–977.
29. Suto A, Wurster AL, Reiner SL, Grusby MJ. 2006. IL-21 inhibits IFN-gamma production in developing Th1 cells through the repression of Eomesodermin expression. J Immunol Baltim Md 1950 177:3721–3727.

6

APPENDIX

The Secreted Protein Library
English summary
Nederlandse samenvatting
List of publications
Author contributions
PhD portfolio
Curriculum vitae
Dankwoord

gene	category	part library
names of the cDNAs of the original secreted protein library used in chapters 2-4		
Q9UQ53	acetylglucosaminyltransferase	original
AMPH	actin family cytoskeletal protein	original
F13A1	acyltransferase	original
AMY1A	amylase	original
AMY2A	amylase	original
AMY2B	amylase	original
AGGF1	angiogenic factor	original
CRTAC1	annexin	original
NELL2	annexin	original
NUCB2	annexin	original
SOSTDC1	antagonist	original
TIMP1	antagonist	original
TIMP2	antagonist	original
TIMP3	antagonist	original
TIMP4	antagonist	original
BPIL1	antibacterial response protein	original
CAMP	antibacterial response protein	original
CD97	antibacterial response protein	original
C10orf58	antioxidant activity	original
APOA1	apolipoprotein	original
APOA2	apolipoprotein	original
APOA5	apolipoprotein	original
APOC1	apolipoprotein	original
APOC2	apolipoprotein	original
APOC3	apolipoprotein	original
APOD	apolipoprotein	original
APOE	apolipoprotein	original
APOF	apolipoprotein	original
APOH	apolipoprotein	original
APOL1	apolipoprotein	original
APOM	apolipoprotein	original
APOO	apolipoprotein	original
CNTNAP3	apolipoprotein	original
EDIL3	apolipoprotein	original
REN	aspartic protease	original
ANXA2	autocrine factor	original
PCDHA10	cadherin	original
PCDHA6	cadherin	original
CRELD2	calcium ion binding	original
CALR	calcium-binding protein	original
SMOC2	calcium-binding protein	original
CALU	calmodulin	original
CA11	carbonate dehydratase	original
GC	carboxylase	original
FCGR3A	cell adhesion molecule	original

gene	category	part library
FCGR3B	cell adhesion molecule	original
FCRLA	cell adhesion molecule	original
LGALS3	cell adhesion molecule	original
PDZD11	cell adhesion molecule	original
VTN	cell adhesion molecule	original
VWF	cell adhesion molecule	original
EDEM2	chaperone	original
CCL14	chemokine	original
CCL15	chemokine	original
CCL16	chemokine	original
CCL19	chemokine	original
CCL2	chemokine	original
CCL21	chemokine	original
CCL26	chemokine	original
CCL3	chemokine	original
CCL4	chemokine	original
CCL5	chemokine	original
CCL8	chemokine	original
CX3CL1	chemokine	original
CXCL1	chemokine	original
CXCL10	chemokine	original
CXCL11	chemokine	original
CXCL12	chemokine	original
CXCL14	chemokine	original
CXCL16	chemokine	original
CXCL2	chemokine	original
CXCL5	chemokine	original
CXCL6	chemokine	original
CXCL9	chemokine	original
IL8	chemokine	original
PF4	chemokine	original
PPBP	chemokine	original
XCL2	chemokine	original
FGG	coagulation factor	original
KNG1	coagulation factor	original
PROS1	coagulation factor	original
C1QTNF1	collagen binding	original
C1QTNF4	collagen binding	original
C1QTNF5	collagen binding	original
C1QTNF6	collagen binding	original
C1QTNF7	collagen binding	original
MMP1	collagenase	original
A2M	complement	original
C2	complement	original
C6	complement	original
C7	complement	original
C8A	complement	original

A

gene	category	part library
C8B	complement	original
CFB	complement	original
CFH	complement	original
CFHR1	complement	original
CFI	complement	original
CFP	complement	original
MASP2	complement	original
GGH	cysteine protease	original
TINAGL1	cysteine protease	original
AHSG	cysteine protease inhibitor	original
CST2	cysteine protease inhibitor	original
CST6	cysteine protease inhibitor	original
CST7	cysteine protease inhibitor	original
CST9L	cysteine protease inhibitor	original
AMH	cytokine	original
CHAD	cytokine	original
CKLF	cytokine	original
CRLF1	cytokine	original
CSF1	cytokine	original
CSF2	cytokine	original
CSF2RA	cytokine	original
CSF3	cytokine	original
CSF3R	cytokine	original
DCN	cytokine	original
EBI3	cytokine	original
FAM19A3	cytokine	original
FAM19A4	cytokine	original
FAM19A5	cytokine	original
GHR	cytokine	original
GREM1	cytokine	original
GREM2	cytokine	original
GRN	cytokine	original
LIFR	cytokine	original
MDK	cytokine	original
PTN	cytokine	original
RARRES2	cytokine	original
SLURP1	cytokine	original
TNFSF12	cytokine	original
TNFSF13	cytokine	original
TNFSF13B	cytokine	original
TNFSF14	cytokine	original
LEPR	cytokine receptor	original
FAM3C	cytokine-like	original
CECR1	deaminase	original
B2M	defense/immunity protein	original
CD8A	defense/immunity protein	original
CRISP2	defense/immunity protein	original

gene	category	part library
CRISP3	defense/immunity protein	original
CRISPLD1	defense/immunity protein	original
CRISPLD2	defense/immunity protein	original
DCD	defense/immunity protein	original
DEFA1	defense/immunity protein	original
DEFA3	defense/immunity protein	original
DEFA4	defense/immunity protein	original
DEFB1	defense/immunity protein	original
DEFB126	defense/immunity protein	original
FAM3A	defense/immunity protein	original
GNLY	defense/immunity protein	original
GP2	defense/immunity protein	original
HAMP	defense/immunity protein	original
HLA-C	defense/immunity protein	original
ICOS	defense/immunity protein	original
IGLL1	defense/immunity protein	original
IGSF21	defense/immunity protein	original
ITFG1	defense/immunity protein	original
LALBA	defense/immunity protein	original
LY86	defense/immunity protein	original
NRP1,NELL1	defense/immunity protein	original
PGLYRP1	defense/immunity protein	original
PGLYRP2	defense/immunity protein	original
PIGR	defense/immunity protein	original
PROZ	defense/immunity protein	original
SFTPD	defense/immunity protein	original
TF	defense/immunity protein	original
TREM1	defense/immunity protein	original
TREM2	defense/immunity protein	original
WIF1	defense/immunity protein	original
DHRS8	dehydrogenase	original
CCL11	development	original
CNTN4	development	original
DKK1	development	original
DKK2	development	original
DKK3	development	original
DKK4	development	original
PTX3	DNA binding protein	original
ANG	endoribonuclease	original
ACE	enzyme	original
ACE2	enzyme	original
CLPS	enzyme modulator	original
FETUB	enzyme modulator	original
FST	enzyme modulator	original
FSTL1	enzyme modulator	original
FSTL3	enzyme modulator	original
CDSN	epidermis development	original

A

gene	category	part library
PLA2G7	esterase	original
PON1	esterase	original
CHRDL1	extracellular matrix	original
COMP	extracellular matrix	original
LEPRE1	extracellular matrix glycoprotein	original
MEPE	extracellular matrix glycoprotein	original
MFAP2	extracellular matrix glycoprotein	original
MMRN2	extracellular matrix glycoprotein	original
MSLN	extracellular matrix glycoprotein	original
NID1	extracellular matrix glycoprotein	original
NID2	extracellular matrix glycoprotein	original
SCUBE1	extracellular matrix glycoprotein	original
SCUBE3	extracellular matrix glycoprotein	original
SPON1	extracellular matrix glycoprotein	original
SPON2	extracellular matrix glycoprotein	original
ATRN	extracellular matrix linker protein	original
LAMA3	extracellular matrix linker protein	original
LAMA4	extracellular matrix linker protein	original
LAMB1	extracellular matrix linker protein	original
LAMC1	extracellular matrix linker protein	original
LAMC2	extracellular matrix linker protein	original
CRTAP	extracellular matrix protein	original
CSPG2	extracellular matrix protein	original
DPT	extracellular matrix protein	original
DSPG3	extracellular matrix protein	original
ECM1	extracellular matrix protein	original
EFEMP1	extracellular matrix protein	original
EFEMP2	extracellular matrix protein	original
ELN	extracellular matrix protein	original
F8	extracellular matrix protein	original
FBLN1	extracellular matrix protein	original
FBLN2	extracellular matrix protein	original
FBLN5	extracellular matrix protein	original
GAS6	extracellular matrix protein	original
IGFALS	extracellular matrix protein	original
LGI1	extracellular matrix protein	original
LGI2	extracellular matrix protein	original
LRG1	extracellular matrix protein	original
LRP8	extracellular matrix protein	original
LRRC54	extracellular matrix protein	original
LUM	extracellular matrix protein	original
MAMDC2	extracellular matrix protein	original
MFAP1	extracellular matrix protein	original
MGP	extracellular matrix protein	original
NRP1	extracellular matrix protein	original
NTN1	extracellular matrix protein	original
OGN	extracellular matrix protein	original

gene	category	part library
OMD	extracellular matrix protein	original
PCOLCE	extracellular matrix protein	original
PCOLCE2	extracellular matrix protein	original
PODN	extracellular matrix protein	original
SPOCK2	extracellular matrix protein	original
TLL2	extracellular matrix protein	original
WISP1	extracellular matrix protein	original
WISP2	extracellular matrix protein	original
ZP2	extracellular matrix protein	original
ZP3	extracellular matrix protein	original
PRELP	extracellular matrix protein(	original
CHI3L1	glycosidase	original
CHIT1	glycosidase	original
HPSE	glycosidase	original
HYAL1	glycosidase	original
CHSS1	glycosyltransferase	original
GALNT1	glycosyltransferase	original
Q96EE4	glycosyltransferase	original
ST3GAL1	glycosyltransferase	original
ST3GAL3	glycosyltransferase	original
ST3GAL4	glycosyltransferase	original
ST6GAL1	glycosyltransferase	original
XYLT2	glycosyltransferase	original
BMP2	growth factor	original
BMP3	growth factor	original
BMP4	growth factor	original
BMP6	growth factor	original
BMP7	growth factor	original
BMP8A	growth factor	original
CSHL1	growth factor	original
CTGF	growth factor	original
CYR61	growth factor	original
FGF1	growth factor	original
FGF10	growth factor	original
FGF12	growth factor	original
FGF13	growth factor	original
FGF14	growth factor	original
FGF16	growth factor	original
FGF2	growth factor	original
FGF21	growth factor	original
FGF23	growth factor	original
FGF4	growth factor	original
FGF5	growth factor	original
FGF7	growth factor	original
GDF11	growth factor	original
GDF15	growth factor	original
GDF3	growth factor	original

A

gene	category	part library
GDF5	growth factor	original
GDF7	growth factor	original
GDF8	growth factor	original
GH2	growth factor	original
HBEGF	growth factor	original
IGF1	growth factor	original
IGF2	growth factor	original
INHA	growth factor	original
MIA	growth factor	original
MIA2	growth factor	original
NELL1	growth factor	original
NOG	growth factor	original
NOV	growth factor	original
NRG1	growth factor	original
PDGFD	growth factor	original
PGF	growth factor	original
PTK6	growth factor	original
REG3A	growth factor	original
REG4	growth factor	original
TFF1	growth factor	original
TFF3	growth factor	original
TGFA	growth factor	original
TGFB2	growth factor	original
TGFB3	growth factor	original
VEGF	growth factor	original
VEGFC	growth factor	original
IGFBP1	growth factor binding	original
IGFBP2	growth factor binding	original
IGFBP3	growth factor binding	original
IGFBP4	growth factor binding	original
IGFBP5	growth factor binding	original
IGFBP7	growth factor binding	original
LECT1	growth factors	original
GNAS	heterotrimeric G-protein	original
ARSJ	hydrolase	original
BTD	hydrolase	original
FUCA2	hydrolase	original
SFN	hydrolase	original
SUMF1	hydrolase	original
DBH	hydroxylase	original
PCSK1N	inhibitor	original
IFNA2	interferon superfamily	original
IFNB1	interferon superfamily	original
IFNG	interferon superfamily	original
CLC	interleukin	original
CTF1	interleukin	original
IL12B	interleukin	original

gene	category	part library
IL16	interleukin	original
IL17D	interleukin	original
IL18	interleukin	original
IL1B	interleukin	original
IL1F5	interleukin	original
IL2	interleukin	original
IL23A	interleukin	original
IL31	interleukin	original
IL32	interleukin	original
IL33	interleukin	original
IL6	interleukin	original
IL7	interleukin	original
ADCK1	kinase	original
ARMET	kinase	original
EIF2AK3	kinase	original
ERBB3	kinase	original
FAM20B	kinase	original
PON3	lactonase	original
MSAP	ligase	original
RNF43	ligase	original
LIPC	lipase	original
LIPF	lipase	original
LIPF,LIPG	lipase	original
LIPG	lipase	original
LIPH	lipase	original
LYPLA3	lipase	original
PLA2G12A	lipase	original
PLA2G2D	lipase	original
PLA2G5	lipase	original
PNLIPRP2	lipase	original
RPH3AL	membrane trafficking regulatory protein	original
SYNPR	membrane trafficking regulatory protein	original
SYP	membrane trafficking regulatory protein	original
SYT5	membrane trafficking regulatory protein	original
SEMA3B	membrane-bound signaling molecule	original
SEMA3C	membrane-bound signaling molecule	original
SEMA3D	membrane-bound signaling molecule	original
SEMA3E	membrane-bound signaling molecule	original
SEMA3F	membrane-bound signaling molecule	original
C14orf112	metabolism	original
ADAM12	metalloprotease	original
ADAM23	metalloprotease	original
ADAM28	metalloprotease	original
ADAM9	metalloprotease	original
ADAMTS1	metalloprotease	original
ADAMTS10	metalloprotease	original

A

gene	category	part library
ADAMTS3	metalloprotease	original
ADAMTS4	metalloprotease	original
ADAMTSL4	metalloprotease	original
ARTS1	metalloprotease	original
CPA1	metalloprotease	original
CPA2	metalloprotease	original
CPA3	metalloprotease	original
CPA3,CPA4	metalloprotease	original
CPA6	metalloprotease	original
CPB2	metalloprotease	original
CPE	metalloprotease	original
CPN1	metalloprotease	original
CPO	metalloprotease	original
CPXM1	metalloprotease	original
CPXM2	metalloprotease	original
CPZ	metalloprotease	original
LNPEP	metalloprotease	original
MMEL1	metalloprotease	original
MMP23B	metalloprotease	original
RNPEP	metalloprotease	original
CMTD1	methyltransferase	original
ADCYAP1	neuropeptide	original
NMB	neuropeptide	original
NMU	neuropeptide	original
NPFF	neuropeptide	original
NPY	neuropeptide	original
NTS	neuropeptide	original
PDYN	neuropeptide	original
PENK	neuropeptide	original
PMCH	neuropeptide	original
PNOC	neuropeptide	original
SCG2	neuropeptide	original
SCG5	neuropeptide	original
TAC1	neuropeptide	original
TAC3	neuropeptide	original
VIP	neuropeptide	original
BDNF	neurotrophic factor	original
GDNF	neurotrophic factor	original
NGFB	neurotrophic factor	original
GSN	non-motor actin binding protein	original
MINP1	nucleotide phosphatase	original
C10orf59	oxidase	original
CD163	oxidase	original
CD5L	oxidase	original
QSCN6	oxidase	original
ERO1A	oxidoreductase	original
SOD3	oxidoreductase	original

gene	category	part library
CTHRC1	oxygenase	original
SPOCK3	peptidase inhibitor	original
ADM	peptide hormone	original
APLN	peptide hormone	original
C12orf39	peptide hormone	original
CALCA	peptide hormone	original
CCK	peptide hormone	original
CFD	peptide hormone	original
CHGA	peptide hormone	original
CHGB	peptide hormone	original
CRH	peptide hormone	original
EDN3	peptide hormone	original
F11	peptide hormone	original
F12	peptide hormone	original
F9	peptide hormone	original
GAL	peptide hormone	original
GALP	peptide hormone	original
GCG	peptide hormone	original
IAPP	peptide hormone	original
INS	peptide hormone	original
INSL4	peptide hormone	original
LEP	peptide hormone	original
MSMB	peptide hormone	original
NPPA	peptide hormone	original
NPPB	peptide hormone	original
NPPC	peptide hormone	original
PLAT	peptide hormone	original
PROK2	peptide hormone	original
PSG1	peptide hormone	original
PSG2	peptide hormone	original
PSG3	peptide hormone	original
PSG4	peptide hormone	original
PSG5	peptide hormone	original
PTHLH	peptide hormone	original
RETN	peptide hormone	original
RLN2	peptide hormone	original
SCG3	peptide hormone	original
SST	peptide hormone	original
STC1	peptide hormone	original
STC2	peptide hormone	original
GPX3	peroxidase	original
GPX7	peroxidase	original
CANT1	phosphatase	original
CILP	phosphatase	original
ENPP5	phosphatase	original
ENPP6	phosphatase	original
ENTPD6	phosphatase	original

A

gene	category	part library
PRG2	phosphatase	original
PRG4	phosphatase	original
SPP1	phosphatase	original
SMPDL3A	phosphodiesterase	original
SMPDL3B	phosphodiesterase	original
CPA4	protease	original
GZMA	protease	original
GZMK	protease	original
GZMM	protease	original
HABP2	protease	original
HGFAC	protease	original
HP	protease	original
HPR	protease	original
KLK11	protease	original
KLK12	protease	original
KLK3	protease	original
KLK4	protease	original
KLK5	protease	original
KLK6	protease	original
KLK9	protease	original
LOX	protease	original
LOXL1	protease	original
LOXL2	protease	original
LTF	protease	original
MMP16	protease	original
MMP19	protease	original
MMP24	protease	original
PCSK1	protease	original
PCSK2	protease	original
PCSK5	protease	original
PCSK9	protease	original
PLG	protease	original
PRSS2	protease	original
PRSS27	protease	original
PRSS3	protease	original
PRSS8	protease	original
TMPRSS11D	protease	original
TMPRSS2	protease	original
TPSAB1	protease	original
TPSB2	protease	original
TPSD1	protease	original
TRH	protease	original
APCS	Protein Phosphatase	original
AGER	receptor	original
AZGP1	receptor	original
CD164	receptor	original
CD40	receptor	original

gene	category	part library
EGFL7	receptor	original
EGFR	receptor	original
EPHA3	receptor	original
FGFR2	receptor	original
FOLR1	receptor	original
FOLR2	receptor	original
FOLR3	receptor	original
GABBR1	receptor	original
IL15RA	receptor	original
IL17RB	receptor	original
IL1RAP	receptor	original
IL1RL1	receptor	original
IL1RN	receptor	original
IL22RA2	receptor	original
IL4R	receptor	original
IL6ST	receptor	original
MATN2	receptor	original
NENF	receptor	original
OLFM2	receptor	original
OLFML3	receptor	original
PDGFRL	receptor	original
PLXDC1	receptor	original
TFRC	receptor	original
TGFBR3	receptor	original
TNFRSF18	receptor	original
TNFRSF1A	receptor	original
TNFRSF1B	receptor	original
TNFRSF6B	receptor	original
VIT	receptor	original
AGR2	reductase	original
AGR3	reductase	original
TXD12	reductase	original
RNASE1	ribonuclease	original
RNASE4	ribonuclease	original
RNASE6	ribonuclease	original
RNASET2	ribonuclease	original
ISG15	ribosomal protein	original
CMA1	serine protease	original
DPP4	serine protease	original
F2	serine protease	original
HTRA1	serine protease	original
HTRA3	serine protease	original
SCPEP1	serine protease	original
AGT	serine protease inhibitor	original
AMBP	serine protease inhibitor	original
PI3	serine protease inhibitor	original
SERPINA10	serine protease inhibitor	original

A

gene	category	part library
SERPINA3	serine protease inhibitor	original
SERPINA4	serine protease inhibitor	original
SERPINA5	serine protease inhibitor	original
SERPINA6	serine protease inhibitor	original
SERPINB2	serine protease inhibitor	original
SERPINB3	serine protease inhibitor	original
SERPINC1	serine protease inhibitor	original
SERPINE2	serine protease inhibitor	original
SERPINF1	serine protease inhibitor	original
SERPING1	serine protease inhibitor	original
SERPINI1	serine protease inhibitor	original
SLPI	serine protease inhibitor	original
SPINLW1	serine protease inhibitor	original
SPINT1	serine protease inhibitor	original
TFPI	serine protease inhibitor	original
TFPI2	serine protease inhibitor	original
WFDC2	serine protease inhibitor	original
ANGPT1	signaling molecule	original
ANGPT2	signaling molecule	original
ANGPTL1	signaling molecule	original
ANGPTL2	signaling molecule	original
ANGPTL3	signaling molecule	original
ANGPTL4	signaling molecule	original
ANGPTL5	signaling molecule	original
ANGPTL7	signaling molecule	original
FCN1	signaling molecule	original
FGA	signaling molecule	original
FN1	signaling molecule	original
FRZB	signaling molecule	original
HHIP	signaling molecule	original
IGFL1	signaling molecule	original
LILRA3	signaling molecule	original
NDP	signaling molecule	original
NPTX2	signaling molecule	original
NXPH1	signaling molecule	original
OLR1	signaling molecule	original
POSTN	signaling molecule	original
RSPO1	signaling molecule	original
RSPO2	signaling molecule	original
RSPO4	signaling molecule	original
SFRP2	signaling molecule	original
SFRP4	signaling molecule	original
SHH	signaling molecule	original
SLIT2	signaling molecule	original
SLIT3	signaling molecule	original
TECT1	signaling molecule	original
TGFBI	signaling molecule	original

gene	category	part library
TNC	signaling molecule	original
TNXB	signaling molecule	original
WNT1	signaling molecule	original
WNT10A	signaling molecule	original
WNT10B	signaling molecule	original
WNT2	signaling molecule	original
WNT3	signaling molecule	original
WNT3A	signaling molecule	original
WNT4	signaling molecule	original
WNT5B	signaling molecule	original
WNT6	signaling molecule	original
WNT7A	signaling molecule	original
WNT7B	signaling molecule	original
WNT8B	signaling molecule	original
WNT9A	signaling molecule	original
STX1A	SNARE protein	original
VAMP1	SNARE protein	original
VAMP2	SNARE protein	original
DAG1	structural protein	original
LAD1	structural protein	original
SFTPC	surfactant	original
DEAF1	transcription factor	original
AFM	transfer/carrier protein	original
ALB	transfer/carrier protein	original
HPX	transfer/carrier protein	original
LCN2	transfer/carrier protein	original
RBP4	transfer/carrier protein	original
SCAMP5	transfer/carrier protein	original
CHSTC	transferase	original
SDF2	transferase	original
CLU	translation initiation factor	original
NPC2	transporter	original
ORM1	transporter	original
ORM2	transporter	original
PLTP	transporter	original
SLC30A3	transporter	original
SV2A	transporter	original
SV2B	transporter	original
TCN1	transporter	original
TCN2	transporter	original
TTR	transporter	original
CD40LG	tumor necrosis factor family member	original
FASLG	tumor necrosis factor family member	original
BLOT	undefined	original
C18orf54	undefined	original
C19orf10	undefined	original
C20orf116	undefined	original

A

gene	category	part library
C2orf30	undefined	original
C2orf40	undefined	original
C3orf29	undefined	original
C3orf40	undefined	original
CBLN4	undefined	original
CLUL1	undefined	original
CN159	undefined	original
CP048	undefined	original
CREG1	undefined	original
CREG2	undefined	original
FAM5B	undefined	original
LRCH3	undefined	original
PRR4	undefined	original
Q6UWT2	undefined	original
Q8TB73	undefined	original
Q969Y0	undefined	original
Q96NZ9	undefined	original
SCRG1	undefined	original
SECTM1	undefined	original
SPOCK1	undefined	original
SRPX2	undefined	original
TEX264	undefined	original
TMEM99	undefined	original
U773	undefined	original
EDN1	vasoconstrictor	original

names of the cDNAs of the extended secreted protein library used in chapter 4

gene	category	part library
ART5	ADP-ribosyltransferase	extension
ESM1	angiogenesis	extension
VASH1	angiogenesis	extension
CA6	anhydrase	extension
BPIFA1	antibacterial	extension
BPIFA2	antibacterial	extension
BPIFB1	antibacterial	extension
BPIFB3	antibacterial	extension
BPIFB5	antibacterial	extension
BPIFB7	antibacterial	extension
BPIFC	antibacterial	extension
ITLN1	antibacterial protein	extension
ITLN2	antibacterial protein	extension
LBP	antibacterial protein	extension
LEAP2	antibacterial protein	extension
LYG2	antibacterial protein	extension
REG3G	antibacterial protein	extension
DEFA5	antibacterial response protein	extension
DEFA6	antibacterial response protein	extension
DEFB118	antibacterial response protein	extension

gene	category	part library
DEFB119	antibacterial response protein	extension
DEFB121	antibacterial response protein	extension
DEFB123	antibacterial response protein	extension
DEFB125	antibacterial response protein	extension
DEFB127	antibacterial response protein	extension
DEFB128	antibacterial response protein	extension
DEFB129	antibacterial response protein	extension
DEFB134	antibacterial response protein	extension
DEFB4A	antibacterial response protein	extension
APOA4	apolipoprotein	extension
APOC4	apolipoprotein	extension
APOOL	apolipoprotein	extension
APOPT1	apoptosis inducer	extension
PGC	aspartic protease	extension
TUFT1	biomineral tissue development	extension
EPDR1	calcium ion binding	extension
EGFL8	calcium-binding protein	extension
SMOC1	calcium-binding protein	extension
FGFBP1	carrier protein	extension
FGFBP2	carrier protein	extension
FCER2	cell adhesion molecule	extension
ICAM4	cell adhesion molecule	extension
LTBP1	cell adhesion molecule	extension
PMEL	cell adhesion molecule	extension
CCL13	chemokine	extension
CCL17	chemokine	extension
CCL18	chemokine	extension
CCL22	chemokine	extension
CCL23	chemokine	extension
CCL24	chemokine	extension
CCL25	chemokine	extension
CCL28	chemokine	extension
CCL3L1	chemokine	extension
CCL7	chemokine	extension
CXCL13	chemokine	extension
CXCL3	chemokine	extension
LECT2	chemokine	extension
PF4V1	chemokine	extension
XCL1	chemokine	extension
COCH	collagen binding	extension
C1QB	complement	extension
C1QC	complement	extension
C1QTNF2	complement	extension
C1QTNF3	complement	extension
C8G	complement	extension
CFHR2	complement	extension
CFHR3	complement	extension

A

gene	category	part library
CFHR4	complement	extension
CFHR5	complement	extension
CRP	complement	extension
CD8B	coreceptor	extension
CER1	cytokine	extension
LIF	cytokine	extension
PZP	cytokine	extension
SCGB1A1	cytokine	extension
SCGB1C1	cytokine	extension
SCGB3A1	cytokine	extension
SEMG1	cytokine	extension
SEMG2	cytokine	extension
CYTL1	cytokine-like	extension
FAM3B	cytokine-like	extension
FAM3D	cytokine-like	extension
GLIPR1L1	defense protein	extension
SFTPA2	defense protein	extension
SPAG11A	defense protein	extension
ULBP2	defense/immunity protein	extension
DHRS11	dehydrogenase	extension
HSD17B13	dehydrogenase	extension
EDA	development	extension
LGI4	development	extension
NYX	development	extension
OTOR	development	extension
OVGP1	development	extension
ENDOD1	endonuclease	extension
SMR3A	endopeptidase inhibitor	extension
SMR3B	endopeptidase inhibitor	extension
FAM20A	enzyme modulator	extension
DOC2A	exocytosis	extension
LGI3	exocytosis	extension
ZG16	extracellular exosome	extension
BCAN	extracellular matrix glycoprotein	extension
EMILIN1	extracellular matrix glycoprotein	extension
EMILIN2	extracellular matrix glycoprotein	extension
EMILIN3	extracellular matrix glycoprotein	extension
FMOD	extracellular matrix glycoprotein	extension
HAPLN3	extracellular matrix glycoprotein	extension
HAPLN4	extracellular matrix glycoprotein	extension
AMBN	extracellular matrix protein	extension
AMELY	extracellular matrix protein	extension
AMTN	extracellular matrix protein	extension
BGN	extracellular matrix protein	extension
CLEC11A	extracellular matrix protein	extension
CLEC3B	extracellular matrix protein	extension
COL20A1	extracellular matrix protein	extension

gene	category	part library
DMP1	extracellular matrix protein	extension
EMID1	extracellular matrix protein	extension
MATN3	extracellular matrix protein	extension
MATN4	extracellular matrix protein	extension
OPTC	extracellular matrix protein	extension
UCMA	extracellular matrix protein	extension
IMPG1	extracellular matrix proteoglycan	extension
HYAL3	glycosidase	extension
MAN2B2	glycosylase	extension
ABO	glycosyltransferase	extension
GALNT2	glycosyltransferase	extension
BMP10	growth factor	extension
BMP15	growth factor	extension
BMP5	growth factor	extension
CSH1	growth factor	extension
CSH2	growth factor	extension
FGF11	growth factor	extension
FGF17	growth factor	extension
FGF19	growth factor	extension
FGF22	growth factor	extension
FGF3	growth factor	extension
FGF6	growth factor	extension
FGF8	growth factor	extension
FGF9	growth factor	extension
FIGF	growth factor	extension
GDF10	growth factor	extension
INHBC	growth factor	extension
INHBE	growth factor	extension
LACRT	growth factor	extension
LEFTY1	growth factor	extension
LEFTY2	growth factor	extension
NODAL	growth factor	extension
PRL	growth factor	extension
TFF2	growth factor	extension
VEGFB	growth factor	extension
VGF	growth factor	extension
WISP3	growth factor	extension
GKN1	growth factor activity	extension
RAB37	GTPase	extension
PTH	hormone	extension
RETNLB	hormone	extension
RLN3	hormone	extension
THPO	hormone	extension
UTS2	hormone	extension
ARSF	hydrolase	extension
ARSG	hydrolase	extension
ARSI	hydrolase	extension

A

gene	category	part library
ARSK	hydrolase	extension
CHIA	hydrolase	extension
DNASE1L2	hydrolase	extension
EPO	hydrolase	extension
GPLD1	hydrolase	extension
IGLC1	immunoglobulin constant	extension
HTN3	innate immune system effector	extension
IFNA1	interferon superfamily	extension
IFNA10	interferon superfamily	extension
IFNA13	interferon superfamily	extension
IFNA14	interferon superfamily	extension
IFNA17	interferon superfamily	extension
IFNA21	interferon superfamily	extension
IFNA4	interferon superfamily	extension
IFNA5	interferon superfamily	extension
IFNA6	interferon superfamily	extension
IFNA7	interferon superfamily	extension
IFNA8	interferon superfamily	extension
IFNB1	interferon superfamily	extension
IFNG	interferon superfamily	extension
IFNW1	interferon superfamily	extension
IL10	interleukin	extension
IL11	interleukin	extension
IL12A	interleukin	extension
IL13	interleukin	extension
IL15	interleukin	extension
IL17A	interleukin	extension
IL17B	interleukin	extension
IL17F	interleukin	extension
IL1A	interleukin	extension
IL1F10	interleukin	extension
IL20	interleukin	extension
IL21	interleukin	extension
IL25	interleukin	extension
IL26	interleukin	extension
IL3	interleukin	extension
IL36A	interleukin	extension
IL36B	interleukin	extension
IL36G	interleukin	extension
IL37	interleukin	extension
IL4	interleukin	extension
IL5	interleukin	extension
IL8	interleukin	extension
IL9	interleukin	extension
IL9R	interleukin	extension
OSM	interleukin	extension
KERA	keratinocyte differentiation	extension

gene	category	part library
KRTDAP	keratinocyte differentiation	extension
CSN2	lactation	extension
CSN3	lactation	extension
PLA1A	lipase	extension
PNLIP	lipase	extension
PNLIPRP1	lipase	extension
LYZL1	lysozyme activity	extension
LYZL2	lysozyme activity	extension
LYZL4	lysozyme activity	extension
LYZL6	lysozyme activity	extension
SYN3	membrane trafficking regulatory protein	extension
SYT12	membrane trafficking regulatory protein	extension
SYT2	membrane trafficking regulatory protein	extension
SYT3	membrane trafficking regulatory protein	extension
SYT4	membrane trafficking regulatory protein	extension
SYT6	membrane trafficking regulatory protein	extension
SYT9	membrane trafficking regulatory protein	extension
GIP	metabolism/signaling molecule	extension
ADAMTS12	metalloprotease	extension
ADAMTS15	metalloprotease	extension
ADAMTS18	metalloprotease	extension
ADAMTSL1	metalloprotease	extension
CNDP1	metalloprotease	extension
CPA5	metalloprotease	extension
MMP26	metalloprotease	extension
MMP28	metalloprotease	extension
MAU2	mitosis	extension
MUC1	mucin	extension
MUC15	mucin	extension
MUC7	mucin	extension
MUCL1	mucin	extension
SOST	negative regulator Wnt signaling	extension
AVP	neuropeptide	extension
CARTPT	neuropeptide	extension
CBLN2	neuropeptide	extension
CORT	neuropeptide	extension
GHRH	neuropeptide	extension
OXT	neuropeptide	extension
PPY	neuropeptide	extension
PTH2	neuropeptide	extension
PYY	neuropeptide	extension
QRFP	neuropeptide	extension
SV2C	neurotransmitter transport	extension
NTF3	neurotrophic factor	extension
NTF4	neurotrophic factor	extension
WNK1	non-receptor serine/threonine protein kinase	extension
ENOX2	nuclease	extension

A

gene	category	part library
RNASE9	nucleic acid binding	extension
CGB	other signaling molecule	extension
LOXL3	oxidase	extension
LOXL4	oxidase	extension
BDH2	oxidoreductase	extension
TMPRSS11E	peptidase	extension
CST8	peptidase inhibitor	extension
CSTL1	peptidase inhibitor	extension
WFDC6	peptidase inhibitor	extension
CALCB	peptide hormone	extension
CGB5	peptide hormone	extension
FSHB	peptide hormone	extension
INSL5	peptide hormone	extension
INSL6	peptide hormone	extension
MLN	peptide hormone	extension
TSHB	peptide hormone	extension
UCN	peptide hormone	extension
UCN2	peptide hormone	extension
UCN3	peptide hormone	extension
ACP6	phosphatase	extension
PIP	phosphatase	extension
PLA2G12B	phospholipase	extension
PLA2G1B	phospholipase	extension
PSG11	pregnancy	extension
PSG6	pregnancy	extension
PSG8	pregnancy	extension
PSG9	pregnancy	extension
A1BG	protease inhibitor	extension
FSTL5	protease inhibitor	extension
IGFBP6	protease inhibitor	extension
LAIR2	protease inhibitor	extension
SFRP1	protease inhibitor	extension
TINAG	protease inhibitor	extension
ADIPOQ	protein hormone	extension
BGLAP	protein hormone	extension
EREG	protein hormone	extension
GAST	protein hormone	extension
GHRL	protein hormone	extension
GPHA2	protein hormone	extension
INSL3	protein hormone	extension
OSTN	protein hormone	extension
CLCN6	receptor	extension
FAS	receptor	extension
FLT1	receptor	extension
LY96	receptor	extension
MYOC	receptor	extension
RTBDN	riboflavin bindin	extension

gene	category	part library
RNASE10	ribonuclease	extension
RNASE11	ribonuclease	extension
RNASE7	ribonuclease	extension
PRH2	salivary secretion	extension
STATH	salivary secretion	extension
LGALS3BP	scavenger receptor	extension
TSPEAR	sensory perception of sound	extension
CELA1	serine protease	extension
CELA2A	serine protease	extension
CELA2B	serine protease	extension
CTRB1	serine protease	extension
KLK10	serine protease	extension
KLK13	serine protease	extension
KLK14	serine protease	extension
KLK15	serine protease	extension
KLK7	serine protease	extension
KLK8	serine protease	extension
PRSS1	serine protease	extension
PRSS22	serine protease	extension
SERPINA1	serine protease inhibitor	extension
SERPINA12	serine protease inhibitor	extension
SERPINA7	serine protease inhibitor	extension
SERPINA9	serine protease inhibitor	extension
SERPINB4	serine protease inhibitor	extension
SERPINB5	serine protease inhibitor	extension
SERPINE1	serine protease inhibitor	extension
SERPINI2	serine protease inhibitor	extension
SPINK1	serine protease inhibitor	extension
SPINK2	serine protease inhibitor	extension
SPINK4	serine protease inhibitor	extension
SPINK7	serine protease inhibitor	extension
WFDC10A	serine protease inhibitor	extension
WFDC10B	serine protease inhibitor	extension
WFDC11	serine protease inhibitor	extension
WFDC5	serine protease inhibitor	extension
WFDC9	serine protease inhibitor	extension
CRIM1	serine-type endopeptidase inhibitor activity	extension
AGRP	signaling molecule	extension
ASIP	signaling molecule	extension
DKKL1	signaling molecule	extension
EDDM3A	signaling molecule	extension
EDDM3B	signaling molecule	extension
EFNA4	signaling molecule	extension
FAM19A1	signaling molecule	extension
FDCSP	signaling molecule	extension
FGB	signaling molecule	extension
FGL1	signaling molecule	extension

A

gene	category	part library
FGL2	signaling molecule	extension
GNRH1	signaling molecule	extension
GRP	signaling molecule	extension
GUCA2B	signaling molecule	extension
IGFL3	signaling molecule	extension
LGALS7B	signaling molecule	extension
MFAP4	signaling molecule	extension
MFAP5	signaling molecule	extension
NXPH2	signaling molecule	extension
NXPH3	signaling molecule	extension
NXPH4	signaling molecule	extension
RSPO3	signaling molecule	extension
S100A7	signaling molecule	extension
SIGLEC6	signaling molecule	extension
VSTM2A	signaling molecule	extension
WNT16	signaling molecule	extension
WNT5A	signaling molecule	extension
WNT9B	signaling molecule	extension
SPATA6	spermatogenesis	extension
IZUMO4	sperm-egg fusion	extension
ZPBP	sperm-egg fusion	extension
ZPBP2	sperm-egg fusion	extension
SCGB1D2	steroid binding	extension
CSN1S1	storage protein	extension
OLFM3	structural protein	extension
SFTA2	surfactant	extension
SFTPB	surfactant	extension
AFP	transfer/carrier protein	extension
LCN1	transfer/carrier protein	extension
LCN10	transfer/carrier protein	extension
LCN12	transfer/carrier protein	extension
LCN6	transfer/carrier protein	extension
LCN8	transfer/carrier protein	extension
OBP2A	transfer/carrier protein	extension
SCGB1D1	transfer/carrier protein	extension
SCGB1D4	transfer/carrier protein	extension
CETP	transferase	extension
GNPTG	transferase	extension
VASN	transforming growth factor beta binding	extension
GIF	transport	extension
LTA	tumor necrosis factor family member	extension
TNF	tumor necrosis factor family member	extension
TNFRSF11B	tumor necrosis factor family member	extension
KLHL11	ubiquitin-protein ligase	extension
C6orf58	undefined	extension
CCDC134	undefined	extension
CCDC70	undefined	extension

gene	category	part library
LYPD6	undefined	extension
PATE2	undefined	extension
PLGLB2	undefined	extension
RSPRY1	undefined	extension

A

English summary

The immune system utilizes a variety of strategies to dispose of pathogens and tumor cells. The immune system is often conceptually split into the innate immune system and the adaptive immune system. The first encompasses all mechanisms that are not tailored to individual pathogens or tumor cells, yet can react quickly, while the latter consists of cells that can mount a pathogen- or tumor cell-specific response which takes time to develop on first encounter. Relevant to this thesis is the secretion of type I interferons by innate immune cells in response to viral infection to instruct other immune cells and cells at risk of infection as well to produce and activate anti-viral proteins. The adaptive immune system includes B cells that can differentiate to secrete antibodies thereby providing humoral immunity, and T cells that support, regulate, or kill other (immune) cells depending on the requirements. A different immune strategy is required for each type of pathogen or tumor cell. Employing the wrong strategy or the generation of a suboptimal response will hinder successful clearance, while an overactive response can lead to tissue or even systemic damage. Immunological communication consists of signals that drive the immune system to a specific response. The cells of the immune system express various receptors that can recognize specific molecules of pathogens, ligands bound to the membrane of both immune- and non-immune cells, as well as soluble ligands. How a cell responds to the signals from its local environment depends on its combined proteome, transcriptome, genome, and metabolic state, meaning every cell may respond differently to the same signal. Immunological communication is therefore incredibly complex and not fully understood.

In this thesis we generated a human secreted protein library (SPL) for use in high-throughput screening to expand our knowledge of immunological communication. The SPL consisted not only of proteins known to be involved in immunological communication, but also non-immunological growth factors, hormones, and enzymes. This library was generated by transfection of HEK293T cells with the individual cDNAs encoding for human secreted proteins. It was confirmed that multiple cytokines were indeed present in their corresponding conditioned media, for other secreted proteins it was assumed that the produced proteins were secreted into the culture medium. Aliquots of the conditioned media were stored ready for use in multiple screens. The first batch of 756 conditioned media was generated in **chapter 2** and extended in **chapter 4** to include 1222 secreted proteins.

In **chapter 2** we employed the SPL to uncover novel modulators of viral infection. HAP1 cells were pretreated with the individual soluble proteins of the SPL to uncover which proteins influence infection with different glycoprotein engineered vesicular stomatitis viruses (VSV). Fibroblast growth factor 16 (FGF16) conditioned medium inhibited VSV. Subsequent experiments with purified recombinant FGF16 showed that it also inhibits coxsackie virus infection, but not lentivirus expressing the VSV glycoprotein, indicating that FGF16 inhibits viral replication in the cytosol, but does not prevent viral entry.

Surprisingly, FGF16 failed to induce the expression of proteins upregulated by type I interferon signaling which are generally known to inhibit viral replication. While the mechanism of FGF16-mediated inhibition of viral infection remains to be resolved, other close relatives of FGF16 in the FGF family (FGF9, FGF20, FGF8B) also inhibited VSV infection of our model cells *in vitro*. Members of multiple FGF subfamilies were therefore identified as a novel class of viral inhibitors.

Another immunological communication process for which we wanted to identify additional modulating factors is B cell differentiation into long-lived antibody secreting cells (ASCs). This process is supported by CD4+ T cells in the germinal center reaction, where they provide B cells with CD40L, IL-21 and IL-4 among other signals. To find hereto unidentified modulators of B cell differentiation into ASCs, naive B cells or IgG+ memory B cells were cultured with the individual soluble proteins of the SPL combined with the CD4+ T cell derived signals CD40L and IL-21 in **chapter 3**. Type I interferons, MAp19, and FASL conditioned media all promoted differentiation of memory B cells into the plasma cell phenotype (CD27+CD38+CD138+). Purified recombinant soluble FASL (sFASL) but not purified recombinant MAp19 replicated this effect. In addition, sFASL treated memory B cells secreted higher amounts of IgG1 and IgG4 compared to CD40L and IL-21 alone. Although FASL is known to induce apoptosis in target cells, further investigation revealed that sFASL did not promote cell death in memory B cells. Instead, the transcription factor BLIMP-1 was expressed by a higher percentage of sFASL treated memory B cells compared to control. These experiments revealed sFASL as an inducer of memory B cell differentiation into ASCs.

T cell receptor activation, co-stimulation and specific cytokines are necessary for naïve T cell differentiation into (specific) effector and memory T cells, yet additional signals may be uncovered as was found in the B cell differentiation screen. In **chapter 4**, CD4+ and CD8+ naive T cells were separately activated in the presence of IL-2, followed by a culture with the individual SPL conditioned media supplemented with IL-15. Half of the ensuing T cells were analyzed for memory T cell content, while the other half was examined for cytokine production capacity. The majority of conditioned media that affected T cell differentiation were known cytokines, of which multiple induced granzyme B (GZMB) in CD8+ T cells. Interestingly, IL-21 was the only cytokine that also induced GZMB in CD4+ T cells. The function of these GZMB expressing CD4+ T cells requires further examination. In addition, multiple hits were not followed up in **chapter 4**, yet may be relevant to improve our understanding of T cell immunology.

Tumor cells may alter the immunological lines of communication for their own gain. Immunotherapy aims to (re)activate immune cells so that they can clear such a tumor. Tumor infiltrating lymphocytes (TILs) can be *ex vivo* isolated, activated and expanded, to be reinfused into a patient. In **chapter 5** we analyzed and cultured TILs from renal cell carcinoma (RCC) patients using established protocols to investigate whether this therapy might be an option in this disease. T cells formed a higher proportion of immune cells in

A

RCC compared to paired kidney tissue. The T cells could be expanded and appeared to recognize autologous tumor digest as evidenced by upregulation of CD137. Yet, these T cells did not express significant levels of IFN-γ, TNF-α or IL-2, which are considered important indicators of anti-tumor T cell function after reinfusion in patients. The cause of this lack of cytokine expression may be found in the presence of RCC-derived immune suppressing factors, or lack of specific stimulating factors in the TIL culture.

As evaluated in the **general discussion**, the SPL has been used successfully to uncover novel modulators of immunological communication, yet improvements can still be made to the type of high-throughput screens as described in this thesis. The SPL itself consists of conditioned media with unknown levels of proteins of interest opposed to purified and quantified proteins. This means the current SPL could not be used to draw conclusions on any individual conditioned medium that did not show an effect. In addition, we may have missed hits due to too low concentrations of certain secreted proteins of interest. The specific culture conditions such as which supporting cytokines were used, timing of the assay, and strength of co-stimulation influenced which additional modulators could be found. Nonetheless, this thesis uncovered new functions of known secreted proteins thereby expanding our knowledge on immunological communication.

A

Nederlandse samenvatting

Het immuunsysteem maakt gebruik van een verscheidenheid aan strategieën om het lichaam te ontdoen van pathogenen en tumorcellen. Conceptueel wordt het immuunsysteem vaak opgedeeld in het aangeboren immuunsysteem en het adaptieve immuunsysteem. Het eerste omvat alle generieke mechanismen die snel kunnen reageren op de aanwezigheid van een pathogeen of tumorcel, terwijl het laatste cellen omvat die een pathogeen- of tumorcel-specifieke reactie kunnen ontwikkelen, maar die meer tijd nodig hebben bij de eerste ontmoeting om zo'n specifieke reactie op te zetten. Relevant voor deze thesis is de secretie van type I interferonen tijdens een virale infectie door het aangeboren immuunsysteem waarmee andere cellen, zowel immuuncellen als niet-immuuncellen die risico lopen om geïnfecteerd te worden, worden geïnstrueerd om antivirale eiwitten te activeren en te maken. Het adaptieve immuunsysteem omvat B cellen, die kunnen differentiëren zodat ze antilichamen kunnen produceren, en T cellen, die andere (immuun)cellen kunnen ondersteunen, reguleren of doden afhankelijk van de omstandigheden. De juiste soort strategie is nodig voor elk type pathogeen of tumorcel. Het inzetten van de verkeerde strategie of het genereren van een suboptimale reactie zit een succesvolle klaring in de weg, terwijl een overactieve reactie kan leiden tot weefselschade of zelfs systemische schade. Alle signalen die het immuunsysteem tot een specifieke reactie aanzetten vallen onder immunologische communicatie. De cellen van het immuunsysteem brengen verschillende receptoren tot expressie die specifieke moleculen, pathogenen, liganden gebonden aan het membraan van andere cellen, of oplosbare liganden kunnen binden. Hoe een cel reageert op een signaal in zijn directe omgeving is afhankelijk van een combinatie van zijn proteoom, transcriptoom, genoom, en metabolische staat. Dit betekent dat elke cel verschillend kan reageren op hetzelfde signaal. Immunologische communicatie is daarom ongelooflijk ingewikkeld en onvolledig begrepen.

In deze thesis hebben we een humane gesecreteerde eiwitten bibliotheek (Engels: *secreted protein library*, SPL) gemaakt voor gebruik in *high-throughput screening* experimenten om onze kennis van immunologische communicatie uit te breiden. De SPL bevat niet alleen eiwitten waarvan bekend is dat ze een rol spelen in immunologische communicatie, maar ook niet-immunologische groeifactoren, hormonen, en enzymen. Deze SPL was gegenereerd door HEK293T cellen te transfecteren met individuele cDNA's die coderen voor humane gesecreteerde eiwitten. Het was bevestigd dat meerdere cytokines inderdaad aanwezig zijn in de corresponderende geconditioneerde media. Voor andere gesecreteerde eiwitten zijn we ervan uitgegaan dat de geproduceerde eiwitten inderdaad in het kweekmedium terecht gekomen waren. Porties van de geconditioneerde media werden opgeslagen voor gebruik in meerdere *screens*. De eerste partij van 756 geconditioneerde media werd gemaakt in **hoofdstuk 2** en uitgebreid met honderden geconditioneerde media in **hoofdstuk 4** zodat de bibliotheek in totaal 1222 gesecreteerde eiwitten bevat.

In **hoofdstuk 2** gebruikten we de SPL om nieuwe regulatoren van virale infectie te ontdekken. HAP1 cellen werden voorbehandeld met de individuele gesecreteerde eiwitten van de SPL om uit te zoeken welke eiwitten infecties met diverse glycoproteïne uitgeruste vesiculaire stomatitis virussen (VSV) kunnen beïnvloeden. Fibroblast groeifactor 16 (FGF16) geconditioneerd medium remde VSV infectie. Vervolgexperimenten met gezuiverde recombinant FGF16 lieten zien dat het ook coxsackievirus infectie kan remmen, maar niet infectie met een lentivirus dat het VSV glycoproteïne tot expressie bracht. Deze bevindingen geven aan dat FGF16 virale replicatie in het cytosol remt, maar het voorkomt niet virale internalisering. Verrassend genoeg stimuleerde FGF16 niet de expressie van eiwitten die normaal door type I interferon signalering tot expressie komen en virale replicatie remmen. Alhoewel het mechanisme van FGF16-gemedieerde remming van virale replicatie nog uitgeplozen moet worden, het is wel duidelijk dat andere leden van de FGF-familie (FGF9, FGF20, FGF8B) ook VSV infectie remden in de modelcellijn *in vitro*. Leden van meerdere FGF-subfamilies zijn daarom geïdentificeerd als een nieuwe klasse van virusremmers.

Een ander immunologisch communicatieproces waarvoor we wilden achterhalen of er nog andere gesecreteerde eiwitten een rol spelen is B cel differentiatie naar langlevende antilichaam secreterende cellen (ASCs). Dit proces wordt ondersteund door CD4$^+$ T cellen in de kiemcentrumreactie waar ze B cellen onder meer CD40-L, IL-21 en IL-4 aanbieden. Om andere modulatoren van B cel differentiatie naar ASCs te vinden werden naïeve B cellen of IgG$^+$ geheugen B cellen gekweekt met de individuele gesecreteerde eiwitten van de SPL gecomplementeerd met CD40L en IL-21 in **hoofdstuk 3**. Type I interferonen, MAp19, en FASL geconditioneerde media bevorderden allen de differentiatie van geheugen B cellen naar het plasmacel fenotype (CD27$^+$CD38$^+$CD138$^+$). Gezuiverde recombinante oplosbare FASL (sFASL), in tegenstelling tot gezuiverde recombinante MAp19, kon dit resultaat repliceren. Daarnaast secreteerden sFASL behandelde geheugen B cellen hogere hoeveelheden IgG1 en IgG4 uit dan geheugen B cellen gekweekt met alleen CD40L en IL-21. Alhoewel sFASL bekend staat om het induceren van apoptose in doelwitcellen werd dit proces niet gestimuleerd in de geheugen B cellen in ons kweeksysteem. In plaats daarvan werd de transcriptiefactor BLIMP-1 door een hoger percentage van sFASL behandelde geheugen B cellen tot expressie gebracht in vergelijking tot de controle. Deze experimenten onthulden dat sFASL differentiatie van geheugen B cellen naar ASCs induceert.

T cel receptor activatie, co-stimulatie, en specifieke cytokines zijn allen nodig om naïeve T cellen naar (specifieke) effector of geheugen T cellen te laten differentiëren. Mogelijk zijn er, net als met de B cel differentiatie *screen* van hoofdstuk 3, nog meer signalen te ontdekken die deze processen beïnvloeden. In **hoofdstuk 4** werden CD4$^+$ en CD8$^+$ T cellen apart geactiveerd in de aanwezigheid van IL-2 en vervolgens gekweekt met de individuele SPL geconditioneerde media gecomplementeerd met IL-15. De helft van de gekweekte T cellen werden geanalyseerd voor de expressie van geheugencel markers,

A

terwijl van de andere helft de cytokineproductiecapaciteit bepaald werd. Het gros van de geconditioneerde media die T cel differentiatie beïnvloedden waren bekende cytokines, waarvan meerdere granzym B (GZMB) expressie in CD8+ T cellen induceerden. Interessant genoeg was IL-21 het enige cytokine dat ook GZMB induceerde in CD4+ T cellen. De functie van deze GZMB producerende CD4+ T cellen vereist nog verder onderzoek. Bovendien waren meerdere bevindingen in hoofdstuk 4 nog niet verder opgevolgd, maar deze kunnen mogelijk wel relevant zijn voor het begrip van T cel immunologie.

Tumorcellen kunnen de immunologische communicatielijnen veranderen voor hun eigen gewin. Immunotherapieën hebben als doel om immuuncellen te (re)activeren zodat ze de tumor kunnen opruimen. Tumor infiltrerende lymfocyten (TILs) kunnen *ex vivo* geïsoleerd, geactiveerd, en geëxpandeerd worden, om vervolgens weer toe te dienen aan de patiënt. In **hoofdstuk 5** analyseerden en kweekten we TILs van niercelcarcinoom patiënten volgens bestaande protocollen om te onderzoeken of TIL-therapie een optie is voor deze ziekte. T cellen vormden een groter deel van de immuuncel populatie in de tumor dan in gepaard nierweefsel. De T cellen konden geëxpandeerd worden en leken autoloog tumordigest te herkennen aangezien ze CD137 tot expressie brachten. Desondanks produceerden deze T cellen geen significante niveaus IFN-γ, TNF-α, of IL-2. Deze cytokines worden gezien als belangrijke indicatoren van anti-tumor T cel functie na infusie in patiënten. De oorzaak van dit gebrek aan cytokine expressie kan mogelijk gevonden worden in de aanwezigheid van immunosuppressieve factoren in de tumor of de afwezigheid van specifieke stimulerende factoren in de TIL kweek.

Zoals geëvalueerd in de **algemene discussie** (Engels: *general discussion*) is de SPL succesvol gebruikt om nieuwe modulatoren van immunologische communicatie te ontdekken, niettegenstaande dat dit type *high-throughput screens* nog zeker verbeterd kan worden. De SPL zelf bestaat uit geconditioneerde media met onbekende niveaus van elk eiwit, terwijl deze ook gezuiverd en gekwantificeerd kunnen worden. Dit betekent dat de huidige SPL niet gebruikt kan worden om conclusies te trekken over een geconditioneerd medium dat geen effect laat zien. Daarnaast hebben we mogelijk interessante bevindingen gemist door een te lage concentratie van deze eiwitten in de geconditioneerde media. Ook de specifieke kweekcondities, waaronder de aanwezigheid van ondersteunende cytokines, tijdsplanning van de proef, en de sterkte van de gebruikte co-stimulatie beïnvloedden welke modulatoren gevonden konden worden. Desondanks zijn dankzij deze thesis nieuwe functies van bekende gesecreteerde eiwitten gevonden waarmee de algehele kennis van immunologische communicatie verbeterd is.

A

List of publications

Wan-Chien Cheng, **Saskia D van Asten**, Lachrissa A Burns, Hayley G Evans, Gina J Walter, Ahmed Hashim, Francis J Hughes, Leonie S Taams. Periodontitis-associated pathogens P. gingivalis and A. actinomycetemcomitans activate human CD14^{+} monocytes leading to enhanced Th17/IL-17 responses. Eur. J. Immunol. (2016). DOI: 10.1002/eji.201545871

Saskia D van Asten, Matthijs Raaben, Benjamin Nota, Robbert M Spaapen. Secretome Screening Reveals Fibroblast Growth Factors as Novel Inhibitors of Viral Replication. J. Virol. (2018). DOI: 10.1128/JVI.00260-18

Saskia D van Asten*, Rosa de Groot*, Marleen M van Loenen, Suzanne M Castenmiller, Jeroen de Jong, Kim Monkhorst, John B A G Haanen, Derk Amsen, Axel Bex, Robbert M Spaapen[#], Monika C Wolkers[#]. T cells expanded from renal cell carcinoma display tumor-specific CD137 expression but lack significant IFN-γ, TNF-α or IL-2 production. Oncoimmunology. (2021). DOI: 10.1080/2162402X.2020.1860482

Anno Saris, Tom D Y Reijnders, Esther J Nossent, Alex R Schuurman, Jan Verhoeff, **Saskia van Asten**, Hetty Bontkes, Siebe Blok, Janwillem Duitman, Harm-Jan Bogaard, Leo Heunks, Rene Lutter, Tom van der Poll, Juan J Garcia Vallejo, ArtDECO consortium and the Amsterdam UMC COVID study group. Distinct cellular immune profiles in the airways and blood of critically ill patients with COVID-19. Thorax. (2021) DOI: 10.1136/thoraxjnl-2020-216256

Saskia D van Asten, Peter-Paul Unger*, Casper Marsman*, Sophie Bliss, Tineke Jorritsma, Nicole M Thielens, S Marieke van Ham, Robbert M Spaapen. Soluble FAS Ligand Enhances Suboptimal CD40L/IL-21-Mediated Human Memory B Cell Differentiation into Antibody-Secreting Cells. J. Immunol. (2021). DOI: 10.4049/jimmunol.2001390

Bárbara Andrade Barbosa, **Saskia D van Asten**, Ji Won Oh, Arantza Farina-Sarasqueta, Joanne Verheij, Frederike Dijk, Hanneke W M van Laarhoven, Bauke Ylstra, Juan J Garcia Vallejo, Mark A van de Wiel, Yongsoo Kim. Bayesian log-normal deconvolution for enhanced in silico microdissection of bulk gene expression data. Nat. Commun. (2021). DOI: 10.1038/s41467-021-26328-2

*/[#] These authors contributed equally

A

Author contributions

Chapter 2

Secretome Screening Reveals Fibroblast Growth Factors as Novel Inhibitors of Viral Replication

Saskia D. van Asten,[1] Matthijs Raaben,[2] Benjamin Nota[3] and Robbert M. Spaapen[1]

[1]Department of Immunopathology, Sanquin Research and Landsteiner Laboratory AMC/UvA, Plesmanlaan 125, 1066 CX Amsterdam, The Netherlands

[2]Department of Biochemistry, The Netherlands Cancer Institute, Plesmanlaan 123, 1066 CX Amsterdam, The Netherlands

[3]Department of Research Facilities, Sanquin Research and Landsteiner Laboratory AMC/UvA, Plesmanlaan 125, 1066 CX Amsterdam, The Netherlands

Conceptualization and experiment design: S.A., M.R. and R.S.
Data acquisition: S.A. and M.R.
Data analysis: S.A., M.R., B.N. and R.S.
Data interpretation: S.A., M.R., B.N. and R.S.
Writing: S.A. and R.S.
All authors have read and approved the manuscript.

Chapter 3

Soluble FAS ligand enhances suboptimal CD40L/IL-21-mediated human memory B cell differentiation into antibody-secreting cells

Saskia D. van Asten[1,2], Peter-Paul Unger[1,2,*], Casper Marsman[1,2,*], Sophie Bliss[1,2], Tineke Jorritsma[1,2], Nicole M. Thielens[3], S. Marieke van Ham[1,2,4], Robbert M. Spaapen[1,2]

[1]Department of Immunopathology, Sanquin Research, Amsterdam, 1066 CX, The Netherlands
[2]Landsteiner Laboratory, Amsterdam UMC, University of Amsterdam, Amsterdam, 1066 CX, The Netherlands
[3]Univ. Grenoble Alpes, CEA, CNRS, IBS, F-38000, Grenoble, France
[4]Swammerdam Institute for Life Sciences, University of Amsterdam, Amsterdam, the Netherlands.

*Authors contributed equally

Conceptualization and experiment design: S.A., P.U., C.M., S.H. and R.S.
Data acquisition: S.A., P.U., C.M., S.B., T.J.
Data analysis: S.A., P.U., C.M., S.B. and R.S.
Data interpretation: S.A., P.U., C.M., S.B., S.H. and R.S.
Writing: S.A. and R.S.
All authors have read and approved the manuscript.

A

Chapter 4

T cells expanded from renal cell carcinoma display tumor-specific CD137 expression but lack significant IFN-γ, TNF-α or IL-2 production

Saskia D. van Asten[1,2,#], Rosa de Groot[2,3,4,#], Marleen M. van Loenen[2,3], Suzanne M. Castenmiller[2,3,4], Jeroen de Jong[5], Kim Monkhorst[5], John B.A.G. Haanen[6], Derk Amsen[2,3], Axel Bex[7,8], Robbert M. Spaapen[1,2*], Monika C. Wolkers[2,3,4*]

[1]Sanquin Research, Dept. of Immunopathology, Amsterdam, The Netherlands
[2]Landsteiner Laboratory, Amsterdam UMC, University of Amsterdam, Amsterdam, The Netherlands
[3]Sanquin Research, Dept. of Hematopoiesis, Amsterdam, The Netherlands
[4]Oncode Institute, Utrecht, The Netherlands
[5]The Netherlands Cancer Institute-Antoni van Leeuwenhoek Hospital (NKI-AvL), Dept. of Pathology, Amsterdam, The Netherlands
[6]NKI-AvL, Dept. of Medical Oncology, Amsterdam, The Netherlands
[7]NKI-AvL, Dept. of Urology, Amsterdam, The Netherlands
[8]Royal Free London NHS Foundation Trust, UCL Division of Surgery and Interventional Science, London, United Kingdom

[#], [*] Authors contributed equally

Conceptualization and experiment design: S.A., R.G. M.L., J.H., A.B. D.A., R.S. and M.W.
Data acquisition: S.A., R.G., M.L., S.C., J.J., K.M. and A.B.
Data analysis: S.A.
Data interpretation: S.A., R.G., M.L., D.A., R.S. and M.W.
Supervision: D.A., R.S. and M.W.
Writing: S.A., R.G., R.S. and M.W.
All authors have read and approved the manuscript.

Chapter 5

Secreted protein library screen uncovers IL-21 as an inducer of granzyme B expression in activated CD4^{+} T cells

Saskia D. van Asten[1,2], Natasja Kragten[2,3], Sophie Bliss[1,2], Derk Amsen[2,3], Monika C. Wolkers[2,3], Klaas van Gisbergen[2,3], Robbert M. Spaapen[1,2]

[1] Sanquin Research, Dept. of Immunopathology, Amsterdam, The Netherlands
[2] Landsteiner Laboratory, Amsterdam UMC, University of Amsterdam, Amsterdam, The Netherlands[3]Sanquin Research, Dept. of Hematopoiesis, Amsterdam, The Netherlands

Conceptualization and experiment design: S.A., N.K., D.A., M.W., K.G. and R.S.
Data acquisition: S.A., N.K. and S.B.
Data analysis: S.A. and S.B.
Data interpretation: S.A., N.K., S.B., D.A., M.W., K.G. and R.S.
Writing: S.A. and R.S.
Editing: S.A., K.G. and R.S.

A

PhD portfolio

Name PhD student: Saskia D. van Asten
PhD period: 01-10-2014 – 01-10-2018
Promotor: Prof. Dr. S.M. van Ham
Copromotor: Dr. R.M. Spaapen

PhD training

	Presentation	Year	ECTS
Courses			
Ensembl course		2014	0.3
AMC PubMed e-learning course		2015	0.1
Sanquin Science Course		2015	0.7
Postgraduate course Advanced immunology		2015	2.9
Expert Cytometry Advanced Flow Cytometry course		2015	0.25
Scientific Writing in English		2016	3
Data scientist with R (online courses from Datacamp)		2017-2018	4
Postgraduate course Systems Medicine		2017	1.5
Seminars, meetings and masterclasses			
Weekly immunopathology (IP) department meetings	Oral 4x	2014-2018	5
Biweekly journal club		2014-2018	2
Weekly Sanquin Research Staff meeting	Oral 2x	2014-2018	5
Biweekly Sanquin seminars		2014-2018	2
Sanquin Science Day		2014	1.8
	Poster	2016	
	Poster	2017	
Monthly IP science evening		2014-2018	1
Master classes			
Prof. dr. Adrian Liston		2015	0.2
Prof. dr. Meinrad Busslinger		2017	0.2
Prof. dr. Johannes Huppa		2017	0.2
Conferences			
Advanced Immunology Summer School (ENII), Porto Cervo, Olbia, Sardinia, IT	Oral + poster	2016	2
Dutch Society for Immunology (DSI) annual meeting, Kaatsheuvel, NL		2014	1.5
DSI annual meeting, Noordwijkerhout, NL	Oral	2015	1.5
	Oral + Poster	2017	1.5
DSI and British Society for Immunology conference, Liverpool, UK	Poster	2016	1.3
Keystone Translational Systems Immunology, Snowbird, Utah, US	Poster	2018	2

	Presentation	Year	ECTS
European Congress of Immunology (ECI), Amsterdam, NL	Poster 2x	2018	2.5
Organizing committee			
Amsterdam Infection and Immunity Institute (AI&II) PhD retreat, Heemskerk, NL		2017	2.5
Teaching			
Mardine Akershoek (internship, 6 months)		2016	2
Masha Bink (internship, 6 months)		2017	2
Parameters of Esteem			
AI&II travel grant		2017	
Nominee in-house Sanquin Seminar Award		2019	

A

Curriculum Vitae

Saskia Désirée van Asten is geboren op 23 september 1991 in Lelystad. In 2009 behaalde ze haar gymnasiumdiploma aan het Nassau Veluwe college in Harderwijk. Vervolgens begon ze aan de bachelor Bio-Farmaceutische Wetenschappen aan de Universiteit Leiden. Ze sloot deze bachelor af met een stage op de afdeling Toxicologie van het Leiden Academic Centre for Drug Research. Hier werkte ze onder begeleiding van Sreenivasa Ramaiahgari en dr. Leo Price aan het door hen ontwikkelde HepG2 3D kweek systeem, bedoeld voor het voorspellen van levertoxiciteit van nieuwe drug compounds. Er werd tijdens de stage onderzocht in hoeverre de genexpressie van voor lever toxiciteit belangrijke genen veranderen door 3D kweek in vergelijking tot 2D kweek, en werd de invloed van meerdere bekende medicijnen op de vitaliteit van in 3D gekweekte HepG2 cellen gemeten.

Na de bachelor volgde de master Bio-Farmaceutische Wetenschappen. Saskia's eerste masterstage vond plaats op dezelfde afdeling als die van haar bachelor, nogmaals onder begeleiding van dr. Leo Price. In deze stage bereidde ze een high-content screen voor met als doel om compounds te identificeren die de invasiviteit van een borstkankercellijn in een 3D celkweek remmen. Haar stage was voorbij na het screenen van een eerste set platen, maar hier werd wel haar interesse voor high-throughput screening geboren. Haar tweede masterstage vond plaats bij King's College London onder begeleiding van Wan-Chien Cheng en dr. Leonie Taams. Het doel van dit onderzoek was om de invloed van het orale pathogeen *Aggregatibacter actinomycetemcomitans* op de *in vitro* cytokineproductie van humane monocyten en CD4$^+$ T cellen te achterhalen. De resultaten van dit onderzoek zijn onderdeel van een wetenschappelijke publicatie.

In 2014 ronde Saskia haar master *cum laude* af en begon ze aan haar PhD onder begeleiding van dr. Robbert Spaapen bij de afdeling Immunopathologie van Sanquin in Amsterdam. Momenteel is ze werkzaam als postdoctoraal onderzoeker onder begeleiding van dr. Juan J. García-Vallejo op de afdeling Molecular Cell Biology & Immunology bij het Amsterdam UMC, locatie VUmc.

A

Dit proefschrift bevat onderzoek over uiteenlopende immunologische onderwerpen. Toch hebben we ze samen kunnen brengen onder het thema immunologische communicatie. Het immuunsysteem kan een immuunreactie alleen beginnen en tot een goed einde brengen als de verschillende (immuun) cellen samenwerken. Het tot een goed einde brengen van een proefschrift vereist eveneens een productieve samenwerking tussen tientallen mensen. Nu zijn mensen niet één op één te vergelijken met immuun cellen (alhoewel online testen me als een Treg indelen), toch heeft ieder zo hun eigen bijdrage geleverd aan het klaren van dit proefschrift. Deze mensen wil ik graag bedanken.

Robbert, als groepsleider ben je altijd heel betrokken geweest. We hadden lange vergaderingen, zowel met de groep als individueel, die uren duurden. Hierdoor heb ik me altijd heel betrokken gevoeld bij de groep ook al had ik mijn eigen projecten. Je vond het ook geen probleem om mij in het lab te helpen bij grote experimenten, zoals het kleuren van een batch van de T cell screen. Jij motiveerde me om altijd dat stapje verder te zetten, ook al heb ik dat bij het schrijven van dit proefschrift niet altijd gewaardeerd. Mede dankzij jou denk ik dat ik een kritische wetenschapper ben geworden.

Marieke, in mijn eerste jaar herkende je al snel de symptomen van een zelf-kritische persoonlijkheid. Impostersyndroom en (lichte) wanhoop overkomt velen van ons, maar jouw positieve kijk en advies stak me altijd een hart onder de riem. Ik heb veel van je geleerd over immunologie, en dan met name over B cellen. Dankjewel dat ik op jouw afdeling mijn promotieonderzoek heb mogen doen en dat je mijn promoter hebt willen zijn.

Derk en *Monika*, jullie hebben jarenlang jullie wijsheid vrijelijk gegeven zodat de verschillende assays, figuren en teksten nog beter werden. Daarnaast heb ik in Monika's groep mogen werken aan het RCC hoofdstuk. *Marleen*, dankzij jouw voorwerk had ik een mooie start op dit hoofdstuk. *Aurélie*, thank you for teaching me how to process kidney and RCC tissue. *Rosa*, de organisatie van het verkrijgen van weefselmateriaal plus de uitgebreide experimenten erna zijn je niet in de koude kleren gaan zitten. Het was veel werk, maar heeft wel interessante data opgeleverd!

Matthijs, het was misschien een zij-projectje voor jou, maar dankzij de vele virusinfecties die jij hebt gedaan hebben we een nieuwe anti-virale familie geïdentificeerd! Na die eerste screen met jou heb ik ook de magische truc geleerd om easy-load puntjes zonder loader netjes in een bakje te krijgen, en dat is nog vaak van pas gekomen.

Klaas en *Natasja*, door jullie had ik eindelijk een assay voor de T cell differentiation screen, ook al leverde het geen mooie hobit-hit op. Natasja heeft me deze assay zelfs geleerd, meegewerkt aan de optimalisatie experimenten, en de eerste run van de

volledige screen. Helaas eindigde deze eerste run met een infectie van alle platen, waar we pas achter kwamen tijdens een marathon facsen op zaterdag. Natasja, ik ben je zeer dankbaar voor je hulp.

Peter-Paul en *Casper*, als B cel mannen hebben jullie respectievelijk de eerste en laatste experimenten van het B cel differentiation screen hoofdstuk gepipetteerd. PP heeft zelfs twee keer de nacht doorgebracht bij de LSR om zo alle platen meten! Zonder jullie was hoofdstuk drie nooit tot een publicatie gekomen.

Voor dit promotieonderzoek is veel gebruik gemaakt van humaan weefsel. Ik wil de afdeling pathologie van het NKI, waaronder de assistent-pathologen, bedanken voor het verwerken van de nier-resecties, en mijn collega's bij Sanquin voor het afnemen en verwerken van bloed. Ik ben daarnaast de RCC patiënten en (gezonde) bloed donoren dankbaar dat ze mee wilden doen aan de diverse studies beschreven in dit proefschrift.

Erik, *Simon* en *Mark*, dankzij jullie draaien de flow cytometers als een zonnetje. En dat was nodig ook voor de duizenden samples die er alleen al voor dit proefschrift gemeten zijn. Om nog maar te zwijgen van de uren die jullie bij de sorters spenderen, en de adviezen die jullie geven om zo reproduceerbaar mogelijk te facsen. Dank!

Groep AP&C: het bestaat niet meer, maar we hebben samen mooie jaren gehad, waarvan vele uren in U212. *Marlieke*, je was erbij toen de groep opgestart werd en in de daarop volgende jaren. Je bent voor mij altijd een bron van inspiratie geweest hoe je zoveel experimenten uit kon voeren, om ze vervolgens in prachtige figuren uit te werken. Je hebt me wegwijs gemaakt in illustrator, en ik heb mijn best gedaan er iets moois van te maken. Ook was je kritisch op mijn werk wanneer dat nodig was. *Twan*, jij bracht meer luchtigheid in de groep. Gelukkig heb je het nooit vervelend gevonden om een taart te bakken, ik vond het geen probleem om ze op te eten. We hebben ook als bureaumaatjes een hoop besproken, je nieuwsgierigheid werkt aanstekelijk. *Sophie*, we've struggled with the experiments that were necessary to finish my thesis. Yet we perseverend, and here we are! You were a fun collegue to work with, I really enjoyed our conversations.

And of course thank you to the the students who joined our group for the ride: *Nour*, *Masha*, *Mardine*, *Milena* and *Kelly*. I hope you all started fulfilling careers.

Annelies, we mochten dan officieel flexplekken hebben, toch zaten we altijd bij elkaar in de buurt. Los van de gezelligheid heb ik veel van je geleerd over het kleuren van cellen voor flow cytometrie, toch wel de belangrijkste techniek voor mijn onderzoek. Maar je was er ook als ik mijn ei even kwijt moest. Dankjewel!

Immunopathologie is een goed georganiseerde afdeling waar ik altijd prettig mijn

A

experimenten heb kunnen uitvoeren. Dit is dankzij de inzet van de (oud-)labmanagers en technicians van de afdeling: *Tineke*, *Gerard*, *Ninotska*, *Miranda*, *Angela*, *Dorina*, *Gijs*, *Pleuni*, *Simone*, *Ingrid*, *Irma*, *Kim*, *Ellen*, *Marja*, *Margreet*, *Helen* en *Mieke*. Vooral Tineke heeft me geholpen met van alles en nog wat, waaronder het verwerken van de vele bestellingen (met name antilichamen), het beantwoorden van praktische vragen, en ze heeft me geleerd nog efficiënter buffycoats te isoleren door middel van de giettechniek. Fantastisch werk allemaal!

Fatima en *Kaoutar*, als secretariaat zullen jullie nooit als co-auteur op een artikel verschijnen, maar toch zijn jullie onmisbaar voor ons werk. Fatima is daarbij een expert in promotie-gerelateerde administratie, wat heel fijn is voor ons OIOs!

De OIOs van IP zijn altijd een hechte club geweest. Alhoewel dansen en playbackshows niet mijn ding zijn hebben jullie altijd veel lol op de afdeling gebracht, wat voor een fijne werksfeer heeft gezorgd. Maar jullie zijn er ook als een van ons een luisterend oor nodig heeft. Dankjewel de rest van mijn (ex-)mede-PhD-studenten: *Sonja*, *Laura L.*, *Mischa*, *Gerben*, *Richard*, *Willem*, *Anouk*, *Astrid* (niet Saskia), *Karin*, *Sanne*, *Anna K.*, *Anna vB.*, *Anno*, *Marein*, *Niels*, *Inge*, *Laura D.*, *Jana*, *Judith*, *Jorn*, *Casper*, *Juulke*, *Nieke* en *Yasmin*.

Ik wil ook de andere meer senior collega's, waaronder de groepsleiders, van de afdeling loven. Zij zijn er om (kritische) vragen te stellen, ons klaar te stomen voor belangrijke presentaties, om zo de kwaliteit hoog te houden. *Anja*, jouw aanwezigheid en inzet zorgde voor goede cellulaire meetings en journal clubs. Maar ook *Theo*, *Diana*, *Gertjan*, *Dörte*, *Henk*, *Ilse*, *Sacha*, *John*, *Rob* en *Lucien* maken/maakten iedereen op de afdeling beter.

Leo en *Leonie*, als mijn stagebegeleiders hebben jullie me geïntroduceerd in de wereld van respectievelijk high-throughput screening en immunologie. Door de ervaringen die ik in jullie labs heb opgedaan werd ik een geschikte kandidaat voor deze PhD. Bedankt daarvoor!

Juan, my current group leader, thank you for giving me the space to finish my PhD and supporting me in my career. By allowing me to work part-time I've managed to somewhat keep my sanity.

Hester, we kennen elkaar al sinds onze SQ-linair dagen als bio-farmaceuten bij Aesculapius. Sindsdien zijn we vele gezellige etentjes samen verder. Jij bent altijd degene geweest die begrijpt wat ik op het lab meemaak, ook al hebben we op dat gebied nooit samengewerkt. Ik hoop nog vele avonden met jou te kunnen kletsen over alles wat in ons leven gebeurt!

Nienke en *Tanja*, jullie betweterige kleine zusje heeft het eindelijk voor elkaar gekregen: ze gaat "afstuderen". Ik heb bij jullie genoeg geklaagd over de negatieve kanten van het promoveren, maar hier kunnen jullie dan eindelijk het mooie resultaat van deze vele jaren zien.

Aernoud en *Elselien*, papa en mama, jullie hebben mij geleerd om altijd naar de beste versie van mezelf te streven. Dat bleef niet alleen bij woorden, want dankzij jullie heb ik zes jaar met de bus naar het gymnasium kunnen gaan, en kon ik later door jullie bijdrage op kamers in Leiden, studeren en zelfs op stage in Londen. Financieel hoeven jullie me al jaren niet meer te ondersteunen, maar jullie zijn er altijd mocht ik weer een keer alles eruit willen gooien. Mijn dank is groot.

Lieve *Lennart*, toen we elkaar ontmoetten zat ik als tweedejaars OIO vol enthousiasme over mijn onderzoek. Deze energie heeft je aangetrokken, maar ook toen het minder leuk was ben je bij me gebleven. Jij hebt me keer op keer weten te overtuigen dat het me zou lukken te promoveren en dankzij jouw geloof in mij heb ik leren programmeren. Ik kijk ernaar uit om, inmiddels als getrouwd stel, samen met jou dit hoofdstuk af te sluiten en een nieuwe te beginnen.

A